DOCTOR OF PHILOSOPHY

# The analysis of the functional role of the cancer-associated, chromosomal breakpoint binding protein Translin in maintaining genome stability.

Alsaiari, Ahad

*Award date:*
2021

*Awarding institution:*
Bangor University

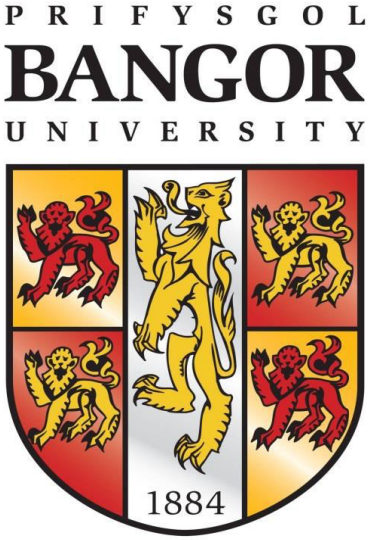


# The analysis of the functional role of the cancer-associated, chromosomal breakpoint binding protein Translin in maintaining genome stability.

A thesis is submitted for the degree of Doctor of Philosophy at Bangor University By

**Ahad Amer Alsaiari**

North West Cancer Research Fund Institute School of Medical Science
University of Bangor
United Kingdom

May,2021

# Declaration

I hereby declare that this thesis is the results of my own investigations, except where otherwise stated. All other sources are acknowledged by bibliographic references. This work has not previously been accepted in substance for any degree and is not being concurrently submitted in candidature for any degree unless, as agreed by the University, for approved dual awards.

---

Yr wyf drwy hyn yn datgan mai canlyniad fy ymchwil fy hun yw'r thesis hwn, ac eithrio lle nodir yn wahanol. Caiff ffynonellau eraill eu cydnabod gan droednodiadau yn rhoi cyfeiriadau eglur. Nid yw sylwedd y gwaith hwn wedi cael ei dderbyn o'r blaen ar gyfer unrhyw radd, ac nid yw'n cael ei gyflwyno ar yr un pryd mewn ymgeisiaeth am unrhyw radd oni bai ei fod, fel y cytunwyd gan y Brifysgol, am gymwysterau deuol cymeradwy.

# Abstract

Translin and Trax are highly conserved, paralogous proteins that are functionally associated with one another. They have been shown to participate in a wide range of biological pathways, including tRNA processing, mRNA regulation in neuronal cells, spermatogenesis function and pre-microRNA degradation during oncogenesis, a role which has given rise to the notion that they could represent a suitable pharmaceutical target for several forms of neoplasia. Translin was originally identified as a cancer-associated, chromosomal breakpoint junction binding protein, which led to the proposal that it functions in the DNA damage response. The aim of this study was to build on previous, unpublished work to further establish how Translin and/or Trax contribute to the maintenance of genomic integrity. Given the conserved nature of the two proteins, their function was investigated using the facile and genetically tractable experimental model, *Schizosaccharomyces pombe*. Preliminary data resulted in the hypothesis that *S. pombe* Translin (Tsn1), but not Trax (Tfx1), is involved in processing genomic RNA:DNA hybrids and could be functionally linked to RNase H activity for genome maintenance control. Here we reveal a functional association between Tsn1 and the RNase H Rnh201, but attribute this to non-RNase H activity of Rnh201, and, counter to our original hypothesis, find no evidence for a role for Tsn1 in RNA:DNA hybrid processing for genome stability maintenance, suggesting a distinct functional pathway. This is extended by exploring the relationship between Tsn1 and Tfx1 with the RNA:DNA helicase, Sen1. Whilst we find no functional relationship between Tsn1 and Sen1, we do reveal a possible functional redundancy between Sen1 and Tfx1, which opens a new avenue of investigation. Previous work has also demonstrated functional redundancy between Tsn1 and the RNA interference-associated RNAse III, Dcr1, which functions in an RNAi-independent fashion to maintain genome stability by displacing RNA polymerase II form the genomic template to avoid genome destabilisation caused by transcription-replication conflicts. Here, we extend this to reveal a complex functional relationship between Dcr1, Tsn1 and Rnh201 and provide a model that proposes an auxiliary role for Tsn1 for displacing RNA polymerase II from genomic DNA to prevent replication-associated genome instability. Finally, we clone the human *TSN* (Translin) gene and demonstrate that it can replace *S. pombe tsn1* encoded function(s) for genome maintenance, and it can do this in the absence of human TSNAX. We also demonstrate that this is not dependent on the RNase activity of human TSN. This not only demonstrates the conservation of this function within the Translin family, but also offers a simple system in which to study this important human oncogene and therapeutic target.

# Acknowledgements

Engaging with this PhD has genuinely transformed my life, and it would not have been achievable without the support and advice that I have been offered by numerous individuals. I would like to thank everyone who, in some manner, has influenced the work conducted for this thesis.

First, I thank God for safeguarding me and enabling me to work. I am very grateful to my supervisor, Dr. Ramsay Macfarlane, who has facilitated this work. I offer him my warmest thanks. His affable leadership and specialist guidance have been priceless during all the phases of this work. His sharp scientific acumen, his ability for finding a way through apparently insoluble practical issues and his capacity to represent complicated ideas as straightforward concepts has been a great advantage. There have been many times when I have been despondent and bewildered about my research's direction, but a supervision with him would rejuvenate my motivation and lift my spirits.

I express my gratitude to all the members of the MacFarlane laboratory, both current and from the past, who have disseminated their scientific knowledge and technical support as well as providing excellent friendship throughout this time. I offer particular thanks to Dr. Natalia Gomez-Escobar who provided me with essential academic advice. Her guidance was of great assistance, and I am thankful for the expert knowledge and aptitudes that she possesses. Further thanks are presented to Dr Jane Wakeman for her support and Dr. Christopher Staples for his ongoing support and for organising his fantastic monthly Journal Club for the sharing of information. I thank Dr. Edgar Hartsuiker for showing me how to work the yeast tetrad dissecting tool, and I cannot omit Dr. David Pryce, who assisted me in commencing from the master's degree until the conclusion of my PhD.

I give a very special thank you to my family. Words are inadequate to describe my gratitude to my mother and my father (God bless his soul), for all the sacrifices that they have undergone on my account. Her prayer for me has kept me going until this point. When it comes to my husband, Musaad, it is hard to convey my appreciation as it knows no bounds. He is my most motivated supporter. If he had not shared his bright optimism, I would be a much grouchier individual; in the absence of his love and support I would not find my way. I am grateful to him, not simply because of what he has sacrificed to put my career ahead in our lives, but because he has been at my side through the rollercoaster of the PhD journey, sharing every step

of the way. I must also thank my beautiful children, Rasil, Faisal and the smallest, Saud, for caring for each other and loving me during the most challenging period of my life. I also thank my brothers, in particular, Abdulhakim and Saleh for being with me in the United Kingdom, and my sisters, Jawaher, Rawia, Arwa, Roaa and Shahad who cheered me on and motivated me to pursue my aspirations. My family will forever be offered additional thanks for all the emotional support. I was constantly aware that they had faith in my skills and wanted an optimal outcome for me. I am so grateful to them for insisting that my life's objectives should be to pursue learning, to be content, to explore myself and to be happy with myself. I would only be able to become acquainted with and value others as I gained these skills.

Finally, I would like to express my gratitude to the Saudi Arabian government for offering Saudi students the opportunities to achieve their aspirations. In particular I would like to thank Taif University for their support and advice.

# List of Abbreviations

ATP: Adenosine Triphosphate

ATM: Ataxia telangiectasia mutated

BIR: break-induced replication

BDNF: Brain-derived neurotrophic factor

bp: base pair

C3PO: component 3 promoter of RISC

*cnt*: central core

CDKs: cyclin-dependent kinases

CDGS: Chromatin-dependent gene silencing

CML: chronic myelogenous leukaemia

cDNA: Complementary DNA

CPT: camptothecin

D-loop: Displacement loop

dH2O: Distilled water

DMSO: Dimethyl sulphoxide

dHJ: double Holliday junction

DNA-PK: DNA-dependent protein kinase

DNA: Deoxyribonucleic acid

dNTP: deoxyribonucleotide triphosphate

dsDNA: double-stranded DNA

DSBR: double strand break repair

dsRNA: double-stranded RNA

DSBs: double strand breaks

EDTA: ethylenediamine tetraacetic acid

EMMG: Edinburgh Minimal Media Glutamic acid

g: Gram

HJ: Holliday junction

HP1: heterochromatin protein 1

HU: hydroxyurea

HR: homologous recombination

5': Five prime end of DNA

3': Three prime end of DNA

IR: ionizing radiation

imr: inner most repeats

L: Litre

kb: kilobase

LB: Luria-Bertani media

kDa: kilo Dalton

LiAC: lithium acetate

MEFs: mice embryotic fibroblasts

miRNA: micro-RNAs

ml: Millilitre

mM: Millimolar

MMC: mitomycin C

MRN: MRE11-RAD50-NBS1 complex

MMS: methyl methane sulfonate

mRNA: messenger RNA

$Na_2HPO_4$; Disodium hydrogen phosphate dihydrate

NE: nuclear envelope

ng: Nanogram

NLS: Nuclear localization signal

NHEJ: non-homologous end joining

otr: outer repeats

ORF: open reading frame

PCR: polymerase chain reaction

pmol: picomole

PTGS: post-transcriptional gene silencing

PEG: polyethylene glycol

pol III: polymerase III

pol II: polymerase II

q-RT-PCR: quantitively real- time PCR

RC: replicative complex

RFB: replication fork barrier

rDNA: ribosomal DNA

RFC: replication factor C clamp loader

RNA pol: RNA polymerase

RISC: RNA-induced silencing complex

RNAi: RNA interference

RNA: Ribonucleic acid

RPA: replication protein A

rNMPs: ribonucleotide monophosphate

RT-PCR: Reverse transcriptase PCR

SDSA: synthesis-dependent strand annealing

SDS: Sodium Dodecyl Sulfate

SPA: synthetic sporulation media

ssDNA: single-stranded DNA

siRNA: small interference RNA

TB-RBP: testis-brain-RNA-binding protein

TRAX: Translin-associated factor X

TGS*:* transcriptional gene silencing

tRNA: transfer RNA

UV: ultra-violet

UTR: untranslated region

YEA: yeast extract agar

YE: yeast extract

YEL: yeast extract liquid

μg: Microgram

μl: Microliter

# Table of Contents

# List of Figures

## Chapter 1



## Chapter 3

# Chapter 4

# Chapter 5



# Chapter 6

# Chapter 7



## Appendices

# List of Tables

## Chapter 2

# Chapter 1: Introduction

# 1. Introduction

## 1.1. Cancer overview

Cancers are an important group of diseases causing high levels of morbidity and mortality, annually claiming approximately 8 million lives globally (Campbell et al., 2020). Thus far, over one hundred different forms and subtypes of cancer, with diverse aetiologies have been characterised; each organ has its own set of distinctive cancers. Whilst cancers are including a wide range of complex diseases, they share many defining characteristics, including genome instability and uncontrolled proliferation of cells that can invade proximal and distal tissues. Mutations in the normal DNA sequence can trigger the formation and progression of cancer; mutated genes may manifest as altered expression and/or altered or lost function (Vargas-Rondón et al., 2018; Nenclares & Harrington, 2020). The extent and type of oncogenic genetic change is variable. They can be simple point mutations that affect just one or a few nucleotides, or they can be large-scale alterations, such as chromosomal translocations, in which large segments of DNA are moved to a different chromosome (see Section 1.3). The effect of both large- and small-scale changes can be significant, resulting in altered chromosome or protein structures (Yi & Ju, 2018; Li et al., 2020). Rather than being a 'one-step' process, the development of cancer development is typically considered to be a cumulative process initiating in one somatic cell which becomes abnormal (clonal origin), although there are exceptions to this, where single chromosomal changes, such as translocations, can drive oncogenesis. As the cancer progresses, malignant tumours can form, which penetrate the basal membrane barrier of the affected tissue, enabling the aberrant cells to metastasise, the process by which tumours invade other tissues.

As well as spontaneous mutations in somatic cells of an adult, individuals can inherit mutations that increase their susceptibility to develop cancer (Wang & Chen, 2020; Campbell et al., 2020). Cancer cells can proliferate because mutations often occur in genes that ordinarily restrict cellular proliferative capacity; these genes are termed tumour suppressor genes. As a result, the genome of cancer cells is unstable, which is a defining characteristic of cancer. However, in contrast to the conventional view that cancers arises gradually over time from several genetic alterations, there is compelling evidence that cancer can also arise from chromothripsis, where the chromosome is 'shattered' and aberrantly rejoined in a single, catastrophic collective of mutation events (Li et al., 2020 ; Dewhurst, 2020).

## 1.2. Hallmarks of cancer

The so called 'hallmarks of cancer' are biological features that the majority of cancers exhibit as the disease develops (Hanahan and Weinberg, 2000; 2011). The proposed common cancer hall marks can be seen in Figure 1.1 and they include 1) angiogenesis, in which there is sustained formation of blood vessels needed to supply oxygen and nutrients to the tumour, and also provide a route for metastatic cellular migration; 2) resistance to apoptosis (programmed cell death), which would normally cull mutated cells from healthy tissue thereby preventing them from becoming cancerous; 3) metastasis, migrating to other sites; 4) enhanced response to signals that promote cell growth; 5) unresponsiveness to signals to inhibit growth; 6) unrestrained ability to replicate. These are the more established hallmarks, but other characteristics of cancer cells have been proposed adding to the set of hallmarks (Figure 1.1). These include the capacity to modulate cell metabolism for the benefit of cell proliferation and, importantly, the ability to evade immune system cells, in particular, B and T lymphocytes, macrophages and natural killer cell, which enables the tumour to express novel tumour specific antigens without triggering immunological destruction (Hanahan and Weinberg, 2011, Nenclares & Harrington, 2020). These hallmarks prove the platform for understanding cancer that will enable the development of anticancer treatments and patient diagnostic/stratification technologies (Meiyanto & Larasati, 2019).

As indicated above, a defining feature of cancer cells is that most of them exhibit genomic instability. (Hanahan and Weinberg, 2011; Bach et al., 2019). Chromosome instability (CIN) is a particular type of genomic instability which arises during mitosis; CIN reflects the failure of chromosomes to segregate correctly. As a result, whole or parts of chromosomes can be lost in one daughter cell and gained in the other, leading to aneuploidy (Duijf & Benezra, 2013; Kawakami et al., 2019). In aneuploid cells, the chromosomal abnormality is not limited to their number, but also considers their structure. Many exhibit irregular structures including deletions, duplications, inversions and translocations (Kawakami et al., 2019). Of these different aberrations, translocation is likely to be the most effective way to produce structural CIN that can lead to gene or gene-promoter fusions, which in turn can create new oncogenes or overexpression of proto oncogenes, genes that become oncogenic upon activation (see below) (Bach et al., 2019).

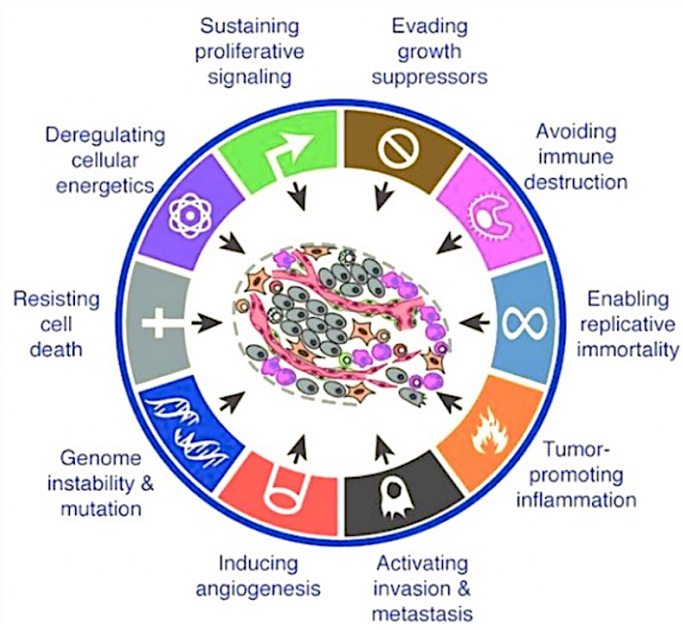


**Figure 1.1. Hallmarks of cancer**

Cancer cells are characterised as exhibiting these attributes; thus, they bear the hallmark of cancer (adapted from Hanahan and Weinberg 2011).

## 1.3. Chromosomal translocations

Identifying translocated chromosomes is important in the clinical setting, as their presence can contribute to disease diagnosis, prognosis and therapeutic strategy, particularly in haematological malignancies (Au et al., 2019). Fusion proteins often arise from chromosomal translocations as well as the bringing together a gene and the regulatory region of another gene. For gene fusions, the chimeric product can potentially have features of both original proteins; for example, the protein-protein interaction domain of one protein and the DNA-binding domain of the other. The chimera binds to the DNA elements specific to one protein and recruits to these genomic regions proteins that interact with the other protein. As a result, the expression of downstream target genes becomes uncontrolled (Schütte et al., 2019).

Numerous factors influence the occurrence of chromosomal translocations. Amongst these is the type of DNA damage that initiates the translocation, the pathway responsible for repairing the break, the location of the lesion in the genome, the state of the chromatin at that location and the stage of the cell cycle that the damage and repair process occurs in. Determining the relative relevance of these different factors is challenging as they are dynamic and intersect with one another. Many of the mechanistic details of translocation events have yet to be elucidated (Gómez-Herreros, 2019) .

Translocations are categorised as either being reciprocal or non-reciprocal. The most common form of translocation is the reciprocal variety, in which breaks drive segments being reciprocally switched between each of the participating chromosomes. Reciprocal, or balanced translocations can occur in the germ line. In these cases, because there is no change in the overall number of chromosomes, carriers can appear phenotypically normal. However, there is a strong risk of infertility, recurrent miscarriage or giving birth to babies with innate physical or mental abnormalities is increased in carriers with this type of translocation. However, reciprocal translocations can be oncogenic when they occur de novo in somatic cells. Non-reciprocal translocation are one-way translocations; only one chromosome transmits an arm to a non-homologous chromosome (Zhang et al., 2010; Chow et al., 2020). Balanced chromosome translocations are reciprocal; the chromosome segments are translocated between the non-homologous chromosomes; genetic material is neither lost nor gained. Unbalanced translocations result in the uneven distribution of chromosome segments, causing one daughter cell to have gained genetic material and the other to have lost it (Harewood & Fraser, 2014).

Nowell and Hungerford (1960) were the first to identify a specific translocation responsible for human cancer. This was the (9;22) (q34; q11) translocation, where the material is reciprocally translocated between chromosomes 9 and 22; 9q34 and 22q11 represents the breakpoint regions. This translocation was identified in chronic myelogenous leukaemia (CML) patients, who have an abnormally short chromosome 22, which is known as the Philadelphia chromosome. The effect of this translocation is a gene fusion of a fragment of the *BCR* gene from region q11 of chromosome 22 with a section of the *ABL1* gene at position q34 on chromosome 9. The fusion of genes results in a *BCR-ABL* hybrid gene on the shortened chromosome 22, which produces hybrid coding mRNA. This abnormal mRNA encodes a constitutively active tyrosine kinase with aberrant oncogenic activity. Myeloid cells with this mutation give rise to apoptosis-resistant CML cells (Nussenzweig, 2010; Burslem et al., 2019; Schütte et al., 2019) .

The burden of mutation is low in approximately 30% of sarcomas, which are rare high-grade tumours. These tumours are distinguishable by having a particular type of chromosomal translocation. In sarcoma, the majority of identified fused genes are those involved in transcription. In alveolar rhabdomyosarcoma (ARMS), desmoplastic small round cell tumour (DSRCT), Ewing sarcoma (ES) and synovial sarcoma, chromosomal translocation produces specific transcription factors that are abnormal (Toomey et al., 2010; Nakano & Takahashi, 2018; Tirado, 2019).

## 1.4. Pathways for repairing DNA double-strand breaks (DSBs)

The genome is exposed to diverse ‘attacks’ from outside and within the cell, damaging the DNA by causing a number of different types of DNA lesions and introducing instability into the genome (Tian et al., 2015; Scully et al., 2019; Cristini et al., 2020). Thus, accurate and rapid repair of the lesions is essential for maintaining the fidelity of the genome and to avoid genetic diseases such as cancer (Uckelmann & Sixma, 2017; Scully et al., 2019; Waterman et al., 2020). The most deleterious lesions are DSBs. In DSBs, both DNA strands break at a particular point, raising the potential for chromosomes to be re-arranged in the repair (Chang et al., 2017; Waterman et al., 2020). It has been postulated that several mechanisms might be responsible for the occurrence of DSBs such as the progression of a DNA replication fork across a nick which leads to the presence of a one sided DNA break during S-phase (see below; Marini et

al., 2019). Free radicals from oxidative stress and cellular metabolism, ionizing radiation and the cleavage of the DNA by nuclear enzymes such as the type II topoisomerases which can cause the transient breakage of both DNA strands also resulting in the formation of DSBs, although replication-associated breakage is thought to be the major source of DSBs with dividing cells (Shibata, 2017). Breakage of the DNA by topoisomerases I on the other hand can lead to single-strand DNA breaks (SSBs) which can then cause the formation of DSBs during the course of subsequent DNA replication. In rapidly dividing cells there exists two major pathways that are capable of repairing DSBs of which are homologous recombination (HR) and nonhomologous DNA end-joining pathway (NHEJ) (Takagi, 2017; Khan & Ali, 2017; Bétermier et al., 2020). Whilst efficient, if the wrong repair pathway is selected to repair breaks, genetic changes that drive cancer can occur. The selection of pathway is partly determined by stage of the cell cycle when the damage occurs; for example, because of sister chromatid availibility during the S and G2 phases, a homologous template can be used as a repair template, thus the HR pathway is the major DSB repair mechanism. Where a homologous template is not in close proximity to a DSB, the NHEJ pathway can mediate the repair. Typically, though, the NHEJ repair pathway is not deployed in the S/G2 phase, but in the other phases, which do not require a template for the DNA to be repaired (Ceccaldi et al., 2016; Zaboikin et al., 2017).

### 1.4.1. Non-homologous DNA end-joining

NHEJ repair does not require a homologous DNA template to join the two ends of DNA together in order to restore duplex integrity (Chaplin & Blundell, 2020). The NHEJ repair pathway mediates the re-ligation of broken DNA ends when a double-ended DSB is present. Unlike HR, the NHEJ pathway can operate independently of cell cycle phases (Zaboikin et al., 2017). NHEJ requires the action of multiple proteins such as Artemis and the Ku heterodimer (Ku70-Ku80 subunit) (Boboila et al., 2012; Chaplin & Blundell, 2020). Errors do occur with imperfect NHEJ repair events, which can lead to fusion of the telomeres and translocations (Wang et al., 2018; Bader et al., 2020a ).

NHEJ is initiated in higher eukaryotes by the Ku70–Ku80 heterodimer, which recognises the DSB and bind to the free ends of DNA. In this position, the dimeric Ku protein forms a scaffold that enables the NHEJ core components, including DNA-PKcs (DNA-PK catalytic subunit), to bind to the damaged ends. Recruited DNA-PKcs forms an active complex of Ku70/Ku80/DNA-PKcs. These complex recruits and phosphorylates the endonuclease,

Artemis. Any overhanging DNA is cleaved from the ends, rendering the DNA ends compatible, ready for ligation (Chang et al., 2017;Li & Xu, 2016; Chaplin & Blundell, 2020).

In several organisms it has been suggested that this pathway is modulated by a MRE11-RAD50-NBS1 (MRN) complex. This same complex is also considered to modulate DNA polymerases and other nucleases that are involved in pre-ligation processing of the DNA ends during NHEJ (Boboila et al., 2012; Chaplin & Blundell, 2020). Ligation of the DNA ends is performed by the XRCC4-DNA Ligase IV complex, resorting the duplex integrity (Figure 1.2).

Due to its direct interaction with the XRCC4/ ligase IV complex, XLF in the NHEJ pathway is presumed to have a role in the repair process. The function of PAXX (paralog of XLF and XRCC4), which is also a XRCC4-like protein, seems to coincide with the function of XLF (Tadi et al., 2016: Ochi et al., 2015; Stinson et al., 2019). These proteins interact with end-processing enzymes for the purpose of bringing together ends that are chemically incompatible. DNA polymerases, such as pol λ and pol μ, fill in gaps and overhangs; Aprataxin removes 5′ adenylate groups produce by unsuccessful ligation; damaged nucleotides are removed by nucleases (e.g., Artemis); tyrosyl-DNA phosphodiesterase 1 (Tdp1) removes topoisomerase I adducts and other 3′ modifications; similarly, Tdp2 removes 5′ DNA-topoisomerase II adducts; and kinase 3′-phosphatase (PNKP) removes 3′ phosphates and adds 5′-phosphates. End incompatibility is resolved in NHEJ by these various processing enzymes (Stinson et al., 2020).

The process of synapsis, which aligns DNA ends for ligation, may also be involved in end processing. Figure 1.3 graphically presents a two-stage model of synapsis. A long-range synaptic complex is formed by the Ku complex and DNA-PKcs; the complex keeps the ends of DNA >100 Å apart. The long-range complex is converted to a short-range complex due to the activity of DNA-PKcs kinase, XLF and Lig4-XRCC4. This brings the ends close together in a ligation-competent state. According to this model, end processing only occurs in the Lig4-dependent short-range synaptic complex state. Such a mechanism requires minimal processing as compatible ends are ligated immediately, and incompatible ends are processed to become compatible, then they are ligated. (Stinson et al., 2019).

### 1.4.2. Homologous recombination pathway (HR)

For tumor suppression and cell viability, homologous recombination (HR) is crucial for mammalian cells due to its essential role in ensuring genomic integrity (San Filippo et al. 2008: Hustedt et al., 2019). This repair mechanism is typically considered to be high fidelity and

largely error-free process because it is using a homologous DNA template, usually a sister chromatid. For HR to be successful, the template must be undamaged (Morati et al., 2020). Both mitosis and meiosis use HR, but it is a programmed event in meiosis, where it is required for inter-homologue connections in meiosis I and genetic material is exchanged between maternal and paternal chromosomes; additionally, this process produces new variants of chromosomes, thus promotes genetic diversity (Wild et al., 2019). The main role of HR in mitosis is the repair of DSBs and single-strand gaps, which can occur due to various damaging events, including DNA replication fork collapse (Kasparek and Humphrey, 2011; Hustedt et al., 2019). Other processes in which HR is involved include repairing DNA inter-strand cross-links (ICLs) and maintaining telomeres (Symington and Gautier, 2011; Crickard et al., 2020).

To repair DSBs HR starts by resecting the broken end, creating single-stranded DNA (ssDNA) overhangs with 3' OH ends. One of these overhangs invades the homologous sequence, becoming a primer to synthesis new DNA using the homologue of the template (Figure 1.4). The MRN complex in mammals (Rad32-Rad50-Nbs1 in fission yeast) acts as a nuclease, promoting resection of the ends of DNA and creating ssDNA. It also assists with the recognition of broken ends of DNA and homologous sequence alignment (Zhao et al., 2017). The Exo I nuclease is also presumed to contribute to the resection procedure in yeast (Szankasi and Smith, 1995; Zhao et al., 2019). The overhangs of the ssDNA are then coated by the single-stranded DNA binding protein RPA (Soniat et al., 2019). The BRCA2/PALB2 complex subsequently eliminates RPA from the ssDNA and loads the essential HR strand-exchange protein RAD51 (Grabarz et al., 2012). Rad51, family of proteins in eukaryotes, or the RecA family of proteins in prokaryotes, mediates the HR pathway by mediating the strand invasion of one DNA molecule into an unbroken homologous duplex, resulting in the formation of a D-loop structure. Rad51 binds to ssDNA ends of a processed DSBs in the presence of ATP (Ait Saada et al., 2018). Upon the hydrolysis of the ATP molecule, Rad51 forms a nucleofilament around the ssDNA. ATP binding thus triggers the binding of Rad51 between homologous DNA strands, strand invasion and strand exchange (Godin et al., 2016). In mammalian cells, Rad51 is only active during the S and G2 phase and occurs only once the nucleofilament is formed leading to the identification of a homologous strand and the invasion of the homologous duplex forming a three-stranded paranemic intermediate. DSBs repair can occur via the following mechanisms: the DSB repair (DSBR) mechanism, the single-strand annealing (SSA) mechanism and the synthesis-dependent strand annealing (SDSA) mechanism (Figure 1.5) (Sakofsky and Malkova, 2017).

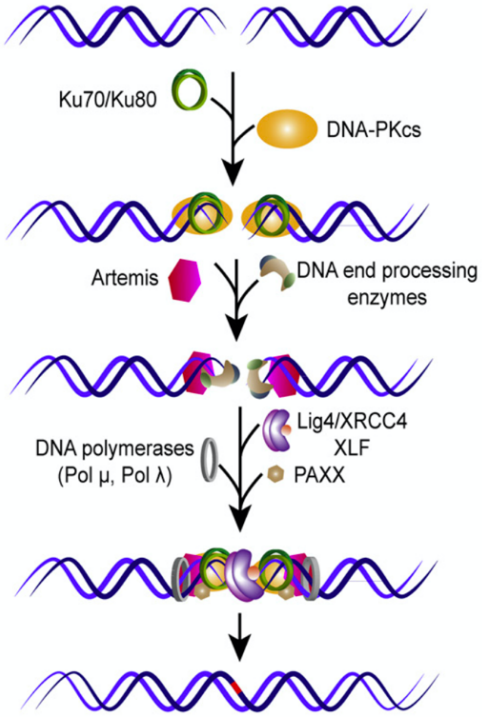


**Figure1.2. Core proteins part of the NHEJ repair pathway**

The Ku70/80 complex recognises DSBs and binds to the DNA ends. This complex recruits DNA-PKcs, which phosphorylates Artemis nuclease, thereby stimulating the actual repair process. Artemis readies the ends of DNA for ligation, which is performed by the LigIV/XRCC4/XLF complex, which rejoins the two ends of DNA (Iliakis et al., 2015).

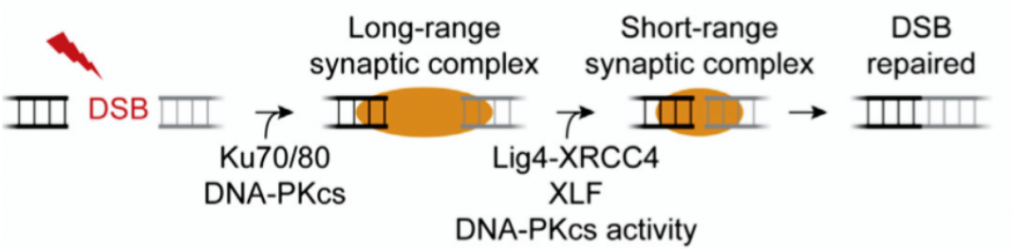


**Figure 1.3. Assembly of mismatched end structures**

Postulated model of two-stage DNA-end synapsis during NHEJ (Stinson et al., 2019).

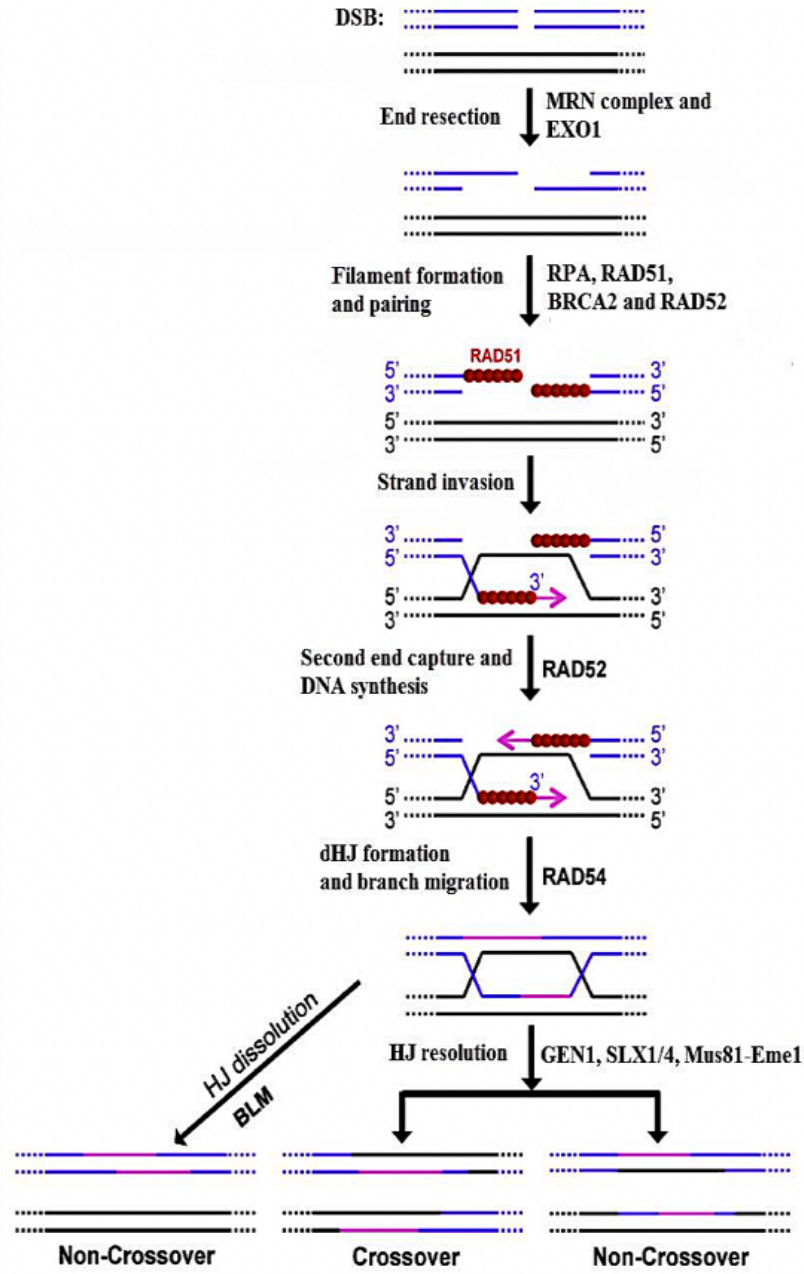


**Figure1. 4. Schematic layout of homologous recombination sequence (HR) repair of a double-strand break**

To begin DNA synthesis, copy and eventually restore genetic information disrupted by DSBs, HR follows a sequence of steps. DSBs are acted upon by MRN. Resection gives rise to ssDNA, which binds to RPA. Subsequently BRCA2 removes RPA then binds to RAD51. dHJs are formed under the influence of RAD52. Invading the homologous template is ssDNA forming a D-loop. The migration of the HJ branch is promoted by Rad54. Resolve proteins, such as GEN1, SLX1/4 Mus81-Eme1 are responsible for HJ resolution; crossover or non-crossover events can result. BLM dissolving HJ results in a non-crossover event case (modified from Suwaki et al., 2011).

### 1.4.2.i The Double Holliday junction repair mechanism

In the DSBR mechanisms, the breakage of the DNA strand results in the formation of a 3′single-stranded DNA overhang. The invasion of the strand at the 3′ overhangs into a homologous DNA sequence leads to the formation of a so-called D-loop, which permits the 3′ invading ends to serve as a primer for DNA synthesis. The second DSB end is then sequestered (second end capture), leading to the formation of two Holliday junctions (HJs) (Figure 1.4) (Wyatt and West, 2014). Following gap-repair DNA synthesis and the ligation of the newly formed strand, the DSB is resolved in a non-crossover or crossover manner (Figures 1.4 &1. 5). There exist three pathways that are required for HJ processing (Mawer and Leach, 2014; Zhou et al., 2019). The BLM helicase topoisomerase IIIα-RMI1/2 (BTR) complex promotes the dissolution of double HJ through the convergent migration of each HJ to form a catenated structure preceded by the topoisomerase-mediated processing of the resultant hemicatenane which leads to the generation of non-crossing DNA strands (Shah et al., 2017). The BTR mechanism is thought to be the predominant double HJ (dHJs) processing mechanism, but two other distinct pathways exist that can resolve both single and double HJs, which are mediated by HJ-specific resolvases (Bizard and Hickson, 2014 ). There are a number of nuclease activities in mammalian cells capable of acting as resolvases on HJs, which can also target other DNA structural intermediates, these are GEN1 and the SLX–MUS complex resolvases (SLX1-SLX4 or MUS81-EME1) (Sarbajna and West, 2014; Falquet and Rass, 2019). Resolvases consist of a DNA-binding domain that specifically interacts with the HJs. This leads to the formation of an HJ-resolvase complex and the insertion of symmetric nicks within the two strands. These resulting nicks can then be ligated by DNA ligases (Shah et al., 2017; Falquet and Rass, 2019).

### 1.4.2.ii The SDSA mechanism

In the SDSA mechanism, the invading strand associated with RAD51 anneals to its complimentary strand in the recipient duplex displacing the non-complimentary strand and creating a D-loop (Paliwal et al., 2013; Ensminger and Löbrich, 2020). The 3′ end of the invading strand again serves as a primer for new DNA replication, using the complimentary strand as a template. For SDSA, BLM and RAD54 proteins are known to disrupt the formation of the nascent D-loop prior to the maturation to a dHJ structure. The BLM-TOPOIIIα-RMI1/2 complex is capable of dissolving de-novo synthesized D-loops while RTEL-1 can reverse the formation of RAD51 generated D-loops (Fasching et al., 2015). The dissociated single-

stranded DNA end, which has been extended by DNA synthesis within the D-loop, re-anneals to the other end of the original DSB and the repair is completed with additional fill in DNA synthesis and DNA ligation (Figure 1.5). This repair mechanism occurs in a non-cross over manner (Fasching et al., 2015) .

#### 1.4.2.iii The SSA repair mechanism

The SSA repair mechanism occurs when the DSBs occurs in two strands of one duplex. Processing of ends or naturally occurring break overhangs can form single-stranded regions located adjacent to the breaks. If these regions contain homologous repeated sequences this permits complementary strands to anneal to each other forming synapsed intermediates (Ramakrishnan et al., 2018). These intermediates then undergo ligation which is mediated by the endonucleolytic cleavage of the non-homologous 3′ ends of the ssDNA tails with DNA polymerase catalyzing the addition of oligonucleotide to gaps in the DNA (Figure 1.5; Onaka et al., 2020). One of the key factors that mediate the resection of DNA in the SSA repair mechanism is the CtIP factor while the excision of the non-homologous regions of the ssDNA overhangs is carried out by RAD52 and ERCC1. RAD52 plays a role in the annealing of ssDNA while ERCC1 carries out its function by forming a complex with the XPF protein which then carries out the cleavage of the ssDNA tails at their respective 3′ ends (Bhargava et al., 2016). SSA that is conducted between inverted DNA strands causes the synthesis of inverted chromosome dimers or folded hairpin-like structures (Figure 1.5).

#### 1.4.2. iv Break-induced replication (BIR)

BIR can be described as a repair pathway that occurs at a single ended DNA duplex break. The single ended DNA break invasion leads to the formation of a RAD51-mediated D-loop (Sakofsky and Malkova, 2017). The invaded 3′ end then serves as a template for DNA synthesis, which causes the migration of the D-loop, which is then continually extended by *de novo* DNA synthesis (Figure 1.5). The repair mechanism is effectuated by the leading strand being utilized as a template for the lagging strand leading to the synthesis of a newly conserved DNA molecule (Figure 5) (Elango et al., 2017). BIR DNA synthesis is catalyzed by the DNA polymerases Polε, Polδ and Polα. Polα is located at the 3′ end, where invasion of the strand occurred and mediates the initiation and synthesis of the lagging and leading strand. Polδ has been suggested to promote the displacement of the DNA strand during the migration of the D-loop complex while Polε might be required for efficient DNA synthesis following the

dissolution of the D-loop complex (Donnianni et al., 2019). BIR has been demonstrated to provide a higher risk of genetic instability due to elevated levels of chromosomal rearrangement/translocations, particularly as BIR can occur between repeat regions in non-homologous chromosomes. Additionally, two factors have been postulated to mediate the formation of frameshift mutations during the BIR repair mechanism: the recurrent dissociation of Polδ from the D-loop during DNA synthesis and a decrease in its efficiency during DNA synthesis for resolving errors during the BIR mechanism (Kramara et al., 2018).

### 1.4.2.1. Homologous recombination and stalled replication forks

A one-sided DSB can arise as a result of the DNA replication fork complex encountering a single-strand break (SSB) in the duplex or a block to replication progression causing stalling and regression of the fork to form a structure that can be processed by nuclease cleavage (Prado, 2018).

DNA replication requires a DNA helicase to separate the inter-strand hydrogen bounds and produces a Y-shape, using energy from ATP hydrolysis. Replication protein A (RPA) is a heterotrimeric complex, which stabilizes the unpaired ssDNA, preventing it from forming intra-strand secondary structures and permitting it to retain replicative template capabilities (Wong et al., 2020) The two ssDNA strands (leading and lagging strands) act as the templates for the replicative polymerases for synthesizing the new daughter strands. As DNA replication occurs, the leading strand goes through continuous, undisrupted strand elongation. As DNA can only be synthesised in a single direction (5' to 3') by DNA polymerases, loops are created on the lagging strand templates. In turn, the lagging strands are replicated in a discontinuous fashion, and numerous short RNA primers initiate synthesis of short stretches of DNA known as Okazaki fragments (Figure 1.6). Once Okazaki fragments come together, the RNA primers are exonucleolytically removed, and subsequently replaced with appropriate deoxyribonucleotides. In turn, these freshly created strands are checked for errors and mis-incorporated bases. Lastly, the Okazaki fragments are connected by DNA ligase enzyme, which then creates two continuous double strands (Lujan et al., 2016; Burgers & Kunkel, 2017; Lewis et al., 2020: Moreno and Gambus, 2020). There are a number of DNA polymerases in eukaryotes, but there are thought to be three core DNA polymerases associated with the majority of DNA replication. DNA polymerase α initiates DNA synthesis on RNA primers for both leading and lagging strands. Once a mature fork is established DNA polymerase α only

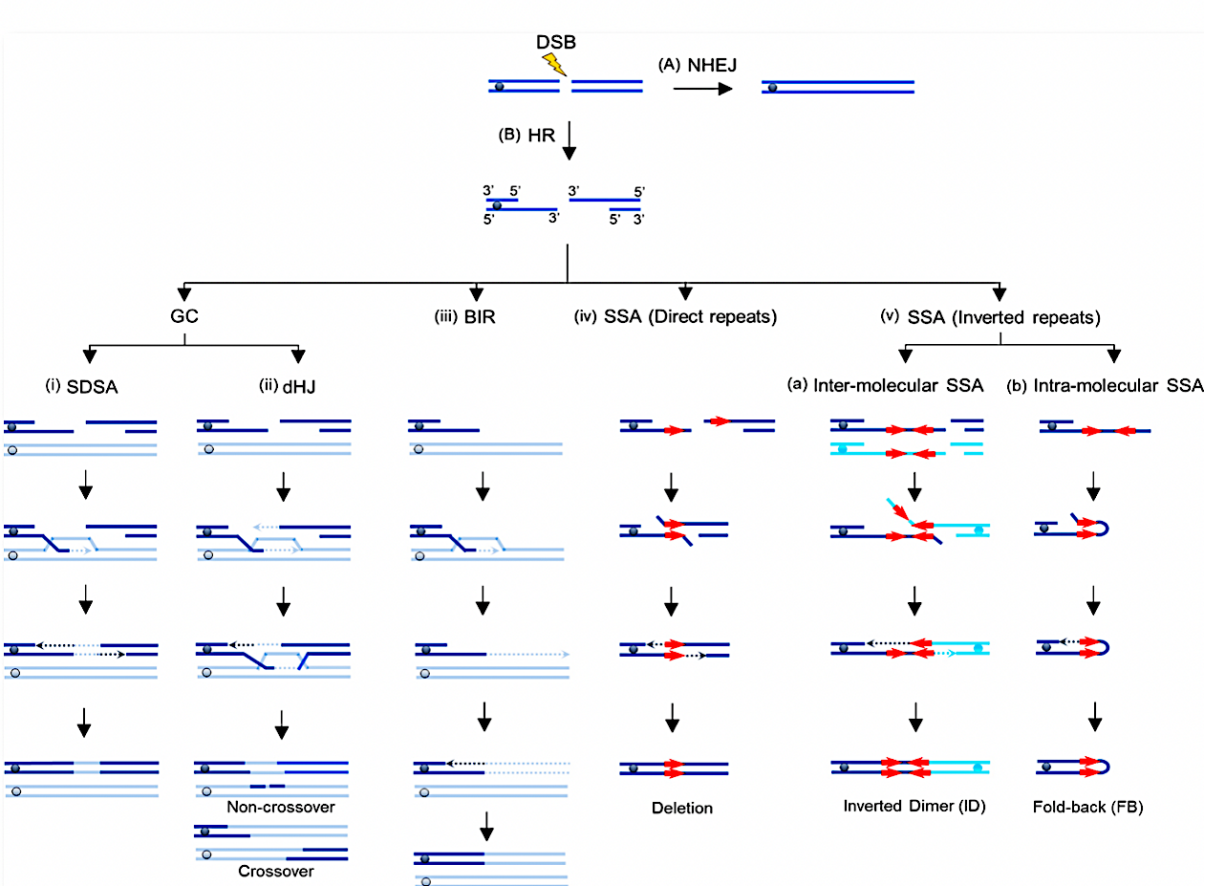


**Figure1.5. The DSB repair pathways.**

During the HR, DSBs can be resolved in the following manner: Homologous recombination wherein the DSBs undergo a resection in the 5′-3′ direction and repair is effectuated by (i) the SDSA pathway whereby the 3′ end invades the homologous DNA template leading to the formation of a displacement loop (D-loop) with the 3′end of the invading strand being used as a template for DNA synthesis. A second round of DNA synthesis is then initiated by the second end of the resected DNA strand leading to the synthesis of non-crossing over products. (ii) the double Holliday Junction (dHJ) pathway mediates DSB repair through the use of a short DNA strand involving the stabilization of the D-loop via the sequestration of the second end of the DSB. DNA synthesis occurs with the resolution/dissolution of the dHJ leading to the formation of non-crossover and cross-over products. (iii) BIR occurs only in the presence of one available DSB end for DNA repair and synthesis. This single DSB end causes the invasion of the DNA strand leading to the start of DNA synthesis that occurs via a migrating bubble proceeded by the asynchronous synthesis of both a leading and lagging strands that act as a template for the synthesis of a fairly conserved new DNA molecule. (iv) SSA occurs in ssDNA that are oriented in the same direction. Resection occurs in the 5′-3′ direction with the exposure of flanking homologous sequences resulting in the annealing of each strand. The non-homologous strands on the other hand are resected at the 3′ end and serve as primers during DNA synthesis and ligation. (va) SSA in inverted DNA repeats can occur between two sister chromatids (inter molecularly) with the resection of the 5′-3′ strand causing the exposure of inverted repeats (IRs) as ssDNA. The annealing of IRs then occurs on two different DNA strands. The removal of non-homologous 3′ end is followed by DNA synthesis that causes the formation of inverted dimers. (vb) intra-molecular SSA occurs when the 5′-3′ resection of the DNA leads to the formation of a ssDNA IRs with SSA occurring between the IRs intra-molecularly. The removal of non-homologous 3′ends and the subsequent DNA synthesis and ligation causes the formation of hairpin-like structures (Ramakrishnan et al., 2018).

serves as a primer polymerase for the individual Okazaki fragments, working with primase to initiate new fragment synthesis. The main DNA polymerase for Okazaki fragment extension is thought to be DNA polymerase δ. For continuous extension of the leading strand, both DNA polymerase δ and DNA polymerase ε have been shown to function in this capacity (Jain et al., 2018).

Other than the described core polymerases, a number of additional important protein complexes, for example the replication factor C clamp loader (RFC), the fork protection complex (FPC) and the proliferating cell nuclear antigen (PCNA) take part in the process. Specifically, they play a role in initiation and replication fork progression used to create collective, known as the replisome. In addition, checkpoint proteins are necessary, which are linked with the replisome to signal to the cell division regulation pathways when DNA replication has been perturbed, thus delaying the onset of cell division until the errors are corrected. Thus the replisome is a major regulator of DNA replication and genome stability (Leman & Noguchi, 2013; Hizume and Araki, 2019 ).

The DNA replication fork progression can be impacted by DNA lesions which stem from different exogenous and endogenous sources (Berti & Vindigni, 2016). Other than unscheduled DNA lesions, replication fork progression can be inhibited by obstacles generated during normal DNA metabolism, such as transcriptions, which can act as a replication fork barrier (RFBs), particularly when the cell is under replicative stress conditions (Gadaleta & Noguchi, 2017; Hizume and Araki, 2019). This in turn can increase the need for HR repair and fork re-establishment. If these processes are perturbed, then this results in greater genome instability (Gadaleta & Noguchi, 2017). Conflicts between replication and transcription machinery are an example of a natural impediment with the potential to impact the DNA replication fork and bring about genomic instability (Castel et al., 2014 ; García-Muse and Aguilera, 2016; Gómez-González and Aguilera, 2019).

Certain drugs can cause a stress on DNA replication fork progression; for example, the ribonucleotide reductase inhibitor hydroxyurea (HU), which blocks DNA synthesis through restricting dNTP synthesis **(**deoxyribonucleotide triphosphate), while the replicative helicase continues unwinding the parental DNA duplex. In turn, the replication forks could collapse as a result and DSBs can form (Petermann et al., 2010; Wong et al., 2020). Drugs such as HU are

frequently used in experimental systems to explore the functional requirements for progression and replicative stress recovery.

It has been shown that S-phase progression in cells which go through oncogene-inducing replication stress need combined functions for stalled replication forks to re-establish and a proposed model of these functions is shown in Figure 1.7 (Liao et al., 2018).

### 1.4.2.2. The role of RNA and RNA polymerase II in DSB repair

Several studies have recently demonstrated the importance of enzymes that interact with the RNA in DNA repair mechanisms (Hawley et al., 2017). The mRNA splicing and transcriptional regulatory machinery appear to be important in DNA repair pathways (Bader et al., 2020). Proteins of DNA repair pathways have been observed to contain RNA-binding motifs thus demonstrating their interaction with RNA-processing enzymes which might occur during the DNA repair process (Domingo-Prim et al., 2020a). RNA endoribonucleases such as Drosha and Dicer might be important in the DNA repair process wherein their depletion caused an impaired mobilization of DNA factors that mediate the repair pathway at the DSB sites with a reduction in both HR and NHEJ repair activity (Francia et al., 2016; Lu et al., 2018). Additionally, NONO and THRAP3, which are RNA-splicing factors, as well as RNA helicases DDX1 and DDX5 are implicated in DNA damage repair (Dutertre et al., 2014; Meng et al., 2020). Studies on the function of RNA-interacting enzymes in DNA repair is still in its infancy. However, studies on so called R-loops have gained acceptance (Hegazy et al., 2020). R-loops are defined as three-stranded nucleic-acid structures which form once a nascent RNA transcript hybridizes with the template DNA strand of a DNA duplex, and the non-template strand remains unpaired (Santos-Pereira and Aguilera, 2015:Belotserkovskii et al., 2018 , Stolz et al., 2019). R-loops are form in many eukaryotic genome regions, including regions transcribed by RNA polymerases I, II, and III (El Hage et al., 2010, Tran et al., 2017, Crossley et al., 2019). In RNA polymerase II (RNAPII)-transcribed genes, research into genome-wide mapping show that R-loops exist normally in high quantities at promotors (Chen et al., 2017, Dumelie and Jaffrey, 2017, Ginno et al., 2012, Nadel et al., 2015, Sanz et al., 2016, Crossley et al., 2019). Several resolution mechanisms take part in the modulation of R-loop presence in cells. Degradation of the RNA within the RNA: DNA hybrid is largely brought on by two enzymes conserved from bacteria to humans, RNase H1 and H2. Specialized RNA:DNA helicases can

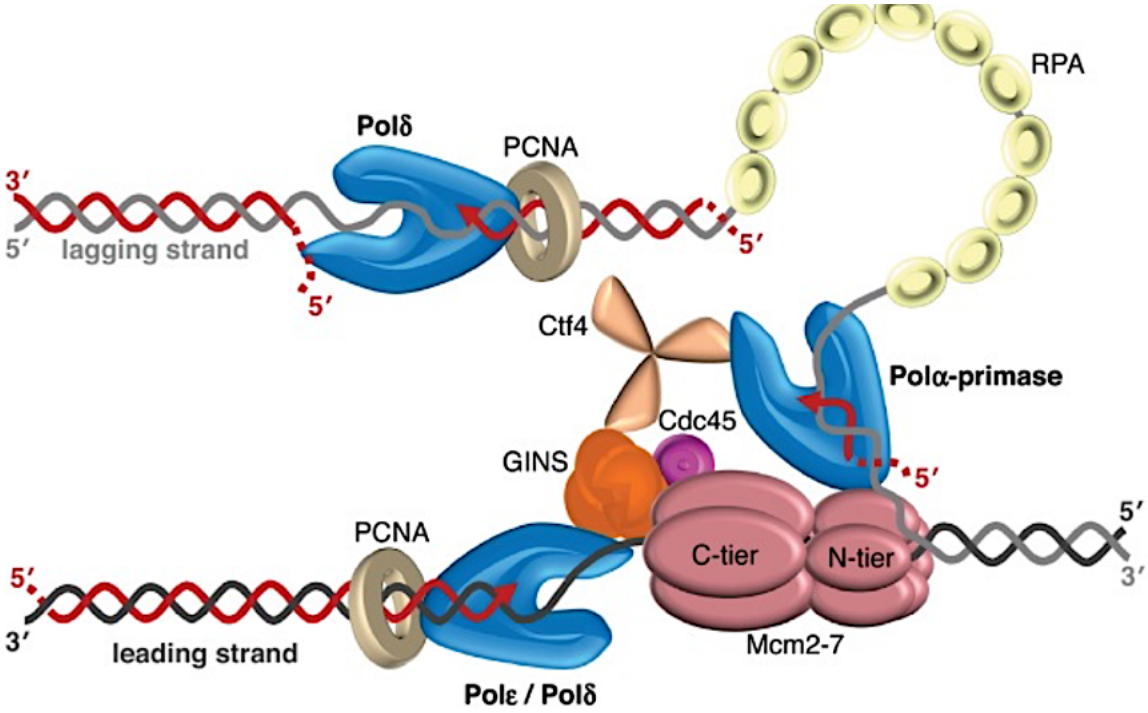


**Figure 1.6. Representation of a core eukaryote replication fork.**

An active Mcm2–7 heterohexamer is located around the leading strand and unwinds the parent duplex via ATP hydrolysis. Polα-primase is distinguished by priming the leading and lagging strands, anchored by Ctf4 to the CMG complex which is (Cdc45-GINS- MCM). Also, Polδ extends the primers on the lagging strand, while Polε is recruited to the leading strand through interactions with the CMG complex. It has been shown that both Polδ and/or Polε can act as the leading strand polymerase. Furthermore, accessory factors (e.g., RPA and PCNA) are also shown (Jain et al., 2018).

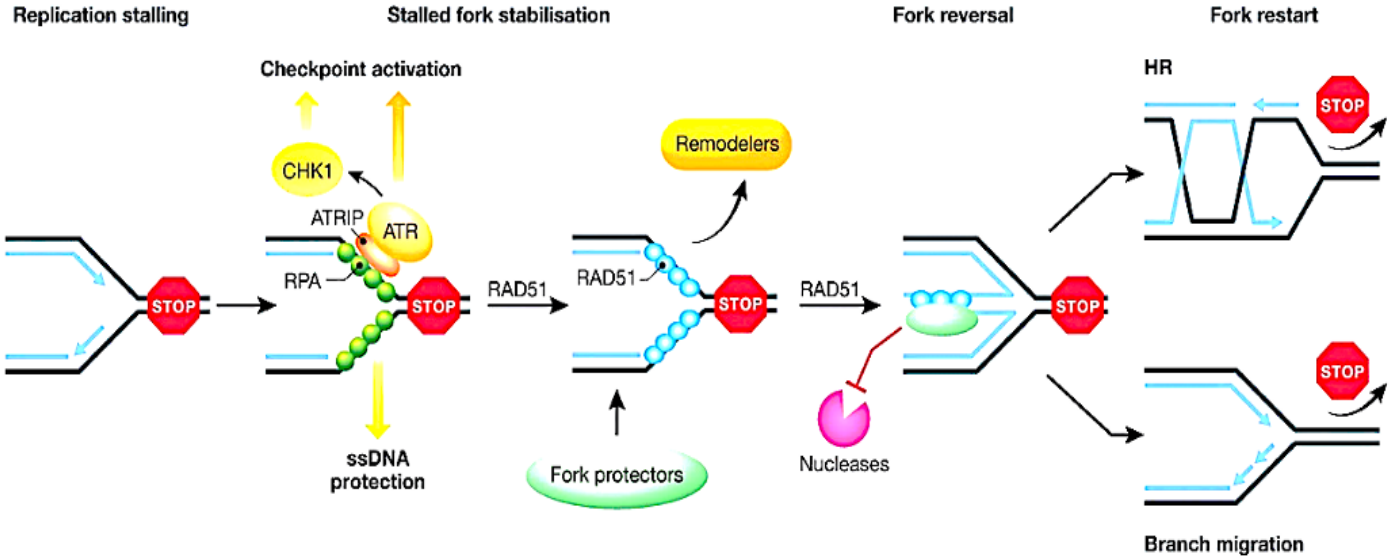


**Figure 1.7. Model for the rescue of stalled replication forks**

Once fork stalling has occurred, ssDNA produced through polymerase–helicase uncoupling is coated by RPA in order to inhibit secondary structure formation. The ssDNA–RPA complex triggers replication checkpoint activation through the ATR and CHK1 kinases. This process will control a large variety of cellular events which support fork recovery. In turn, RAD51 replaces RPA and guides replication fork reversal to enable fork repair. A number of other replication fork remodels are involved in this function (e.g., SMARCAL1). A number of fork protectors are in place to shield these reversed forks from deleterious fork degradation, which have the ability to destabilize stalled forks. Lastly, once replication stress is mitigated, stalled replication forks are able to be started once more in an HR-dependent fashion (top right), or with branch migration (bottom right) (Liao et al., 2018).

responsible for the unwinding the RNA from the hybrid (see below) (Belotserkovskii et al., 2018).

## 1.5. RNA:DNA hybrids

Formation of RNA:DNA hybrids takes place when the annealing of nascent RNA transcripts to their template DNA strand occurs; in the context of a DNA duplex (as opposed to a transcript from a ssDNA) a so called R-loop can be formed (although the term R-loop is now applied more widely to any RNA:DNA hybrid, irrespective of whether the RNA is annealed to ssDNA or dsDNA). It is, to some degree, assumed that R-loops are a naturally occurring phenomena in transcription and replication (Fragkos & Naim, 2017; Wahba et al., 2013; Felipe-Abrio et al., 2015; García-Rubio et al., 2018; Jimeno et al., 2019). Modern studies have connected RNA: DNA hybrids to cellular processes at the molecular level. RNA:DNA hybrids participate in a wide range of processes and they can play diverse roles in different systems, or within the same system under differing circumstances. An example of this is where RNA:DNA hybrids are shown to both cause DSBs or stimulate their repair (Crossley et al., 2019; Yasuhara et al., 2018). The formation of RNA:DNA hybrids have been observed to cause DNA damage leading to genome instability in both prokaryote and eukaryote cells (Rondón & Aguilera, 2019; Jimeno et al., 2019). RNA:DNA hybrids have been observed to cause the stalling of DNA replication forks, and halting transcription elongation, a consequence potentially being the formation of DSBs (Gómez-González and Aguilera, 2019). Additionally, increased hybrid formation at transcription and replication conflict sites display a high propensity towards recombination initiation, thus demonstrating the tumorigenic potential of these structures (Brambati et al., 2015; Castel et al., 2014; Lin & Pasero, 2012; Rondón and Aguilera, 2019).

Because of the creation of an R-loop, a section of ssDNA on the non-template strand becomes exposed. Due to the inherent vulnerability of ssDNA, exposed segments are implicated in DNA breaks and mutagenesis. For example, DNA deaminases, such as mammalian AID, which convert cytidine to uracil, can target the exposed ssDNA in the R-loop. This can give rise to a notch in the DNA in case uracil is processed by the base excision repair machinery (BER). Mismatch repair proteins may process the nicked DNA, forming a DNA DSB. A known example of when this process occurs is when immunoglobulin undergoes class switch

recombination (CSR) (Muramatsu et al., 2000; Yu et al., 2003; Gómez-González and Aguilera, 2007).

As revealed by other studies, the activation of ATM is promoted by R-loops. There are several endonucleases, including FEN1, XPF and XPG that are capable of cleaving R-loop-associated ssDNA. These cleavages result in DSBs or single-strand breaks (SSBs). Furthermore, ssDNA can develop bulky and weak secondary structures, such as G-quadruplexes and hairpins. These structures obstruct DNA replication and are vulnerable to breaking (Hamperl et al., 2017; Dutta et al., 2011; Marabitti et al., 2019; Rinaldi et al., 2021).

A number of experimental approaches have been used in order to investigate the presence and levles of RNA:DNA hybrids at sites of DNA damage (Lu et al., 2018; Domingo-Prim et al., 2019; Cohen et al., 2018). After DSB induction, it was has been shown that damage-induced long non-coding RNAs (dilncRNAs) are transcribed by RNAPII at both sides of the DSB, in a bi-directional manner (Storici and Tichon, 2017). With S-phase and G2, at the point where CtIP is phosphorylated and DNA end resection receives preference, dilncRNAs can base-pair to assist end resectioning generating RNA:DNA hybrids on ssDNA tracts (Domingo-Prim et al., 2019; D'Alessandro et al., 2018). In the case of fission yeast, RNA:DNA hybrids are proven to control DNA end resection and recruitment of the ssDNA-binding protein RPA (Figure 1.8) (Ohle et al., 2016). It is further suggested that they also have vital functions in mammalian cells, specifically with the promotion of HR through the direct recruitment of BRCA1, a protein which controls HR by binding RAD51 and boosting its recombinase activity (Zhao et al., 2017; D'Alessandro et al., 2018). However, even though there are clearly positive impacts resulting from RNA:DNA hybrids when it comes to HR repair, RNA: DNA hybrids at DSB must be resolved to permit completion of repair (Domingo-Prim et al., 2019; Cohen et al., 2018). Higher levels of dilncRNAs, as well as greater RNA:DNA hybrid levels, are seen at DSBs in line with the depletion of the exosome subunit EXOSC10 in human cells, which inhibits the recruitment of RPA at the damaged sites and restricts HR repair (Domingo-Prim et al., 2020b). RNA:DNA hybrid development assists in the construction of HR machinery, while their stabilization should be blocked in order to achieve RPA recruitment thereafter. Establishment and resolution of RNA:DNA hybrids is under strict control and is a central component of some DSB repair mechanisms (Domingo-Prim et al., 2020b). The mechanism(s) which cause RNA:DNA hybrids to stimulate DSB resection and DSB repair choice are not yet fully understood (Jimeno et al., 2019, Marini et al., 2019).

The existence of R-loop in cells is modulated by multiple resolution mechanisms. RNA:DNA hybrid degradation is achieved by two human conserved enzymes RNase H1 and H2. RNase H1 constitutes an N-terminal domain that binds to the RNA:DNA hybrid and a C-terminal domain that possesses endonuclease properties (Lockhart et al., 2019). RNase H2 on the other hand is constituted of three distinct protein sub-units; one catalytic subunit (RNH201) and two accessory subunits (RNH202 and RNH203) (Tsukiashi et al., 2019). These sub-units consists of 301, 308 and 166 amino acids respectively and, unlike RNAse H1, are also involved in the removal of rNTPS that have been mis-incorporated into newly synthesized DNA (Kojima et al., 2018). Moreover, RNA:DNA hybirds can be unwound by specific RNA:DNA helicases such as senataxin (Cohen et al., 2018).

## 1.6. Translin and Trax

Human Translin was originally discovered in a screen for proteins that bind to the breakpoint junctions of chromosomal translocations in human lymphoid tumours (Aoki et al., 1995). Translin was found to bind strongly to single-stranded DNA and consensus sequence motifs of 5'-GCCC(A/T)(G/C)(G/C)(A/T)-3' and 5'-ATGCAG-3' were identified from chromosome translocation breakpoint junctions from a range of malignancies (Aoki, et al., 1995, Kasai, et al., 1997). The binding of Translin to the breakpoint junction of chromosome has been shown in patients with the Philadelphia chromosome in chronic myeloid leukaemia (CML) translocation t(9;22) (q34;q11) (Martinelli et al., 2000) and another patient with acute myeloid leukaemia (AML) with the t(9;11)(p22;q23) translocation (Atlas, et al., 1998; Martinelli, et al., 2000). Due to the identification of Translin binding sequences at the reciprocal translocation breakpoints between CHOP on chromosome 12 (long arm) and fused in sarcoma (FUS) on chromosome 16 (short arm), Translin is also considered to be implicated in liposarcoma development (Hosaka, et al., 2000; Kanoe, et al., 1999). Since these early studies numerous other tumour-associated chromosomal translocation breakpoints have been recognised as being Translin DNA binding sites. Also of note is the fact that hotspots of human male meiotic recombination also feature Translin binding sites, possibly suggestive of a natural role in meiotic recombination (Badge et al., 2000; Abeysinghe, et al, 2003). The chromosomal translocation breakpoints-associated Translin-binding sites led to the proposition that Translin has a role to play in recombination regulation (Parizotto et al., 2013; McFarlane & Jaendling,

2010). However, to date the mechanism for this putative role has not been elucidated and has since been questioned, following the discovery that Translin-null mutants in a range of eukaryotes, including *Drosophila,* mice, and *S. pombe* do not exhibit recombination-associated errors or problems, including meiotic recombination, NHEJ or DNA damage repair (Claussen, et al., 2006; Yang, S. & Hecht, 2004; Jaendling, et al., 2008).

'Translin', whose name derives from 'translocation', is a protein of approximately 26 kDa (Jaendling & McFarlane, 2010). In humans, the protein is composed of 228 amino acids (Lluis, et al., 2010; Jaendling & McFarlane, 2010). The Translin gene in mice encodes the testis–brain RNA-binding protein (TB-RBP) (Wu, et al., 1997), and the murine protein is implicated in regulating mRNA in neurons and spermatogenesis (Li et al., 2008; Jaendling & McFarlane, 2010). The role of Translin in neurons may account for the abnormal behaviour observed in Translin-deficient *Drosophila* and mice (Stein, et al., 2006; Suseendranathan, et al., 2007).

Using a yeast two-hybrid screen in which Translin was used as 'bait', the protein, Translin-associated factor X (TRAX), was identified, which is approximately 33 kDa. Trax and Translin encoding genes are paralogous (Aoki, Ishida, & Kasai, 1997 ), demonstrating an association between Trax and Translin proteins. The stability of Trax is determined by the presence and stability of Translin, a functional feature conserved in many organisms emphasising an intimate functional relationship between these proteins (Yang & Hecht, 2004; Jaendling, et al, 2008).

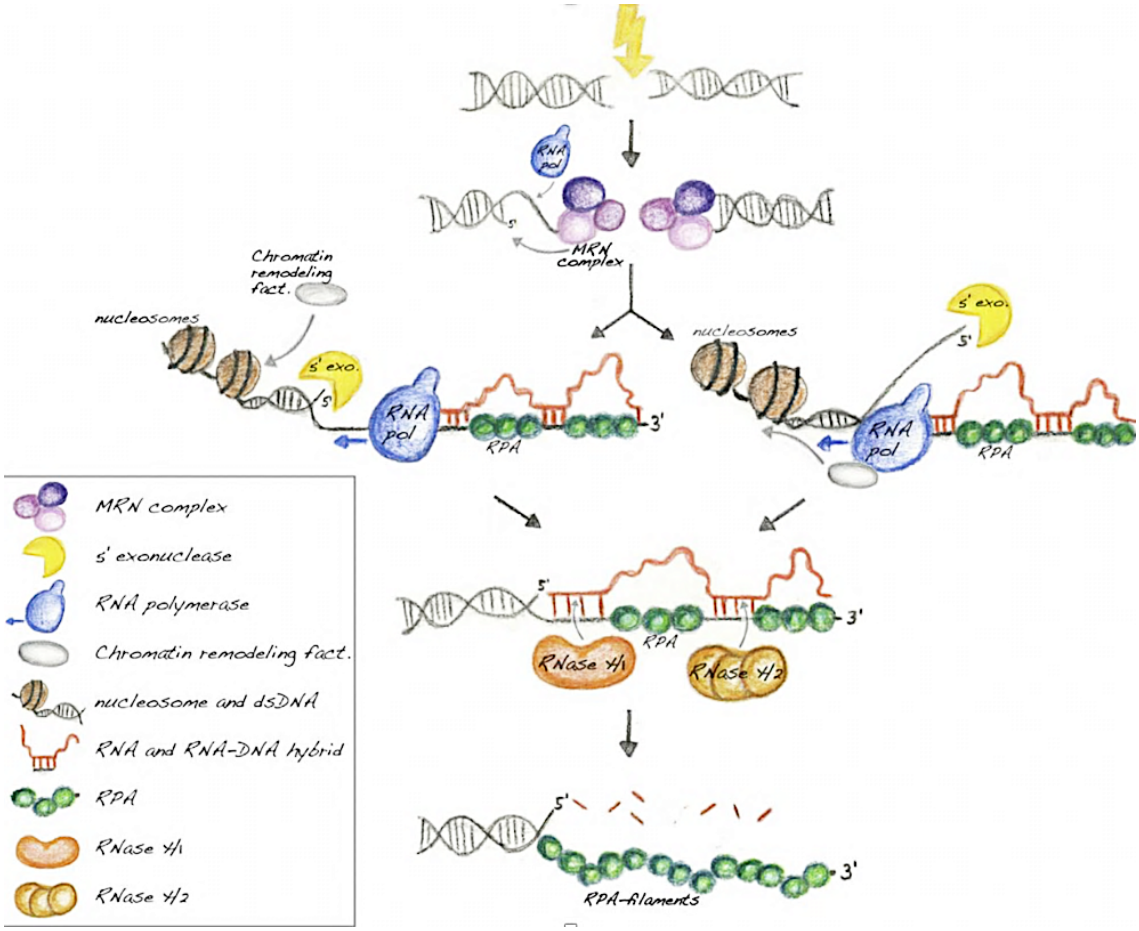


**Figure 1.8. Proposed role for RNA:DNA hybrids in the HR-mediated repair of DSBs**

The formation of DSBs cause the MRN complex to be recruited to the break, where, together with it, exonuclease, Exo1, and other factors resect the DSB ends in a 5'→3' manner. This creates overhangs of ssDNA with free 3' OH ends. Transcription is initiated by the recruitment of RNA Pol II is to the ssDNA overhangs. RNA:DNA hybrids form as the newly synthesised RNA transcripts are annealed to their template ssDNA. The hybrids may terminate RNA Pol II transcription, thereby regulating the end resection process; it also recruits the ssDNA-binding RPA complex to the resected DNA strand. RNase H enzymes (RNase H1 and RNase H2) then degrade the RNA:DNA intermediates, enabling RPA to be loaded onto the ssDNA overhangs. This facilitates the repair of DSBs to be completed efficiently (modified from Ohle et al., 2016).

Orthologues of both Translin and Trax are ubiquitous in eukaryotes, although there is some notable exception, such as the budding yeast, *Saccharomyces cerevisiae* (Chennathukuzhi, et al., 2003; Claussen, et al., 2006; Jaendling, et al., 2008; Jaendling & McFarlane, 2010). A single orthologue is also found in *Archaea*, indicating a primitive ancestry (Parizotto et al., 2013).

### 1.6.1. Biochemical Characteristics of Translin and Trax

The level of evolutionary conservation between the amino acid sequence of mouse and human Translin is very high, varying by just three amino acids out of 228 amino acids. Translin in humans and fission yeast are 37.9% identical and 66.7% similar, the protein in fission yeast is made up of 220 amino acids. However, overall Translin and Trax show considerable sequence homology between diverse eukaryotic species including fission yeast, human, *Drosophila* and other mammals (Laufman, et al.,2005: Zhang et al., 2016).

Translin protein can form a homo-octameric ring structure, as demonstrated by multiple microscopic and biochemical studies (Kasai et al., 1997; Jaendling & McFarlane, 2010; Gupta et al., 2019a). This structure is similar to proteins that are associated with DNA recombination, replication and repair, further suggestive of a role in these recombination control. Translin binds ssDNA, dsRNA and ssRNA (Kasai, et al, 1997; Eliahoo, et al, 2014; Jaendling & McFarlane, 2010). Tranlsin and Trax can also form a hetero-octamer of 2 units of Trax and 6 units of Translin in a barrel like structure, which is also known as C3PO (Sahu et al., 2014; Zhang et al., 2016: Mo et al., 2018). The hetero-octamer produced by a combination of Translin and Trax possesses Trax-dependent RNase activity. Compared to the Translin homo-octamer, the hetero-octameric complex has an enhanced ssDNA binding capacity, with a partially decreased association with ssRNA, while the Translin homo-octamer has a greater affinity for ssRNA (Jaendling & McFarlane, 2010; Fu et al., 2016). More recently, specific amino acids within the human Translin protein structure have been identified (Y85, R86, H88, R92 and K193) which provide a substantial portion of the RNA binding affinity (Gupta et al., 2019b). In murine studies, Trax has been observed to modulate the binding behaviour of Translin, preventing it from binding to RNA and promoting its binding to ssDNA sequences (Chennathukuzhi, et al., 2003; Jaendling & McFarlane, 2010; Cho et al., 2004).

Large bodies of research indicate a regulatory function for Trax and Translin in spermatogenesis and neuronal interactions. In the case of the mouse model, Translin is

associated with unique RNA sequences of target mRNAs at the end of the 3′ UTRs (untranslated regions), suggesting a role for Translin in RNA transportation and stabilisation in both the brain and testes (Han et al., 1995). Furthermore, some have suggested a putative Translin role in posttranscriptional gene expression regulation in male germ cells, given that Translin binds and stabilises a germ cell-associated miRNA (Yu & Hecht, 2008). A possible role for the Translin/Trax complex is indicated in the function and development of the CNS, demonstrated in neuronal mammalian cells where the complex facilitates targeting of neuronal dendrites with brain-derived neurotrophic factor (BDNF) mRNA, Disruption of the Translin/Trax complex binding sequence in *BDNF* mRNA is connected with neural human behavioural conditions, and this evidence supports the putative CNS role for the complex ( Chiaruttini et al., 2009; Jaendling & McFarlane, 2010 ).

Translin and Trax have been suggested to have a role in the management of mitotic cell proliferation in mammalian cells (Yang & Hecht, 2004) as evidenced by a correlation between Translin levels and cell proliferation rate when comparing basal levels of protein expression with expressed levels during mitotic division. In addition, Kasai et al., (2018) described the association between the human Translin gene (*TSN)* overexpression and increased cell proliferation. The same authors identified variation in expressed levels of *TSN* throughout the cell cycle, with expression starting in the S phase and peaking in the G2/M phase, again supporting the proposal that Translin has a function in DNA replication and enhanced cell division mechanism (Kasai et al., 2018). Confocal microscopy appeared to demonstrate a role for Translin in hastening the microtubular organisation and segregation of the chromosome during mitosis (Ishida et al., 2002).

Contemporary research has identified a putative role for Translin/Trax in memory formation. Specifically, enduring forms of synaptic plasticity and memory are depended on *de novo* protein synthesis; however, the association between learning and implementation of this process still needs to be elucidated. The Translin/Trax complex may promote learning-induced memory via suppression of microRNA-mediated translational silencing at activation of synapses (Park et al., 2017, 2020).

### 1.6.2. Translin and Trax contribute to DNA repair

Translin and Trax are postulated to contribute to DNA repair processes. Evidence for this comes from various studies, including experiments in which etoposide or mitomycin C was

administered to HeLa cells, which resulted in the relocation of Translin from the cytoplasm to the nucleus (Wang et al., 2016; Gupta et al., 2019a). The absence of a nuclear localisation signal (NLS) in Translin needed for targeting the nucleus, gives rise to the hypothesis that Translin nuclear transport is reliant upon its interactions with different kinds of proteins, such as Trax, that do bear this signal (Laufman et al., 2005). Furthermore, following X-ray exposure, mice that lacked Translin demonstrated impaired hematopoietic stem cell recovery; this may indicate that Translin has function in cell repairing cells following damage to DNA in a cell type and/or tissue-specific fashion (Jaendling & McFarlane, 2010). Despite these findings, efforts to determine the role Translin plays in DNA repair of mouse embryotic fibroblasts (MEFs) have failed to identify differences between the quantity of breaks and gaps in DNA, or cell maintenance present in TB-RBP-null fibroblasts and unexposed cell lines (Yang et al., 2004). Furthermore, exposing *S. pombe tfx1* and *tsn1* null mutants to other chemicals that damage DNA did not reveal any deficiencies in DNA damage recovery (Jaendling et al., 2008).

Evidence from various studies reveals that in response to DNA damage, both Trax and Translin can bind with other proteins. To illustrate the point, in a bait and prey yeast-two hybrid system, mouse Translin bound to the GADD34 protein, which inhibits apoptosis (GADD34 is induced by damage to DNA and growth arrest) (Hasegawa & Isobe, 1999; Gupta et al., 2019 a). GADD34 is known to be a translation initiator (Patterson et al., 2006). Based on this, it is postulated that the role of Translin, together with GADD34, may not be to repair DNA damage directly, rather it may be involved in RNA processing/binding activity (Gupta et al., 2019). However, in response to cell damage, it is thought that GADD34 transports Translin from the cytoplasm to the nucleus (Hasegawa et al., 2000).

In cells that have been exposed to γ radiation, C1D protein binds with Trax, which is an activator of DNA-dependent protein kinase (DNA-PK); where C1D is implicated in both the HR and NHEJ pathways that repair DNA (Yavuzer et al., 1998; Jackson et al., 2016; Chern et al., 2019). In mammalian cells, Trax appears to contribution to DNA damage repair as murine studies suggest Trax contributes to DSB repair by participating in the ATM-mediated pathway, assisting the stabilisation of the MRN complex (Wang et al., 2016; Chien et al., 2018; McFarlane & Wakeman, 2020). That Trax plays significant role in repair DNA is evidenced by ATM being rendered ineffective by dysfunctional Trax (Wang et al., 2016; Chien et al., 2018; McFarlane & Wakeman, 2020). However, thus far, it is not clear what, if any, functional capacity Translin plays in DNA damage repair, and the role of Trax in regulating ATM appears

to be independent of Translin. The question of whether Trax and Translin exhibit any functional role in recombinant and DNA repair activities that can account for their initially proposed role in translocation formation has yet to be determined (Jaendling & McFarlane, 2010; McFarlane & Wakeman, 2020).

### 1.6.3. Contribution of Translin and Trax in RNA interference (RNAi)

Gene expression in diverse eukaryotic organisms is regulated by RNAi transcription and/or post-transcriptional level (Kalantari et al., 2016; Ranjan et al., 2019). RNAi processes uses non-coding small RNA molecules, which are about twenty to thirty nucleotides in length; it regulates gene activity by modulating and preventing translation of transcripts or targeting them for degradation (Holoch & Moazed, 2015; Meng & Lu, 2017). There are two pathways by which RNAi exert an effect: 1) post-transcriptional gene silencing (PTGS), that prevents cytoplasmic mRNAs from being translated; 2) chromatin-dependent gene silencing (CDGS), that promotes the formation of heterochromatin, thereby suppressing the transcription of specific genes (Creamer & Partridge, 2011). There are also a number of small RNAs known as regulatory RNAs, which have key roles in the RNAi pathway (Ranjan et al., 2019). These include microRNAs (miRNAs), the small interfering RNAs (siRNAs) that stimulate transcriptional degradation and PIWI-interacting RNAs (piRNAs), the latter being involved in regulating transposon transcription in animal germline cells (Holoch & Moazed, 2015; Schuster et al., 2019; Gutbrod and Martienssen, 2020) miRNAs and siRNAs are the primary mediators of the RNAi pathway and they are both implicated in PTGS and CDGS. In contrast, piRNAs are charged with inhibiting ‘parasitic’ DNA.

Double-stranded long RNA molecules (dsRNA) initiate the PTGS RNAi process. dsRNA is made by several methods, including long-hairpin RNAs formed by intramolecular base paring within a single transcript and antisense transcription, which results in inter-molecular base pairing of complementary transcripts. For miRNAs, these are formed by a transcription of a primary-miRNA (pri-miRNA), which forms intra-strand stem loop structures, which are digested in the nucleus to for precursor miRNAs (pre-miRNAs), which are exported to the cytoplasm, where they are further processed by Dicer to form mature functional miRNAs (O’Brian et al., 2018; McFarlane & Wakeman, 2020). dsRNA formed by inter molecular base pairing of anti-sense transcripts are thought to be processed directly by Dicer, which cleaves the dsRNA molecules into siRNA duplexes that are twenty to twenty-five nucleotide (nt) in terms of length (O’Brian et al., 2018). These duplex segments are combined into the RNA-

induced silencing complex (RISC) that exhibits endoribonuclease activity. RISC, which is essential for RNAi processes, is composed of effector proteins such as Argonaut. After the RISC has been loaded with duplex siRNA, one strand of the siRNA, known as the 'passenger' strand, is discarded, whilst the other strand remains bound to the complex, where it acts as a 'guide' strand, which targets the RISC complex to its cognate target mRNA. The sequence of siRNA guide strand will base pair perfectly to the target mRNA, targeting RISC to degrade the specific mRNA and prevent protein production (Kalantari et al., 2016; Ranjan et al., 2019). In both *Drosophila melanogaster and* human cells, after the duplex siRNA is loaded onto the RISC, the siRNA passenger strand is cleaved by the endoribonuclease activity of a complex known as component 3 promoter of RISC (C3PO). C3PO is the Translin/Trax hetero-octomer and there are other auxiliary factors in this process, such as Hen1, R2D2 and Loqs-PD (Figure 1.9) (Liu et al., 2018).

It has been suggested that the RNAi role of C3PO in may be restricted to higher order eukaryotic organism. For instance, C3PO functions as a ribonuclease in the filamentous fungus *Neurospora crassa*, processing pre-tRNAs to become mature tRNA, rather than contributing to the RNAi pathway. After pre-tRNAs are processed by ribonuclease P (RNase P), sequences are removed from the 5' end by C3PO (Li et al., 2012). Also, C3PO is credited with having a role in tRNA in embryonic fibroblast cells in mice (Li et al., 2012). C3PO also has a potential countering the silencing activity undertaken by miRNAs and siRNAs, as it can degrade pre-miRNAs. This implies that C3PO is a silencing mediator, which is contrary to its role in *Drosophila*, where it promotes silencing (Asada et al., 2014; Fu et al., 2016; Liu et al., 2018), This miRNA degrading function is oncogenic (see below), but the role it plays, if any, in normal cellular function is currently unclear (McFarlane & Wakeman, 2020).

### 1.6.4. Translin and Trax contribute to oncogenesis

Aside from the proposed role in oncogenesis via potentially serving as a driver of chromosomal translocations, the Translin/Trax complex has been implicated as a major oncogenic factor in Dicer-deficient tumours (Asada et al., 2014). The RNAase III enzyme, Dicer, has a number of roles in cell process, including being a key regulator of miRNA biogenesis and maturation (Johanson et al., 2013). pre-miRNAs are processed by Dicer to become mature miRNAs, some of which have tumour suppressing functions (Hata & Kashima, 2016; Mei et al., 2016; McFarlane & Wakeman, 2020). Around 30% of human gene expression is regulated by miRNAs and deregulated miRNA is detected in many cancers (Ali Syeda et al., 2020). The

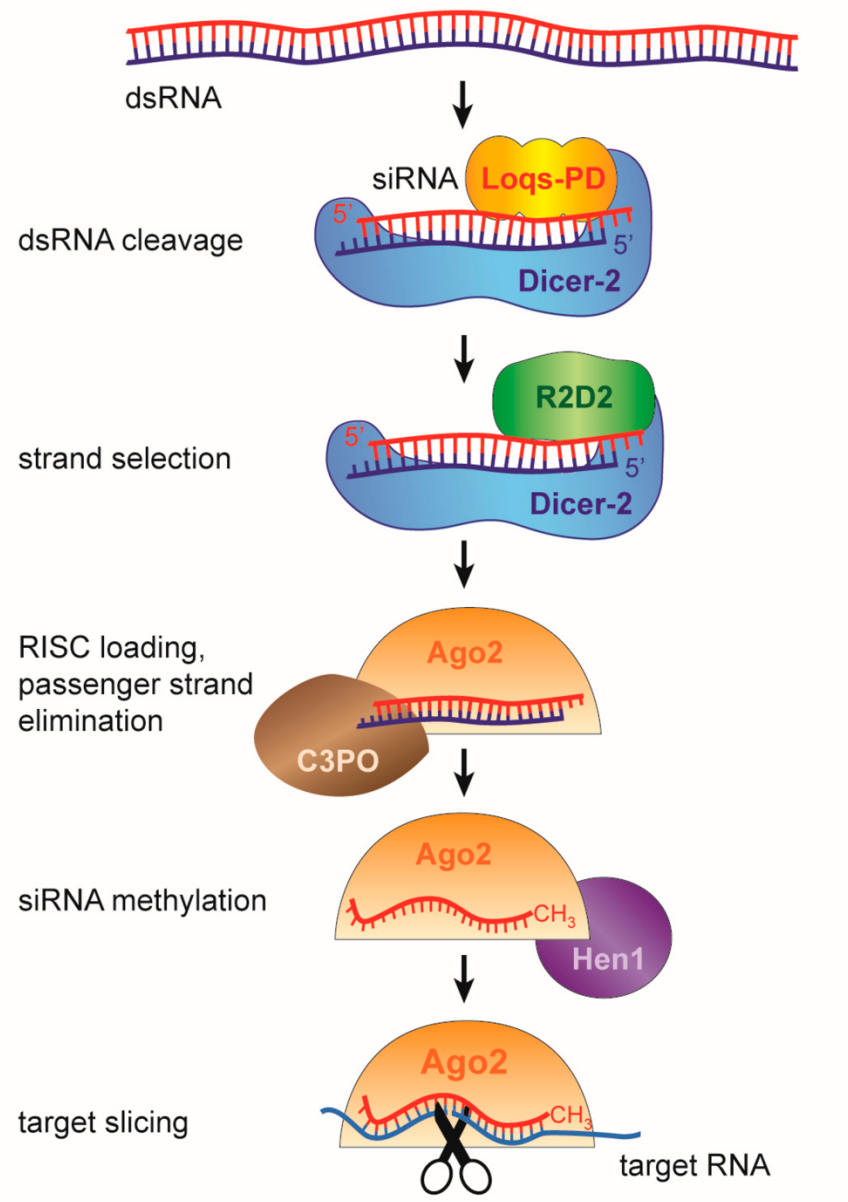


**Figure 1.9. Scheme of gene silencing in eukaryotes mediated by RNAi**

The small interfering RNA (siRNA) pathway in *Drosophila melanogaster*. Dicer-2 processes double-stranded RNA precursors, obtained from different sources, to produce short interfering RNAs of approximately 21 nucleotides in length. The siRNA duplex is incorporated into Argonaute2 that includes the RISC complex; the guide strand of the siRNA duplex is kept and the passenger strand is degraded. The mechanism used by the guide strand for the recognition of target RNA is Watson-Crick base pairing. Argonaute then cleaves the target site (Schuster et al., 2019).

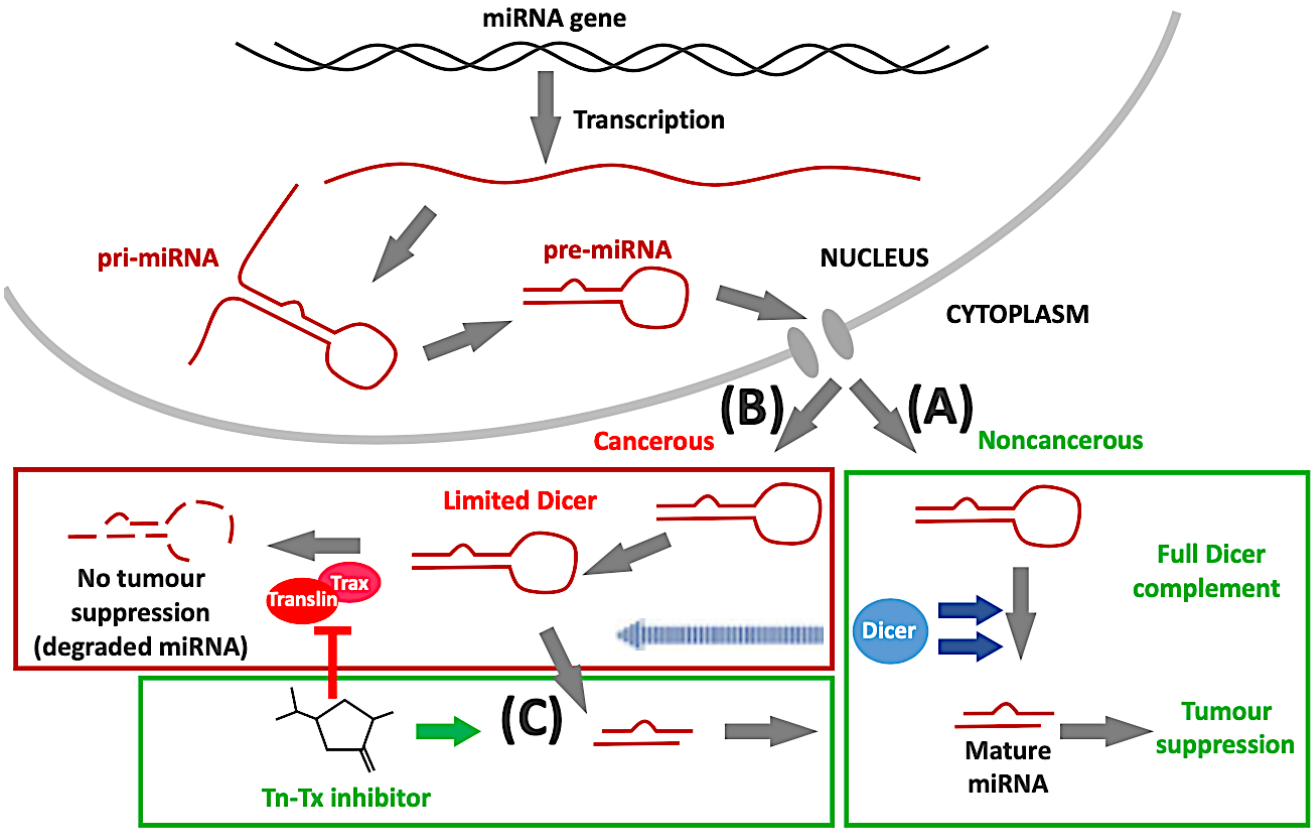


**Figure 1.10. Limiting Dicer Prevents the Maturation of Tumour Suppressor miRNA through a Translin-Trax (Tn-Tx)-Dependent Pathway**

Transcription of primary-miRNAs (pri-miRNAs) from miRNA genes takes place in the nucleus. pri-miRNAs are processes in the nucleus by Drosha to become pre-miRNAs. These are subsequently exported to the cytoplasm. (A) Where the levels of the ribonuclease, Dicer, is normal (i.e. in healthy cells), pre-miRNAs are processed to form mature miRNAs, some of these maintain the non-cancerous state, by adopting tumour-suppressing functions. (B) Limiting Dicer, such as by *DICER1* haploinsufficiency, results in reduced processing of pre-miRNAs due to limited levels of Dicer activity. In this case Tn-Tx ribonuclease can compete for pre-miRNAs and degrade them, resulting in insufficient mature tumour-suppressing miRNAs initiates the oncogenic pathway. (C) In the presence of small-molecule Tn-Tx inhibitors, the limited levels of Dicer are able to process the pre-miRNAs. This facilitates the maturation of sufficient tumour-suppressing miRNAs to ameliorate the oncogenic state (McFarlane & Wakeman, 2020).

observation that several oncogenic and tumour-suppressive mRNAs are inhibited by miRNAs has given rise to the notion that these RNAs work variously as tumour genes or oncogenes (Gurtner et al., 2016; Hata & Kashima, 2016). A notable difference between cancer and normal tissue is that in the former, pre-miRNAs accumulate and there are fewer mature miRNAs (Gurtner et al., 2016). Poor patient outcomes are associated with Dicer deficiency, occurring in up to 40% of cancers. Dicer is defined as a haploinsufficient tumour suppressor (Gurtner et al., 2016; Foulkes et al., 2014; Asada et al., 2016; McFarlane & Wakeman, 2020).

The tumour suppression and processing activity of miRNA is adversely affected by their depletion as a consequence of Dicer deficiency (Hata & Kashima, 2016; Asada et al., 2014; McFarlane & Wakeman, 2020). But the reduction in Dicer-induced formation of miRNA is not the only mechanism that affects the generation of miRNA; in the absence of normal Dicer-mediated pre-miRNA processing the pre-miRNAs become the targets of the ribonuclease catalytic activity of Trax /Translin (TSNAX /TSN). In *DICER1* haploinsufficiency, the C3PO complex acts as an RNase enzyme, degrading pre-miRNAs, preventing them from forming into mature tumour suppressing miRNAs, resulting in oncogenic transformation (Figure 1.10). Both miRNA and tumour suppression are restored by the inhibition of C3PO and indeed new small molecule inhibitors that target the Translin-Trax ribonuclease activity have been developed as potential oncological therapeutics (Asada et al., 2014; Asada et al, 2016; McFarlane & Wakeman, 2020).

## 1.7. *Schizosaccharomyces pombe* as a eukaryotic model

Much of the understanding of eukaryotic molecular biology has emerged through studying model organisms, such as the fission yeast *Schizosaccharomyces pombe* (Hoffman et al., 2015 ; Hayles & Nurse, 2018 ; Lock et al., 2018; Sabatinos & Forsburg ,2010; Holič et al., 2020). First identified in Germany by Saare and his colleagues after it was isolated from a consignment of contaminated millet beer from East Africa. The organism gained its “Pombe” (which is Swahili for ‘beer’) name in the 1890s from Ziedler and Lindner who isolated a pure culture of *S. pombe* and described it in depth. *S. pombe* became a model organism for use in experiments during the 1950s (Hoffman et al., 2015; Hayles & Nurse, 2018; Ďúranová et al ., 2019). The *S. pombe* genome consists of three chromosomes, numbered I, II and III, and their respective sizes are approximately 5.6, 4.8 and 3.6 Mb (Petrova et al., 2013). According to the PomBase database, these three chromosomes contain 5135 annotated genes (Lock et al., 2018), and the

first draft sequence of the *S. pombe* genome was completed in 2002 (Wood et al., 2002). The level of gene conservation is high, with 3535 of the 5135 protein-encoding genes having confirmed orthologues present in humans or vertebrates, with 914 of these genes being linked to diseases (Wood et al., 2002).

Interestingly, some of the genes that are conserved in *S. pombe* and humans are not evident in other model yeasts, such as the budding yeast *Saccharomyces cerevisiae* (Koyama et al., 2017). Examples of *S. pombe* genes that do not have *S. cerevisiae* orthologues but do have human orthologues, are *tsn1* (Translin) and *tfx1* (Trax) (see Section 1.6). Additionally, unlike *S. cerevisiae, S. pombe* has a full complement of RNAi components making it an excellent model system for RNAi and cellular epigenetics investigations (Buhler & Gasser, 2009; Hayles & Nurse, 2018). Several regions of the *S. pombe* genome, including the centromere, telomeres, mating-type and the rDNA locus, exhibit unique heterochromatic features (see the next section for detail). Epigenetic regulation observed in these regions is comparable with that of other organisms (Holoch and Moazed, 2015a; Wang et al., 2016: Shipkovenska et al.,2020). Thus, the features of *S. pombe* make it an appropriate model for this study.

### 1.7.1. *S. pombe:* Heterochromatin loci

There is an essential relationship between the organisation of chromatin and function in eukaryotes. Histone proteins make up the majority of chromatin. The nucleosome is the fundamental structural constituent of chromatin. The nucleosome is an octamer made up of pairs of each of the four core histones H3, H4, H2A and H2B, which is wrapped by approximately 147 base pairs of DNA (McGinty and Tan, 2015; Chen et al., 2016; Tolsma and Hansen, 2019). Distinct nucleosomes are associated by linker DNA (up to 80 bp), which is associated with the linker histone, H1. Each core histone has a flexible N-terminal tail that protrudes into the nucleoplasm. The tail is amenable to modification by diverse enzymes, which can alter the structure of the chromatin, which in turn can alter the accessibility of DNA. Acetylation and methylation are common post-translation modifications of histone tails (Maeshima et al., 2014; Timsina & Qiu, 2019).

Basically, chromosomes comprise of two distinct type of domain. Firstly, euchromatic domains, which are considered to be the transcriptionally active regions of the genome. The second domain type is the heterochromatic domains, in which the DNA is largely unavailable for DNA binding factors and consequently these domains are transcriptionally silent (Iglesias

et al., 2020). There are two categories of heterochromatin, facultative and constitutive. Facultative heterochromatin includes genes repressed in a cell type-specific manner, whereas constitutive heterochromatin is made up primarily by repetitive sequences and transposons positioned at consistent placements across different cell types, which remains transcriptionally silent in almost all cell types. These type include pericentromeric regions, which are transcribed (at an extremely low level) (Thomas et al. 2018;Talbert and Henikoff, 2018; Marsano et al., 2019; Gerlitz, 2020). Heterochromatin is vital for many cellular applications it is produced via methylation of histone tails by Clr4/Suv39h, which occurs at histone H3 at lysine 9 (H3K9me), and thereafter completed by incorporation of various chromodomain proteins, such as Swi6 and Chp2 in *S. pombe* [Heterochromatin protein 1 (HP1 orthologues)] (Iglesias et al., 2020). These epigenetic changes affect an area of the N terminal tail of histones that is highly conserved across many species, including humans and yeasts (Liu et al., 2020).

In the fission yeast, *S. pombe,* heterochromatin occurs at a number of locations; however, the locations, such as the silent mating-type locus, pericentromeric regions and subtelomeres (Iglesias et al., 2020), have structural similarities as they all contain specific DNA repeat sequences known as *dg* and/or *dh* repeats. These common areas are heterochromatin nucleation sites (Holla et al., 2020).

#### 1.7.1.i. Centromeres

In the eukaryotic genome every chromosome comprises distinct functional regions, including centromeres that are vital to maintain effective chromosomal segregation (Westhorpe & Straight, 2014; Sullivan, 2020). In most eukaryotes centromeres consist of highly repetitive DNA sequences and the chromatin is mostly heterochromatic (Zocco et al., 2016; Wang et al., 2016a; Steiner & Henikoff, 2015; Navarro and Cheeseman, 2020). The main function of the centromere within the chromosome is as a location for assembly of the multi-factor kinetochore, which, when assembled, operates as an anchor structure for spindle microtubules; establishment of heterochromatin at centromeres is important for precise chromosome segregation during both mitosis and meiosis (Krassovsky et al., 2012; Moreno-Moreno et al., 2017; Schmidt & Cech, 2015; Mutazono et al., 2017; Sullivan, 2020; Ideue and Tani, 2020). Failures in the function and structure of the centromere can result in chromosome mis-segregation, which is an oncogenic driver due to the resulting loss or gain of chromosomes (Westhorpe & Straight, 2014; Steiner & Henikoff, 2015; Remo et al., 2020) .

The centromeres in *S. pombe* vary in size from 40-100 kb, and they are each comprised of three distinct areas, including the essential central core (*cnt)* where the kinetochore develops (Figure 1.11). The nucleosomes of the *cnt* region are distinctive and they include Cnp1 (CENP-A orthologue) as an alternative to H3. This region is protected by a pair of inverted innermost repeats *(imr)* that contain tRNA genes within their sequences, which operated as chromatin boundaries, separating the Swi6-containing heterochromatin from the Cnp1-containing region (Talbert and Henikoff, 2020). Furthermore, the *imr* regions are protected by outer repeat regions (*otr)*, comprising of repeating *dg* and *dh* sequences, critical to production of heterochromatin in the centromere (Figure 1.11).

By controlling epigenetic modifications of chromatin, RNAi can suppress the formation of heterochromatin and/or transcription of individual genes. This process, which is known as transcriptional gene silencing (TGS) extends to modulating DNA methyltransferases and histones (Holoch & Moazed, 2015; Castel & Martienssen, 2013). The *S. pombe* model of RNAi pathways that mediate the formation of heterochromatin have been studied most thoroughly (Alper et al., 2012; Pushpavalli et al., 2012; Holoch & Moazed, 2015). The studies have shown that the creation of heterochromatin is mediated by nuclear siRNAs which targets the emerging centromeric nascent RNA molecules that RNA polymerase II produces (Holoch & Moazed, 2015; Smurova and De Wulf, 2018). Mutation of any of the *S. pombe* canonical RNAi pathway genes such as Argonaute (*ago1*), Dicer (*dcr1*), and RNA-dependent RNA polymerase (*rdp1*) affects heterochromatin function at the centromeres, as Swi6 (HP1) is unable to localise and H3K9 methylation is lost (Thakur et al., 2015; Creamer & Partridge, 2011; Chan & Wong, 2012; Gutbrod and Martienssen, 2020). With help from an RNA-dependent RNA polymerase complex (RDRC), the RNAi (CDGS) process commences in this species of yeast with RNA polymerase II (RNA Pol II) transcribing the pericentromeric DNA repeat into dsRNA. Dicer then processes the dsRNAs into siRNAs that bind to the Argonaute siRNA chaperone complex (ARC). In turn, they are added to the RNA-induced transcriptional silencing (RITS) complex containing Ago1, Chp1 and Tas3. As RNA transcripts emerge from the DNA repeats (centromere), the RITS complex binds to nucleosomes through the Chp1 chromodomain protein. This recruits the Clr4- Rik1-Cul4 (CLRC) complex to the centromeric repeats; Clr4 (histone methyltransferase) of the CLRC complex adds a methyl group to lysine 9 on H3 (Figure 1.11).

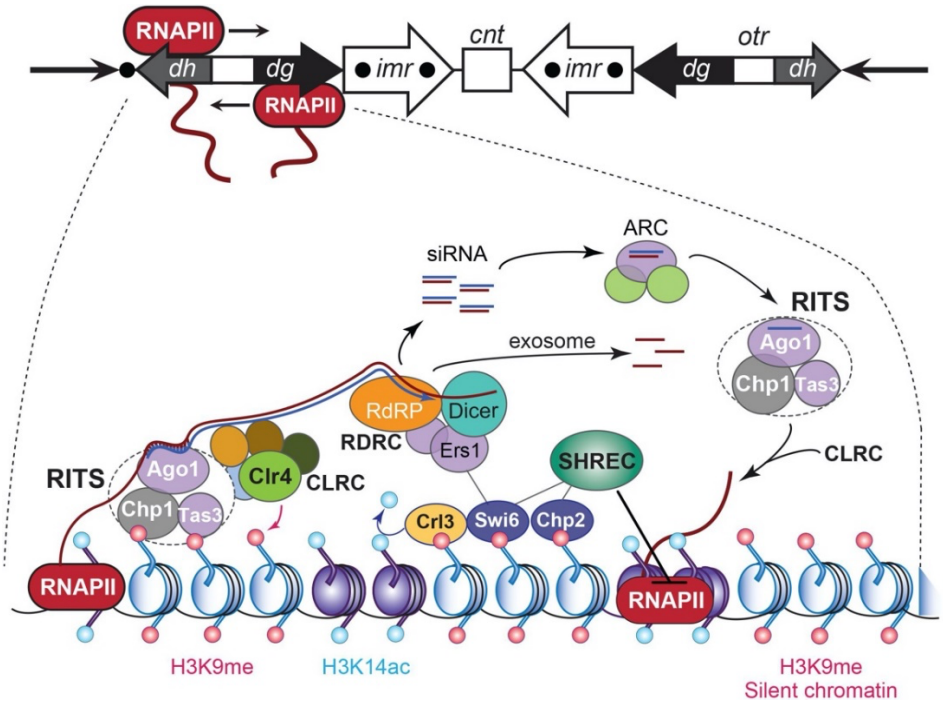


**Figure 1.11. Formation and maintenance of RNA-modified heterochromatin at the centromere (CEN) of *S. pombe.***

Upper panel: Schematic illustration of the *S. pombe* centromeres. *cnt* and *imr* are the two principal sequences that make up the centromeric domain. The *cnt* and *imr* sequences are bordered by the *otr,* which is composed of repeating *dg* and *dh* sequences. Lower panel: Illustrates the components involved in regulating heterochromatic-state CEN sequences adjoining the central core domain. Ago1, Chp1 and Tas3 make up the RNA-induced transcriptional silencing (RITS) complex, which binds to the ssRNA transcripts that are produced by the *otr* sequence repeats. Binding is achieved through siRNA–RNA base pairing interactions and through nucleosomes locating histone H3, which is methylated at Lys9 (H3K9me). RDRC/Dicer is recruited by RITS, thereby initiating dsRNA synthesis, siRNA synthesis and methylation of H3K9 by CLRC methyltransferase. The siRNAs are transferred from RDRC/Dicer to the RITS complex due to the catalytic action of the Argonaute siRNA chaperone complex (ARC). Exosomes degrade the transcript ssRNAs present in the siRNAs. Chromatin transcription is silenced by chromodomain HP1 proteins, Swi6 and Chp2 being recruited by H3K9me, which localises the Snf2/HDAC repressive complex (SHREC). This complex remodels the chromatin remodelling, thereby inhibiting the activity of RNAPII (Smurova and De Wulf, 2018).

A binding site for the Swi6 protein forms on the modified histone (H3K9me); this is key to heterochromatin being able to assemble and spread. Finally, Chp1 recruits the RDRC complex (containing Rdp1), which synthesises more dsRNAs that Dcr1 cleaves in readiness for methylation (Figure 1.11) (Kalantari et al., 2016; Smurova and De Wulf, 2018).

#### 1.7.1.ii Telomeres

Telomeres are highly repetitive sequences of nucleoprotein-like structures located at each end of linear eukaryotic chromosomes (Zocco et al., 2016; Chatterjee, 2017; Wang et al., 2016a; Lorenzi et al., 2015). The purpose of telomeres is to protect the ends of chromosomes from being mistaken for DSBs during DNA replication and from being degraded (Buhler & Gasser, 2009; Vancevska et al., 2017; Lorenzi et al., 2015; Bettin et al., 2019).Telomerase is a special reverse transcriptase enzyme tasked with maintaining the telomeres by extending the DNA at the ends of chromosomes (Hsu & Lue, 2017; Buhler & Gasser, 2009; Oh et al., 2016; Mizukoshi & Kaneko, 2019). Also, telomeres are integral to chromosomes adhering to the nuclear envelope; this attachment is important for organising and localising chromosomes within the nucleus (Chikashige et al., 2009; Kupiec, 2014; Li et al., 2017). To avoid the coding areas at the ends of chromosomes from becoming dysfunctional, the length and function of telomeres is maintained by protein complexes, known as shelterins (Vancevska et al., 2017; Eberhard et al., 2019). Ultimately, the integrity of telomeres, telomerase and shelterins is essential to maintaining the genome, as cancer and a number of other genetic diseases are associated with telomeric dysfunction (Chatterjee, 2017; Sarek et al., 2015; Van Emden et al., 2019). Originally, the heterochromatic state of telomeres was thought to be transcriptionally inactive (Novo & Londoño-Vallejo, 2013; Lorenzi et al., 2015; Udroiu and Sgura, 2020). However, subsequent research noted that RNA polymerase II (RNA Pol II) transcribe telomeres into G-rich telomeric repeat-containing RNA (TERRA) molecules (Feretza et al., 2017; Azzalin & Lingner, 2015; Cusanelli & Chartrand, 2015; Rippe & Luke, 2015; Maicher et al., 2014; Wang et al., 2015; Bettin et al., 2019). Transcription of these large, non-coding molecules starts at the sub-telomere and continues towards the telomere. Identified first in humans, (Schoeftner & Blasco, 2008; Azzalin et al., 2007;Feretzaki et al., 2019), TERRA is thought to be associated with various functions related to telomeres. These include controlling the length of telomeres, regulating the activity of telomerase, telomeric heterochromatin and DNA damage responses (Azzalin & Lingner, 2015; Cusanelli & Chartrand, 2015; Maicher et al., 2014; Rippe & Luke, 2015; Wang et al., 2015; Bettin et al., 2019). The integrity and

stability of the genome is dependent upon regulation of the expression of TERRA (Cusanelli & Chartrand, 2015; Brieño-Enríquez et al., 2018; Bettin et al., 2019). Based upon the evidence provided by studies of human cells and budding yeast indicate that in the absence of telomerase, the productive recombination of telomeres is maintained by the up-regulation of TERRA. This corresponds to the increased incidence of telomeric RNA-DNA hybrids (see Section 1.5)(Hu et al., 2019).

*S. pombe* not only synthesises TERRA, but it also creates distinctive telomeric and sub-telomeric- related transcripts. These include a C-rich, antisense transcript from the telomeric RNA repeats, known as ARIA and the sub-telomeric heterochromatic transcripts, ARRET and αARRET; the latter do not have telomeric sequences (Figure 1.12) (Bah et al., 2012; Greenwood & Cooper, 2012; Azzalin & Lingner, 2015; Lorenzi et al., 2015). To establish heterochromatin in *S. pombe*'s sub-telomeric regions, which are rich with the H3K9me and Swi6 modifications, RNAi is needed (Moravec et al., 2016). Compared to the levels of transcription in centromeric heterochromatin, the telomeric and sub-telomeric levels of transcription are unaffected by mutation of the RNAi genes, *ago1* or *dcr1* suggesting a pathway redundancy (Greenwood & Cooper, 2012). Furthermore, the researchers found that the core components of shelterin are responsible for regulating *S. pombe* transcripts. Specifically, mutation of either Taz1 or Rap1, which are double-strand telomere-binding proteins, leads to an increase in the number of all telomeric and sub-telomeric transcripts (Greenwood & Cooper, 2012). Taz1 also has a role in subduing the sub-telomeric RecQ-like *tlh* genes, which are orthologues of the *BLM* gene in humans (Hansen et al., 2006). Typically, these are silent genes, and their function has yet to be determined; however, in emergencies arising from a telomerase deficit, these genes appear to be involved in telomeric metabolism (Mandell et al., 2005). Mutation of *ago1, dcr1* and other RNAi components has little impact upon the expression of *tlh*; this is similar to telomeric transcript regulation (Hansen et al., 2006). At the ends of chromosomes, Taz1 contributes to diverse functions including maintaining the length of telomeres, regulating the recruitment of telomerase, DNA damage responses, as well as inhibiting transcription at telomeres and sub-telomeres (Pan et al., 2015; Harland et al., 2014).

### 1.7.1.iii Mating type

In *S. pombe,* three mating-type cassettes are present, specifically the expressed *mat1* domain, which is held in either the M (minus) or P (plus) state, and two silent domains, *mat2-P* and *mat3-M* (Yamada-Inagawa et al., 2007). Switching of mating-type results from a single-stranded DNA break during replication followed by gene conversion recombination between the expressed *mat1* locus and either *mat2-P* or *ma3-M* donor cassettes. The K region, between the *mat2-P* and *ma3-M* cassettes, and the cassettes are heterochromatic areas (Klar, 2007; Seike et al., 2019; Hylton et al., 2020). Silencing is depended on various DNA sequences, including the *cenH* region, an area which is 96% homologous with the repeating *dg* and *dh* regions of the centromere. *cenH* operates as a nucleation point for heterochromatin assembly (Verdel and Moazed, 2005; Thon et al., 2019). Heterochromatin is produced at the mating-type loci (*mat2/3*) via a similar process to the sequestration of Clr4 H3K9 methyltransferase to centromeres by RNAi factors. An alternate pathway operates via binding of transcription factors Pcr1 and Atf1 in the region between *mat3* and *cenH,* which then initiates RNAi-independent recruitment of Swi6 and Clr4 (Jia et al., 2004; Greenstein et al., 2020). Knockout of any RNAi components is insufficient to induce silencing, which necessitates the additional knockout of either of the genes encoding the transcription factors Atf1 and Pcr1. The implication of this is that Swi6 heterochromatin maintenance occurs via two redundant pathways (Jia et al., 2004 ; Greenstein et al., 2020).

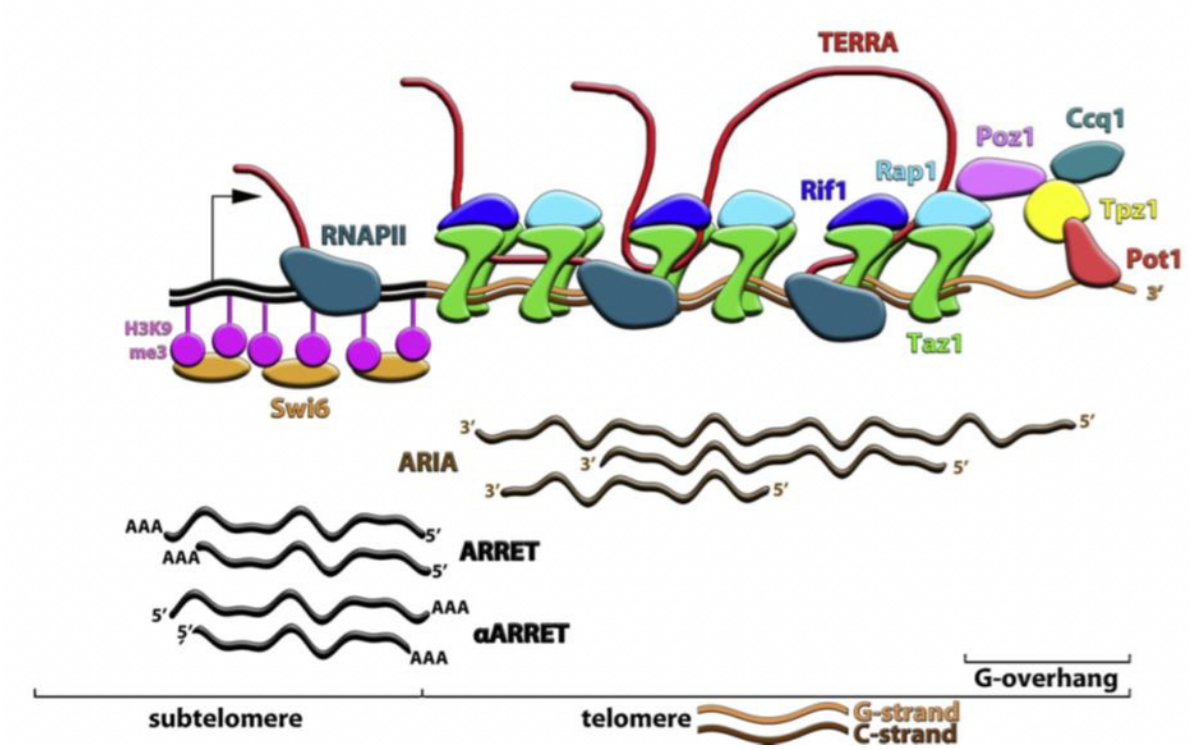


**Figure 1.12. Schematic illustration of the components involved in creating RNA species at the ends of chromosomes in fission yeast**

To protect telomeres in *S. pombe,* a multiprotein complex comprised of the shelterin components Taz1, Rap1, Rif1, Poz1, Tpz1, Pot1 and Ccq1 binds to telomeric repeats. The chromosome ends are rich in the H3K9me3 and Swi6 heterochromatin factors; however, in *S. pombe* TERRA is produced, primarily from RNA Pol II transcription. This starts in the sub-telomeric regions (black arrow) and progresses towards the telomeres at the ends of the chromosome; Taz1 may be the binding interface between TERRA and the telomeres. Not only do the ends of *S. pombe* chromosomes produce TERRA, they also create ARIA, ARRET and αARRET (adapted from Bah et al., 2012).

## 1.8. Hypothesis

Our overarching hypothesis at the onset of this work was that Tsn1 and/or Tfx1 function to maintain genome stability in the absence of Dcr1. This hypothesis extends an unpublished preliminary observation made by others in the McFarlane Group, which seems to suggest a requirement for Tsn1 in the absence of Dcr1.

## 1.9. Aims and Objectives

- We aim to determine/confirm whether Tsn1 and/or Tfx1 function to maintain genome stability in the absence of RNAse H activity.
- We aim to establish whether Tsn1 and/or Tfx1 function to maintain genome stability in the absence of *sen1*.
- We aim to determine the relationship of the RNAi gene *dcr1* to the RNase H genes, *rnh1* and *rnh201* in the control of genome stability, which might offer insight into the function of Tsn1.
- We aim to establish whether human Translin functions in genome stability control and whether this might be linked to Trax function.
- We aim to determine whether the postulated functional requirement for Tsn1 in genome stability maintenance is dependent on conserved RNAse domain function.

# Chapter 2: Materials and Methods

# 2. Materials and Methods

## 2.1. Yeast and bacterial Media

### 2.1.1. Strains used in this study

Table 2.1 details the media used for both yeast and bacteria. Tables 2.2, 2.3 and 2.4 respectively list the plasmids, *Escherichia coli* strains and *S. pombe* strains used in this study. To create the desired mutant strains, either the *de novo* deletion method was applied (Bähler et al., 1998) or standard genetic crosses (Sabatinos & Forsburg, 2010). PCR analysis of the genomic DNA was conducted to verify specific gene deletions within a given *S. pombe* strain.

### 2.1.2. Media

Bacterial media, supplements and reagents for yeast were acquired from Fisher Scientific, Sigma-Aldrich and Becton Dickinson; whilst, with some exceptions, buffers and enzymes were bought from New England Biolabs.

For the minimal media, Edinburgh minimal media Glutamic acid (EMMG) was used with required supplements (e.g., amino acids and/or the nucleobases adenine and/or uracil) added to achieve a final concentration of 250 mg/l (Petersen & Russell, 2016). The concentration of antibiotics added to the media was 100 μg/ml for all the antibiotics used; namely, ampicillin (Sigma-Aldrich), hygromycin (Sigma-Aldrich), geneticin (G418) (Sigma-Aldrich) and nourseothricin (Werner BioAgents).

**Table 2.1. Yeast and bacterial media recipe**

| **YEA** | **(1 L)** |
|---|---|
| Glucose | 30 g |
| Yeast extract | 5 g |
| Agar | 14 g |
| **YEL** | **(1 L)** |
| Glucose | 30 g |
| Yeast extract | 5 g |
| **SPA** | **(1 L)** |
| Glucose | 10 g |
| Potassium dihydrogen orthophosphate | 1 g |
| Agar | 30 g |
| Minerals | 0.1 ml |
| Salts | 20 ml |
| Vitamins | 1 ml |
| **EMMG** | **(1 L)** |
| L-Glutamic acid, Monosodium salt | 3.75 g |
| Potassium hydrogen phthalate | 3 g |
| Di-sodium hydrogen phosphate, $Na_2HPO_4$ | 2.2 g |
| Glucose | 20 g |
| Minerals | 0.1 ml |
| Salts | 20 ml |
| Vitamins | 1 ml |
| Agar | 30 g |
| **LBA** | **(1 L)** |
| Sodium chloride | 10 g |
| Tryptone | 10 g |
| Agar | 14 g |
| Yeast extract | 5 g |
| Ampicillin (50mg/ml) | 2 ml |
| **Vitamins (x1000)** | **(1 L)** |
| Nicotinic acid | 10 g |
| Biotin | 10 mg |
| *Myo*-inositol | 10 g |
| Pantothenic acid | 1 g |

| **Salts (x50)** | **(1 litre)** |
|---|---|
| Calcium chloride dihydrate<br>Disodium sulphate<br>Potassium chloride<br>Magnesium chloride hexahydrate | 0.735 g<br>2 g<br>50 g<br>52.5 g |
| **Minerals (x10, 000)** | **(1 litre)** |
| Copper sulphate<br>Manganese sulphate<br>Iron chloride hexahydrate<br>Zinc sulphate septahydrate<br>Potassium iodide<br>Citric acid<br>Molybdic acid<br>Boric acid | 0.4 g<br>4 g<br>2 g<br>4 g<br>1 g<br>10 g<br>0.4 g<br>5 g |

## 2.2. Plasmid Extraction from *E. coli*

The QIAGEN Miniprep kit has been used to separate plasmids from *E. coli* and was performed according to the manufacturer's instructions. Strains of *E. coli* preserved at -80°C were streaked on Luria-Bertani agar (LBA), comprising ampicillin as required, then incubated at 37°C overnight. Cells were centrifuged for 5 mins at 3,000 *g*. 250 µl of P1 buffer with RNase A was prepared and the centrifuged cells were resuspended in it. The suspension was moved to an Eppendorf tube, after that 250 µl of P2 lysis buffer was added for cell lysis. Invert mixing has been repeated up to five times, then 350 µl of N3 neutralising/binding buffer was added. To homogenise the tube contents, invert mixing was performed, again for up to 5 times. The tube was then spun at 12,000 *g* for 10 mins. The resultant pellet was removed, and the supernatant was transferred to a QIAprep tube (QIAGEN). The supernatant was centrifuged again for up to 1 min. The supernatant was drawn off and the pellet was washed in 500 µl of washing buffer and spun again for up to 1 min at 12,000 *g*. The supernatant was drawn off, and the pellet was washed with 750 µl of PE buffer then spun at 12,000 *g* for 30-60 secs. Then the supernatant was then discarded. Elution buffer (EB) of 50 µl was used to clear the plasmid DNA from the filter

**Table 2.2. Plasmids used in this study**

| Plasmid | Description |
|---|---|
| pARC782 (*kanMX6 amp*$^{R}$) | Plasmid for deletion of the yeast gene using selectable marker kanMX6, which confers resistance to Kanamycin |
| pYL16 (*natMX6 amp*$^{R}$) | Plasmid for deletion of the yeast gene using selectable marker natMX6, which confers resistance to Nourseothricin. |
| pFA6a (*hphMX6 amp R)* | Plasmid for deletion of the yeast gene using the selectable marker hphMX6 which confers resistance to Hygromycin |
| pREP3X | The REP3X are derived from the REP. The original REP/RIP vectors include an ATG at the 5' end of the polylinker; the X-series eliminates ATG and inserts a *Xho*I site. |
| pREP3X::*rnh1* | pREP3X with the full open reading frame of *S. pombe rnh1* cloned into the *Xho*l and *Bam*H1 restriction site |
| pREP3X::*pac1* | pREP3X with the full open reading frame of *S. pombe pac1* cloned into the *Xho*l and *Bam*H1 restriction site |
| pREP3X::Sp*tsn1* | pREP3X with the full open reading frame of *S. pombe tsn1* cloned into the *Xho*l and *Bam*H1 restriction site |
| pREP3X::Hs*TSN* | pREP3X with the full open reading frame of Human *TSN* cloned into the *Xho*l and *Bam*H1 restriction site |
| pREP3X::Sp*dcr1* | pREP3X with the full open reading frame of *S. pombe dcr1* cloned into the *Xho*l and *Bam*H1 restriction site |
| pREP3X:Sp*tsn1::*E152A | pREP3X with the full open reading frame of *S. pombe tsn1* gene carrying the E152A mutation cloned into the *Xho*l and *Bam*H1 restriction site |
| pREP3X::Sp*tsn1::*R86G | pREP3X with the full open reading frame of *S. pombe tsn1* gene carrying the R86G mutation cloned into the *Xho*l and *Bam*H1 restriction site |
| pREP3X::Hs*TSN::*E150G | pREP3X with the full open reading frame of Human *TSN* gene carrying the E150G mutation cloned into the *Xho*l and *Bam*H1 restriction site |
| pREP3X:: Hs*TSN::*R92G | pREP3X with the full open reading frame of Human *TSN* gene carrying the R92G mutation cloned into the *Xho*l and *Bam*H1 restriction site |
| pREP3X::*rnh201* | pREP3X with the full open reading frame of *S. pombe rnh201* cloned into the *Xho*l and *Bam*H1 restriction site |
| pREP3X::Sp*tfx1* | pREP3X with the full open reading frame of *S. pombe tfx1* cloned into the *Xho*l and *Bam*H1 restriction site |
| pREP3X::Hs*TSNAX* | pREP3X with the full open reading frame of human *TSNAX* cloned into the *Xho*l and *Bam*H1 restriction site |

**Table 2.3. *E. coli* strains used in this study**

| **Bangor strain number** | ***E. coli* strain** | **Source** |
|---|---|---|
| BE9 | NEB 10-beta *E. coli* (pARC782 *kanMX6 amp*$^{R}$) | McFarlane collection |
| BE183 | NEB 10-beta *E. coli* (pYL16 *natMX6 amp*$^{R}$) | Edgar. Hartsuiker |
| BE193 | NEB 10-beta *E. coli* (pFA6a *hphMX6 amp*$^{R}$) | Oliver Fleck |
| BE294 | NEB 10-beta *E. coli (*pREP3X::*rnh1*) | This research |
| BE299 | NEB 10-beta *E. coli* (pREP3X::*pac1*) | McFarlane collection |
| BE303 | NEB 10-beta *E. coli* (pREP3X::Sp*tsn 1*) | McFarlane collection |
| BE304 | NEB 10-beta *E. coli (*pREP3X::Hs*TSN*) | McFarlane collection |
| BE307 | NEB 10-beta *E. coli* (pREP3X::Sp*dcr1*) | McFarlane collection |
| BE308 | NEB 10-beta *E. coli* (pREP3X:: Sp*tsn1::*E152A) | McFarlane collection |
| BE309 | NEB 10-beta *E. coli* (pREP3X::Sp*tsn1::*R86G) | McFarlane collection |
| BE310 | NEB 10-beta *E. coli* (pREP3X::Hs*Tsn1::*E150G) | McFarlane collection |
| BE311 | NEB 10-beta *E. coli (*pREP3X::Hs*Tsn1*-R92G) | McFarlane collection |
| BE312 | NEB 10-beta *E. coli* (pREP3X:: *rnh201*) | McFarlane collection |
| BE313 | NEB 10-beta *E. coli (*pREP3X::Sp*tfx1)* | McFarlane collection |
| BE314 | NEB 10-beta *E. coli* (pREP3X::Hs*TSNAX)* | McFarlane collection |

## 2.3. Gene deletions using the PCR method

Gene open reading frames were deleted from the *S. pombe* genome using a method explained by Bähler et al. (1998). The primers for PCR used 80 bp homologous sequences that were downstream and upstream of the open reading frame for the genes to be targeted for deletion. These sequences contained 20 bp sequences that were homologous to the target PCR template plasmids that conferred antibiotic resistance. In some cases, *natMX6* cassettes were used, in other cases *kanMX6* or *hphMX6* cassette were used. Table 2.5 presents the oligonucleotide sequences used. The primers were created using the online Bähler lab genome regulation programme (http://www.bahlerlab.info/cgibin/PPPP/pppp_deletion.pl).

Before PCR, the primer and plasmid were diluted 10-fold in 1X TE buffer (EDTA 1.0 mM and 10 mM Tris-HCl preserved at pH 8.0). In of the 50 µl PCR reactions was the following: 10 µl 5x PhusionTM GC buffer, 1 µl of DNA template (20 ng of plasmid DNA), 1 µl of 20 ng/µl each of forward and reverse primers, 1 µl of 10 mM dNTPs, 1 µl high fidelity Phusion polymerase (NEB), 2.5 µ of DMSO and 32.5 µl of sterile dH2O. Amplification of the selected marker cassettes was achieved as follows: 98°C for 1 min, after that 40 cycles of 10 secs at 98°C, 30 secs at 59°C, then 1 min 50 secs at 72°C, finalised by a further 5 mins at 72°C. To purify the PCR products, the phenol/chloroform method was used.

## 2.4. Phenol/ chloroform purification of DNA

To an Eppendorf tube containing the DNA solution, at a ratio of 1:1, 0.1 M NaCl and an equivalent quantity of chloroform/phenol was appended. The tube was centrifuged at 12,000 *g* for 15 mins. The aqueous supernatant was transferred to a fresh tube in which a three-fold quantity of 100 % ethanol was added. To precipitate the DNA, the tube was left for 1 hour at –80°C. The DNA was centrifuged at 13,000 *g* for 15 mins then washed with 70% ethanol. The resultant pellet was left to dry for 5 mins. The pellet was then resuspended in 50 µl of 1x TE buffer.

## 2.5. Transformation of *S. pombe* cells using a DNA knockout cassette

A single colony of a selected *S. pombe* strain was used to inoculate 5 ml of YEL (supplemented with 250 mg/ml adenine for *ade6* mutants) and incubated overnight at 30°C in a rotary incubator. In the morning, 100 ml of pre-warmed YEL containing supplemental adenine (250 mg/) was inoculated with 100-200 µl of the overnight culture at a concentration of of 1x $10^7$ cells/ml then left overnight to incubate at 30°C in a rotary incubator. The next day the cells were centrifuged for 5 mins at 3,000 *g,* washed with sterile $dH_2O$, then spun again at 3,000 *g* for 5 mins. The cells have been resuspended in one ml sterile $dH_2O$ and moved to the Eppendorf tubes. Cells were washed with one ml of 0.1 M LiAc/1X TE; then, cells were resuspended in LiAC/TE to maintain cell density at 2 x $10^9$ cells/ml. After that, 100 µl of cell suspension was drawn off and mixed with 10-20 µg of cassette DNA and 2 µl of 10 mg/ml sheared herring testis DNA (Invitrogen). The mixture was incubated at room temperature for 10 mins then 270 µl of 40% PEG/LiAC/TE (maintained at 7.5 pH) was added. After mixing gently, the cells were incubated for 1 hour in a 30°C water bath. After that DMSO of 42 µl was added, then for 5 mins, the cells were exposed to heat shock at 42°C. After cooling for 10 mins and washing with 1 ml sterile $dH_2O$, the mixture was centrifuged for 3 mins. The cells were then resuspended in 0.5 ml sterile $dH_2O$ and plated, with 100 µl of the mixture being applied to each YEA plate (not selective). Plates were incubated at 30°C for 18 hours. Finally, cells were replica plated onto fresh YEA plates comprising the selective antibiotic then incubated at 30°C.for 3-4 days

## 2.6. Transformation with plasmids

To transform *S. pombe* strains with plasmids, the lithium acetate (LiAC) technique, as stated in Section 2.5 was adopted. The only variation to that procedure is that plasmid DNA of 1 µg was used, in terms of choosing transformants, cells were plated on specific EMMG media before being incubated at 30°C for 5-8 days.

**Table 2.4. *S. pombe* strains used in this project**

| Strain number | Genotype | Source |
|---|---|---|
| BP90 | *h¯ ade6-M26 ura4-D18 leu1-32* | McFarlane collection |
| BP89 | *h+ ade6-M26 ura4-D18 leu1-32* | McFarlane collection |
| BP743 | *h¯ rad3-136* | McFarlane collection |
| BP1079 | *h¯ ade6-M26 ura4-D18 leu1-32 tsn1:: kanMX6* | McFarlane collection |
| BP1089 | *h¯ ade6-M26 ura4 -D18 leu1-32 tfx1:: kanMX6* | McFarlane collection |
| BP2746 | *h¯ ade6-M26 ura4-D18 leu1-32 dcr1:: ura4*$^{+}$ | McFarlane collection |
| BP2748 | *h¯ ade6-M26 ura4-D18 leu1-32 tsn1:: kanMX6 dcr1:: ura4*$^{+}$ | McFarlane collection |
| BP2750 | *h¯ ade6-M26 ura4-D18 leu1-32 tfx1:: kanMX6 dcr1::ura4*$^{+}$ | McFarlane collection |
| BP3401 | *h¯ ade6-M26 ura4-D18 leu1-32 rnh1::kanMX6* ( iso 1) | This research |
| BP3402 | *h¯ ade6-M26 ura4-D18 leu1-32 rnh1::kanMX6* (iso 2*)* | This research |
| BP3403 | *h¯ ade6-M26 ura4-D18 leu1-32 rnh1::kanMX6* (iso 3) | This research |
| BP3404 | *h¯ ade6-M26 ura4-D18 leu1-3 rnh1::kanMX6* (iso 4) | This research |
| BP3405 | *h¯ ade6-M26 ura4-D18 leu1-32 rnh201::kanMX6* (iso 1) | This research |
| BP3406 | *h¯ ade6-M26 ura4-D18 leu1-32 rnh201::kanMX6* ( iso 2) | This research |
| BP3407 | *h¯ ade6-M26 ura4-D18 leu1-32 rnh201::kanMX6 (*iso 3) | This research |
| BP3408 | *h¯ ade6-M26 ura4-D18 leu1-32 rnh201::kanMX6* (iso 4) | This research |

| | | |
|---|---|---|
| BP3409 | *h¯ ade6-M26 ura4-D18 leu1-32 rnh201::kanMX6* (iso 5) | This research |
| BP3410 | *h¯ ade6-M26 ura4-D18 leu1-32 rnh1::kanMX6 rnh201::hphMX6* (iso 1) | This research |
| BP3411 | *h¯ ade6-M26 ura4-D18 leu1-32 rnh1::kanMX6 rnh201::hphMX6* ( iso 2*)* | This research |
| BP3412 | *h¯ ade6-M26 ura4-D18 leu1-32 tfx1::natMX6 rnh1::kanMX6* (iso 1*)* | This research |
| BP3413 | *h¯ ade6-M26 ura4-D18 leu1-32 tfx1::natMX6 rnh1::kanMX6* (iso 2*)* | This research |
| BP3414 | *h¯ade6-M26 ura4-D18leu1-32 tfx1::natMX6 rnh201::kanMX6* (iso 1*)* | This research |
| BP3415 | *h¯ ade6-M26 ura4-D18 leu1-32 tfx1::natMX6 rnh201::kanMX6* (iso 2) | This research |
| BP3416 | *h¯ade6-M26ura4-D18leu1-32 tfx1::natMX rnh201::kanMX6* (iso 3) | This research |
| BP3417 | *h¯ ade6-M26 ura4-D18 leu1-32 rnh201::kanMX6 tsn1::natMX6* (iso 1*)* | This research |
| BP3418 | *h¯ ade6-M26 ura4-D18 leu1-32 rnh201::kanMX6 tsn1: natMX6* (iso 2) | This research |
| BP3419 | *h¯ ade6-M26 ura4-D18 leu1-32 rnh201::kanMX6 rnh1::natMX6* (iso 1) | This research |
| BP3420 | *h¯ ade6-M26 ura4-D18 leu1-32 rnh201::kanMX6 rnh1::natMX6* (iso 2) | This research |
| BP3424 | *h¯ ade6-M26 ura4-D18 leu1-32 tfx1::natMX6 rnh1::kanMX6 rnh201::hphMX6* (iso 1) | This research |
| BP3425 | *h¯ ade6-M26 ura4-D18 leu1-32 tfx1::natMX6 rnh1::kanMX6 rnh201::hphMX6* (iso 2) | This research |
| BP3426 | *h¯ ade6-M26 ura4-D18 leu1-32 tsn1::kanMX6 rnh1::natMX6* (iso1 ) | This research |
| BP3427 | *h¯ ade6-M26 ura4-D18 leu1-32 tsn1::kanMX6 rnh1::natMX6* (iso 2) | This research |
| BP3428 | *h¯ ade6-M26 ura4-D18 leu1-32 sen1::kanMX6* (iso 1) | This research |
| BP3429 | *h¯ ade6-M26 ura4-D18 leu1-32 sen1::kanMX6* (iso 2*)* | This research |

| | | |
|---|---|---|
| BP3441 | *h⁻ ade6-M26 ura4-D18 leu1-32 sen1::kanMX6 tsn1::natMX6* (iso 1*)* | This research |
| BP3442 | *h⁻ ade6-M26 ura4-D18 leu1-32 sen1::kanMX6 tsn1::natMX6* (iso 2*)* | This research |
| BP3443 | *h⁻ ade6-M26 ura4-D18 leu1-32 sen1::kanMX tsn1::natMX6* (iso 3*)* | This research |
| BP3444 | *h⁻ ade6-M26 ura4-D18 leu1-32 sen1::kanMX6 tfx1::natMX6* (iso 1*)* | This research |
| BP3445 | *h⁻ ade6-M26 ura4-D18 leu1-32 sen1::kanMX6 tfx1:: natMX6* (iso 2) | This research |
| BP3446 | *h⁻ ade6-M26 ura4-D18 leu1-32 sen1::kanMX6 tfx1::hphMX6* (iso 3) | This research |
| BP3447 | *h⁻ ade6-M26 ura4-D18 leu1-32 sen1::kanMX6 tfx1::hphMX6* (iso 4) | This research |
| BP3448 | *h⁻ ade6-M26 ura4-D18 leu1-32 sen1::kanMX6* (iso1) | This research |
| BP3449 | *h⁻ ade6-M26 ura4-D18 leu1-32 sen1::kanMX6* (iso2) | This research |
| BP3472 | *h⁻ ade6-M26 ura4-D18 leu132 rnh1::kanMX6 rnh201::hphMX6 (*pREP3X) | This research |
| BP3473 | *h⁻ ade6-M26 ura4-D18 leu1-32 rnh1*::*kanMX6 rnh201*::*hphMX6* (pREP3X::*rnh1*$^{+}$) | This research |
| BP3474 | *h⁻ ade6-M26 ura4-D18 leu1-32 dcr1*::*natMX6 tsn1*::*kanMX6* (pREP3X) | This research |
| BP3475 | *h⁻ ade6-M26 ura4-D18 leu1-32 dcr1*::*natMX6 tsn1*::*kanMX6* (pREP3X::*rnh1*$^{+}$) | This research |
| BP3476 | *h⁻ ade6-M26 ura4-D18 leu1-32 dcr1*::*natMX6*(pREP3X) | This research |
| BP3477 | *h⁻ ade6-M26 ura4-D18 leu1-32 dcr1*::*natMX6* (pREP3X::*rnh1*$^{+}$) | This research |
| BP3478 | *h ⁻ade6-M26ura4-D18leu1-32 rnh201*::*kanMX6 tsn1*::*natMX6* (pREP3X) | This research |
| BP3479 | *h ⁻ade6M26 ura4-D18 leu1-32 rnh201*::*kanMX6 tsn1*::*natMX6 (*pREP3X::*rnh1*$^{+}$) | This research |
| BP3482 | *h⁻ ade6-M26 ura4-D18leu1-32dcr1*::*natMX6 (*pREP3X::*pac1*$^{+}$) | This research |

| | | |
|---|---|---|
| BP3483 | *h⁻ ade6-M26 ura4-D18 leu1-32 dcr1*::*natMX6 tsn1*::*kanMX6* (pREP3X::*pac1*$^{+}$) | This research |
| BP3484 | *h⁻ ade6-M26 ura4-D18leu1-32 rnh201*::*kanMX6 tsn1*::*natMX6* (pREP3X::*pac1*$^{+}$ ) | This research |
| BP3485 | *h⁻ ade6-M26 ura4-D18leu1-32 rnh1*::*kanMX6 rnh201*::*hphMX6* pREP3X::*pac1*$^{+}$) | This research |
| BP3486 | *h⁻ ade6-M26 ura4-D18 leu1-32 dcr1*::*natMX6* (pREP3X::Sp*tsn*1$^{+}$) | This research |
| BP3487 | *h⁻ ade6-M26 ura4-D18 leu1-32 dcr1*::*natMX6* (pREP3X::Hs*TSN*$^{+}$) | This research |
| BP3488 | *h⁻ ade6-M26 ura4-D18 leu1-32 dcr1*::*natMX6 tsn1*::*kanMX6* (pREP3X::Sp*tsn*1$^{+}$) | This research |
| BP3489 | *h⁻ ade6-M26 ura4-D18 leu1-32 dcr1*::*natMX6 tsn1*::*kanMX6* (pREP3X::Hs*TSN* $^{+}$) | This research |
| BP3490 | *h⁻ ade6-M26 ura4-D18 leu1-32 dcr1*::*natMX6 tsn1*::*kanMX6* (pREP3X::*dcr1*$^{+}$) | This research |
| BP3491 | *h⁻ ade6-M26 ura4-D18leu1-32 rnh201*::*kanMX6* tsn1::*natMX6* (pREP3X::Sp*tsn*1$^{+}$) | This research |
| BP3492 | *h⁻ ade6-M26 ura4-D18leu1-32 rnh201*::*kanMX6 tsn1*::*natMX6* (pREP3X::Hs*TSN* $^{+}$) | This research |
| BP3493 | *h⁻ade6-M26 ura4-D18leu1-32 rnh201*::*kanMX6 tsn1*::*natMX6* (pREP3X::*dcr1*$^{+}$) | This research |
| BP3494 | *h⁻ ade6-M26 ura4-D18 leu1-32 dcr1*::*natMX6* (pREP3X::Sp*tsn1::*E152A) | This research |
| BP3495 | *h⁻ ade6-M26 ura4-D18 leu1-32 dcr1*::*natMX6* (pREP3X::Sp*tsn1::*R86G) | This research |
| BP3496 | *h⁻ ade6-M26 ura4-D18 leu1-32 dcr1*::*natMX6* (pREP3X::Hs*TSN ::*E150A) | This research |
| BP3497 | *h⁻ ade6-M26 ura4-D18 leu1-32 dcr1*::*natMX6 tsn1*::*kanMX6* (pREP3X::Sp*tsn1::*E152A ) | This research |
| BP3498 | *h⁻ ade6-M26 ura4-D18 leu1-32 dcr1*::*natMX6 tsn1*::*kanMX6* (pREP3X::Sp*tsn1::*R86G) | This research |
| BP3499 | *h⁻ ade6-M26 ura4-D18 leu1-32 dcr1*::*natMX6 tsn1*::*kanMX6* (pREP3X::Hs*TSN::*E150A ) | This research |
| BP3500 | *h⁻ ade6-M26 ura4-D18 leu1-32 rnh201*::*kanMX6 tsn1*::*natMX6* (pREP3X::Sp*tsn1::*E152A ) | This research |

| | | |
|---|---|---|
| BP3501 | *h⁻ ade6-M26 ura4-D18 leu1-32 rnh201*::*kanMX6 tsn1*:: *natMX6* (pREP3X::Sp*tsn1*::R86G) | This research |
| BP3502 | *h⁻ ade6-M26 ura4-D18 leu1-32 rnh201*::*kanMX6 tsn1*::*natMX6* (pREP3X::Hs*TSN*::E150A ) | This research |
| BP3503 | *h⁻ ade6-M26 ura4-D18 leu1-32 dcr1*::*natMX6* (pREP3X::Hs*TSN*::R92G) | This research |
| BP3504 | *h⁻ ade6-M26 ura4-D18 leu1-32 dcr1*::*natMX6 tsn1*::*kanMX6* (pREP3X::Hs*TSN*::R92G) | This research |
| BP3505 | *h⁻ ade6-M26 ura4-D18 leu1-32 rnh201*::*kanMX6 tsn1*::*natMX6* (pREP3X::Hs*TSN*::R92G) | This research |
| BP3506 | *h⁺ ade6-M26 ura4-D18 leu1-32 rnh1*::*kanMX6* (iso1) | This research |
| BP3507 | *h⁺ ade6-M26 ura4-D18 leu1-32 rnh1*::*kanMX6* (iso2) | This research |
| BP3508 | *h⁺ ade6-M26 ura4-D18 leu1-32 rnh1*::*kanMX6* (iso3) | This research |
| BP3509 | *h⁺ ade6-M26 ura4-D18 leu1-32 rnh1*::*kanMX6* (iso4) | This research |
| BP3510 | *h⁻ ade6-M26 ura4-D18 leu1-32 dcr1*::*natMX6 tsn1*::*kanMX6* (pREP3X::*rnh201*$^{+}$) | This research |
| BP3511 | *h⁻ ade6-M26 ura4-D18 leu1-32 rnh1*::*kanMX6 rnh201*::*hphMX6* (pREP3X::*rnh201*$^{+}$) | This research |
| BP3512 | *h⁻ ade6-M26 ura4-D18 leu1-32 dcr1*::*natMX6 tsn1*::*kanMX6* (pREP3X-Hu*TSNAX*$^{+}$) | This research |
| BP3513 | *h⁻ ade6-M26 ura4-D18 leu1-32 dcr1*::*natMX6 tsn1*::*kanMX6* (pREP3X::Sp*tfx1*$^{+}$) | This research |
| BP3514 | *h⁻ ade6-M26 ura4-D18 leu1-32 rnh201*::*kanMX6 tsn1*::*natMX6* (pREP3x::Hu*TSNAX*$^{+}$) | This research |
| BP3515 | *h⁻ ade6-M26 ura4-D18 leu1-32 rnh201*::*kanMX6 tsn1*::*natMX6* (pREP3x::Sp*tfx1*$^{+}$) | This research |
| BP3516 | *h⁻ ade6-M26 ura4-D18 leu1-32 rnh1*::*kanMX6 rnh201*::*hphMX6* (pREP3X::Hu*TSNAX*$^{+}$) | This research |
| BP3517 | *h⁻ ade6-M26 ura4-D18 leu1-32 rnh1*::*kanMX6 rnh201*::*hphMX6* (pREP3X::Sp*tfx1*$^{+}$) | This research |
| BP3518 | *h⁻ ade6-M26 ura4-D18 leu1-32 dcr1*::*ura4 rnh1*::*kanMX6* (iso1) | This research |

| | | |
|---|---|---|
| BP3519 | *h⁻ ade6-M26 ura4-D18 leu1-32 dcr1*::*ura4 rnh1*::*kanMX6* (iso2) | This research |
| BP3520 | *h⁻ ade6-M26 ura4-D18 leu1-32 dcr1*::*ura4 rnh1*::*kanMX6* (iso3) | This research |
| BP3521 | *h+ ade6-M26 ura4-D18 leu1-32 dcr1*::*ura4 rnh1*::*kanMX6* (iso1) | This research |
| BP3522 | *h+ ade6-M26 ura4-D18 leu1-32 dcr1*::*ura4 rnh1*::*kanMX6* (iso2) | This research |

## 2.7. Genomic DNA extraction

Single colonies of a selected strain were inoculated into 5 ml YEL and incubated at 30°C until the culture was concentrated. Then Cells were extracted at 3,000 *g*, washed with one ml of sterile $dH_2O$, centrifuged at 3,000 *g*, and then resuspended in 1 ml of sterile $dH_2O$. Cells were moved to screw-cap tubes and centrifuged at 3,000 *g*. A mixture was made of 200 µl) phenol chloroform, acid washed beads (300 mg) and 200 µl of lysis buffer (1 ml Triton-X100, 5 ml 10% SDS, 5 ml 1 M NaCl, 0.5 ml TE 100X, in sufficient sterile $dH_2O$ to take the volume to 50 ml). A Bead-Beater (FastPrep120, ThermoSavant) was used for 30 secs to destabilize the cells, which were then centrifuged at 12,000 *g* for 15 mins. The supernatant was removed and then it was added to one ml of 100% ethanol. It was kept at –20°C for 1 hour then centrifuged at 12,000 *g* for 12 mins. The resultant pellets were washed in one ml of 70% ethanol, dried with air, and then resuspended in 100 µl of 1x TE buffer.

## 2.8. Confirmation of gene knockout by PCR screening

Genomic DNA for the candidate knockout strains was extracted. Various "check primers", were designed within and outside of the region of the desired genes, together with primers within the knockout cassettes (provided in Table 2.6). For 50 µl PCR reaction, 1 µl of a 10% dilution of extracted genomic DNA in TE buffer, 1 µl of 20 ng/µl of both forward and reverse primers, 25 µl of BioMix red (BioLine) and 23 µl sterile $dH_2O$ was used. The following PCR protocol was used: initial heating at 96°C for 1 min; 30 cycles of 1 min at 96°C; 30 secs at X°C, and 72°C as needed (letting 15–30 secs/kb); final elongation was conducted at 72°C for 5 mins. The primers set determined the annealing temperature (X°C), therefore it was variable. To visualise the size and quality of the PCR products, 1% agarose gel was used.

**Table 2.5. PCR primers utilised to delete target genes**

| Primer name | Sequence | Notes |
|---|---|---|
| rnh1-kanMX6-F | 5′TTGCAAAGTTTTGGGAAAAACTCCCAAG TTTTACTAAGTTTTACTATTTTAAAGCTAT TTTTGAATCTTCGCATTACGAACGGATCCC CGGGTTAATTAA-3′ | Forward primer for the Kanamycin cassette to replace the rnh1 |
| rnh1-kanMX6-R | 5′GAGTAGACGAAAATTATACGGCAAATTT CAAAAGAATGTACCTATATCCATTTTTTAC AGCGCTCATCATAGATGACCATGAATTCG AGCTCGTTTAAAC -3′ | Reverse primer for the Kanamycin cassette to replace the rnh1 |
| tfx1-natMX6-F | 5′-TATAGACTTATACATTTATAC CTTCCA CACGGCTTTGCTGAATTGAGGATATTATA AAACTTTAACCGAATTTGCCAAATCGGAT CC CCGGGTTAATTAA -3′ | Forward primer for the Nourseothricin cassette to replace the *tfx1* |
| tfx1-natMX6-R | 5′-ATTATGATTTTCAAAAGCTGCAAAACA GAAAAACTTTTAATAAACTAGTAAGGTGT CTGTCGAGAGCTGTCGATCATATATGAAT TCGAGCTCGTTTAAAC -3′ | Reverse primer for the Nourseothricin cassette to replace the *tfx1* |
| tsn1-natMX6-F | 5′-TTATTTGCATACTGAAAACATCATTCG AATATCAACACTACTCAACAGCATACATT ACAGATTAAGTCGACGGATCCCCGGGTT AATTAA-3′ | Forward primer for the Nourseothricin cassette to replace the *tsn1* |
| tsn1-natMX6-R | 5′-ATATTAAAAAAGCAATTTTATCGG CTCAATTTTAGTCAAGCGTACAGCTGG CAAATAAATTGTTAGCAATGAATTCGA GCTCGTTTAAAC-3′ | Reverse primer for the Nourseothricin cassette to replace the *tsn1* |
| rnh201-kanMX6-F | 5′TATTTTTTTATTCAGTTTTGAGCCAAAT ATTAGAAGTACTCTGATAATTCTTTAAAA GATACAAAGCAGCAATCTCAACCGGATCC CCGGGTTAATTAA-3′ | Forward primer for the Kanamycin cassette to replace the *rnh201* |
| rnh201-kanMX6-R | 5′GATTTTAAGCATAAATGTAAATTCGTAT CACTCTCACAATTAGTCTTAGGCAAAAGT AGTGACAGAGTATAGTAACTAAAGATTCG AGCTCGTTTAAAC-3′ | Reverse primer for the Kanamycin cassette to replace the rnh201 |
| sen1-kanMX6-F | 5′TTGCAAAGTTTTGGGAAAAACTCCCAAG TTTTACTAAGTTTTACTATTTTAAAGCTAT TTTTGAATCTTCGCATTACGAACGGATCCC CGGGTTAATTAA-3′ | Forward primer for the Kanamycin cassette to replace the *sen1* |
| sen1-kanMX6-R | 5′AGTAGACGAAAATTATACGGCAAATTTC AAAAGAATGTACCTATATCCATTTTTTACA GCGCTCATCATAGATGACCATGAATTCGA GCTCGTTTAAAC-3′ | Reverse primer for the Kanamycin cassette to replace the *sen1* |

**Table 2.6. Non-deletion targeting PCR primer sequences used in this study**

| Primer name | Sequence | Notes |
|---|---|---|
| Tfx1 check-forward | 5′-CAAATAGTCATCTTGATTTGC-3′ | Upstream of *tfx1* Open Reading Frame |
| Tfx1 check-reverse | 5′-TCTAACATATAGAAAGCAGCG-3′ | Downstream of *tfx1* Open Reading Frame |
| Tfx1-int-Forward | 5′-ATAAGAGGGAGAAAATTATTC G-3′ | Forward primer within *tfx1* |
| Tfx1-int-Reverse | 5′-CTCCTCGGGAGGAGTTGC -3′ | Reverse primer within *tfx1* |
| Tsn1-check-Forward | 5′-GAT CTA AACAACCCA AGC G-3′ | Upstream of *tsn1* Open Reading Frame |
| Tsn1- check-Reverse | 5′-GCATTCATCATAGGACTGCC-3′ | Downstream of *tsn1* Open Reading Frame |
| Tsn1-int-Forward | 5'-AAACTGACTGCAGAGGTC G-3' | Forward primer within *tsn1* |
| Tsn1-int-Reverse | 5'-GAACACAGAGATAGTACTGC- 3' | Reverse primer within *tsn1* |
| Dcr1 check-Forward | 5′-AGTATTCTGCTCGTGTGATTG-3 | Upstream of *dcr1* Open Reading Frame |
| Dcr1 check-Reverse | 5′-TGATTGAAACTCGAGATGCTTTG-3′ | Downstream of *dcr1* Open Reading Frame |
| Dcr1-int Forward | 5′-ATTCGACGAATGTCATCATGC-3′ | Forward primer within *dcr1* |
| Dcr1-int-Reverse | 5′-AGACGATATCATCAGTCACACG-3′ | Reverse primer within *dcr1* |
| KanMX6-Forward | 5′-CGGATGTGATGTGAGAACTG-3′ | Forward primer within kan cassette |
| KanMX6-Reverse | 5′-CAGTTCTCACATCACATCCG-3′ | Reverse primer within kan cassette |
| NatMX6-Forward | 5′-CATGGGTACCACTCTTGACG- 3' | Forward primer within nat cassette |

| | | |
|---|---|---|
| NatMX6-Reverse | 5′-CTCAGTGGCAAATCCTAACC- 3' | Revers primer within nat cassette |
| HphMX6-Forward | 5′-CTGTGTAGAAGTACTCGCCG-3′ | Forward primer within hph cassette |
| HphMX6-Reverse | 5'-AACTTCTCGACAGACGTCGC-3′ | Reverse primer within hph cassette |
| rnh1 check-Forward | 5'-CAGTCGCGGAGATCTAACTAGC-3′ | Upstream of *rnh1* Open Reading Frame |
| rnh1 check-Reverse | 5'-GCATTATGCAAAACGAGAACAA-3′ | Downstream of *rnh1* Open Reading Frame |
| rnh1-int-Forward | 5'-AGGGATGAGGCGTCGGATCA-3′ | Forward primer within *rnh1* |
| rnh1-int-Reverse | 5'-TTTGCTCTTCCCCAGCCAAC-3′ | Reverse primer within *rnh1* |
| rnh201 check-Forward | 5'-GATTGCTAGGAGATGACTCGCT-3′ | Upstream of *rnh201* Open Reading Frame |
| rnh201 check-Reverse | 5'-AAGTCTCATGCCAGCCATATTT-3′ | Downstream of *rnh201* Open Reading Frame |
| rnh201-int-Forward | 5'-CGAATCCCGCAAAATCGAAT-3′ | Forward primer within *rnh201* |
| rnh201-int-Reverse | 5'-GAAGCTAAACTCACGATGGG-3′ | Reverse primer within *rnh201* |
| sen1-check-Forward | 5'-CAACGTTTATTTGGGTCCATTT-3′ | Upstream of *sen1* Open Reading Frame |
| sen1-check-R | 5'-TCAATTGGCCTTCTTCACCTAT-3′ | Downstream of *sen1* Open Reading Frame |
| sen1-int-Forward | 5'-TACTGAAATAAGAATTTCTT-3′ | Forward primer within *sen1* |
| sen1-int-Reverse | 5'-TAACAGAAATGATACAACTG-3′ | Reverse primer within *sen1* |
| pAW1-Forward | 5′-AGTTTAACTATGCTTCGTCGGC-3′ | Forward primer within *ura4* cassette |
| pAW1-Reverse | 5′-ACACGACATGTGCAGAGATGC-3′ | Reverse primer within *ura4* cassette |
| act1-Forward | 5′-ATGGAAGAAGAAATCGCAG-3′ | Forward primer within *act1* |
| act1-Reverse | 5′-CAAAACAGCTTGAATAGC-3′ | Reverse primer within *act1* |

| | | |
|---|---|---|
| nmt promoter pREP F1 | 5′-GAAGTTCCTCGACAAGC-3′ | Forward primer within pREP3X |
| Hs translin F-(*Bam*H1) | 5′CGCGGATCCATGTCTGTGAGCGAGATCTTCG-3′ | Forward primer used to synthesis the first strand of cDNA for Human tsn1. |
| rnh1-F qPCR | 5′ACTGGTATATAGTACATGGGATGAG 3′ | Forward qPCR primer for amplification of rnh1 |
| rnh1-R qPCR | 5′-AATTCCTGAGCAGCCTCATAG -3′ | Reverse qPCR primer for amplification of rnh1 |
| Pac1-F qPCR | 5′-GTCATTGAAGAACCCTCCTCTC -3′ | Forward qPCR primer for amplification of pac1 |
| Pac1-R qPCR | 5′-TCAGACCGTAAAGGTGGTAATG-3′ | Reverse qPCR primer for amplification of pac1 |
| rnh1F cloning (*Xho*l) | 5′CCGCTCGAGATGGGTGGAAATAAGCGTGC-3′ | Forward primer used to synthesis the first strand of cDNA for rnh1 |
| rnh1 R cloning (*Bam*H1) | 5′CGCGGATCCTTACTCAGAAGCTCCTCGCC-3′ | Reverse primer used to synthesis the first strand of cDNA for rnh1. |

## 2.9. Yeast meiotic crosses

Culturing of 2.5 x $10^7$ samples of *S. pombe* cells of opposite mating type ($h^+$ and $h^-$) was undertaken in 5 ml yeast-extract liquid (YEL) with 250 mg/l supplemental adenine. This was followed by mixing in a 1.5 ml Eppendorf centrifuge tube in identical 750 µl volumes for every strain. Microcentrifugation was performed on the cells, with aspiration of the supernatant. 1 ml sterile distilled water was used to wash the pellet again before being subjected to renewed centrifugation. After pellet resuspension in 50 µl distilled sterile water, cells were spotted on SPA, plates containing 250 mg/l adenine, uracil, and leucine, and incubated for 3-4 days. From mating spots cells were scraped from plates and introduced into 1 ml of an aqueous solution of 0.6% β-glucuronidase (Sigma) in an Eppendorf tube. Spores were released from the asci and vegetative cells were eradicated through mixture and incubation of the suspension for 16 hours at 25°C. The next step was addition of ethanol in a proportion of 30% and five-minute incubation at ambient temperature. The spores were subjected to 60secs centrifugation in an

Eppendorf microcentrifuge, followed by elimination of the supernatant and resuspension of the spore pellets in 1 ml distilled sterile water. To enable viable spores to grow, plating of dilutions on to YEA was undertaken. After three-day plate incubation at 33°C, replica plating of colonies on selective media was performed according to requirements.

For isolation of new strains using tetrad analysis, asci were removed from SPA plates and spores spotted onto YEA using a yeast tetrad dissecting instrument from Singer Instruments Ltd.

## 2.10. Iodine staining for mating-type test

Unlike vegetative cells, *S. pombe* spores contain a starch-like compound. To test for the presence of mating, mating mixes on SPA are exposed to iodine vapours following 3 days under mating conditions. Positive and negative response to iodine being respectively indicated by the black colouring of spore-containing materials and the yellow colouring of materials comprising solely vegetative cells after five minutes of exposure.

## 2.11. Spot test

A single colony of the required *S. pombe* strain was incubated until late log phase at 30°C in 5 ml YEL containing 250 mg/l supplemental adenine. Then using a light microscope (40X), the following day the cells were counted using a haemocytometer. Sterile $dH_2O$ was applied to resuspend cells to get a concentration of 5 x $10^6$ cells/ml. The cell mixture was serially diluted four times; 10 µl of each dilution was spotted onto YEA plates supplemented with 250 mg/l adenine and the appropriate concentration of drug, where appropriate (Table 2.7). Using the appropriate solute, a set of plates was also made, and cell dilutions were spotted onto these as controls. Plates were incubated for 3-4 days at the right temperature. This same procedure was used for minimal media conditions for strains containing plasmids, but YEL and YEA were exchange for EMMG liquid and EMMG agar containing appropriate supplements respectively.

**Table 2.7. drugs used in this study**

| Drug | Working concentrations used |
|---|---|
| Methyl Methanesulfonate (MMS) | (0.0075%, 0.01%) |
| Mitomycin C (Sigma) | (2, 3 mM) |
| Hydroxyurea (HU) (Sigma) | (8, 9, 10 mM) |
| Camptothecin (Sigma) | (4, 5, 6, 8 μg/ml) |
| Phleomycin | (3,5 μg/ml) |

## 2.12. Storage of *S. pombe* Strains

Single colonies were introduced into 5 ml of YEL supplemented with 250 mg/l of adenine and left to grow. The cultures were shaken until cell saturation. Glycerol was added to 700 μl of culture to get a final concentration of 30%. The cultures were vortexed before storing them at -80°C. For strains containing plasmids YEL was replaced with liquid EMMG containing appropriate supplements.

## 2.13. Ultraviolet (UV) irradiation of *S. pombe*

Following the protocol described in Section 2.9, 10 μl of each serial dilution of *S. pombe* was spotted onto YEA plates supplemented with 250 mg/l of adenine (250 mg/l) and left to dry. Plates were then exposed to UV irradiation (70 and 100 J/$m^2$; CL-1000 UV cross linker). They were then incubated for 3-4 days at the right temperature.

## 2.14. Cloning of *S. pombe* open reading frames

### 2.14.1. RNA Extraction and DNase treatment

Single colonies were introduced into 5 ml of YEL supplemented with 250 mg/l of adenine and cultured overnight in an orbital incubator at 30°C until they reached the exponential phase ($OD_{600}$ of 0.6–0.8). Then RNA was extracted with the assistance of MasterPure ™ Yeast RNA Purification Kit (Epicentre). 1.5 ml of culture was centrifuged for 1 min at 3,000 *g*. The supernatant was aspirated off. A 300 µl mixture containing of RNA extraction reagent and 2 µl of 50 µg/µl proteinase K, was added to the tubes. The tubes were incubated for 15 mins at 70°C; during the incubation period, the tubes were mixed at 4 mins intervals. The tubes were positioned on ice sheet for 4 mins. Then the tubes were filled with 175 µl of MPC protein precipitation reagent. Mixtures were centrifuged at 4°C at 10,000 *g* for 10 mins. The supernatant was moved to another Eppendorf tube containing 500 µl of isopropanol. The tubes were inverted then centrifuged at 10,000 *g* for 10 mins at 4°C. Excess isopropanol was excluded and just after it, the pellets were resuspended in 200 µl DNase I solution (comprised of 175 µl of deionised water, 5 µl of RNase-free DNase I and 20 µl of DNase buffer (100 mM Tris-HCl (pH 7.5), 25 mM MgCl2, 1 mM CaCl2)). The samples were incubated for 15 mins at room temperature. Then to each tube, 200 µl of MPC protein precipitation reagent and 200 µl of 2X T and C Lysis Solution were added. Tubes were vortexed then placed on ice for 3 mins. After cooling, the samples were centrifuged at 10,000 *g* up to 10 mins at 4°C. after this step, the supernatant was then moved to a fresh Eppendorf tube with an addition of 500 µl of isopropanol. Then, the tubes were inverted and centrifuged again at 10,000 *g* for 10 mins at 4°C. Excess isopropanol was removed carefully. Then using 1 ml of 70% ethanol, the pellets were washed twice. After removing the ethanol, the RNA was resuspended in 350 µl of TE buffer. To protect the RNA, 1 µl of RiboGuardTM RNase Inhibitor was added.

Lastly, the RNA was treated with RNase-free DNase (Promega) by combining 1 µl RNase-Free DNase with 1 µg of RNA, 1 µl of RNase-Free DNase reaction buffer up to 10 µl nuclease-free water. Tubes were incubated at 37°C for 30 mins. After this duration, 1 µl of DNase Stop Solution (Promega) was added. The tubes were incubated for 10 mins at 65°C. Then the RNA has been preserved at-20°C.

### 2.14.2. Synthesis of cDNA

Synthesis of a cDNA from total RNA was achieved by employing the SuperScriptTM III first-strand synthesis kit (Invitrogen, Cat#18080-051) in line with the manufacturer's guidelines. The kit came with the necessary primers and reagents. Preparation of two sterile PCR tubes was undertaken. The content of the first tube included 2 µg total RNA, 1 µl of 50 µM oligo (dT), and 1 µl of 10 mM dNTP mix, with the remaining volume consisting of 10 µl DEPC-treated water. After five-minute incubation at 65°C, the tube was kept on ice for a minimum of 60 secs. The content of the second tube included 2 µl of 2 ml RT buffer, 4 µl of 25 mM magnesium chloride, 2 µl of 0.1 M DTT, 1 µl RNaseOUTTM and 1 µl SuperScriptTM III RT. After gentle mixing of the compositions of the two tubes into a new single tube, flash spin was performed for collection, followed by 50 mins incubation at 50°C and further 5 mins incubation at 85°C. A flash spin was conducted again after tube chilling on ice. Following addition of 1 µl RNase H, 20 mins incubation was performed at 37°C. The cDNA thus obtained was placed in storage at -20°C.

PCR amplification on *rnh1* was conducted by employing MyTaqTM Red Mix (Bioline) alongside 2µl cDNA. The applied PCR procedure with 10-pmol/µl Rnh1F cloning (*Xho*l,5 units) and Rnh1 R cloning (*Bam*H1,10 units) consisted of one 3 min cycle at 95°C, 35 30 sec cycles at 95°C, one 20 sec cycle at 62°C, and one 30 sec cycle at 72°C. An extension step was subsequently performed for 5 mins at 72°C. The Macherey-Nagel, Cat.No. 740609 kit was then employed to conduct culm clean on the reaction (see Section 2.14.3), followed by elution in 50-µl buffer EB.

## 2.14.3. Digestion and Purification of PCR products from agarose gel

For testing purposes, digestion of the vector and the insert by *Bam*H1 and *Xho*I was performed through the general digestion protocol issued by New England BioLabs (NEB). A 50 µl volume of the insert and vector was supplemented with a mixture consisting of 6 µl of 5 ml cutsmart buffer, 2µl water and 2µl *Bam*H1 (10 units) and *Xho*l (5 units) enzymes. The digestion reaction was subjected to 2 hour incubation at 37°C. The mixture was subsequently enriched with 16 µl 5x DNA loading dye. The sample was loaded on 1% agarose and run for one hour at 100 V. The gel was visualised under UV light, while vector and insert removal was performed with a

fresh sterile scalpel. The guidelines set out by the manufacturer were followed when using the PCR clean-up gel extraction kit (Macherey-Nagel, Cat.No. 740609). The Eppendorf tube was weighed both before and after the removed fragment of DNA (gel slice) was added to the tube. According to the guidelines, 200 µl buffer NTI had to be added for each 100 mg agarose gel. Therefore, 274 µl buffer NTI was added to the tube, which was then incubated for 10 mins in a heating block at 50°C. Furthermore, the incubating sample was vortexed at 2 min intervals until full dissolution of the gel slice. NucleoSpin gel and PCR clean-up column were added to a collection tube that contained the whole sample. The tube was then centrifuged for 30 secs at 10,000 *g*, with removal of flow-through. 700 µl buffer NT3 was used to enrich the column, after which the tube was centrifuged again for 30 secs at 10,000 *g*, with removal of flow-through. The previous procedure was subsequently performed again, in line with the manufacturer's guidelines. The tube that contained the column was centrifuged for 60 secs at 10,000 *g* to fully remove the buffer NT3. The column was introduced into a new Eppendorf tube with 20 µl buffer NE, which was subjected to 5 mins incubation at 70°C. The final step was centrifugation for 1 min at 10,000 g. The next procedure was dephosphorylation of the vector through addition of 1 µl shrimp alkaline phosphate, 6 µl 5 ml CutSmart buffer, and 3 µl water to 50 µl vector. The Macherey-Nagel Cat. No. 740609 kit was used according to the manufacturer's guidelines for column cleaning of the vector. Since the vector exceeded 7 Kb, sample elution was performed in 50 µl buffer EB at 70°C. A last quantification and quality verification were subsequently undertaken by using the nano drop. The insert was merged with the vector through DNA ligation; with the ligation reaction being performed with 100 ng total DNA. The ratio of vector to insert was about 1:3 and was determined based on http://www.insilico.uni-duesseldorf.de/Lig_Input.html.

### 2.14.4. High-efficiency transformation of *E. coli*

The process of NEB 10-beta Competent *E. coli* transformation was commenced by adding 5 µl of 100 ng plasmid DNA to a vial of NEB 10-beta Competent *E. coli* (a derivative of DH10b), which were mixed gently. After the solution was kept on ice for half an hour, the cells were subjected to 30 secs heat-shock at 42°C and placed on ice again for 5 mins. 950 µl S.O.C. medium was subsequently added at ambient temperature and the tube was horizontally shaken for one hour at 37°C and 200 r.p.m. This was followed by spreading of 100 and 200 µl from

each transformation of a selective plate that had been warmed beforehand, which was then incubated overnight at 37°C.

### 2.14.5. PCR colony screening

Eppendorf tubes containing 20 µl purified water were used for resuspension of five colonies extracted from two overnight plates. Preparation of a master mix sufficient for five PCR reactions (one extra) was achieved by mixing the required reagents in an Eppendorf tube: 75 µl MyTaq, 6 µl of 10 pmol/µl forward primer1 (1:10 dilution) 6 µl of 10 pmol/µl reverse primer1 (1:10 dilution) and 33 µl distilled water. After a quick centrifugation, 20 µl of the mix was poured in every one of the five PCR tubes. The tubes were subsequently enhanced with 5 µl resuspended colony. The samples were incubated in the PCR analyser for a 3 min cycle at 95°C, 35 30 secs cycles at 95°C, one 20 sec cycle at 62°C, and one 30 sec cycle at 72°C. An extension step was then performed for 5 mins at 72°C. To acquire the result, the PCR products were run on 1% agarose gel.

## 2.15 Quantitative PCR

For the *pac1* and *rnh1* qRT–PCR experiments, the QuantiTect SYBR Green PCR Kit (Qiagen; 204054) was used to PCR amplify cDNA using a CFX96 real-time system (Bio-Rad) in accordance with the manufacturer's instructions. For a 20 µl reaction mixture, the following were combined: 10 µl of SYBRTM Green master mix, 4 µl of the diluted cDNA (including 2.5 µl of nuclease-free water and 1.5 µl cDNA and), 4µl of 10 pmol/µl forward and reverse primers and 2 µl of sterile $dH_2O$. Triplicate samples were prepared and loaded into PCR plates (BioRad) and he following PCR protocol was used: 3 mins at 95°C, then 40 cycles at 95°C for 10 secs, 30 secs at 60°C, and 10 secs at 95°C. Table 2.6 details the oligonucleotide sequences used in these experiments.

# Chapter3: Investigation of genetic association between *tsn1* and RNAse H encoding genes.

# 3.1. Introduction

For cells to proliferate, accurate DNA replication is essential. Evolution has that ensure DNA replication is high fidelity (Kang, et al, 2018; Williams, Lujan & Kunkel, 2016; Potenski& Klein, 2014). However, endogenous or exogenous agents can alter the chemical composition and structure of DNA or cause barriers to DNA replication progression (Bouwman & Crosetto, 2018; Parker, Botchan & Berger, 2017). The consequences of not remedying replicative perturbations can be mutagenic and/or cytotoxic. Whilst there are various DNA abnormalities that threaten genomic stability, the presence of ribonucleotides in the DNA backbone is common. Additionally, transient annealing occurs between chromosomal DNA and RNA strands (often referred to as R-loops), or single and tandem ribonucleotides (rNMPs) resulting in RNA:DNA hybrids, which can potentially impede replication fork progression (Cornelio, et al, 2017; Williams, Lujan & Kunkel, 2016: Kellner, and Luke, 2020). For example, R-loops can develop during transcription when developing mRNA molecules fail to separate from the DNA template strand. During replication, large quantities of single rNMPs can be incorporated into the freshly formed DNA by the action of replicative polymerases. Moreover, should the rNMPs used to synthesise the lagging strand primer persist the hybrid structures also endure. To generate the full lagging strand from Okazaki fragments, these primers must first be removed (Zheng& Shen, 2011; Vaisman et al., 2013). This has implications for normal DNA replication and other genomic behaviour, ultimately disrupting the chromosome (Cornelio, et al, 2017).

The elimination of deleterious rNMPs and/or RNA:DNA hybrids is undertaken by several nucleases (Fragkos & Naim, 2017; Belotserkovskii et al., 2018). These enzymes act with specificity, hydrolysing the phosphodiester bond between deoxyribonucleotides and ribonucleotides.

RNase H1 (Rnh1) and RnhH201 (Rnh201) are ribonucleotide-specific ribonucleases that eliminate RNA:DNA hybrids. Rnh201, is composed of a heterotrimeric complex with Rnh202 and Rnh203, the complex has ribonucleotide excision repair (RER) activity, which has been demonstrated using the enzymes extracted from fission yeast *S. pombe* and *E. coli* (Vaisman, and Woodgate, 2015; Sparks, et al, 2012; Hyjek, Figiel and Nowotny, 2019).

In each of these organisms, RNase H201 is the principal enzyme responsible for removing rNMPs. RNase H2 activity is encoded by the *rnhB* gene in *E. coli* and the catalytic subunit by *rnh201* in *S. pombe*. These ribonucleases act with specificity, removing RNA fragments from the DNA template strand by hydrolysing the phosphodiester bonds between RNA and DNA that are present. They also hydrolyse the phosphodiester bonds of individual rNMPs present in the DNA double-stranded molecules (Williams, Lujan & Kunkel, 2016; Kojima, et al, 2018; Lockhart, et al, 2019).

The cleavage activity of type I ribonucleases is dependent upon the presence of a fragment with no less than four consecutive ribonucleotides within the DNA strand. RNase H1 enzyme is encoded by *rnhA* in prokaryotes and by *rnh1* in eukaryotes (Williams, Lujan & Kunkel, 2016; Kojima, et al, 2018; Lockhart, et al, 2019).

Whilst R-loops are thought to cause replicative stress, it is also thought that they are needed to help repair, particularly for DSB, where it is proposed RNA Pol II makes new RNA:DNA hybrids at the site of damage and this is needed to recruit the repair factors (Zhao et al., 2017; D'Alessandro et al., 2018). It is thought that this is the reason the *S. pombe rnh1*Δ *rnh201*Δ double mutant is sensitive to DNA damaging agents, as they cannot process the RNA:DNA hybrids and so fail to complete the DSB repair. So, in *S. pombe* Rnh1 and Rnh201 have a positive role in repair and RNase H activity is also essential for the repair of DSBs (Ohler et al., 2016). The contribution from both RNase H1 and RNase H2 means that there is redundancy in the RNase H pathways, thus enabling successful DSB repair should one pathway fail (Ohle et al., 2016).

Translin was originally thought to be involved mediating chromosomal rearrangements (Aoki et al., 1995; Gajecka et al., 2006). Based on that and the increased affinity that Tsn1 in *S. pombe* has for RNA than for DNA (Jaendling & Mcfarlane, 2010), we suggest that Tsn1 could be involved in reducing the stability of RNA:DNA hybrids throughout the genome; this reduces transcription-DNA replication conflicts, thus saving the stability of the chromosomes. This led us to hypothesize that Tsn1 and/or Tfx1 might function in an RNase H-associated pathway.

# 3.2. Results

## 3.2.1. Assessment of a role for *tsn1* in an RNAse H-associated pathway

To determine whether *tsn1* function is redundant with RNAse H activity appropriate double mutants were required (*tsn1*Δ *rnh1*Δ and *tsn1*Δ *rnh201*Δ). To create the desired mutant strains, direct gene mutation method was used (Bähler et al., 1998). Genetic crossing was not used in this present data, as a study by the McFarlane group (unpublished) noted that the mating outcomes of strains with the *tsn1*Δ mutation did not follow Mendelian patterns of segregation. This indicates that *tsn1*Δ may be associated with meiotic haplo-insufficiency or be a poison-antidote meiotic driver (Hu et al., 2017; Nuckolls et al., 2017). In support of this, a study by Dudin et al. (2017) that aimed to identify non-essential mutations of *S. pombe* associated with aberrant mating and sporulation processes, found that the frequency of sporulation defects was high for *tsn1*Δ mutants. Additionally, Blyth and co-workers (2018) also observed meiotic defects in *tsn1*Δ mutants, supporting the proposal that there is an unknown function for Tsn1 in maintaining genetic and or epigenetic stability in meiosis, further justifying the direct deletion approach for mutant generation; therefore, in this study, *de novo* deletion (direct gene mutation) were created from mitotically dividing cells. No less than two mutants were created for each strain.

Single mutants were firstly created for *rnh1* [*rnh1*Δ (BP3401)] and *rnh201* [*rnh201*Δ (BP3405)] from the parent strain (BP90). Double mutants, *tsn1*Δ *rnh1*Δ (BP3426), *rnh201*Δ *tsn1*Δ (BP3417) and *rnh1*Δ *rnh201*Δ (BP3410) were created from deleting the required gene from the single mutant *tsn1*Δ (BP1079), *rnh201*Δ (BP3405) and *rnh1*Δ (BP3401) (see Table 2.4) (a minimum of two isolates were isolated and tested for each genotype). *hphMX6* (hygromycin-resistant) *natMX6* (nourseothricin-resistance) and *kanMX6* (kanamycin-resistant) genes were used as deletion marker genes. To amplify the gene replacement cassettes, PCR was used with primers of 80 bp homologous sequences that were upstream and downstream contiguous with the open reading frames (ORFs) of the genes to be deleted. The primers also comprised a 20 bp sequence that was homologous to the appropriate antibiotic-resistant marker within a marker-carrying plasmid (Figure 3.1). Marker cassette PCR product was transformed into the appropriate *S. pombe* strains and mutant candidates were selected for screening (details in Section 2.5). To assess whether the deletions were successful, three sets of PCR primers were used for each of the genes deleted (Figures 3.2), Successful of *rnh1*Δ,

*rnh201*Δ, *rnh1*Δ *rnh201*Δ, *rnh1* Δ *tsn1*Δ , *rnh201* Δ *tsn1*Δ deletion was confirmed in Figure 3.3, 3.4, 3.5, 3.6 and 3.7 respectively.

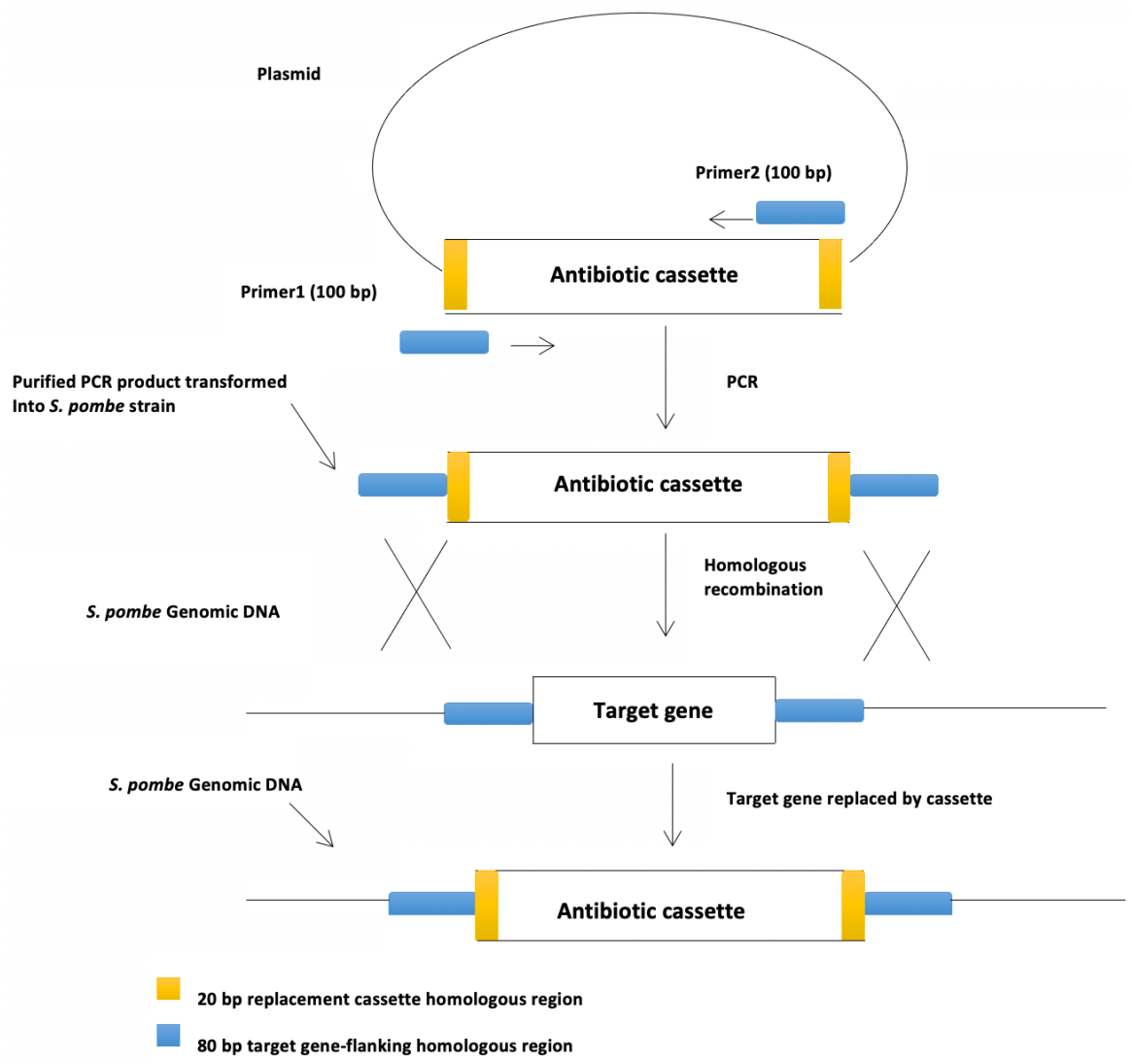


**Figure 3.1. Schematic illustration depicting the target gene knockout process**

The amplification of selectable antibiotic resistant cassettes uses various plasmids with distinct gene selections as templates. Primers contained a 20 bp (yellow box) sequence that was homologous to the plasmid containing the target antibiotic resistant marker, and containing 80 bp homologous sequences, flanking the ORF upstream and downstream of the target gene destined for deletion (blue box). The marker cassette replaces the target gene via a homologous recombination reaction.

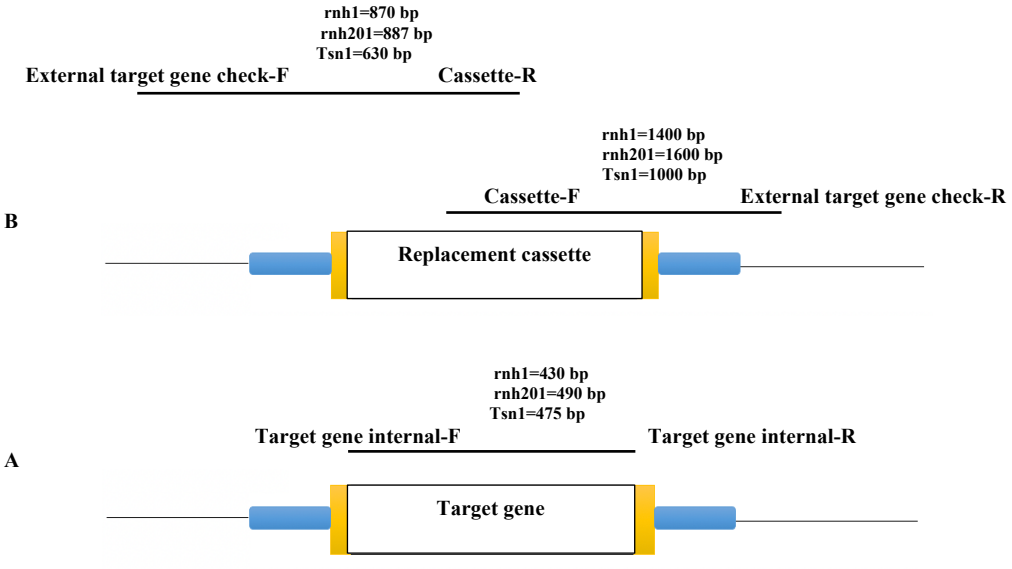


**Figure 3.2. Schematic image of the position of the primers used to verify the gene of interest had been deleted.**

Following the process reported by Bähler et al. (1998), antibiotic resistant cassettes were used to replace all the deleted target genes. Confirmation of the deletion was made using three sets of checking primers. A- One primer set targets the gene to be deleted internal-F/target gene internal-R; no PCR products of the candidate genes should be generated once they have been successfully replaced with the cassette genes. B-Due to the presence of the cassettes, PCR using the external target gene check-F/cassette-R and cassette-F/external target gene check-R primer sets should yield appropriately sized products from the candidates with successfully deleted genes, but not from strains where successful deletion has failed to occur.

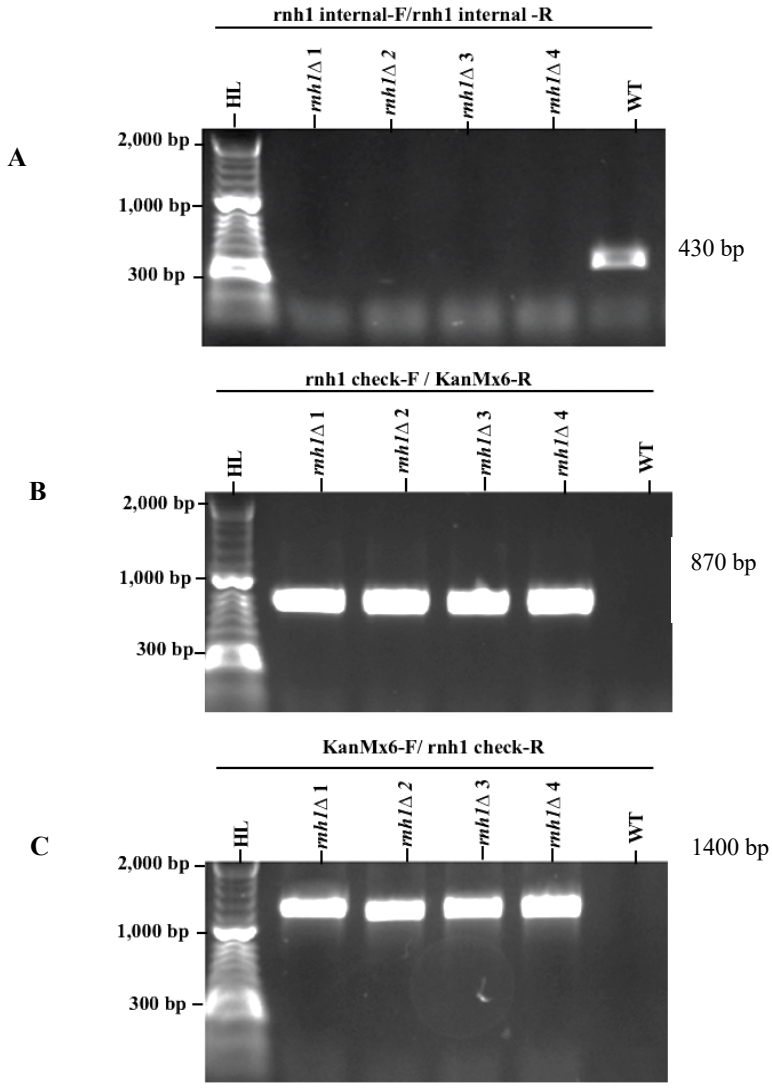


**Figure 3.3. PCR screening for successful *rnh1*Δ deletion.**

**A.** Image of agarose gels of PCR products for the WT strain (BP90) and *rnh1*Δ single mutant candidates. The *rnh1*gene internal PCR product is generated using rnh1-internal-F and rnh1-internal-R primers measures 430 bp. No PCR products are detectable in the successful *rnh1*Δ candidate strains. **B**. The PCR primers rnh1 check-F and kanMX6-R were used to check the WT and *rnh1*Δ candidate strains. Whilst no bands were detected in the WT, the *rnh1*Δ strains exhibit a band of approximately 870 bp. **C.** To amplify the WT and *rnh1*Δ candidate strains, the kanMX6-F and rnh1check-R primers were used. 1400 bp product is evident in the *rnh1*Δ strains, but not the WT strain. H = Hyper ladder.

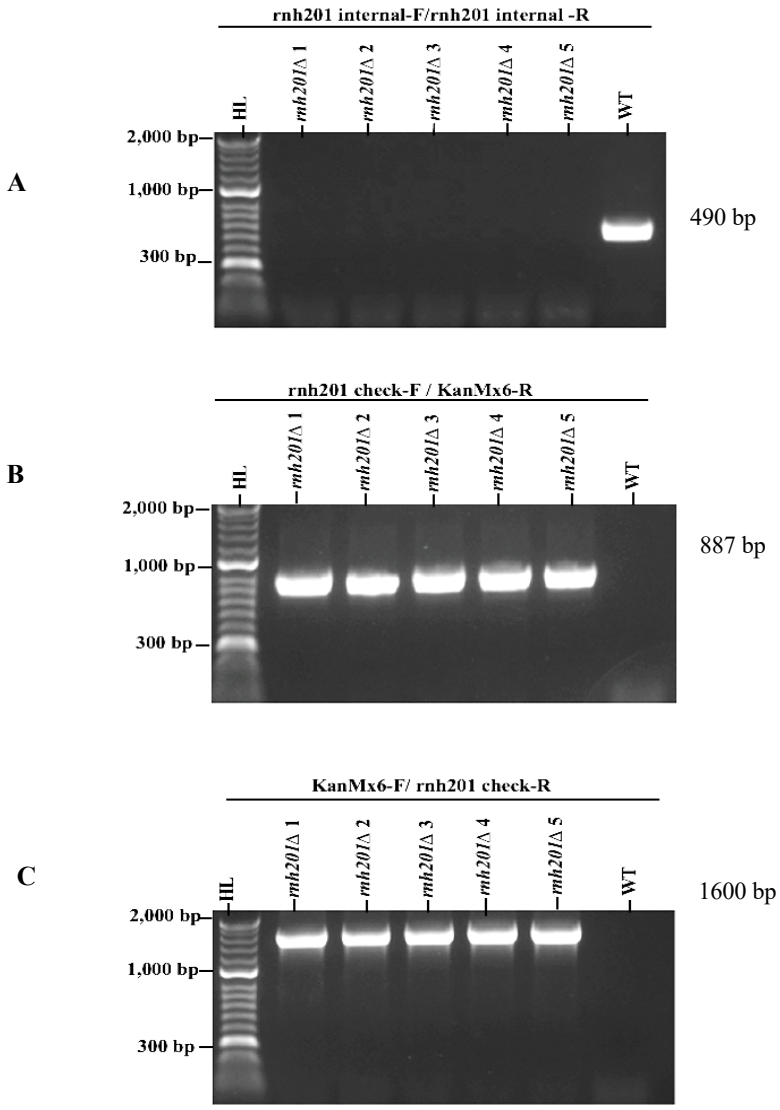


**Figure 3.4. PCR screening of successful *rnh201*Δ deletion.**

**A**. Image of agarose gels for PCR products for the WT strain (BP90) and *rnh201*Δ single mutant candidates. The r*nh201*gene internal PCR product is generated using rnh201-internal-F and rnh201-internal-R primers measures. No PCR products are detectable in the successful *rnh201*Δ candidate strains. **B**. The PCR primers rnh201 check-F and kanMX6-R were used to check the WT and *rnh201*Δ candidate strains. Whilst no bands were detected in the WT, the *rnh201*Δ strains exhibit a band of approximately 887 bp. **C.** To amplify the WT and *rnh201*Δ candidate strains, the kanMX6-F and rnh201check- R primers were used. 1600 bp product is evident in the *rnh201*Δ strains, but not the WT strain. H = Hyper ladder.

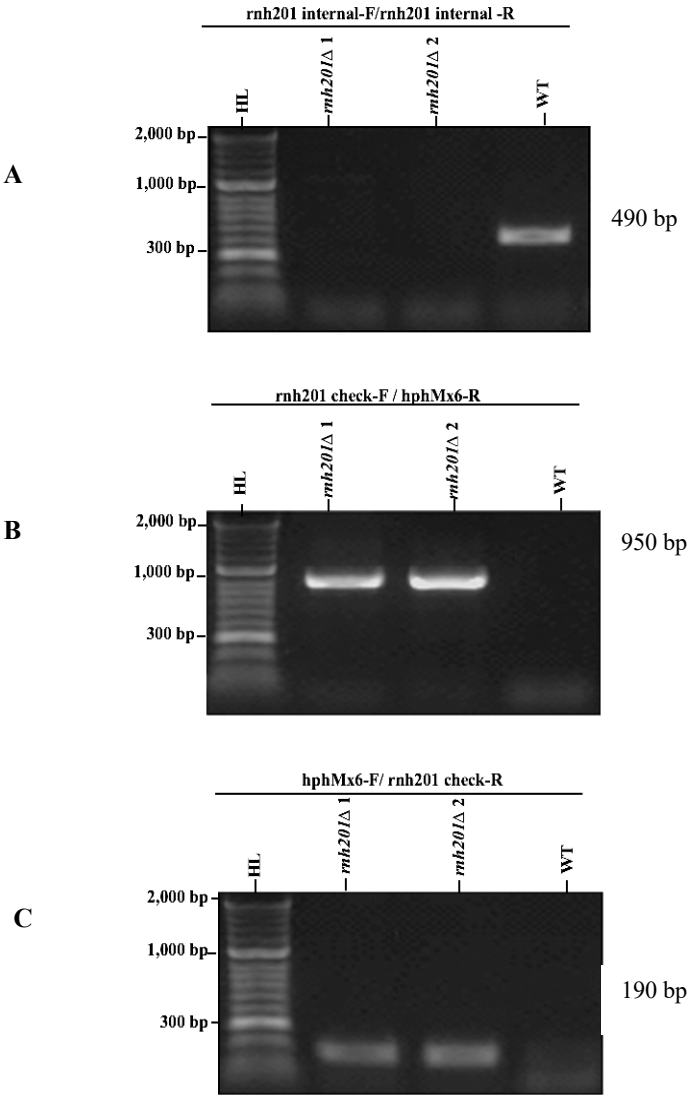


**Figure 3.5. PCR screening of successful *rnh1*Δ *rnh201*Δ double mutant deletion.**

**A.** Image of agarose gels for PCR products for the WT strain (BP90) and *rnh201* gene deletion *in rnh1*Δ background. The *rnh201* gene internal PCR product is generated using rnh201-internal-F and rnh201-internal-R primers measures 490 bp. No PCR products are detectable in the successful *rnh201*Δ candidate strains. **B**. The PCR primers rnh201 check-F and hphMX6-R were used to check the WT and *rnh201*Δ candidate strains. Whilst no bands were detected in the WT, the *rnh201*Δ strains exhibit a band of approximately 950 bp. **C.** To amplify the WT and *rnh201*Δ candidate strains, the hphMX6-F and rnh201check- R primers were used. 190 bp product is evident in the *rnh201*Δ strains, but not the WT strain. H = Hyper ladder.

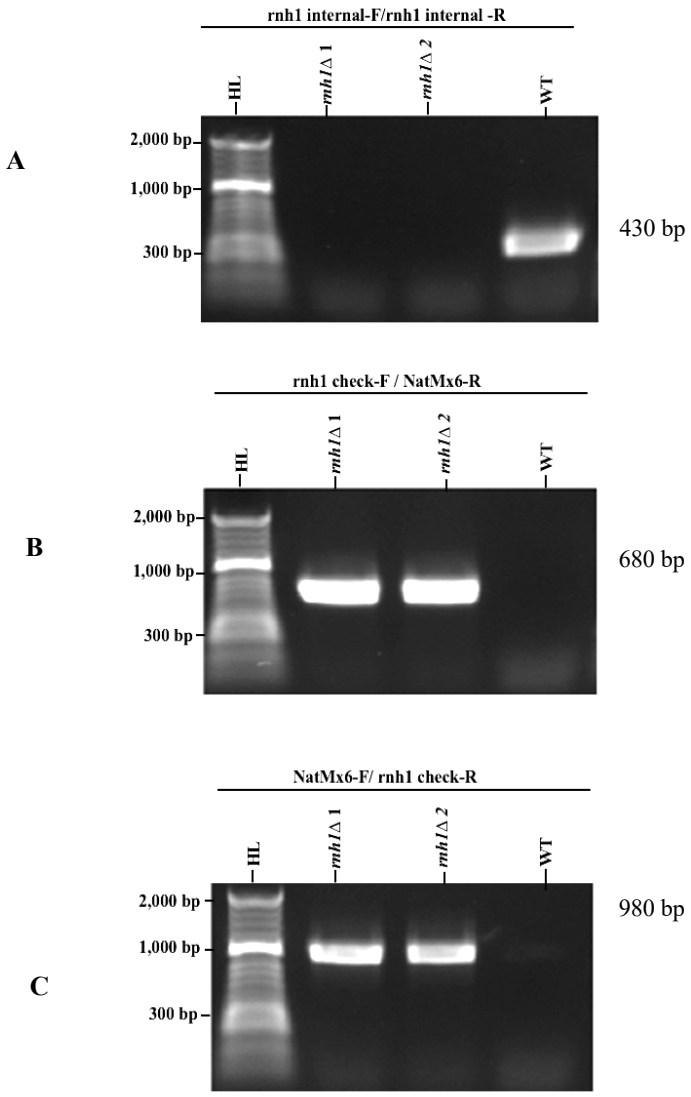


**Figure 3.6. PCR screening of successful *tsn1*Δ *rnh1*Δ double mutant deletion.**

**A.** Image of agarose gels for PCR products for the WT strain (BP90) and *rnh1* gene deletion *in tsn1*Δ *background.* The *rnh1*gene internal PCR product is generated using rnh1-internal-F and rnh1-internal-R primers measures 430 bp. No PCR products are detectable in the successful *rnh1*Δ candidate strains. **B**. The PCR primers rnh1 check-F and natMX6-R were used to check the WT and *rnh1*Δ candidate strains. Whilst no bands were detected in the WT, the *rnh1*Δ strains exhibit a band of approximately 680 bp. **C.** To amplify the WT and *rnh1*Δ candidate strains, the natMX6-F and rnh1check- R primers were used. 980 bp product is evident in the *rnh1*Δ strains, but not the WT strain. H = Hyper ladder.

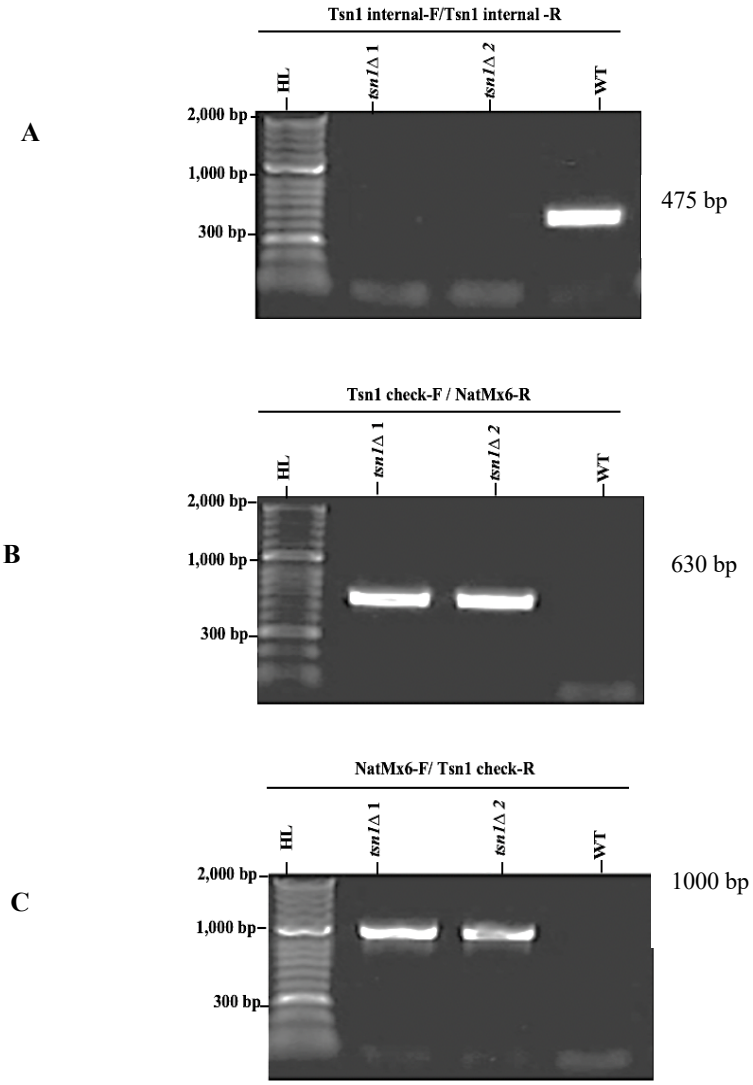


**Figure 3.7. PCR screening of successful *rnh201*Δ *tsn1*Δ double mutant.**

**A.** Image of agarose gels for PCR products for the WT strain (BP90) and *tsn1*gene deletion in *rnh201*Δ background. The *tsn1*gene internal PCR product is generated using tsn1-internal-F and tsn1-internal-R primers measures 475 bp. No PCR products are detectable in the successful *tsn1*Δ candidate strains. **B**. The PCR primers tsn1 check-F and natMX6-R were used to check the WT and *tsn1*Δ candidate strains. Whilst no bands were detected in the WT, the *tsn1*Δ strains exhibit a band of approximately 630 bp. **C.** To amplify the WT and *tsn1*Δ candidate strains, the natMX6-F and tsn1check- R primers were used. 1000 bp product is evident in the *tsn1*Δ strains, but not the WT strain. H = Hyper ladder.

### 3.2.2. Assessment of a role for *tsn1* for DNA damage response in the absence of RNase H activity.

As described earlier, eukaryotic cells have evolved several mechanisms to prevent the spontaneous creation/stabilisation of RNA:DNA hybrids. These mechanisms include the RNase H1 and H2 enzymes that degrade RNA component of RNA:DNA hybrids (Ohle, et al, 2016; Zhao, et al, 2018). Thus, we postulated whether *tsn1* has a function that is redundant with an RNase H activity encoded by *rnh1* and *rnh201.* Both genes are thought to provide redundant function (although *rnh201*Δmutants do exhibit sensitivity to DNA damage under certain circumstances: see Section 3.2.5). Therefore, the appropriate double mutant strains of *S. pombe* that had been constructed were exposed to various DNA-damaging drugs and their responses assessed. Agents used included hydroxyurea (HU) which is responsible to inhibit DNA replication (Figure 3.8), phleomycin which is responsible for making DNA DSBs (Figure 3.9), methyl methane sulfonate (MMS) which is alkylates DNA (Figure 3.10), and camptothecin (CPT) which is a topoisomerase inhibitor (Figure 3.11). In each of the experiments a *rad3-136* mutant was used as positive control (*rad3* is a checkpoint control gene); the *rnh1*Δ *rnh201*Δ double mutant also serves as a positive control, as loss of both RNAse H encoding genes results in a defective DNA damage response (Ohle et al., 2016). Compared to WT, neither *rnh1*Δ nor *rnh201*Δ single mutants showed sensitivity to DNA damaging agents under these conditions. Compared to the WT and the *tsn1*Δ *rnh1*Δ double mutant exhibited no overt sensitivity to any of the agents tested (Figure 3.8-3.11). However, the *tsn1*Δ *rnh201*Δ double mutant was hypersensitive to HU (Figure 3.8) and phleomycin (Figure 3.9) and showed mild sensitivity to MMS (Figure 3.10) but, unlike the *rnh1*Δ *rnh201*Δ double mutant, the *tsn1*Δ *rnh201*Δ double mutant showed no sensitivity to CPT (Figure 3.11).

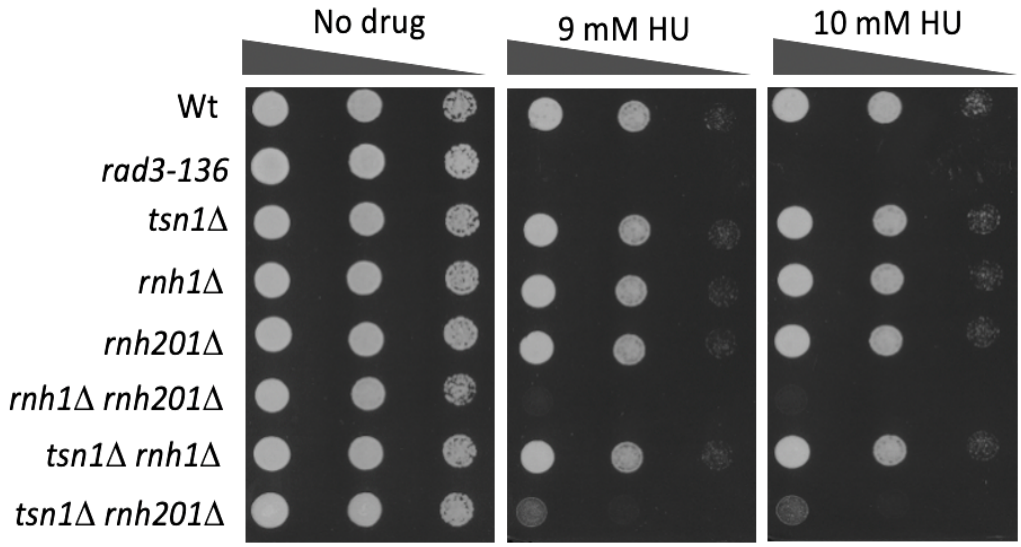


**Figure 3.8. Increased the sensitivity of the *tsn1*Δ *rnh201*Δ to hydroxyurea (HU).**

*S. pombe* cultures were serially diluted (x10 increments) then spotted onto YEA with and without HU. Mutants were spotted onto two different concentrations of hydroxyurea (9 mM and 10 mM) and were then incubated at 30°C for 3 days. The *rad3-136* mutant was the positive control. The *rnh1*Δ *rnh201*Δ and *tsn1*Δ *rnh201*Δ double mutants exhibited hypersensitivity compared with the WT and the *tsn1*Δ *rnh1*Δ double mutant.

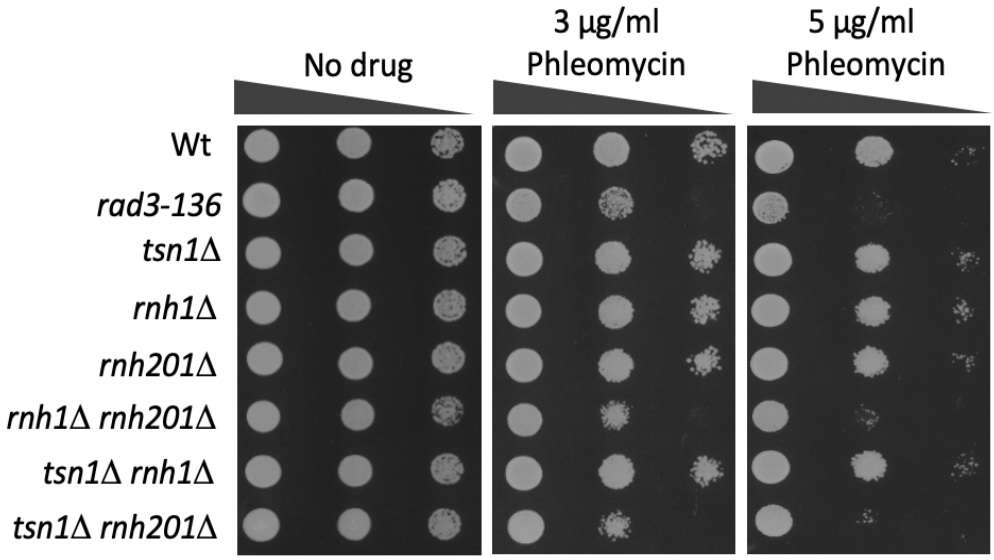


**Figure 3.9. Increased the sensitivity of the *tsn1*Δ *rnh201*Δ to phleomycin.**

*S. pombe* cultures were serially diluted (x10 increments) then spotted onto YEA with and without phleomycin. Mutants were spotted onto two different concentrations of phleomycin (3 µg /ml and 5 µg /ml) and were then incubated at 30°C for 3 days. The *rad3-136* mutant was the positive control. The *rnh1*Δ *rnh201*Δ and *tsn1*Δ *rnh201*Δ double mutants exhibited hypersensitivity compared with the WT and the *tsn1*Δ *rnh1*Δ double mutant.

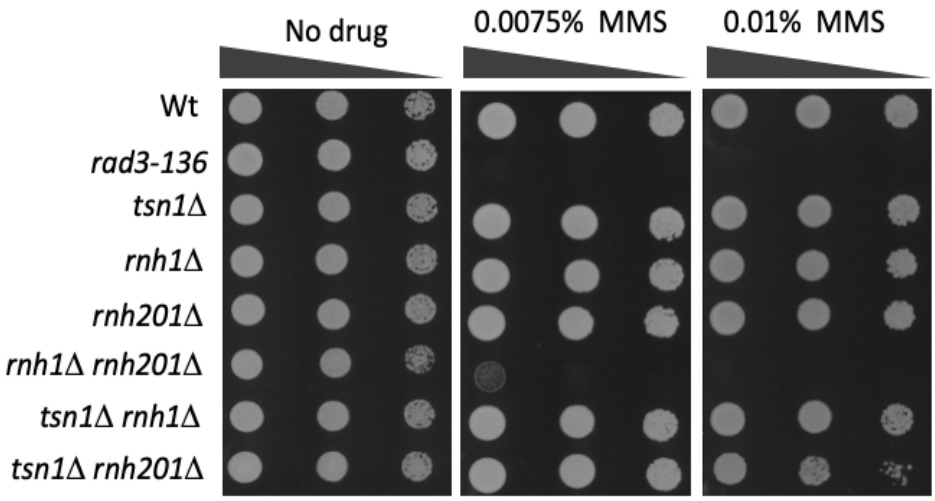


**Figure 3.10. Sensitivity spot test of Methyl methane sulfonate (MMS).**

*S. pombe* cultures were serially diluted (x10 increments) then spotted onto YEA with and without MMS. Mutants were spotted onto two different percentages of MMS (0.0075% and 0.01%) and were then incubated at 30°C for 3 days. The *rad3-136* mutant was the positive control. The *rnh1*Δ *rnh201*Δ double mutant exhibited hypersensitivity compared with the WT and the *tsn1*Δ *rnh1*Δ double mutant. The *tsn1*Δ *rnh201*Δ double mutant exhibited a very mild sensitivity at higher levels of MMS.

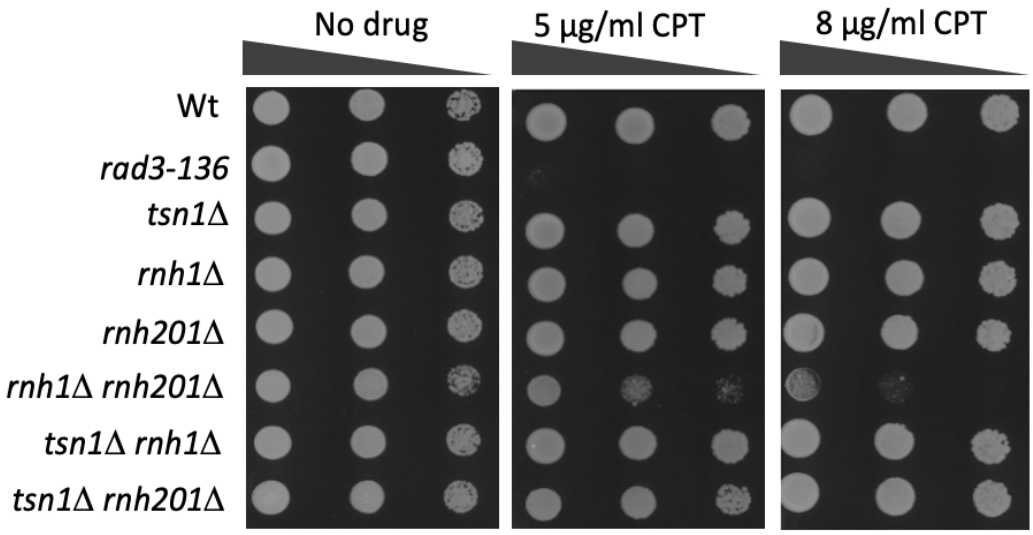


**Figure 3.11. Sensitivity spot test of Camptothecin (CPT).**

*S. pombe* cultures were serially diluted (x10 increments) then spotted onto YEA with and without CPT. Mutants were spotted onto two different concentration of CPT (5 µg /ml and 8 µg /ml) and were then incubated at 30°C for 3 days. The *rad3-136* mutant was the positive control. The *rnh1*Δ *rnh201*Δ double mutant exhibited hypersensitivity compared with the WT and the *tsn1*Δ *rnh1*Δ double mutant. The *tsn1*Δ *rnh201*Δ double mutant also exhibited no apparent sensitivity to CPT.

### 3.2.3. Assessment of a potential role for *tfx1* in maintaining genome stability in the absence of RNAse H function

Having demonstrated a role for *tsn1* in maintaining genome instability in the absence of *rnh201*, we wished to determine whether the *tfx1* gene, which, for humans, encodes the partner protein to Tsn1, is also required. To do these double mutants of *tfx1*Δ *rnh1*Δ and *tfx1*Δ *rnh201*Δ were required. To create the strains, all the target genes were replaced with antibiotic-resistant cassettes, following the PCR-based gene targeting approach characterised by Bähler et al. (1998). Genes were deleted from the *tfx1*Δ single mutant (BP3384) to derive the double mutants, *tfx1*Δ *rnh1*Δ (BP3412) and *tfx1*Δ *rnh201*Δ (BP3414). To replace the *rnh1* and *rnh20* genes the *kanMX6* gene cassette was used. To amplify the replacement cassettes, PCR was used with primers of 80 bp homologous sequences that were upstream and downstream contiguous with the *rnh1* and *rnh201* open reading frames (ORFs), with 20 bp of homologous sequence to the plasmid that carries the *kantMX6* gene. PCR screening was conducted to confirm the correct genes had been deleted from the candidate strains (Figures 3.12 and 3.13). For each construct, two separate isolates were evaluated (although following checks only one was allocated a primary BP strain designation).

### 3.2.4. *tfx1* is not required for recovery from DNA damage in the absence of RNAse H activity

To assess whether *tfx1* is required for recovery from DNA damage in the absence of *rnh1* or *rnh201* we investigate the sensitivity of *tfx1*Δ *rnh1*Δ and *tfx1*Δ *rnh201*Δ double mutants to a number of DNA damaging agents. The results of the DNA damaging agents are presented below; different agents exert different effects: HU inhibits DNA replication (Figure 3.14), CPT is a topoisomerase inhibitor (Figure 3.15), Mitomycin C, a potent DNA crosslinker (Figure 3.16), UV irradiation creates multiple adducts (Figure 3.17), and MMS, alkylates DNA (Figure 3.18). Consistent with other research, the *rnh1*Δ *rnh201*Δ double mutant exhibited heightened sensitivity to the all-DNA damaging agents tested (Ohle et al., 2016; Zhao et al., 2018). In contrast, no increase in sensitivity to the DNA damaging agents was detected in the *tfx1*Δ *rnh1*Δ or *tfx1*Δ *rnh201*Δ double mutants when compared against the WT or *rnh1*Δ and *rnh201*Δ single mutants for any agents tested. Taken together, the data presented in this chapter infers that when Rnh201 is absent, Tsn1, but not Tfx1, contributes to the response to repair DNA damage caused by particular agents.

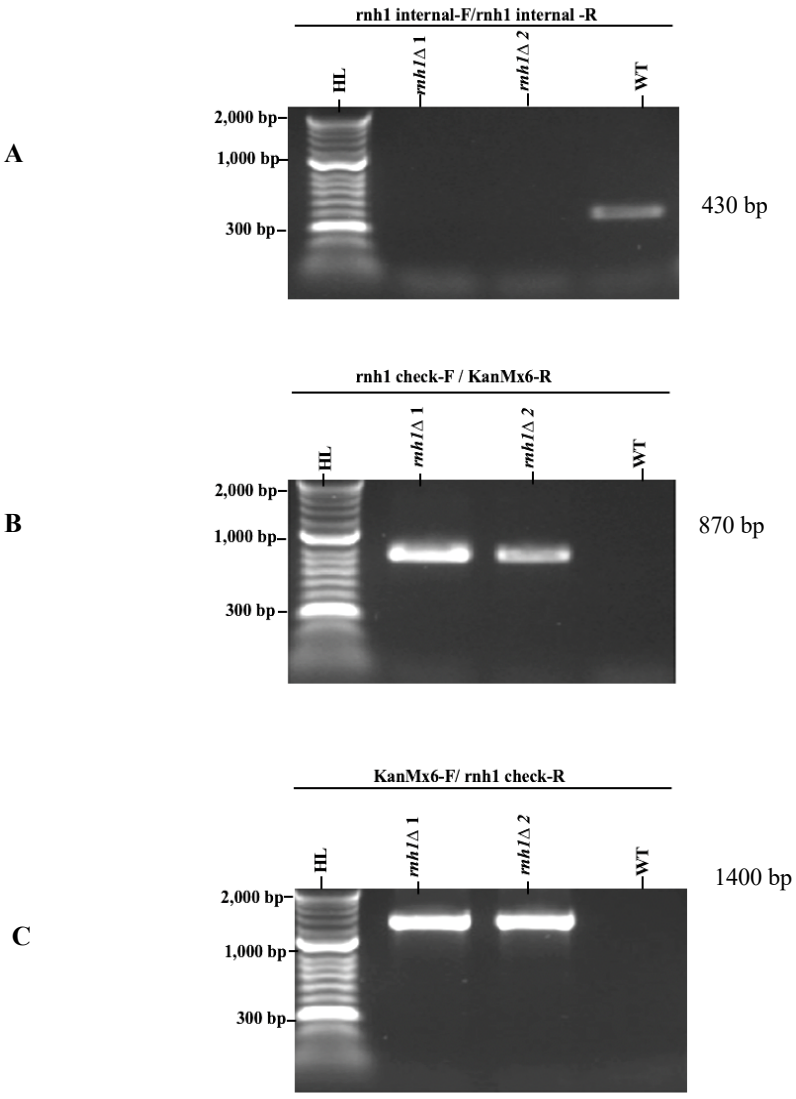


**Figure 3.12. PCR screening of potential *tfx1*Δ *rnh1*Δ double mutants.**

**A.** Image of agarose gel runs PCR products for the WT strain (BP90) and *rnh1*Δ mutant candidates. The *rnh1*gene internal PCR product is generated using rnh1-internal-F and rnh1-internal-R primers measures 430 bp. No PCR products are detectable in the successful *rnh1*Δ candidate strains. **B**. The PCR primers rnh1 check-F and kanMX6-R were used to check the WT and *rnh1*Δ candidate strains. Whilst no bands were detected in the WT, the *rnh1*Δ strains exhibit a band of approximately 870 bp **C.** To amplify the WT and *rnh1*Δ candidate strains, the kanMX6-F and rnh1check-R primers were used. 1400 bp product is evident in the *rnh1*Δ strains, but not the WT strain. H = Hyper ladder.

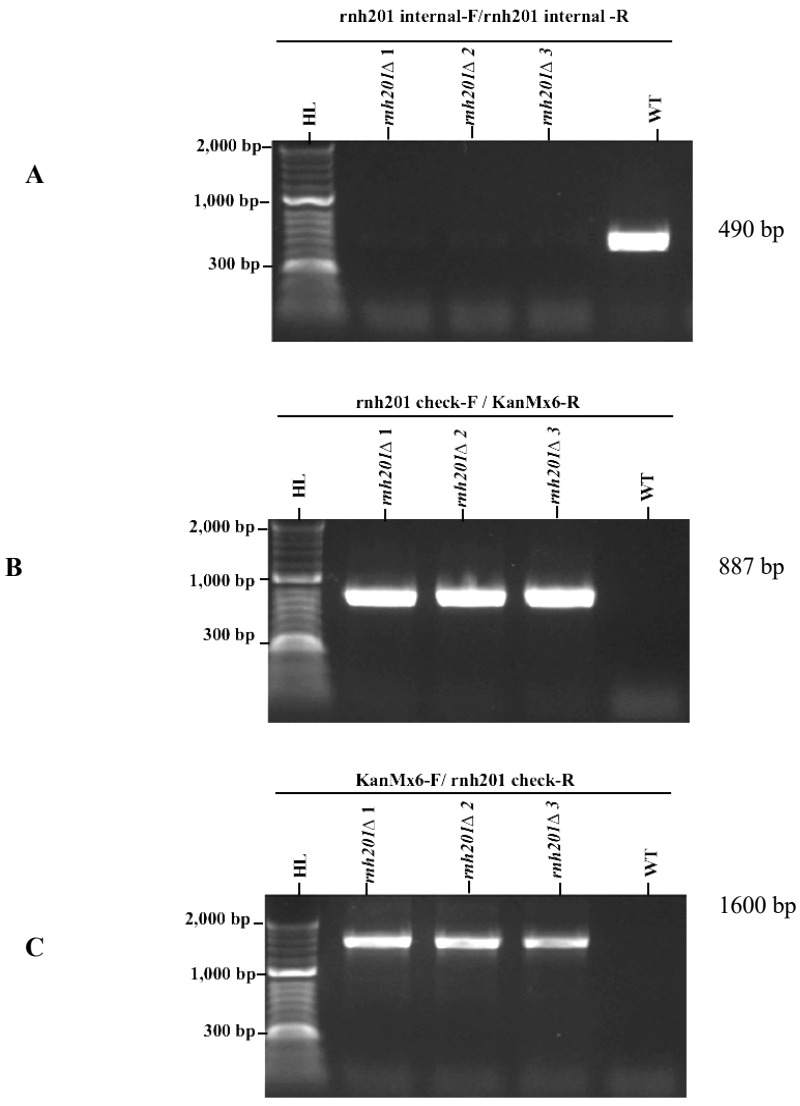


**Figure 3.13. PCR screening of potential *tfx1*Δ *rnh201*Δ double mutants.**

**A**. Image of agarose gel runs PCR products for the WT strain (BP90) and *rnh201*Δ mutant candidates. The *rnh201*gene internal PCR product is generated using rnh201-internal-F and rnh201-internal-R primers measures 490 bp. No PCR products are detectable in the successful *rnh201*Δ candidate strains. **B**. The PCR primers rnh201 check-F and kanMX6-R were used to check the WT and *rnh201*Δ candidate strains. Whilst no bands were detected in the WT, the *rnh201*Δ strains exhibit a band of approximately 887 bp **C.** To amplify the WT and *rnh201*Δ candidate strains, the kanMX6-F and rnh201check- R primers were used. 1600 bp product is evident in the *rnh201*Δ strains, but not the WT strain. H = Hyper ladder.

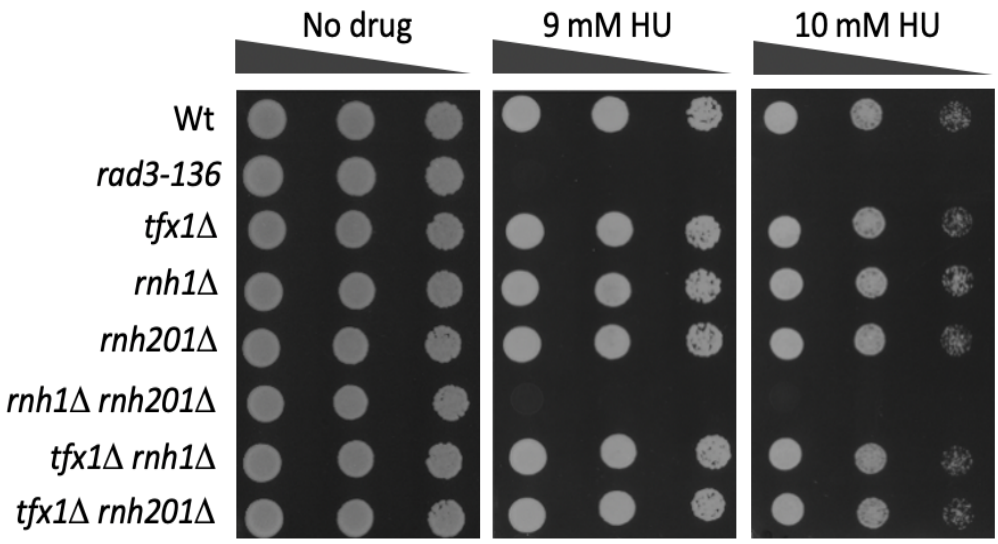


**Figure 3.14. Sensitivity spot test of hydroxyurea (HU).**

*S. pombe* cultures were serially diluted (x10 increments) then spotted onto YEA with and without HU. Mutants were spotted onto two different concentration of hydroxyurea (9 mM and 10 mM) and were then incubated at 30°C for 3 days. The *rad3-136* mutant was the positive control. The *rnh1*Δ *rnh201*Δ double mutant exhibited hypersensitivity compared with the WT and the *tfx1*Δ *rnh1*Δ double mutant. The *tfx1*Δ *rnh201*Δ double mutant also exhibited no apparent sensitivity to HU.

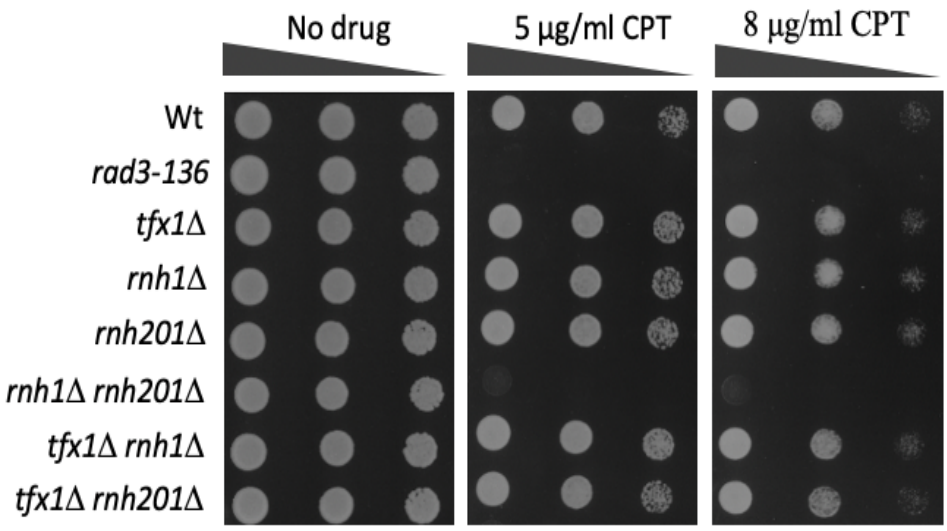


**Figure 3.15. Sensitivity spot test of Camptothecin (CPT).**

*S. pombe* cultures were serially diluted (x10 increments) then spotted onto YEA with and without CPT. Mutants were spotted onto two different concentrations of Camptothecin (5 mg/ml and 8 mg/ml) and were then incubated at 30°C for 3 days. The *rad3-136* mutant was the positive control. The *rnh1*Δ *rnh201*Δ double mutant exhibited hypersensitivity compared with the WT and the *tfx1*Δ *rnh1*Δ double mutant. The *tfx1*Δ *rnh201*Δ double mutant also exhibited no apparent sensitivity to CPT.

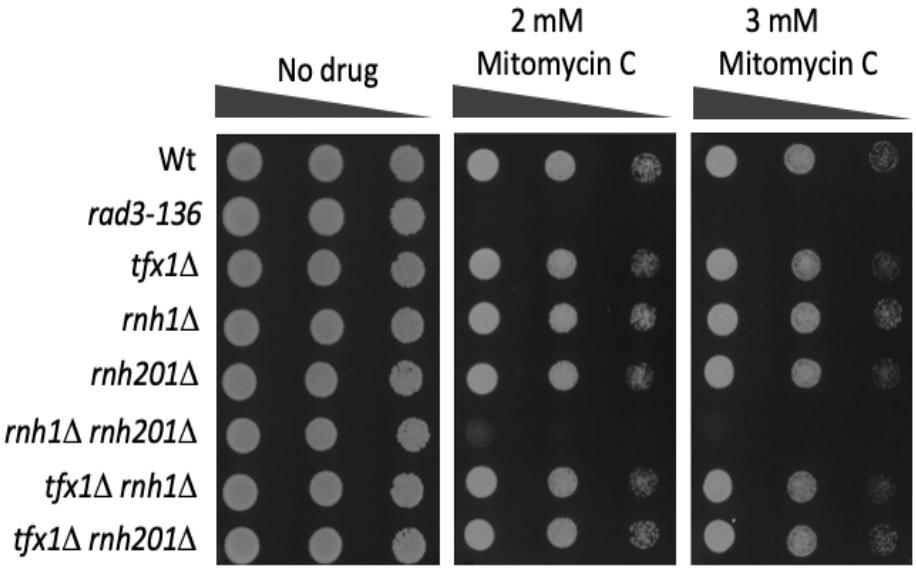


**Figure 3.16. Sensitivity spot test of Mitomycin C (MMC).**

*S. pombe* cultures were serially diluted (x10 increments) then spotted onto YEA with and without MMC. Mutants were spotted onto two different concentration of Mitomycin C (2 mM and 3 mM) and were then incubated at 30°C for 3 days. The *rad3-136* mutant was the positive control. The *rnh1*Δ *rnh201*Δ double mutant exhibited hypersensitivity compared with the WT and the *tfx1*Δ *rnh1*Δ double mutant. The *tfx1*Δ *rnh201*Δ double mutant also exhibited no apparent sensitivity to MMC.

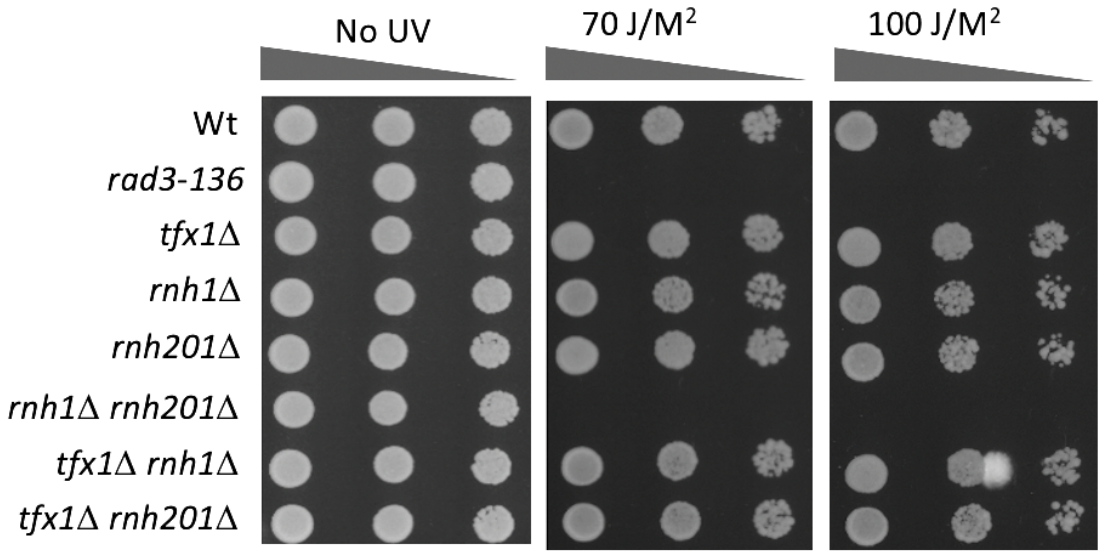


**Figure 3.17. Sensitivity spot test of UV irradiation.**

*S. pombe* cultures were serially diluted (x10 increments) then spotted onto YEA with and without UV. Mutants were spotted onto two different doses of ultraviolet irradiation (70 J/M$^2$ and 100 J/M$^2$) and were then incubated at 30°C for 3 days. The *rad3-136* mutant was the positive control. The *rnh1*Δ *rnh201*Δ double mutant exhibited hypersensitivity compared with the WT and the *tfx1*Δ *rnh1*Δ double mutant. The *tfx1*Δ *rnh201*Δ double mutant also exhibited no apparent sensitivity to UV.

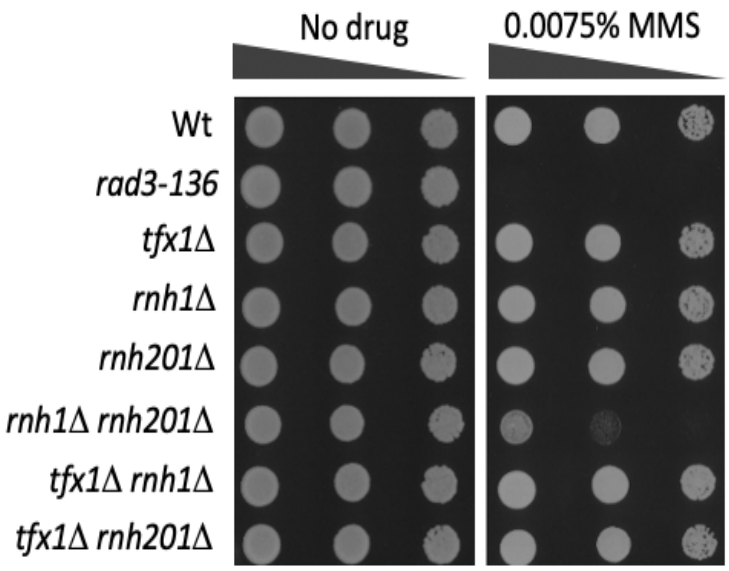


**Figure 3.18. Sensitivity spot test of Methyl methane sulfonate (MMS).**

*S. pombe* cultures were serially diluted (x10 increments) then spotted onto YEA with and without MMS. Mutants were spotted onto one percentage of Methyl methane sulfonate **(**0.0075%) and were then incubated at 30°C for 3 days. The *rad3-136* mutant was the positive control. The *rnh1*Δ *rnh201*Δ double mutant exhibited hypersensitivity compared with the WT and the *tfx1*Δ *rnh1*Δ double mutant. The *tfx1*Δ *rnh201*Δ double mutant also exhibited no apparent sensitivity to MMS.

### 3.2.5. *rnh201* is required for the recovery from replicative stress in exponentially growing cells.

During this study we noted that *rnh201*Δ mutants appeared to show a sensitivity to replicative stress induced by HU in some experiments and not others (for example, when *rnh201*Δ mutants are used in minimal media – see Chapter 6). Previous studies had reported different findings. Ohle et al. (2016) had found no sensitivity of an *rnh201*Δ single mutant to HU, as is the case in our experiments reported in this chapter. However, Zhao et al. (2018) challenged the findings of Ohle et al. (2016) and demonstrated that an *rnh201*Δ single mutant was sensitive to the replicative stress caused by HU treatment. We hypothesized that the discrepancy between the groups arose due to the state of the cultured cells used for the spot test. In our experiments we had largely used what we believed to be late exponential stage cultures. We postulated that the sensitivity of the *rnh201*Δ mutant might only be apparent when cells were growing very rapidly or under conditions that might induce elevated rNMP misincorporation (e.g., growth in minimal media). To test this hypothesis, we grew *rnh201*Δ and *rnh1*Δ single mutants and employed spot test analysis for response to HU for cells taken from the same culture, but at distinct stage of the culture progression. Three stage were used: lag (pre-exponential), log (exponential) and post-log stationary phase. Figure 3.19 shows that the *rnh201* Δ single mutant, but not *rnh1*Δ mutant is sensitive to HU when the cells are in exponential phase, but not other phases. The *rnh1* Δ *rnh201* Δ and the *rnh1*Δ mutants behave uniformly at all culture states. This explains the discrepancy among the *rnh201*Δ sensitives seen between the previous reports (Ohle *et al.,* 2016; Zhao *et al*., 2018), that is each lab might have been spotting the cells from distinct culture points.

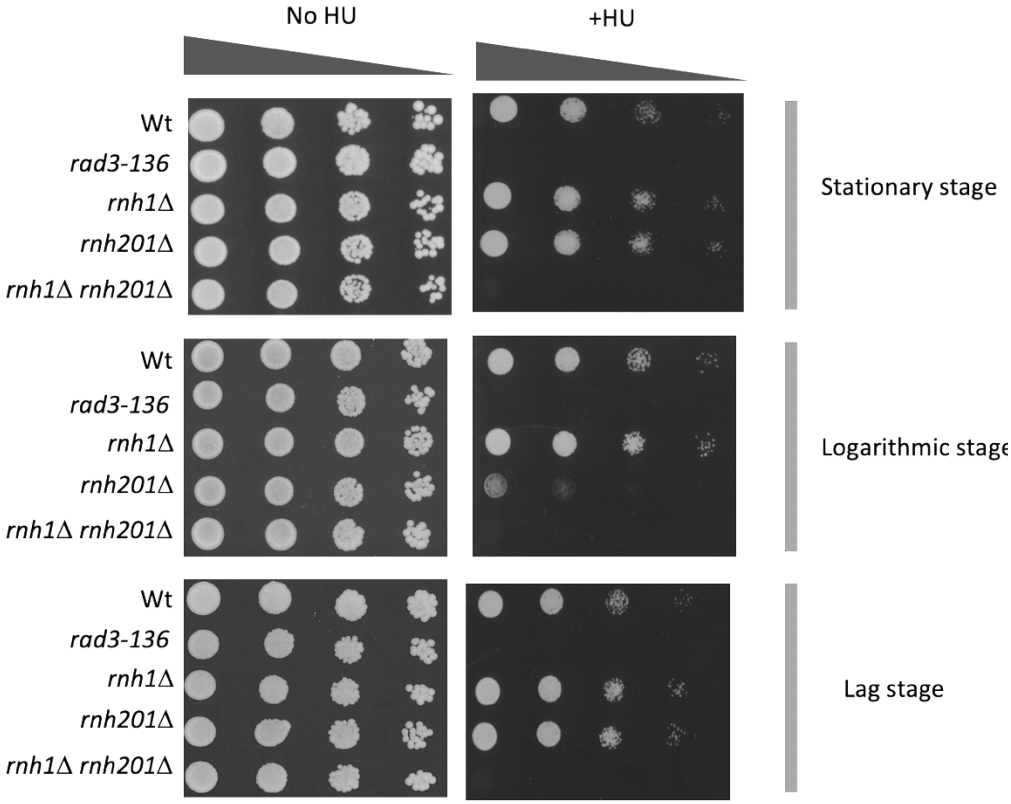


**Figure 3.19. *rnh201*Δ single mutant only exhibits a replicative stress response defect caused by hydroxyurea (HU) when in exponential growth.**

*S. pombe* cultures were serially diluted (x10 increments) then spotted onto yeast extract agar (YEA). Mutant strains were exposed to one contraction (10 mM) of HU at each of three culture stages (the same culture was employed for testing each stage), namely, stationary phase (top), log phase (middle) and lag phase (bottom). The plates were incubated at 30°C for 3 days. Positive controls were provided by *rad3-136* cells and *rnh1*Δ *rnh201*Δ double mutant, both of which showed hypersensitivity at all stages. The results indicate that during the log phase, *rnh201*Δ single mutant was sensitive to HU. The *rnh1*Δ mutant exhibited no sensitivity at any phase.

### 3.2.6. Analysis of *tsn1* requirement in the absence of *rnh201* for cells from log phase culture.

The finding that the *rnh201*Δ mutant had distinct responses when sensitivity was checked from mid-log phase cultures led us to speculate that other sensitivities, we report might vary with culture status of the strains. Given this, we duplicated all results presented here using cells spotted from mid-log phase and found that only the *rnh201*Δ mutant behaves in this fashion. The *tsn1*Δ and *tfx1*Δ single mutants exhibit no notable or reproducible DNA damage response phenotype under any condition tested, and the *rnh201*Δ*tsn1*Δ double mutant exhibits hypersensitivity to HU relative to *tsn1* Δ and *rnh201*Δ under all conditions tested (Figure 3.20). Assessment of other damaging agents did not reveal any additional sensitivity for any strain or damaging agent (Figures 3.21-3.23), suggesting this is specific for the type of damage that is induced by HU, most likely this reflects the need for Rnh201 in removal of mis-incorporated rNMPs during periods of rapid DNA replication.

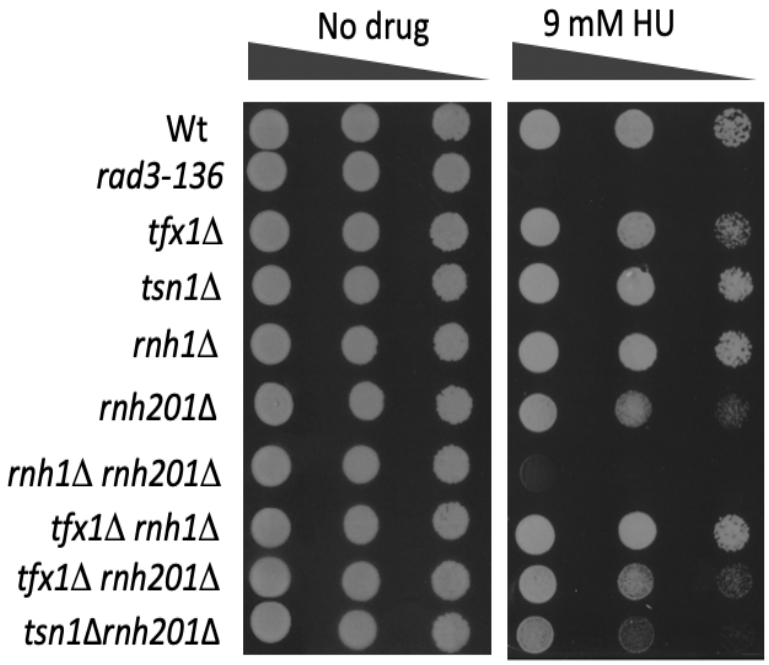


**Figure 3.20. Loss of *rnh201* causes HU sensitivity for log phase growth cells.**

*S. pombe* cultures were serially diluted (x10 increments) then spotted onto YEA. Log phase cells were spotted onto 9 mM HU then incubated at 30°C for 3 days. The *rad3-136* cells were the positive control. The double mutant, *rnh1*Δ *rnh201*Δ*,* exhibited hypersensitivity as positive control. Compared with the WT, the *rnh201*Δ single mutant exhibited sensitivity to the HU, but consistent with non-mid-log phase cells the *rnh201* Δ *tsn1* Δ mutant exhibited increased sensitivity relative to the *rnh201* Δ single mutant.

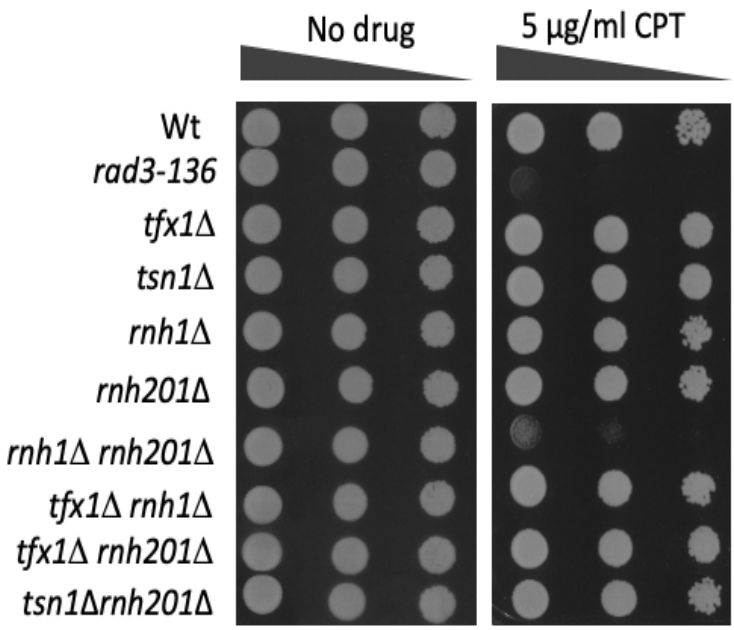


**Figure 3.21. Loss of *rnh201* causes no CPT sensitivity for log phase growth cells.**

*S. pombe* cultures were serially diluted (x10 increments) then spotted onto YEA. Log phase cells were spotted onto 5 µg/ml CPT then incubated at 30°C for 3 days. The *rad3-136* cells were the positive control. The double mutant, *rnh1*Δ *rnh201*Δ, exhibited hypersensitivity as positive control. Compared with the WT, the *rnh201*Δ single mutant exhibited no sensitivity to the CPT, also consistent with non-mid-log phase cells the *rnh201* Δ *tsn1* Δ mutant exhibited no sensitivity relative to the *rnh201* Δ single mutant.

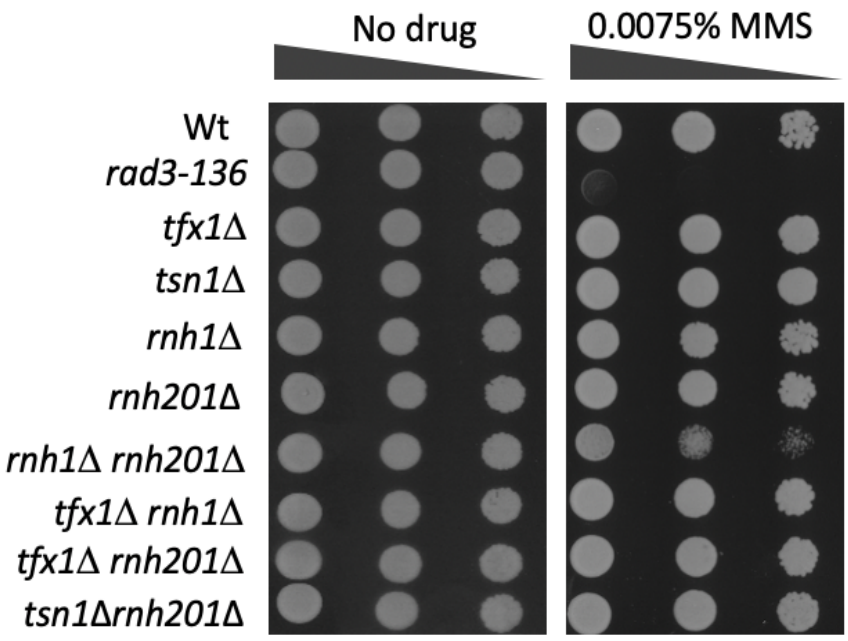


**Figure 3.22. Loss of *rnh201* causes no MMS sensitivity for log phase growth cells.**

*S. pombe* cultures were serially diluted (x10 increments) then spotted onto YEA. Log phase cells were spotted onto 0.0075% MMS then incubated at 30°C for 3 days. The *rad3-136* cells were the positive control. The double mutant, *rnh1*Δ *rnh201*Δ*,* exhibited hypersensitivity as positive control. Compared with the WT, the *rnh201*Δ single mutant exhibited no sensitivity to the MMS, also consistent with non-mid-log phase cells the *rnh201* Δ *tsn1* Δ mutant exhibited no sensitivity relative to the *rnh201* Δ single mutant.

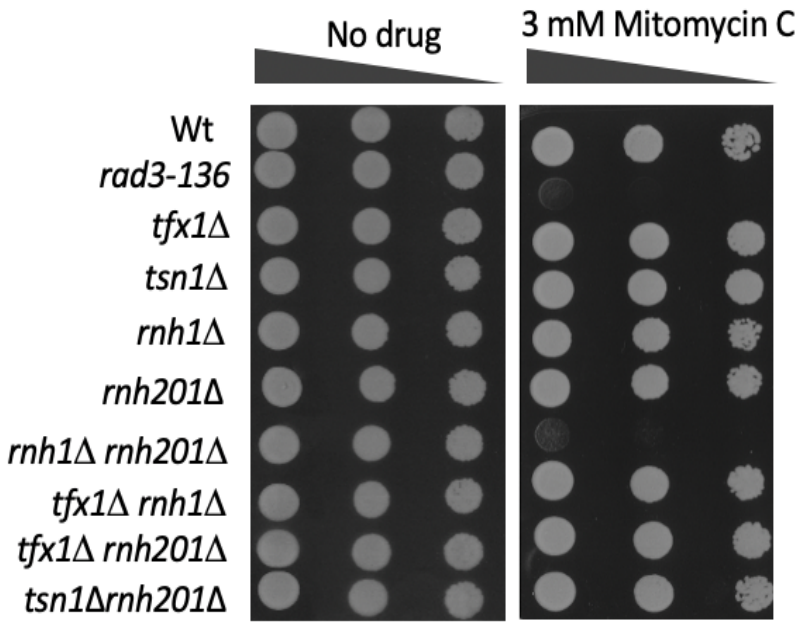


**Figure 3.23. Loss of *rnh201* causes no MMC sensitivity for log phase growth cells.**

*S. pombe* cultures were serially diluted (x10 increments) then spotted onto YEA. Log phase cells were spotted onto 3 mM MMC then incubated at 30°C for 3 days. The *rad3-136* cells were the positive control. The double mutant, *rnh1*Δ *rnh201*Δ, exhibited hypersensitivity as positive control. Compared with the WT, the *rnh201*Δ single mutant exhibited no sensitivity to the MMS, also consistent with non-mid-log phase cells the *rnh201* Δ *tsn1* Δ mutant exhibited no sensitivity relative to the *rnh201* Δ single mutant.

## 3.3. Discussion

Formation of RNA:DNA hybrids takes place when the annealing of nascent RNA transcripts to their template DNA strand occurs in the context of a DNA duplex (Fragkos & Naim, 2017; Wahba et al., 2013; Felipe-Abrio et al., 2015; García-Rubio et al., 2018; Jimeno et al., 2019). RNA:DNA hybrids can lead to chromosome instability, through transcription replication conflicts, which can result in genetic diseases such as cancer (Zimmer & Koshland et al., 2016). Ordinarily, RNA:DNA hybrids are suppressed by the highly conserved ribonuclease enzymes, RNase H1 and RNase H2, which degrade the RNA component of the RNA:DNA hybrid. Consequently, the RNase H enzymes contribute to preventing transcription replication conflicts and preventing genome instability (Ohle et al., 2016; Zhao et al., 2018; Amon & Koshland et al., 2016). The deletion of both RNase H1 and RNase H2 coding genes results in defects in DNA damage recovery and can inhibit HR-mediated DSB repair. The implication of this is that the RNase H pathways are required redundantly to both avoid DNA damage and to repair DSBs (Ohle et al., 2016), although, Zhao et al. (2018) argue that RNase H activity is only needed for some types of DNA break repair.

Previously, the McFarlane group have showing that in the absence of Dcr1, Tsn1 is involved in recovering from some forms of DNA damage, such as replicative stress; however, Tfx1 is not (unpublished data). This was the first evidence for a direct role for Tsn1 in DNA damage recovery in *S. pombe*. Given that Dcr1 is implicated in suppressing RNA:DNA hybrid levels in an RNAi-independent pathway, it was postulated that Tsn1 might have a role in one of the RNase H pathways. This led us to evaluate whether Tsn1 (and/or Tfx1) has functions in one of the RNase H pathways and the data presented here suggest that Tsn1, but not Tfx1, does indeed have a role to play in the recovery from DNA damage for several genotoxic and DNA replicative stress agents in the absence of Rnh201, the catalytic subunit of *S. pombe* RNAse H2.

The *tsn1*Δ *rnh201*Δ double mutant was sensitive to HU, which contrasts with the *tsn1*Δ *rnh1*Δ double, which had no sensitivity (Figure 3.8). The reasons for this could be that more ribonucleotides were incorporated into DNA, which might be combined with faults in the ribonucleotide excision repair (RER), R-loop processing or RNA primer removal. However, HU might affect rNMP pools with possible knock-on effects on ribonucleotide incorporation.

Thus, these findings show that Tsn1 assists in the repair of damaged DNA, perhaps by destabilising RNA:DNA hybrids in a pathway redundant with Rnh201. The *rnh201*Δ *tsn1*Δ strain also showed greater sensitivity to phleomycin than WT, this drug is recognised as being able to generate DSBs. The increased sensitivity to phleomycin of *tsn1*Δ *rnh201*Δ compared to that of *tsn1,* suggests Tsn1 could contribute to repairing DNA DSBs.

Translin and Trax are involved in various biological processes where RNA, but not DNA molecules need regulating. The data presented here could indicate that RNA:DNA hybrids generated by RNA pol II appear to need the involvement of Tsn1 for processing when other factors are missing, such as Rnh201. This could be explained by the nucleic acid binding and RNAse capabilities of Tsn1 (Jaendling and McFarlane, 2010), and one possibility is that Tsn1 provides an RNAse H-like activity that functions redundantly with Rnh201. These findings may also explain why Translin is implicated in chromosomal translocation generation, as these could be sites of RNA:DNA hybrid formation where Translin function is required. Prior to this work, little evidence has been given to implicate Translin directly in the recovery from DNA damage, although haematopoietic stem cells in Translin-deficient mice recover more slowly after ionizing irradiation (Fukuda et al., 2008). Wang et al. (2016) successfully demonstrated that Trax is involved in DNA repair in mammalian cells, as it recruits the ATM kinase to DSB sites, but they found no evidence for involvement of Translin.

In contrast to the *tsn1*Δ *rnh201*Δ double mutant, which does not exhibit sensitivity to all DNA damaging agents tested, the *rnh1*Δ *rnh201*Δ double mutant appears hypersensitive to all tested agents. Additionally, if *rnh201*Δ *tsn1*Δ exhibits sensitivity, then the *rnh1*Δ *rnh201*Δ double mutant exhibited an increased sensitivity. Together, these findings show that the functions lost in the *rnh1*Δ *rnh201*Δ double mutant are not all lost in the *tsn1*Δ *rnh201*Δ double mutant as in most cases some damage tolerance is maintained. The majority of the DNA damaging agents indicated that the increased sensitivity of the *rnh201*Δ *tsn1*Δ double mutant appears to be associated with damage in S phase of the cell cycle. Conversely, the fact that the non-S phase-specific damage agent, MMS, failed to confer any evident sensitivity to the *rnh201*Δ *tsn1*Δ double mutant (Figure 3.10). MMS might also ‘damage’ RNA species, including RNA in hybrids (Hans E et al., 2013), and that might be another explanation for not seeing any sensitivity when exposure the cell to MMS.

CPT is an extremely selective inhibitor of DNA topoisomerase I (TOP I), which is a nuclear monomeric enzyme. Its principal role is to discharge some of the rotational tension that occurs within intracellular DNA during normal duplication and transcription processes (Kjeldsen et al., 2018). This effect is achieved by temporarily breaking on strand of the DNA duplex, rotating the duplex and then re-annealing the broken strand to reform a continuous duplex. The reannealing function is compromised by CPT and chromosomal breaks can result when the replisome encounters the unclosed nick. The *rnh201*Δ *tsn1*Δ double mutant was not sensitive to CPT, this might indicate that whilst DSBs caused by CPT are associated with DNA replication, these breaks do not require Tsn1, but they do require RNAse H activity as the double mutant is sensitive to CPT. It has been demonstrated that RNA pol II generates new transcripts at the sites of DSBs and that the RNA molecules formed are required for correct DSB repair and require RNAse H activity to remove them (Domingo-Prim et al. 2020). The CPT data appear to indicate that RNAse H activity is required for CPT recovery, but that Tsn1 is not required. This suggests that Tsn1 is required for recovery from genomic damaging replicative stress caused by HU, but not by CPT, which forms DSBs via a unique pathway. It could simply be the case that Tsn1 is required to avoid RNA:DNA hybrids in the genome from becoming genotoxic particularly when there is an additional stress (in this case, induced by HU), but is not required for the removal of RNA:DNA hybrids involved in the DSB repair pathway. This hypothesis is further supported by the lack of sensitivity of the *rnh201*Δ *tsn1*Δ double mutant to MMC, a DNA cross linking agent that inhibits replisome progression that is unlikely to be associated with genomic RNA:DNA hybrids. The phleomycin data challenge this simple model, as the *rnh201*Δ *tsn1*Δ mutant is sensitive to this agent. Phleomycin is thought to generate DSBs and serve as a mimetic of ionizing irradiation. It might be the case that Tsn1 is required for some DSB recovery, but not DSBs associated with a covalently associated protein, such as Top1 inhibited by CTP.

A modest degree of sensitivity to HU was observed in *rnh201*Δ (Figure 3.19) although this is dissimilar to that shown in Figures 3.8 and 3.14. This is likely to be a consequence of the proliferative state of cells at the moment of agent administration. Within the log phase there is a high rate of cellular proliferation; hence, at this point, HU has a greater effect. Changes in gene duplication and transcription occur in the stationary cell phase owing to the surplus carbohydrate reservoir present (Zhao et al. 2016). Thus, the response of the cells to the DNA-

damaging agent may vary according to their proliferative state when the agent is added. Despite this, no notable DNA damage response phenotypes were identified in the experiments for the *tsn1*Δ and *tfx1*Δ single mutants, so this phenomenon is specific to the *rnh201*Δ mutant. The hypersensitivity to HU exhibited by the *rnh201*Δ *tsn1*Δ double mutant in all the experimental scenarios is consistent when compared to *tsn1*Δ and *rnh201*Δ (Figure 3.20). Further DNA-damaging agent were appraised, but no enhanced sensitivity in response to these was noted in any of the strains (Figures 3.21-3.23). Thus, it appears that this phenomenon is particular to damage caused by HU.

In summary, the data presented in this chapter indicate that Tsn1, but not Tfx1, is required for the recovery from some, but not all, types of DNA damage in the absence of Rnh201. This could indicate that Tsn1 functions in the Rnh1 pathways for RNA:DNA hybrid processing, but if this were the case, then Tsn1 is not as critical to this pathway as Rnh1, as the *rnh201*Δ *tsn1*Δ mutant does not exhibit the same gamut of DNA damage response phenotypes as the *rnh201*Δ *rnh1*Δ mutant. Moreover, Tsn1 only appears to be involved in recovery from certain types of DNA damage. We hypothesis that it plays a role in processing some types on nucleic acid intermediates, possibly RNA:DNA hybrids, in some, but not all damage avoidance/repair pathways. For example, we postulate that Tsn1 helps to prevent RNA:DNA hybrids generated during transcription from causing genotoxic replicative barriers. These data are the first to demonstrate a link between Tsn1 and RNAse H activity, or other activities mediated by Rnh201. It remains a formal possibility that Tsn1 serves in a rMNP removal pathway and is redundant with Rnh201 in this activity, rather than RNA:DNA hybrid removal. The further analyses presented in subsequent chapters explore the many questioned opened by these novel findings.

# Chapter 4: Analysis of *tsn1* and *tfx1* function in genome stability regulation in the absence of *sen1*

# 4.1. Introduction

Preservation of genomic integrity necessitates that during each cell division DNA is replicated accurately and in its entirety. However, there are numerous factors that may hinder the activity of DNA replication forks (RFs). Such hindrances must be overcome in order to circumvent fork stalling/collapse and subsequent chromosomal instability. Transcription is a notable impediment to the RF. In eukaryotes, DNA synthesis is negatively influenced by conflicts between RFs and transcription bubbles. These give rise to errors in chromosome upkeep and an elevated rate of recombination (Helmrich et al., 2011; 2013; Hamperl et al., 2017; Tran et al., 2017; Wu et al. 2020).

DNA-bound RNA polymerase subunits and RNA:DNA hybrids that are created in the transcription process need to be removed. The latter, which arise inherently in the course of transcription, are generally around eight base pairs. They are usually removed when the RNA polymerase becomes uncoupled from the DNA (Aguilera and Garcı́a-Muse, 2012; Barroso et al. 2019; Domingo-Prim et al. 2020 ; Gómez-González et al. 2020). At specific loci within the chromosomes, elongated RNA:DNA hybrids can also materialise in the wake of RNA synthesis via the reannealing of novel RNAs to template DNA, supplanting the non-template DNA strand. The development of these configurations, which are referred to as R-loops, are favoured in association with genes that have an elevated transcription rate and GC bias. In higher eukaryotes they may encompass up to one kilobase (Aguilera and Garcı́a-Muse, 2012; Skourti-Stathaki et al., 2014; Kuznetsov et al. 2018; Vanoosthuyse 2018; García-Muse and Aguilera 2019). R-loop production is augmented following head to head collisions between RFs and complexes undergoing active transcription (Hamperl et al., 2017; Lang et al., 2017; Allison and Wang 2019; Wu et al. 2020). RNase H enzymes break down RNA molecules that participate in the DNA:RNA hybrids and these enzymes are essential for R-loop degradation (Zimmer and Koshland 2016 ; Zhao et al. 2018 ; Lockhart et al. 2019). Moreover, RNA:DNA hybirds can be unwound by specific RNA:DNA helicases such as Senataxin (Cohen et al., 2018; Cohen 2019; Dutta et al. 2020).

Two conditions that affect the neural system, namely, amyotrophic lateral sclerosis type 4 (ALS4) and ataxia-ocular apraxia type 2 (AOA2), have been associated with a deficiency of the conserved DNA/RNA helicase Senataxin (Yüce-Petronczki and West, 2012; Bennett and

La Spada, 2018; Richard et al., 2020; Dutta et al., 2020). Despite the existence of awareness about this correlation, knowledge is still limited with regard to the manner in which various mutations of this helicase are involved in the development of conditions with different pathologies (Groh et al., 2017). It has been established that Senataxin represents the yeast Sen1 helicase ortholgue and there have been consistent reports about the fact that the transcription termination of a minimum of one subset of RNA pol II-transcribed genes depends significantly not only on human Senataxin, but also on budding yeast Sen1 (Ursic et al., 1997; Steinmetz et al., 2006; Skourti Stathaki et al., 2011; Porrua & Libri, 2013; Han et al, 2017). Nevertheless, it is unlikely that these two orthologues participate in this process in exactly the same way; one reason for this is that the involvement of budding yeast Sen1 in RNA Pol II transcription termination of occurs as a component of the Nrd1-Nab3-Sen1 (NNS) complex; human cells do not display conservation of this complex. Evidence has been put forth in support of the participation of both human Senataxin and budding yeast Sen1 in other processes as well, such as DNA damage repair (Li et al., 2016; Andrews et al., 2018; Cohen et al., 2018; Rawal et al. 2020) and the solving of incongruities between transcription and replication (Yüce & West, 2013; Rivosecchi et al., 2019a). It has been demonstrated that budding yeast Sen1 and fission yeast Sen1 are capable of translocation in a 5′–3′ direction on single-stranded DNA or RNA *in vitro* (Han et al., 2017; Martin Tumasz & Brow, 2015). Furthermore, sit has been argued that both budding yeast Sen1 and human Senataxin have long, co-transcriptional RNA-DNA hybrids as an essential substrate *in vivo* (Groh et al., 2017; Rivosecchi et al., 2019a). According to existing models, the occurrence of a correlation between transcription termination and flaws of DNA repair is confirmed by the fact that when Senataxin is no longer active R-loops become stabilised. Nevertheless, there is an opposing argument to this idea, which is that the presence of RNA:DNA hybrids is not an absolute prerequisite for the direct dissociation of pre-assembled RNA Pol II transcription elongation complexes by budding yeast Sen1 *in vitro* via translocation on newly formed RNA (Porrua & Libri, 2013; Han et al., 2017). From this, it can be implied that Sen1 might achieve regulation of transcription through functions unrelated to R-loops.

Sen1 and Dbl8 are the two Senataxin orthologues that are expressed by the fission yeast *Schizosaccharomyces pombe*. However, it is worth noting that the absence of one or both of these homologues does not have a major impact on the transcription termination at RNA pol II-transcribed genes (Lemay et al., 2016; Larochelle et al., 2018). Furthermore, knowledge about the functions played by the Senataxin enzymes of *S. pombe* is still limited. Yu et al.

(2013) demonstrated that Dbl8 was present at DNA double-strand break sites, whilst both Legros et al. (2014) and Rivosecchi et al. (2019a) observed that Sen1 of *S. pombe* had a physical association with RNA Pol III and was also mobilised to particular tRNA genes. In spite of such observations, it is yet to be definitively established what role Sen1 plays at RNA Pol III-transcribed genes. Meanwhile, as has been reported by Hamada et al. (2001) and Shukla and Bhargava (2018), the adequate recruitment of RNA Pol III in *S. pombe* cannot occur without the aid of an upstream TATA box, which is responsible for helping TFIIIC with TFIIIB recruitment as well. After loading, RNA Pol III is capable of achieving transcription termination on its own when it reaches a signal of transcription termination consisting of a basic stretch of five thymine residues on the non-template strand, according to transcription assays carried out *in vitro* (Mishra & Maraia, 2019). With regard to the number of residues making up the transcription termination signal, it is important to highlight that it may not be the same for every gene and organism (Arimbasseri et al., 2013).

Among the different subunits that make up the NNS-complex, the only one that displays catalytic activity is Sen1. The composition of Sen1 consists of a conserved central domain that is homologous to the helicases belonging to the Super Family 1 (SF1), and on each side of this conserved central domain are extensions of N-terminus and C-terminus, which take part in the interactions between proteins. To provide further details, a number of studies have suggested that the role fulfilled by the N-terminal domain is that of mediator of the interaction with RNA pol II, whereas the C-terminal domain comprises sequences that are of significance for determining the position of Sen1 in the nucleus (Ursic et al., 2004; Chen et al., 2014; Han et al., 2017). What is more, according to the findings of several different studies, transcription is terminated in a flawed manner *in vivo* under certain circumstances, such as when the N-terminal domain is deleted or when the helicase domain undergoes mutations (Chen et al., 2014; Finkel et al., 2010; Han et al. 2020). In addition, it is of note that, in the majority of eukaryotic organisms, no other protein that belongs to the NNS-complex exhibits conservation besides Sen1.

It has previously been noted that the *tsn1*Δ *rnh201*Δ double mutant showed enhanced sensitivity to some DNA damaging agents but the *tfx1*Δ *rnh201*Δ did not (Chapter 3). In *S. cerevisiae,* RNA:DNA hybrids duplex unwinding by Sen1 can lead to the eradication of these hybrids (Stuckey et al., 2015). This observation gave rise to the possibility that *tsn1,* but not *tfx1,* may act in an RNA:DNA hybrid removal/avoidance pathway that functions is either

redundant or overlapping with a Sen1-dependent pathway. Here we will apply genetic analysis to assess these possibilities.

# 4.2. Results

## 4.2.1. Construction of *sen1* gene null mutants

In view of the association between *tsn1* and an *S. pombe* RNase H pathway, it was decided to explore the genetic interaction between *tsn1* and the primary *S. pombe SEN1* orthologue, *sen1* (the other being *dbl8*), which is the first orthologue identified and has now been shown to be linked to RNA Pol III displacement. This might indicate that it could help prevent recombination at tRNA genes, which are known replication pause sites that can become recombination hotspots (Pryce et al. 2009).

A single *sen1*Δ mutant (BP3428) was generated from BP90, the parent strain. The resulting *sen1*Δ strain was employed as the parental strain for the generation of new double mutants. The creation of all the strains was via the PCR-based gene targeting approach, utilising antibiotic-resistant cassettes for gene replacement (Bähler et al., 1998). Deletion of the *tsn1* and *tfx1* genes from *sen1*Δ background produced the two double mutants *sen1*Δ *tsn1*Δ (BP3441) and *sen1*Δ *tfx1*Δ (BP3444); each genotype had at least two isolates. For the deletion of *sen1, tsn1 and tfx1,* the antibiotic *kanMX6, natMX6* and *hphMX6* were deployed as the replacement cassettes (note that *tfx1* gene was replaced with two different antibiotic cassettes in distinct strains). In order to mediate gene replacement, PCR was used with 80 bp homologous sequence primers positioned upstream and downstream adjacent to the open reading frames (ORFs) for *sen1, tsn1* and *tfx1.* A 20 bp sequence, homologous to the antibiotic resistant markers on the plasmids for *kanMX6, natMX6* and *hphMX6*, was also contained within the primers. The resultant purified PCR product was then chemically transformed into the appropriate *S. pombe* strains (Section 2.5). Three groups of primers were used for confirmatory PCR to check that gene deletion had been accomplished for the *sen1, tsn1* and *tfx1* genes (Figures 4.1-4.4).

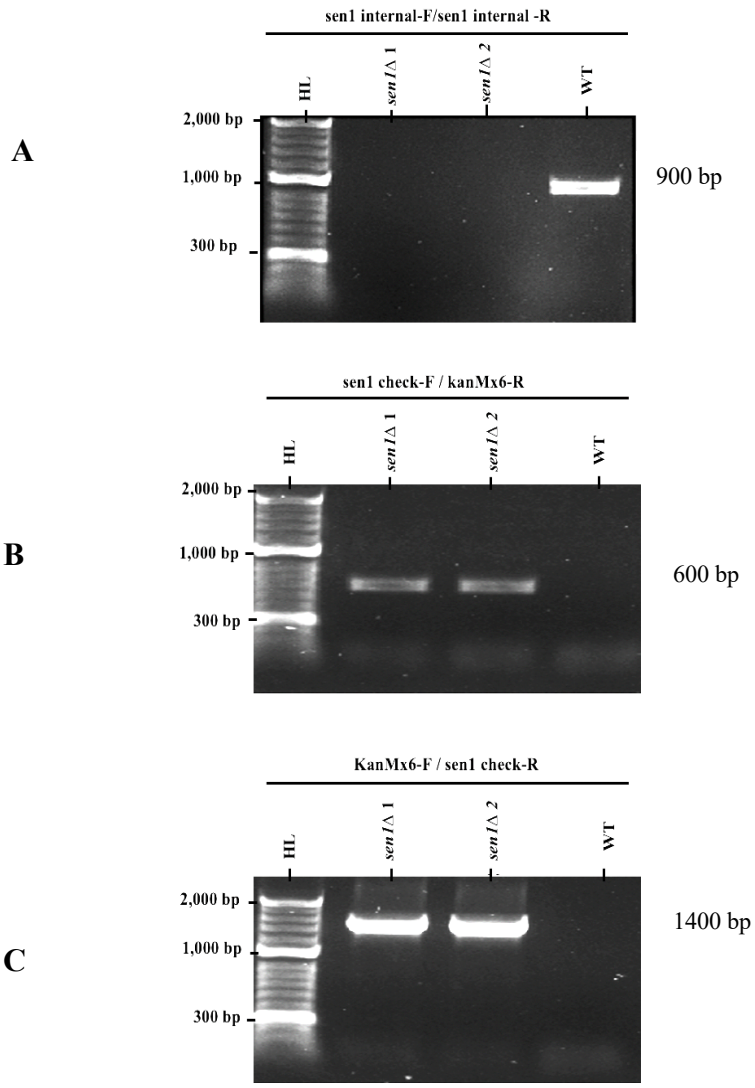


**Figure 4.1. PCR screening for successful *sen1*Δ deletion.**

**A.** Image of an agarose gel of the PCR products for the WT strain (BP90) and two *sen1*Δ single mutant candidates. The *sen1* gene internal PCR product is generated using sen1-internal-F and sen1-internal-R primers and the predicted product is 900 bp. No PCR products are detected in the successful *sen1*Δ candidate strains. **B**. To assess the 5' end of the *sen1*Δ locus the PCR primers sen1 check-F and kanMX6-R were used to check the WT and *sen1*Δ candidate strains. Whilst no bands were detected in the WT, the *sen1*Δ strains exhibit a band of approximately 600 bp **C.** To check the 3' end of the deleted *sen1* Δ locus PCR was conducted on genomic DNA from WT and *sen1*Δ candidate strains using the kanMX6-F and sen1check-R primers. A band for the correct size was apparent at approximately 1400 bp in the *sen1*Δ strains, but not the WT strain. H = Hyper ladder.

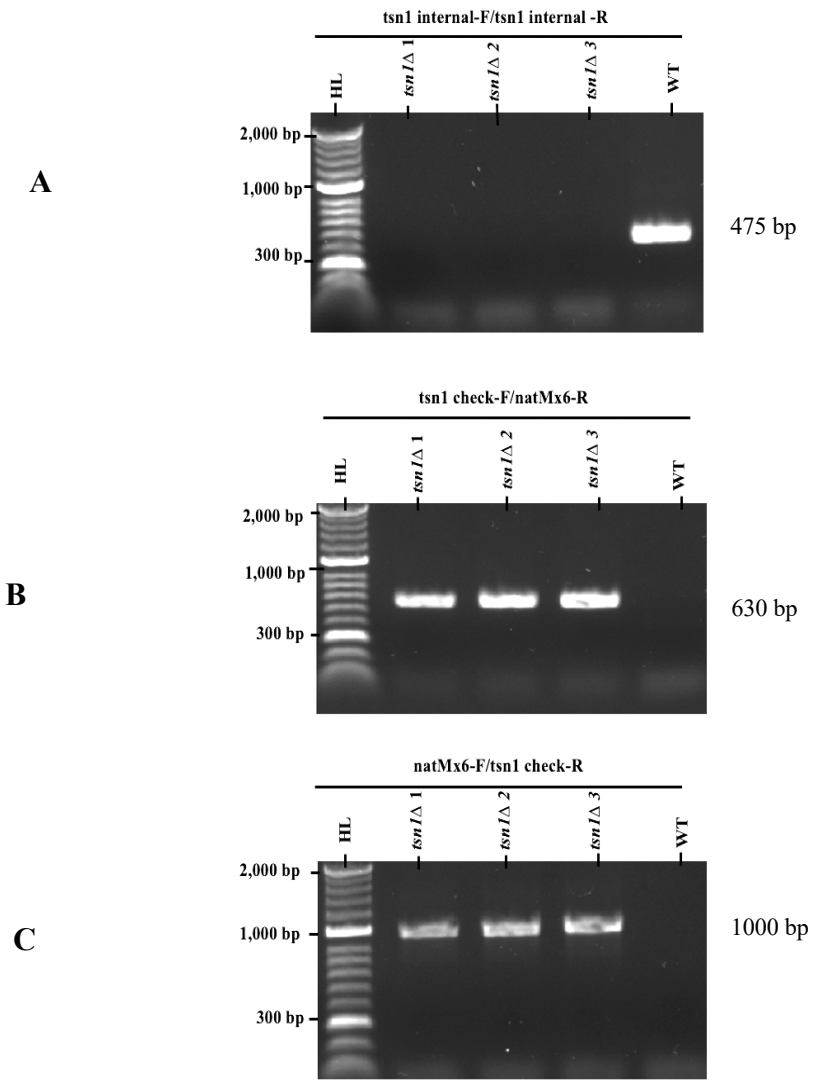


**Figure 4.2. PCR screening of successful *sen1*Δ *tsn1*Δ double mutant deletion.**

**A.** Image of an agarose gel of the PCR products for the WT strain (BP90) and three *tsn1* gene deletion *in sen1*Δ background. The *tsn1* gene internal PCR product is generated using tsn1-internal-F and tsn1-internal-R primers and the predicted product is 475 bp. No PCR products are detected in the successful *tsn1*Δ candidate strains. **B**. To assess the 5' end of the *tsn1* Δ locus the PCR primers tsn1 check-F and natMX6-R were used to check the WT and *tsn1*Δ candidate strains. Whilst no bands were detected in the WT, the *tsn1*Δ strains exhibit a band of approximately 630 bp **C.** To check the 3' end of the *tsn1* Δ locus PCR was conducted on genomic DNA from WT and *tsn1*Δ candidate strains using the natMX6-F and tsn1check- R primers. A band for the correct size was apparent at approximately 1000 bp in the *tsn1*Δ strains, but not the WT strain. H = Hyper ladder.

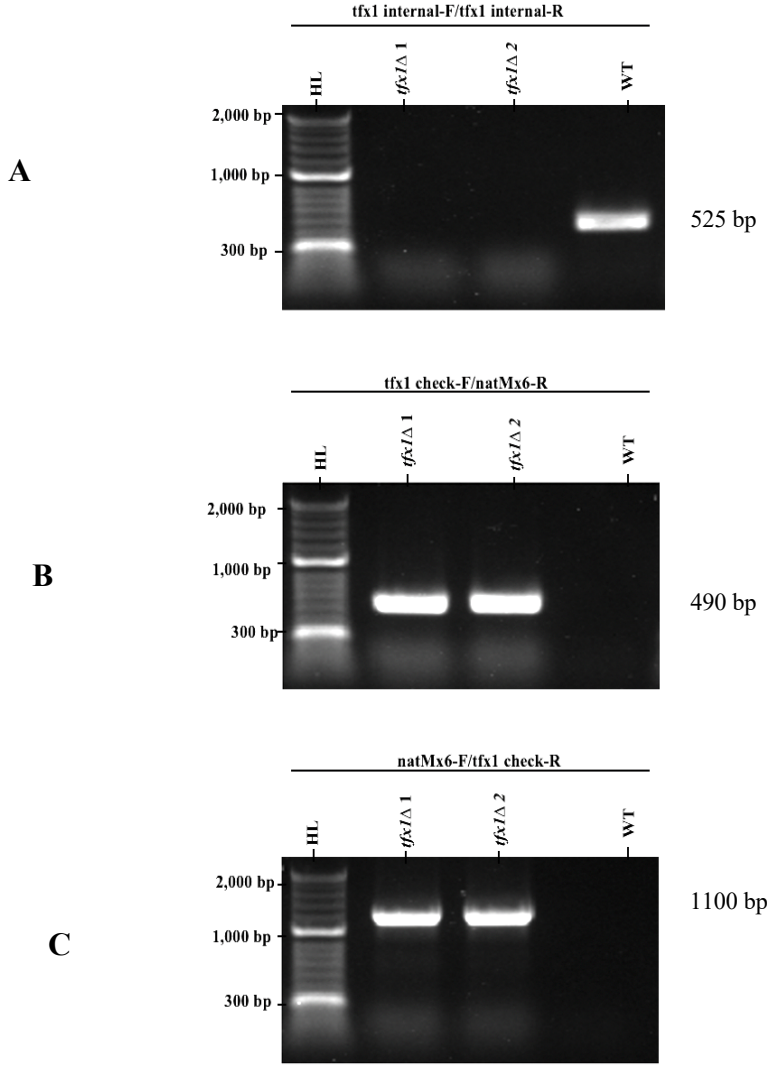


**Figure 4.3. PCR screening of successful *sen1*Δ *tfx1*Δ double mutant deletion (using *natMX6* for *tfx1* replacement).**

**A.** Image of an agarose gel of the PCR products for the WT strain (BP90) and two *tfx1* gene deletion *in sen1*Δ background. The *tfx1* gene internal PCR product is generated using tfx1-internal-F and tfx1-internal-R primers and the predicted product is 525 bp. No PCR products are detectable in the successful *tfx1*Δ candidate strains. **B**. To assess the 5' end of the *tfx1*Δ locus the PCR primers tfx1 check-F and natMX6-R were used to check the WT and *tfx1*Δ candidate strains. Whilst no bands were detected in the WT, the *tfx1*Δ strains exhibit a band of approximately 490 bp **C.** To check the 3' end of the *tfx1*Δ locus PCR was conducted on genomic DNA from WT and *tfx1*Δ candidate strains using the natMX6-F and tfx1check- R primers. A band for the correct size was apparent at approximately 1100 bp in the *tfx1*Δ strains, but not the WT strain. H = Hyper ladder.

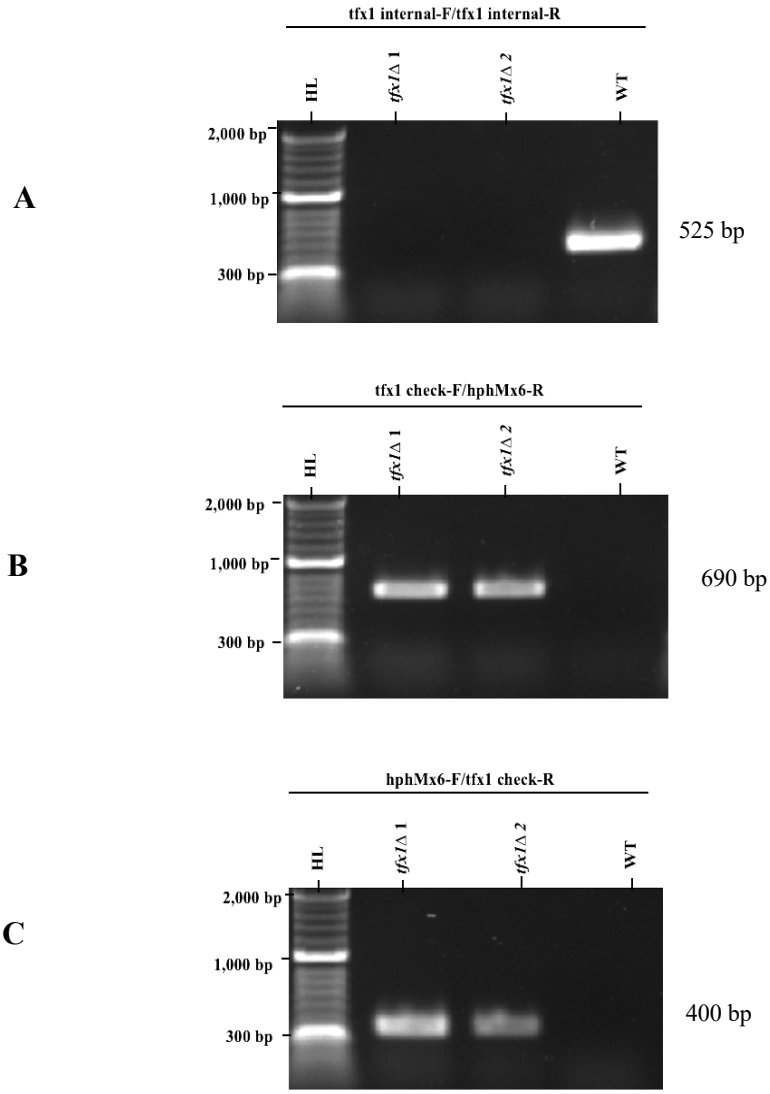


**Figure 4.4. PCR screening of successful *sen1*Δ *tfx1*Δ double mutant deletion (using *hphMX6* for *tfx1* replacement).**

**A.** Image of an agarose gel of the PCR products for the WT strain (BP90) and two *tfx1* gene deletion *in sen1*Δ background. The *tfx1* gene internal PCR product is generated using tfx1-internal-F and tfx1-internal-R primers and the predicted product is 525 bp. No PCR products are detectable in the successful *tfx1*Δ candidate strains. **B**. To assess the 5' end of the *tfx1*Δ locus the PCR primers tfx1 check-F and hphMX6-R were used to check the WT and *tfx1*Δ candidate strains. Whilst no bands were detected in the WT, the *tfx1*Δ strains exhibit a band of approximately 690 bp **C.** To check the 3' end of the *tfx1*Δ locus PCR was conducted on genomic DNA from WT and *tfx1*Δ candidate strains using the hphMX6-F and tfx1check- R primers. A band for the correct size was apparent at approximately 400 bp in the *tfx1*Δ strains, but not the WT strain. H = Hyper ladder.

### 4.2.2. Investigation of the relationship between *sen1* and *tsn1/tfx1*

Results from the sensitivity of the double mutant *tsn1*Δ *rnh201*Δ to the phleomycin and HU, and the fact that Sen1 is postulated to facilitate a discrete RNA:DNA eradication mechanism, raised the query as to whether a DNA damage response defect that was observed for the *tsn1*Δ *rnh201*Δ strain is also apparent in the *sen1* Δ double mutant strains. This led to the exploration of the sensitivity of the *sen1*Δ *tsn1*Δ and *sen1*Δ *tfx1*Δ double mutants to DNA damaging drugs. Spot tests were therefore performed using a variety of DNA damaging agents. These encompassed HU, which acts by perturbing DNA replication (Figure 4.5); CPT, which blocks topoisomerase (Figure 4.6); MMS, which is a DNA alkylator (Figure 4.7); and mitomycin C which is a potent DNA crosslinking agent (Figure 4.8). The results revealed that *sen1*Δ exhibits some sensitivity to HU and the *sen1* Δ *tfx1*Δ double mutant seems to exhibit elevated sensitivity to HU relative to the *sen1*Δ single mutant, while *sen1*Δ *tsn1* Δ does not. Whilst the *sen1* Δ single mutant exhibited no sensitivity to MMC, the double mutant appears to have a very mild sensitivity to this agent (Figure 4.8).

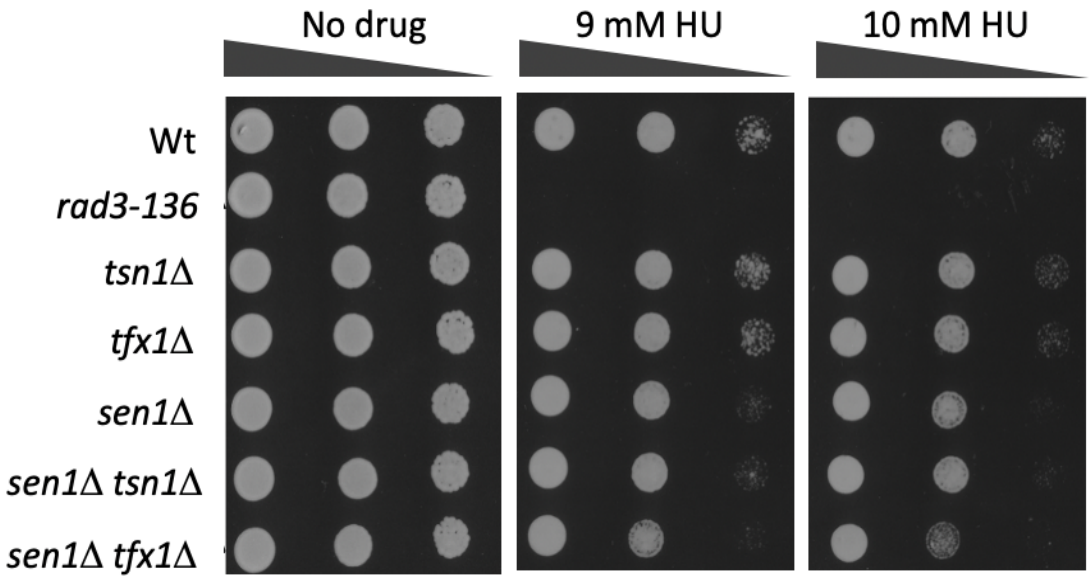


**Figure 4.5. Increased the sensitivity of the *sen1*Δ *tfx1*Δ to hydroxyurea (HU).**

*S. pombe* cultures were serially diluted (x10 increments) then spotted onto YEA with and without HU. Cells were spotted onto two different concentrations of hydroxyurea (9 mM and 10 mM) and were then incubated at 30°C for 3 days. The *rad3-136* mutant was the positive control. The *sen1*Δ single mutant exhibits a clear sensitivity to HU. The *sen1*Δ *tsn1* Δ double mutant exhibited no added sensitivity compared to the *sen1*Δ single mutant. However, the *sen1*Δ *tfx1*Δ double mutant exhibited high sensitivity than the *sen1*Δ single mutant.

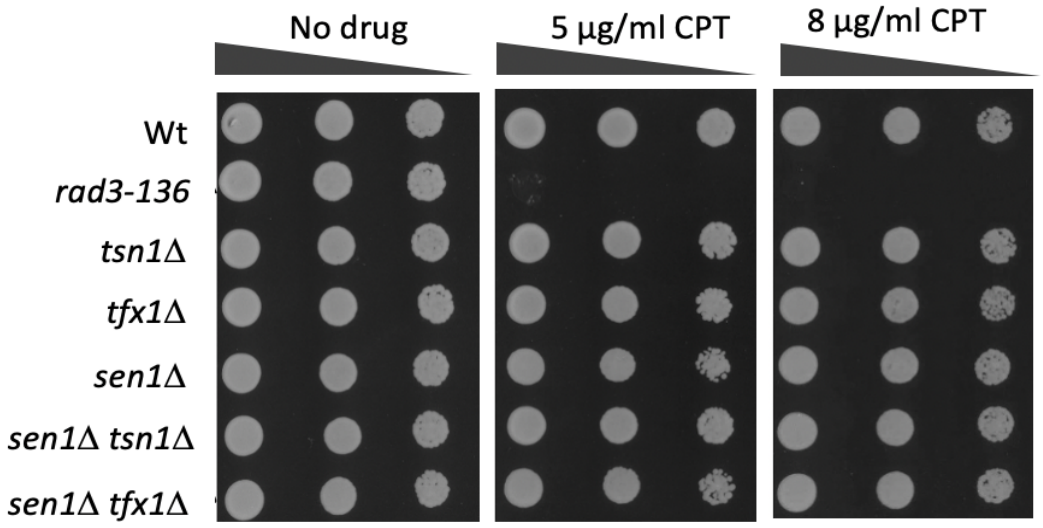


**Figure 4.6. Sensitivity spot test of Camptothecin (CPT).**

*S. pombe* cultures were serially diluted (x10 increments) then spotted onto YEA with and without CPT. Cells were spotted onto two different concentration of CPT (5 µ g/ml and 8 µg/ml) and were then incubated at 30°C for 3 days. The *rad3-136* mutant was the positive control. No strains exhibited any sensitivity to CPT relative to the Wt.

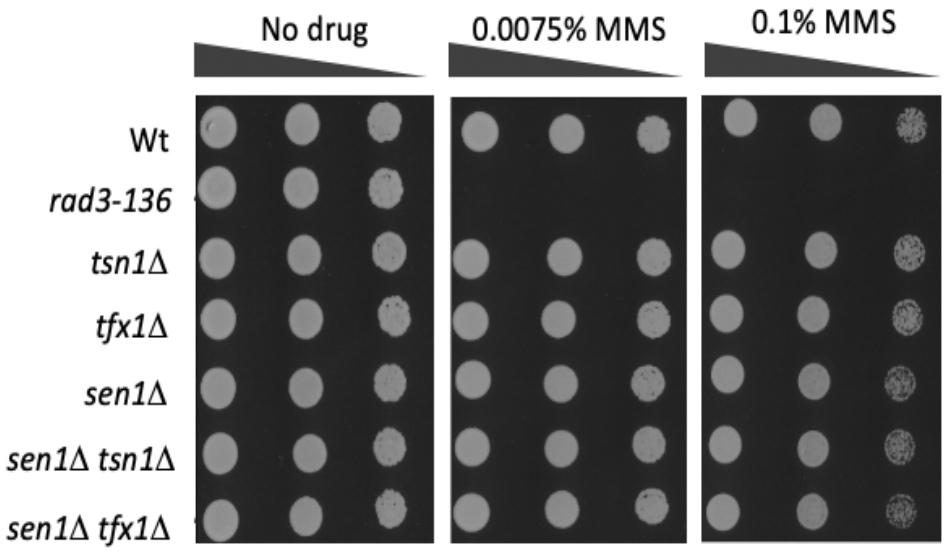


**Figure 4.7. Sensitivity spot test of Methyl methane sulfonate (MMS).**

*S. pombe* cultures were serially diluted (x10 increments) then spotted onto YEA with and without MMS. Cells were spotted onto two different percentages of MMS (0.0075% and 0.01%) and were then incubated at 30°C for 3 days. The *rad3-136* mutant was the positive control. No strains exhibited any sensitivity to MMS relative to the Wt.

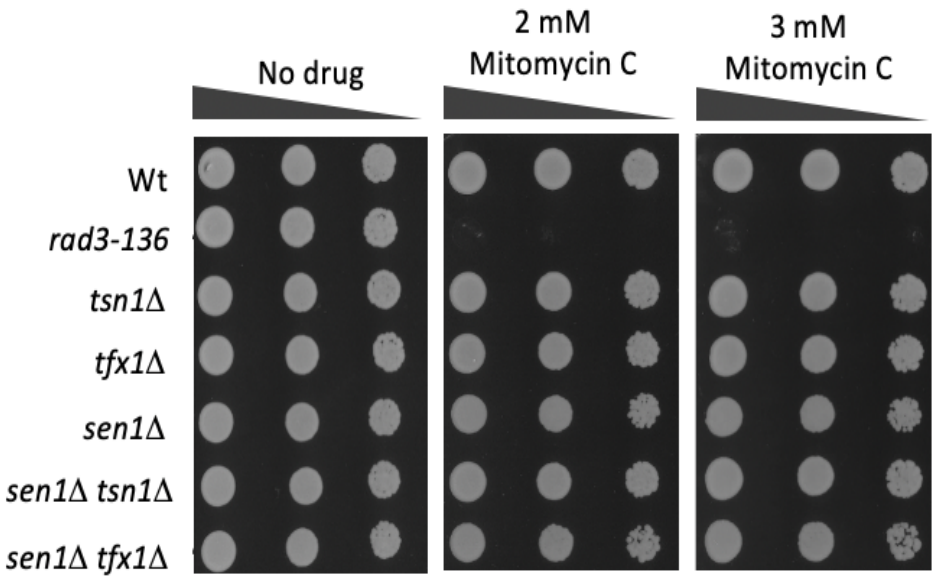


**Figure 4.8. Sensitivity spot test of Mitomycin C (MMC).**

*S. pombe* cultures were serially diluted (x10 increments) then spotted onto YEA with and without MMC. Cells were spotted onto two different concentration of Mitomycin C (2 mM and 3 mM) and were then incubated at 30°C for 3 days. The *rad3-136* mutant was the positive control. The *sen1*Δ *tsn1* Δ, *tsn1* Δ and *sen1*Δ strains exhibited no sensitivity compared with the WT. The strain sen1Δtfx1Δ exhibited a mild sensitivity to MMC relative to the WT and *sen1*Δ and *tsn1*Δ single mutants.

## 4.3. Discussion

Different biological processes are influenced by Translin and Trax in a way that is specific to the species and tissue (Jaendling & McFarlane, 2010; McFarlane & Wakeman, 2020). It seems that the modulation of RNA molecules (e.g., mRNAs, tRNA precursors, microRNAs, and siRNA passenger strands) is critical for most of their biological functions (Jaendling & McFarlane, 2010; Gomez-Escobar et al., 2016). In spite of this knowledge, it has not yet been fully established what the functional importance of the binding ability to chromosomal translocation breakpoint junctions is (Aoki et al., 1995; McFarlane & Wakeman, 2020). Furthermore, there is evidence that Translin and Trax modulate the abundance of telomere transcripts, both acting in distinct ways. Changes to the levels of telomeric transcripts appears to be tolerated under laboratory condition, as neither single mutant of *S. pombe tfx1* or *tsn1* exhibit overt negative phenotypes. However, correlation has been reported between Translin and Trax disruption and diminished proliferation of cells in mammals (Yang & Hecht, 2004; Yang et al., 2004; Ishida et al., 2002; Gomez-Escobar et al., 2016), although it is possible that this may be due to non-telomeric function defects in mammalian cells. Additionally, the *tsn1*Δ and *tfx1*Δ mutants of the fission yeast exhibit a single defect, namely, incorrect modulation of telomeric transcripts. Therefore, *S. pombe* is an appropriate system for investigating this key role of these proteins when other biological functions do not show any disruption.

*S. pombe* Telomeric DNA provides the template for specific RNA molecules termed TERRAs, which are also found in human cells; moreover, the sub-telomeric regions are also transcribed into other RNAs, including ARRETs (Cusanelli & Chartrand, 2015; Azzalin & Lingner, 2015; Maicher et al., 2014; Rippe & Luke, 2015; Wang *et al.*, 2015; Lalonde and Chartrand 2020). Many different roles of telomeres are underpinned by TERRAs, such as response to DNA damage, regulation of telomeric length, modulation of telomerase activity, and development of telomeric heterochromatin (Wang et al., 2015;Maicher et al., 2014; Cusanelli & Chartrand, 2015; Rippe & Luke, 2015; Bettin et al. 2019). Tsn1 and Tfx1 of the fission yeast function to control ARRETs and TERRAs, with Tsn1 suppressing TERRAs and Tfx1 suppressing ARRETS, although the functional significance of this is unclear as single mutants of *tsn1* and *tfx1* have no overt genome stability defects (Jaendling et al., 2007; Gomez-Escobar et al., 2016; Kwapisz and Morillon, 2020). Gomez-Escobar et al. (2016) concluded that the regulation of telomeric and sub-telomeric transcripts by Tfx1 and Tsn1 was based on a mutual mechanism.

This, in conjunction with the finding that the *sen1*Δ *tfx1*Δ double mutant is extremely sensitive to the HU (Figure 4.5), could suggest a role for Sen1 in sub-telomeric ARRET control. If there is a correlation between the HU sensitivity of the *sen1*Δ *tfx1*Δ double mutant and telomeric transcripts, it may be worthwhile examining this phenotype in the HAATI strain background, which is telomere deficiency (Jain et al., 2010).

The nucleic acid structures with three strands and comprising a RNA:DNA hybrid and a displaced DNA strand are known as R-loops (RLs) (Fragkos & Naim, 2017; Wahba et al., 2013; Felipe-Abrio et al., 2015; García-Rubio et al., 2018; Jimeno et al., 2019). Such RLs are particularly enriched in genomic regions with GC skew and a transcript with G abundance. Although they have essential physiological functions in cells, RLs may cause the genome to become unstable when they occur in excessive levels. Toubiana and Selig (2018) argued that telomeric sequences were ideal for the formation of RLs as telomeric repeats had ideal GC skew and due to the identification of TERRAs. Telomeric RLs occur in normal cells in humans with transcription of minimal TERRA levels, implying that they may have a physiological function in the upkeep of telomeres. Several researchers have shown that, according to the cellular recombinogenic capacities, excessively high TERRA transcription associated with a number of human pathologies increases the levels of telomeric RLs and induces a range of cellular effects (Toubiana & Selig, 2018; Bettin et al., 2019). Given their ability to change their favourable action to unfavourable one depending on circumstances, telomeric RLs must be closely modulated, as demonstrated by their investigation in different organisms. It can be concluded that, for purposes of telomere maintenance, both Tfx1 and Sen1 are required by the Tfx1-reliant telomeric RNAs forming RNA:DNA hybrids, with the *sen1*Δ *tfx1*Δ double mutant being significantly sensitive to agents causing DNA damage.

It is of note that a correlation has been established between *sen1* and displacement of RNA Pol III, which could assist in hindering recombination at tRNA genes referred to as replication pause sites with the potential to turn into recombination hotspots (Pryce et al., 2009). This warrants additional examination of the enhanced recombination observed earlier in the *dcr1*Δ *tsn1*Δ double mutant strains (MacFarlane group, unpublished data; H. Al-Ahmadi, PhD thesis, Bangor University; Al-Thagafi, PhD thesis, Bangor University; O. Al-Zahrani, PhD thesis, Bangor University).

Pryce et al. (2009) reported a plasmid-by-chromosome recombination system for assessment of recombination occurring at a tRNA gene. The robust activity of replication fork barrier (RFB) exhibited by tRNA genes was proven through the application of the above-mentioned system to evidence that the progression of DNA replication fork was delayed by a fission yeast tRNA gene (Pryce et al., 2009). Succinctly, the procedure involved inserting the tRNA gene $tRNA^{GLU}$ separately in the two orientations in the *Bst*XI site at the *ade6* locus of the genome of fission yeast. Orientation 1 was associated with expectation of direct collision between RNA Pol III, the mediator of tRNA gene transcription, and the replication system (Pryce et al., 2009); in this case, no significantly higher recombination frequency was exhibited by the *dcr1Δ* mutation and *dcr1*Δ *tsn1*Δ double mutant by comparison with the WT strain. On the other hand, for orientation 2, there was expectation of direct collision between the replication fork and RNA Pol II, which is known to transcribe the tRNA non-template strand of tRNA genes (Castel et al., 2014), and in this context, recombination frequency nearly doubled by comparison with the WT strain due to Dcr1 loss. It is notable in that, the recombination frequency increased even more owing to *tsn1* mutation in the *dcr1*Δ background in the case of orientation 2, but not orientation 1. However, loss of *tfx1* resulted in no recombination in either orientation. This means that the genome stability role associated with Tsn1 seems to be distinct from the DNA damaging agent sensitivity seen in the *sen1Δ tfx1Δ* double mutant, further suggestive of a specific role for Tfx1 at telomeres, which is also consistent with the conclusions of Gomez-Escobar et al. (2016).

Interestingly, the need for *tfx1* in the *sen1*Δ background is only apparent in response to HU damage, and very mildly in response to MMC damage. This suggests a very specific role, as opposed to a wider role in DNA damage recovery. In humans, TRAX is required for assisting ATM responding to DNA damage (Wang et al., 2016). If this were the case in *S. pombe* it is reasonable to assume other damaging agents would result in a more overt set of DNA damage response phenotypes. Collectively, we speculate that Tfx1 in *S. pombe* is plays a specific replication inhibition response at telomeric regions and that this is an auxiliary role to the role played by Sen1.

To summarise, these findings show that, when *sen1* is not present, recovery from certain forms of DNA damage is dependent on Tfx1, not Tsn1. It can thus be speculated that, Sen1 and Tfx1 are in functionally redundant pathways that relate to control of replication-associated defects involved in telomeric transcript regulation, possibly RNA:DNA hybrid processing at the

telomeres. If this is correct, is appears to be distinct from a role for Tsn1, further indicating that Tsn1 and Tfx1 are functionally discrepant, at least in *S. pombe*. These phenomena offer tantalizing insight into important new regulator roles for these disease-associated factors the details of which require further assessment.

# Chapter 5: Investigate the genetic relationship of *dcr1* to the RNase H genes in controlling genome stability.

# 5.1. Introduction

In eukaryotic organisms, gene silencing is governed by RNAi (Gutbrod and Martienssen, 2020). RNAi was first used to describe the ability of double-stranded RNA (dsRNA) molecules extrinsically added to cells to silence the chromosomal expression of homologous sequences within the nematode *Caenorhabditis elegans* (Fire et al., 1998; Agrawal et al., 2003; Moazed, 2009; Fischer, 2010; Massirer and Pasquinelli, 2013; Almeida et al., 2019). Small interfering RNAs (siRNAs) are between 20 and 30 nucleotides have been recognised as essential factors in the control of which genes are either silenced or active, together with the degree of activity of the latter (Moazed, 2009; Holoch and Moazed, 2015; Gutbrod and Martienssen, 2020).

The RNAi apparatus contributes to the development and maintenance of heterochromatin in eukaryotes including advanced telomere, centromere, mating-type loci and rDNA such as seen in *S. pombe* (Djupedal and Ekwall, 2009; Klar, 2007; Martienssen and Moazed 2015). If core RNAi regulatory genes are knocked out, e.g., *ago1* and *dcr1,* heterochromatic H3K9 methylation is diminished resulting in reduced heterochromatin and impaired genome function and chromosomes segregation (Tadeo et al., 2013; Sadeghi et al., 2015; Holoch & Moazed, 2015; Yang et al., 2018; Gutbrod and Martienssen, 2020).

In *Homo sapiens* and *Drosophila melanogaster,* the Translin-TRAX (C3PO) complex is a key factor in the RNAi pathways. It assists in the subtraction of passenger strands from siRNAs, thus playing a role in silencing governed by the RNAi RISC complex (Liu et al., 2009; Jaendling & McFarlane, 2010; Tian et al., 2011; Ye et al., 2011; Holoch & Moazed, 2015; Zhang et al., 2016).

It has been observed by the McFarlane Group that sensitivity to various DNA damaging agents is increased in the *dcr1*Δ*tsn1*Δ double mutant relative to the *dcr1*Δ single mutant. Therefore, a genetic association between *tsn1* and *dcr1* has been demonstrated. Dcr1 has been demonstrated to contribute via an RNAi-independent mechanism to the removal of RNA Pol II from the genome and thus protect the genome from RNA polymerase II – replisome collisions (Castel et al., 2014). Given this and the finding that *tsn1* is in a distinct genetic pathway to *dcr1*, we propose that Tsn1 and Dcr1 function in distinct pathways to maintain genome stability,

possibly to remove RNA Pol II or the RNA:DNA hybrids that might result from stalled RNA Pol II. This proposal is in keeping with the nucleic acid binding and RNAse functions of Tsn1 (Jaendling & McFarlane, 2010), and may explain why Translin is associated with chromosomal translocation site in human malignancies.

Transcription replication conflicts can arise from transcription-produced RNA:DNA hybrids, which in turn can disrupt genomic integrity and, potentially, cause aberrations that may induce malignant change (Zimmer & Koshland , 2016; Rondón and Aguilera, 2019). It has also been shown that enhanced sensitivity to several DNA damaging agents is seen in the *rnh201*Δ *tsn1*Δ double mutant (Chapter 3). RNase H201 has a role of eradicating ribonucleotides included in error in DNA replication and unprocessed Okazaki fragments (Kojima et al., 2018). Genome stability maintenance relies on RNase H activity in *S. pombe.* Deletion of both RNaseH1 and RNaseH201 genes (*rnh1* and *rnh201*) results in an inability to tolerate DNA replicative stress and other DNA damage, indicating that the two pathways of RNase H function redundantly in genome maintenance (Ohle et al., 2016). Tsn1, but not Tfx1, appears to function redundantly with Rhn201, but not Rnh1 (Chapter 3).

Given the elevated sensitivity of both the *dcr1*Δ *tsn1*Δ and *rnh201*Δ *tsn1*Δ double mutants to the DNA replication stressing agent HU relative to *the dcr1*Δ single mutant, we hypothesised that Dcr1 and Tsn1 could operate within the distinct RNase H pathways. Based on the genetic evidence, one pathway is predicted to involve Dcr1 and Rnh201, whilst the other is predicted to involve Tsn1 and Rnh1. Such a hypothesis not only fits the current experimental data but also predicts that a *dcr1*Δ *rnh1*Δ will be hypersensitive to HU, whereas *dcr1*Δ *rnh201*Δ will not be. In order to evaluate this hypothesis, *dcr1*Δ *rnh1*Δ and *dcr1*Δ *rnh201*Δ strains were constructed and tested for replicative stress (HU) response.

# 5.2. Results

## 5.2.1. Relationship between *dcr1* and RNase H genes (*rnh1* and *rnh201*)

In order to appraise any association of *dcr1*with RNAse H activity, relevant double mutants, i.e., *dcr1*Δ *rnh1*Δ and *dcr1*Δ *rnh201,* were necessary. The latter was created by colleagues within the laboratory; the strain utilised in the spot tests presented underwent PCR to verify its genotype.

The generation of the *dcr1*Δ *rnh1*Δ double mutant was a little more problematic using the direct deletion methodology, the reasons for this were not clear, but one possibility was that the double mutant exhibited synthetic lethality, so viable double mutants could not be generated.

To assess for synthetic lethality the four spores produced from one meiosis can be appraised using tetrad dissection of asci; this technique is used within the field of yeast genetics, offering the ability to establish linkage, to recognise distinct phenotypes related to double mutants, or to appraise particular meiotic aberrations with only a low number of tetrads (Escorcia & Frosburg, 2018). *h*+ and *h*- single mutant strains are crossed on SPA medium for a period of 3 days. A micromanipulator is employed in order to segregate spores from mature asci developed following mating on SPA plates to positions that are 5 mm distance from each other in a linear configuration on a YEA plate. Spores are left to sporulate and to form colonies. If there is no genetic linkage, then genes will segregate according to Mendelian distribution and one of the four spores would contain a double mutant. If all four spores produce a viable colony, and one is the double mutant, then there is no synthetic lethality.

A cross was conducted between the *dcr1*Δ $h^-$ and *rnh1*Δ $h^+$ strains, from which numerous tetrads were acquired (although this cross did yield some non-standard asci relative to the wild-type control, but we have previously noted that this is a feature of RNAi pathway gene mutants, suggesting a meiotic defect; data not shown). Wild-type and mutant cross tetrads were dissected, and four viable spores were obtained for approximately half of the four spore asci from the cross with the mutant strains (some four spore asci did not give four viable colonies and this is thought to reflect a meiotic segregation phenotype for RNAi genes, which we have previously observed) (Figure 5.1). PCR analysis of cells from colonies of asci producing four viable spores revealed that the double mutant was obtained as per Mendelian segregation

patterns (examples shown in Figure 5.1 – blue circles). Furthermore, meiotic crosses were performed in order to acquire a random spore pool according to the protocol presented in Section 2.0. The replica plates of colonies on selective media were necessary; again, viable *dcr1*Δ *rnh1*Δ double mutants were obtained indicating that the double mutant does not exhibit synthetic lethality. Examples of five double mutants assessed by PCR analysis are shown in Figure 5.2 and 5.3. Of the five double mutant strains verified by PCR, mating type was tested by iodine staining (iodine staining mated cells following mating of strains of unknown mating type with both *h*+ and *h*- strains can indicated the mating type of the unknown strain) and both *h*+ and *h*- double mutants were obtained, as would be expected in the absence of linkage to the mating type locus (Figure 5.4).

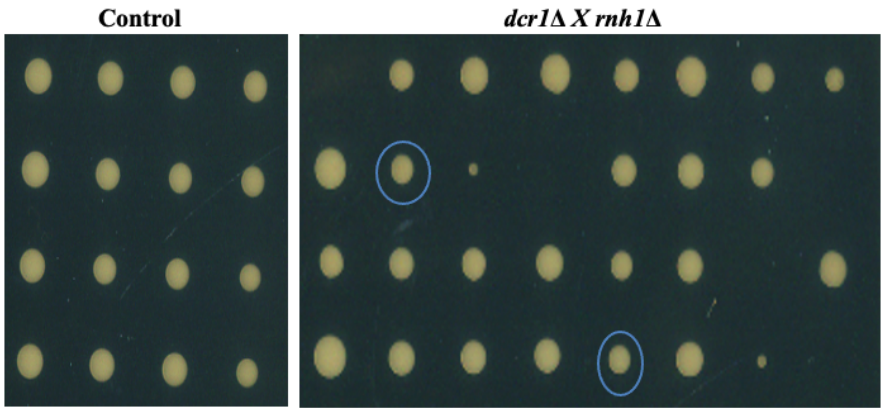


**Figure 5.1. Tetrad dissection for the isolation *dcr1* Δ *rnh1*Δ double mutants.**

Two typical dissections are illustrated. Dissected spores were cultured on YEA for 4 days at a temperature of 30°C. **A.** depicts a tetrad dissection plate of spores from a wild-type cross (BP89 X BP90): **B.** Shows spores from the *dcr1*Δ X *rnh1*Δ cross. Double *dcr1*Δ *rnh1*Δ mutants (verified by PCR) are shown by the blue circles; these colonies are of uniform size relative to all other colonies indicating there is no notable growth defect under these conditions.

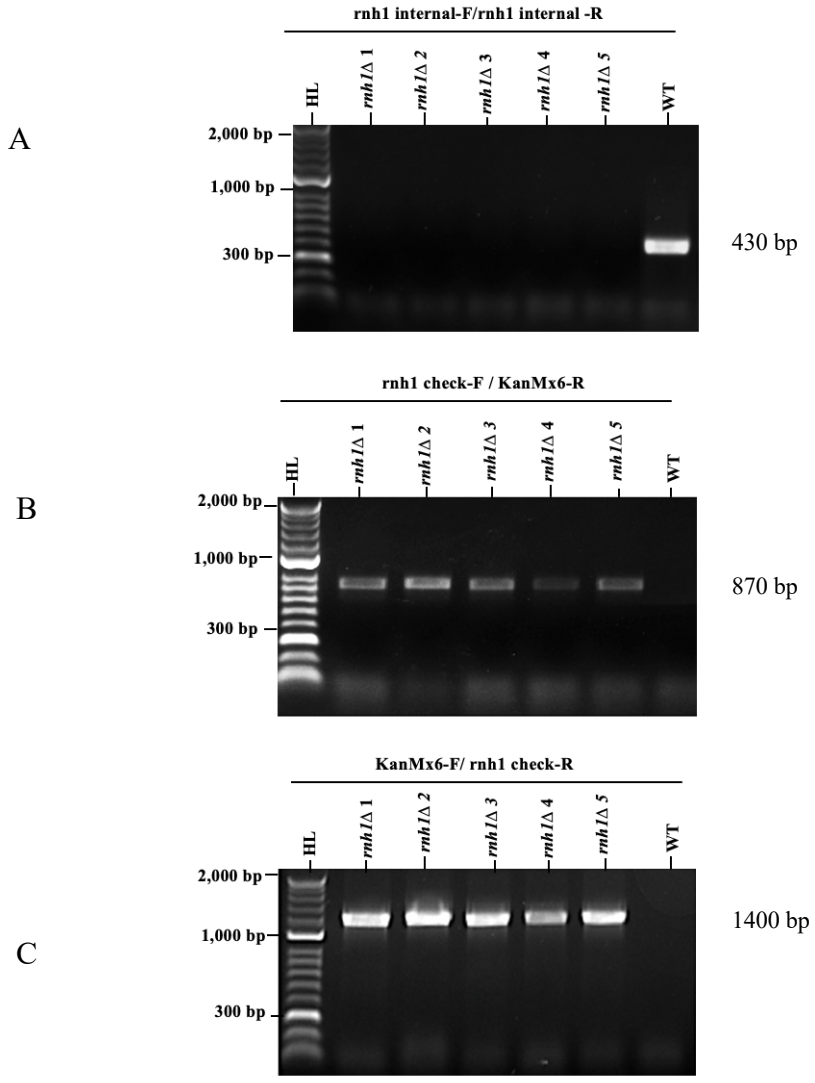


**Figure 5.2. PCR verification of *dcr1*Δ *rnh1*Δ double mutants.**

**A.** Image of agarose gels of PCR products for the WT strain (BP90) and *rnh1*Δ single mutant candidates *in dcr1*Δ background. The *rnh1*gene internal PCR product is generated using rnh1-internal-F and rnh1-internal-R primers measures 430 bp. No PCR products are detectable in the successful *rnh1*Δ candidate strains. **B**. The PCR primers rnh1 check-F and kanMX6-R were used to check the *rnh1*Δ candidate strains. The *rnh1*Δ strains exhibit a band of approximately 870 bp. **C.** To amplify the *rnh1*Δ candidate strains, the kanMX6-F and rnh1check-R primers were used. 1400 bp product is evident in the *rnh1*Δ strains. H = Hyper ladder.

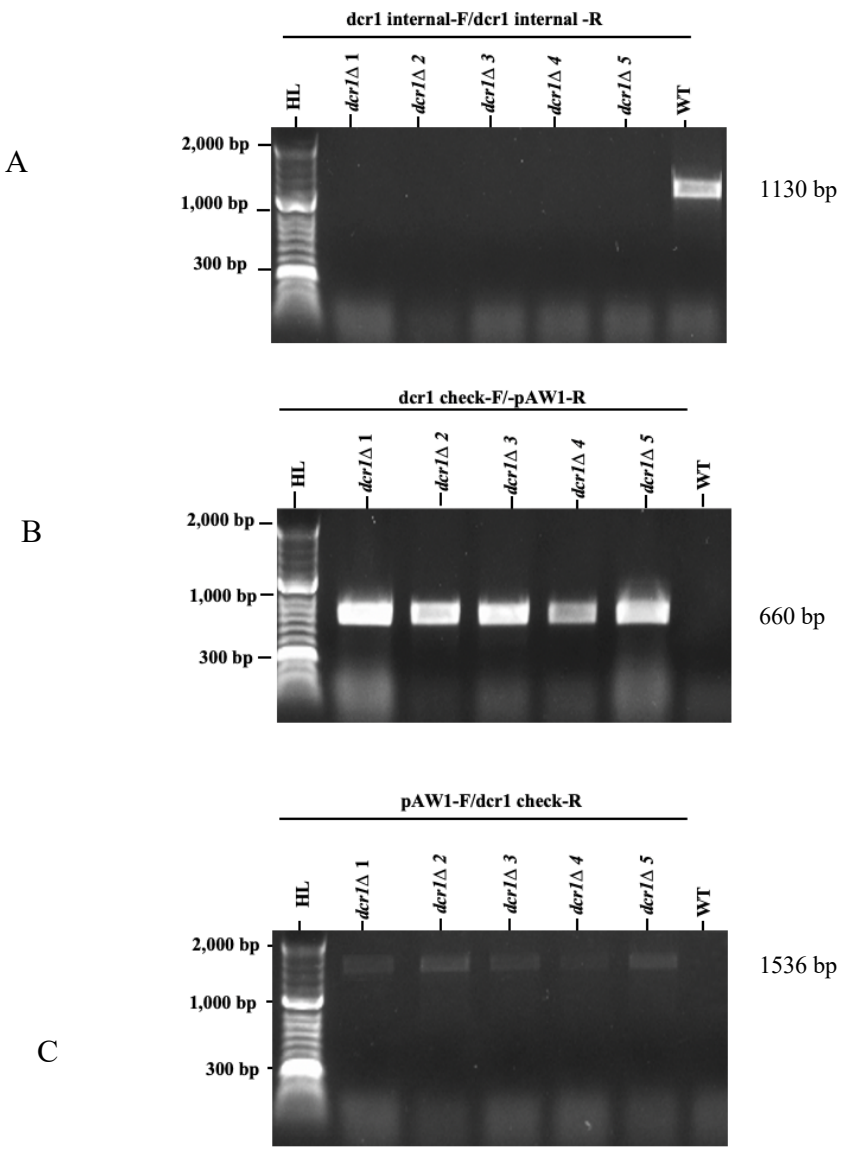


**Figure 5.3. PCR verification of *dcr1*Δ *rnh1*Δ double mutants.**

**A.** Image of agarose gels of PCR products for the WT strain (BP90) and *dcr1*Δ single mutant candidates *in rnh1*Δ background. The *dcr1*gene internal PCR product is generated using dcr1-internal-F and dcr1-internal-R primers measures 1130 bp. No PCR products are detectable in the successful *dcr1*Δ candidate strains. **B**. The PCR primers dcr1 check-F and pAW1-R were used to check the *dcr1*Δ candidate strains. The *dcr1*Δ strains exhibit a band of approximately 660 bp. **C.** To amplify the *dcr1*Δ candidate strains, the pAW1-F and dcr1check-R primers were used. 1536 bp product is evident in the *dcr1*Δ strains. H = Hyper ladder.

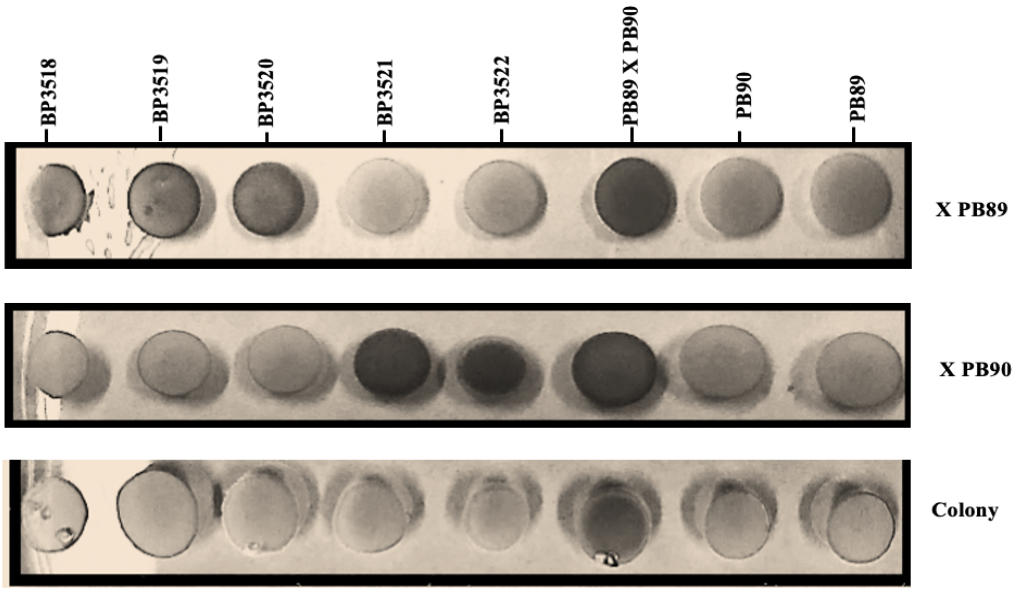


**Figure 5.4. Examination of mating type status by iodine staining.**

The image illustrates the mating type of the *dcr1*Δ *rnh1*Δ double mutants. The mating mixes on SPA are exposed to iodine vapours following 3 days under mating conditions. Positive and negative response to iodine being respectively indicated by the black colouring of spore-containing materials which in this case *is dcr1*Δ *rnh1*Δ $h^{+}$strain and the yellow colouring of materials comprising solely vegetative cells (BP90, BP89 and *dcr1*Δ *rnh1*Δ$h^{-}$) after five minutes of exposure to iodine vapours.

### 5.2.2. *dcr1* exhibits genetic interaction with *rnh201* for DNA damage response control

To address the hypothesis that Dcr1 and Rnh1 function in distinct DNA damage response pathways (see above) we tested the newly created double mutants (*dcr1*Δ *rnh1*Δ and *dcr1*Δ *rnh201*Δ) for their response to DNA damaging agents. A range of such agents were used for spot tests. In these experiments, the DNA damaging agents that were tested encompassed the DNA replication inhibitor, HU (Figure 5.5), the DNA alkylating agent, MMS (Figure 5.6), the topoisomerase inhibitor, CPT (Figure 5.7) and UV, which provokes numerous adducts (Figure 5.8). Compared with the WT, little or no change in sensitivity to the above damaging agents were observed in the *tsn1*Δ and *rnh1*Δ single mutants, although the *tsn1*Δ does appear to show a mild sensitivity that has not previously been observed. The reason for this was not clear. A modest sensitivity to HU was noted in the *dcr1*Δ and *rnh201*Δ single mutants. Unexpectedly, sensitivity was notably increased in the *dcr1*Δ *rnh201*Δ double mutant relative to the single mutants but not in the *dcr1*Δ *rnh1*Δ double mutant (this observation has subsequently been verified by a co-worker within the group who also revalidated the genotypes by PCR analysis of genomic DNA). The latter exhibited a very slight increased sensitivity to HU, CPT and UV. In contrast to the single mutants, *rnh1*Δ and *rnh201*Δ, the double mutant *dcr1*Δ *rnh201*Δ failed to demonstrate any increase in sensitivity following MMS and CPT. Interestingly, the *dcr1*Δ *rnh201*Δ double mutant actually appears to have reduced sensitivity to CTP relative to the *dcr1*Δ single mutant, suggesting that loss of *rnh201* partially suppresses the need for *dcr1* in response to CTP.

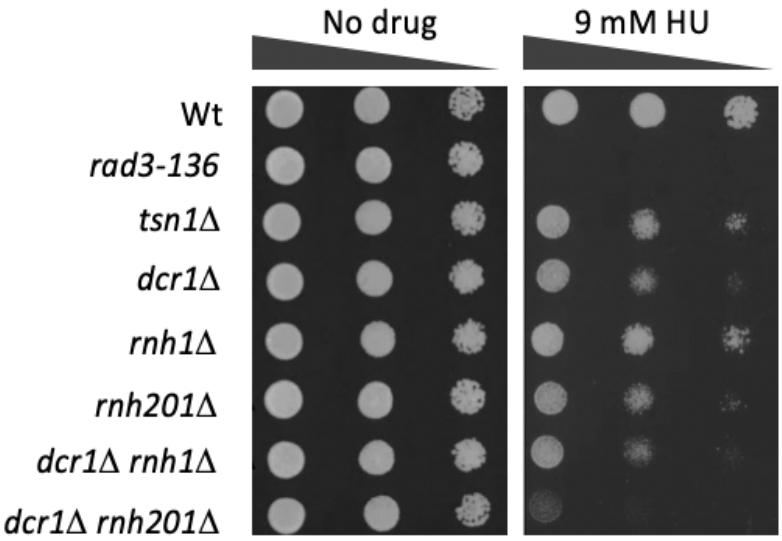


**Figure 5.5. Increased the sensitivity of the *dcr1*Δ *rnh201*Δ to hydroxyurea (HU).**

*S. pombe* cultures were serially diluted (x10 increments) then spotted onto YEA with and without HU. Cells were spotted onto (9 mM of hydroxyurea) and were then incubated at 30°C for 3 days. The *rad3-136* mutant was used as a positive control. The *dcr1*Δ *rnh201*Δ double mutant show hypersensitivity to HU compared with the *rnh1*Δ and *rnh201*Δ single mutant, but the *dcr1*Δ *rnh1*Δ double mutant show no increased sensitivity.

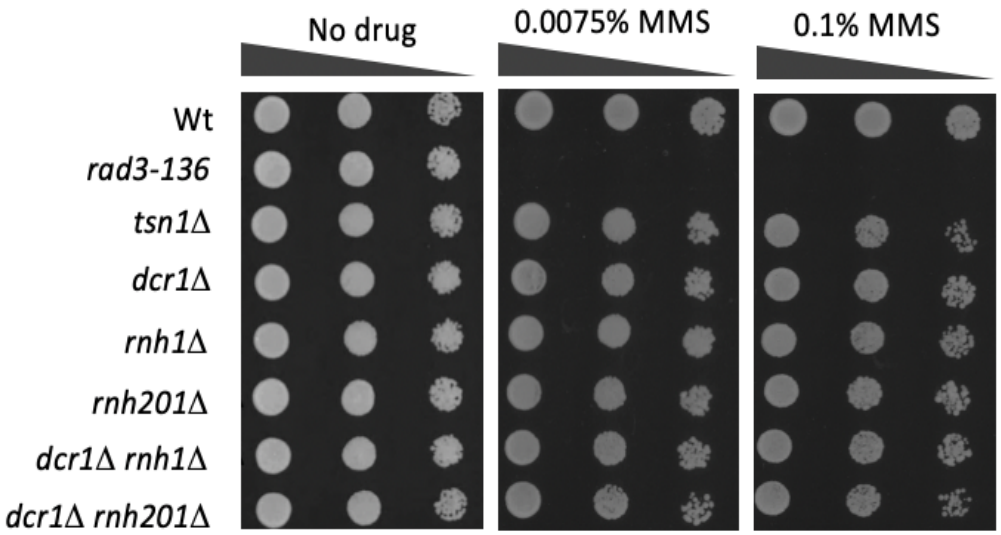


**Figure 5.6. Sensitivity spot test of Methyl methane sulfonate (MMS).**

*S. pombe* cultures were serially diluted (x10 increments) then spotted onto YEA with and without MMS. Cells were spotted onto two different percentages of MMS (0.0075% and 0.01%) and then incubated at 30°C for 3 days. *rad3-136* was used as a positive control. The double mutants *dcr1*Δ *rnh1*Δ and *dcr1*Δ *rnh201*Δ show no increase sensitivity to the MMS compared with WT and the *dcr1*Δ single mutant.

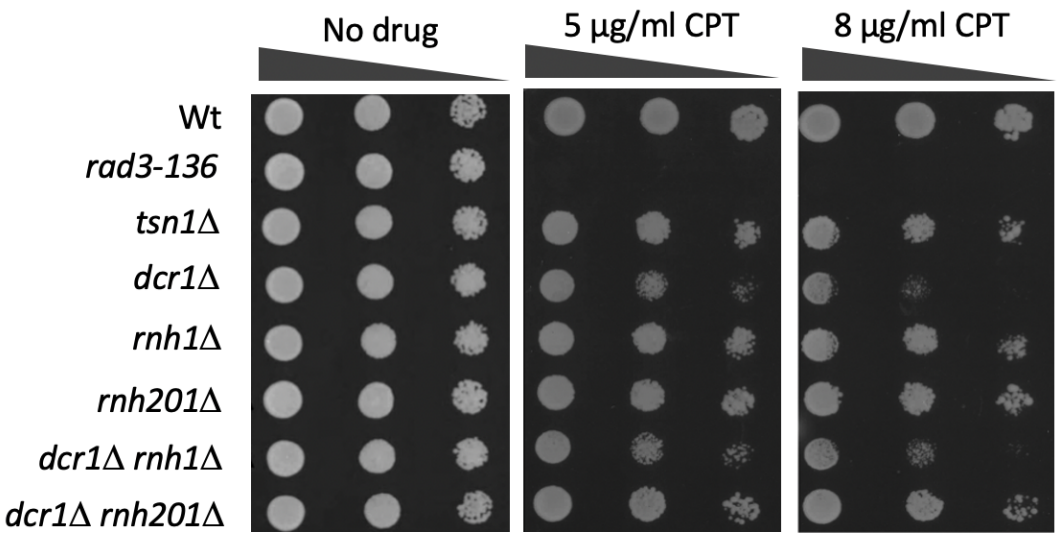


**Figure 5.7. Increased the sensitivity of the *dcr1*Δ *rnh1*Δ to Camptothecin (CPT).**

*S. pombe* cultures were serially diluted (x10 increments) then spotted onto YEA with and without CPT. Cells were spotted onto two different concentration of CPT (5 µg/m and 38 µg/ml CPT) and then incubated at 30°C for 3 days. *rad3-136* was used as a positive control. The *dcr1*Δ and *dcr1*Δ *rnh1*Δ double mutants show increased sensitivity to CPT compared with WT and *dcr1*Δ *rnh201*Δ double mutant. The *dcr1*Δ *rnh201*Δ double mutant does not exhibit the same level of sensitivity as seen for the *dcr1*Δ single mutant.

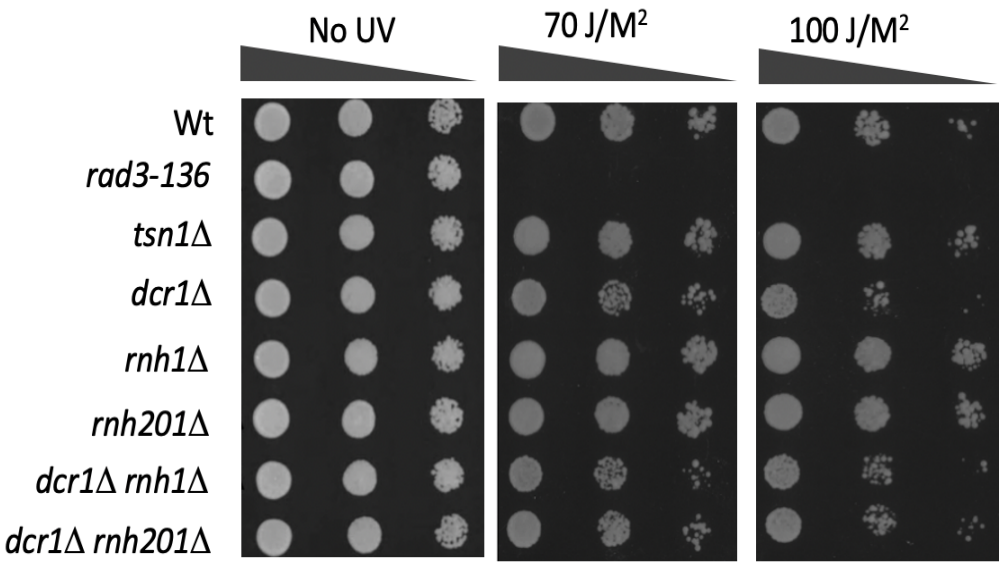


**Figure 5.8. Increased the sensitivity of the *dcr1*Δ *rnh1*Δ to UV.**

*S. pombe* cultures were serially diluted (x10 increments) then spotted onto YEA with and without UV. Cells were spotted onto two different doses of ultraviolet irradiation (70 J/M$^2$ and 100 J/M$^2$) and were then incubated at 30°C for 3 days. *rad3-136* was used as a positive control. The *dcr1*Δ and *dcr1*Δ *rnh1*Δ double mutants show increased sensitivity to UV compared with WT and *dcr1*Δ *rnh201*Δ double mutant.

## 5.3. Discussion

When it was first observed that Translin attaches to chromosomal translocation breakpoint junctions in human malignancies, the notion that Translin is involved in the regulation of recombination was broached (Aoki et al, 1995; Jaendling & McFarlane, 2010;). However, the precise function, if any, in this regard is still to be elucidated. Earlier work evaluating Tsn1 and Tfx1 in *S. pombe* reported that these genes are not primary factors in recombination and its associated mechanisms, e.g., repair of DNA damage (Jaendling et al., 2008). The two pairing proteins have been proposed to be involved in RNA metabolism governance by several researchers, including possible participation in the RNAi pathway (Liu et al., 2009; Ye et al., 2011; Zhang et al., 2016). However, the exact association between Translin, TRAX and malignancy-related chromosomal translocations, together with their interplay with RNA metabolism, remains undetermined.

In the last few years, Dcr1, an RNAi regulator in *S. pombe,* was reported to exhibit a function that was independent of RNAi in the avoidance of DNA damage. Dcr1 eradicates RNA pol II-mediated highly recombinogenic RNA:DNA hybrids from specific areas where there is collision between transcription and replication, e.g., rDNA and tRNA genes, an action which preserves the integrity of the genomic material (Castel et al., 2014; Ren et al., 2015). It is thought to do this by assisting in the removal of RNA polymerase II and associated RNA:DNA hybrids, which it does via a mechanism that is independent of its RNAse activity (Castel et al., 2014). Subsequently, it has been shown by the McFarlane Group that *dcr1*Δ mutant sensitivity to some DNA damaging agents and substances that inhibit replication is markedly enhanced after including the extra *tsn1*Δ mutation, as observed in the data of co-workers previously.

This significant discovery suggested that Tsn1 plays a role in the DNA damage/prevention response when Dcr1 is lacking, thus connecting the function of Translin to the process of genomic maintenance. This is the first association of this conserved protein to malignancy-inducing mechanism, which could include chromosomal translocations. In view of the first hypothesis relating to the part played by Translin in controlling chromosomal rearrangement breakpoints (Aoki et al., 1995; Gajecka et al., 2006), and the heightened attraction of Tsn1 in *S. pombe* for RNA as opposed to DNA (Jaendling & McFarlane, 2010), it was postulated that Tsn1 may have a subsidiary function to Dcr1 in decreasing the integrity of RNA:DNA hybrids

within the genetic material, repressing transcription-DNA replication-associated recombination when Dcr1 was not present, and thus salvaging genomic stability.

In the absence of Dcr1, RNA:DNA hybrid levels increased (Castel et al, 2014). When the levels of RNA:DNA hybrids rises during replication, cells become vulnerable to impaired DNA replication, for instance as induced by HU. Thus, the question as to whether Dcr1 was additionally a component of one of the pair of RNase H pathways was posed. Of note was that the *dcr1*Δ *rnh201*Δ double mutants demonstrated heightened sensitivity to the effects of HU relative to the *dcr1*Δ *rnh1*Δ, thus implying that Dcr1 is directly associated with the *rnh1* mediated pathway (Figure 5.5).

The *dcr1*Δ *rnh201*Δ double mutant strain showed resistant to the CPT compared with *dcr1*Δ and *dcr1*Δ *rnh1*Δ mutant strains. We could imply that the *rnh201*Δ supress the *dcr1*Δ phenotype. This result might suggest that the loss of *rnh201* may free up Rnh1 to mediate a positive function that suppresses the need for *dcr1* in maintaining genomic stability (Figure 5.7).

A co-worker has recently used RNA:DNA immunoprecipitation (DRIP) at distinct genomic loci, the rDNA locus and tRNA genes, indicating levels of genomic RNA:DNA hybrids when *dcr1* and *tsn1* are both mutated (Gomez-Escobar, unpublished data) (Figure 5.9). Of particular note, was that the two mutants, *tsn1*Δ and *tfx1*Δ, displayed equivalent RNA:DNA hybrid level elevations to those identified in the single mutant, *dcr1*Δ. If the higher levels of RNA:DNA hybrids by themselves are enough to cause dysfunctional replication and thus sensitivity to substances that impact this process (e.g., HU), then HU sensitivity would be expected in the *tsn1*Δ and *tfx1*Δ single mutants, which is not the case. This is an important finding as it indicates that the levels of elevated RNA:DNA hybrids previously observed (Castel et al., 2014) alone are not sufficient to sensitise to replicative stress. Although the absence of Tsn1 and Tfx1 leads to elevated RNA:DNA hybrid levels, the intracellular coping strategies to maintain genome stability remain functional and can tolerate these elevated levels. It should also be noted that at the loci tested the levels of RNA:DNA hybrids are not statistically significantly elevated in the *dcr1* Δ *tsn1* Δ double mutant relative to the *dcr1*Δ single mutant (Figure 5.9). However, if Dcr1 is lacking, the cell is no longer in a position to tolerate replicative stress, and Castel and co-workers (2014) suggested that the stress inducing factor is RNA polymerase II retained on the template, removal of which requires Dcr1. This might also suggest that Tsn1, but not Tfx1, is involved in RNA polymerase II ejection from the DNA template when Dcr1 function is lost.

Further recent preliminary work within the group demonstrates that this might well be the case (Gomez-Escobar, data not shown).

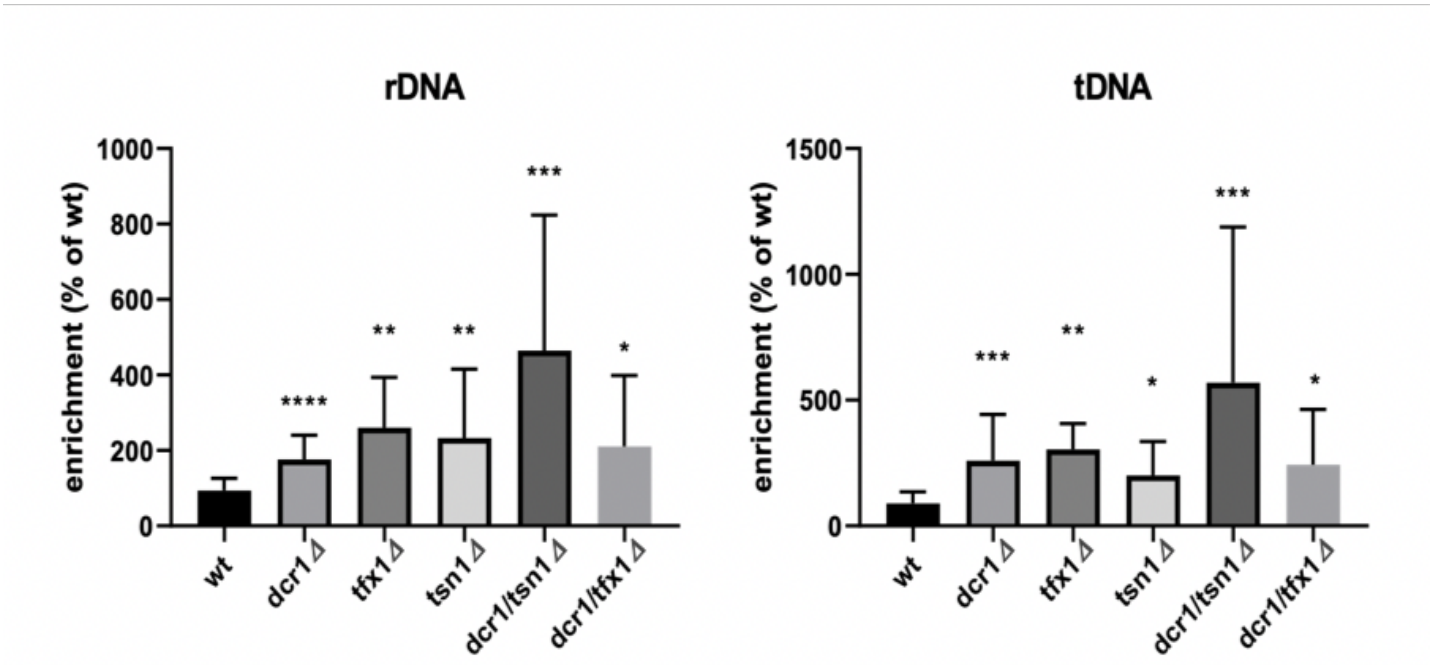


**Figure 5.9. Analysis of the RNA:DNA levels by DNA:RNA immunoprecipitation (DRIP)**.

The bar graphs illustrate the raised titres of RNA:DNA hybrids at two diverse gene loci, i.e. the rDNA and tRNA genes in all mutants, including the *dcr1*Δ*tsn1*Δ double mutant. Error bars represent standard error of the mean; * $P < 0.05$, ** $P < 0.01$, *** $P < 0.001$, **** $P < 0.0001$ [$n \geq 5$ in all cases; T- test]. Depicted data represent one set from a minimum of three independent repeats (adapted from Dr Natalia Gomez-Escobar, unpublished data).

Figures 5.5–5.7 show that compared to other samples, WT cells exhibit more growth. The most probable reason for this observation is related to the duration of the incubation. WT on plates that are incubated for longer than 3 days continues to grow, becoming more condensed. This phenomenon was not observed for other strains incubated for lengthy duration. Therefore, these findings are consistent with typical results. However, to minimise the risk of normal cells becoming contaminated or experiencing abnormal growth, plates should be left in the incubator for a duration of 3 to 4 days.

In conclusion, the current results show that where Dcr1 is lacking, Tsn1 and Rnh201 are involved in replicative stress tolerance. The finding that the *dcr1*Δ *rnh201*Δ double mutant but not the *dcr1*Δ *rnh1*Δ double mutant was sensitive to replicative stress means our original hypothesis that there are two pathways in operation for removal of RNA:DNA hybrids, one being Tsn1 Rnh1 dependent, the other being Dcr1 Rnh201 dependent, is wrong. The meaning of the results presented here and how they relate to other data will be discussed in the final chapter.

# Chapter 6: *S. pombe* and human Translin function in genome stability maintenance via an RNAse-independent mechanism.

# 6.1. Introduction

Translin comprises 228 amino acids and has numerous functions which include the capability to bind to both DNA and RNA. It was first identified as a protein that associated with chromosomal translocation breakpoint junctions in human lymphomas (Aoki et al., 1995). It was noted that relocalisation of Translin to the nucleus occurred in response to DNA damage; this, in combination with its ability to bind to breakpoints suggested that it was involved in a DNA repair pathway and it was referred to as a recombinase (Jaendling and McFarlane, 2010). As demonstrated in the previous chapters, *S. pombe* Translin (Tsn1) appears to be required for an auxiliary pathway in genome stability control. Given this, we wished to further assess the mechanism of this role and to determine the relevance to human Translin (TSN) function.

Extrinsic agents that are potentially poisonous to the genome include radiation and some chemicals (Aguilera and García-Muse, 2013). However, intrinsic nuclear mechanisms, including transcription and replication, can also lead to instability of the genome (Gaillard et al., 2013; Costantino and Koshland, 2015; Gómez-González and Aguilera, 2019). Transcription can give rise to hypermutation and recombination, partly due to transcription-replication conflicts (Aguilera and García-Muse, 2012; Skourti-Stathaki and Proudfoot, 2014; Blin et al., 2019). Loss of genomic integrity can result from RNAs reannealing to their original DNA template strand, thus generating RNA:DNA hybrids (R-loops) (García-Muse and Aguilera, 2019 :Rondón and Aguilera, 2019; Wells et al., 2019; Brambati et al., 2020; Hegazy et al., 2020; Niehrs and Luke, 2020; Rinaldi et al., 2021).

In the absence of working transcription elongation factors, the genome may become unstable through the disturbance of transcription and replication by R-loops; this generates replication stress and DSBs (Aguilera and García-Muse, 2012; Crossley et al., 2019). If ribonucleotides are accidently embedded into DNA during replication, this may also result in the creation of very localised RNA:DNA hybrids (Williams et al., 2016; Nava et al., 2020). Resolution of RNA:DNA hybrids can be achieved by over expression of RNAase H class proteins, which eradicate the RNA components of RNA:DNA hybrids (Drolet et al., 1995; Gaillard et al., 2013; Lockhart et al., 2019).

It has already been documented that the double mutants, *dcr1*Δ *tsn1*Δ and *tsn1*Δ *rnh201*Δ*,* have increased sensitivity to some DNA damaging agents; it was proposed that this sensitivity is associated with the structural integrity of the RNA:DNA hybrids. In view of this, we set out to

over express RNase H in these cells in order to examine whether this could suppress the replicative stress phenotype (HU sensitivity), which would implicate Tsn1 in R-loop removal. In order to confirm the phenotype is Tsn1 associated and to assess the relevance to humans we conducted over expression experiments using *S. pombe* and human Translin genes (*tsn1* and *TSN*, respectively). Extending this, mutations have been made in key domains in both *S. pombe tsn1* and human *TSN* to gain insight into the mechanism of action of these conserved factors.

# 6.2. Result

## 6.2.1. Overexpression of *rnh1* (RNAse H1) fails to suppress the *dcr1*Δ *tsn1*Δ replicative stress phenotype.

The *dcr1*Δ *tsn1*Δ double mutant exhibits sensitivity to HU, suggesting a role for *tsn1* in replicative stress tolerance in the absence of Dcr1. We propose that this could be due to the role for Tsn1 in processing R-loops to prevent them causing genotoxic transcription-replication conflicts. R-loops can be resolved by RNAse H activity, so to determine whether elevated R-loops cause the replicative sensitivity in the *dcr1*Δ *tsn1*Δ double mutant we set out to over produce RNAse H1 by over expressing *rnh1*. If elevated R-loop levels are causing the double mutant phenotype then *rnh1* overexpression will suppress the HU sensitivity phenotype of the double mutant, *dcr1*Δ *tsn1*Δ.

The *rnh1* open reading frame was cloned into pREP3X, which is a thiamine-repressible shuttle vector, so as to give rise to *rnh1* gene overexpression. Figure 6.1A depicts maps of the pREP3X*::rnh1* plasmid together with its restriction sites. The pREP3X vector includes a potent regulatable yeast promoter, *nmt* (no message in thiamine). The entire length of *S. pombe rnh1,* with a size of 979 bp, was amplified utilising appropriate primers, Phusion high-fidelity PCR Master Mix and a GC buffer (see Appendix 1). *rnh1* bands were removed from the gel. They then underwent purification and incubation with *Xho*I *and Bam*HI to enable directional cloning to occur (see Appendix 2.A). pREP3X was digested using the same enzymes and then purified, as illustrated in Appendix 2.B. The entire length of *rnh1* was subsequently ligated into the purified and digested vector, utilising 1:3 proportions. Efficacious identification of ligated plasmids in *E. coli* was conducted employing resistance to ampicillin.

Following transformation of the ligation mix into *E. coli*, analysis was performed on colonies in order to check that relevant colonies were selected. The positive PCR data for numerous colonies are displayed in Appendix 3; these results indicate that they included recombinant plasmid pREP3X*::rnh1*. Colony number two was selected for subsequent affirmation. Additional analysis deploying *nmt* promoter and cloning primers was performed on the selected colony in order to prove that *rnh1* cloning into the pREP3X vector was satisfactory, prior to confirmatory DNA sequencing (see Appendix 4).

The construct was transformed into the following strains, *dcr1*Δ*, dcr1*Δ *tsn1*Δ and *rnh201*Δ *tsn1*Δ. In this experiment, the *nmt* thiamine-repressible promoter governs the *rnh1* expression

in pREP3X::*rnh1*. *nmt* is the most frequently utilised promoter for heterologous gene expression in *S. pombe* (Matsuyama et al., 2008) and is suppressed by supplementing media with 15 μM thiamine. Thus, in order to confirm phenotype suppression, EMMG media without thiamine is used. Thiamine is a constituent of YEA medium, which is typically deployed for fission yeast, and so it is unable to be utilised for *S. pombe* when the goal is *nmt* regulated expression. However, it was utilised in this study as a gene 'off' control. HU, an inhibitor of DNA replication, is the replicative stress agent deployed in this experiment.

The *dcr1*Δ *tsn1*Δ double mutant was transformed with pREP3X and pREP3X::*rnh1* to create distinct strains (Section 2.5). The *rnh1*Δ *rnh201*Δ (pREP3X) strain served as a negative control, whereas the *rnh1*Δ *rnh201*Δ (pREP3X*::rnh1*) strain was employed as a positive control to show the *nmt* promoter and the *rnh1* gene were functioning correctly (Figure 6.2).

The result demonstrated that in the thiamine lacking EMMG media, overexpression of *rnh1* failed to inhibit the *dcr1*Δ *tsn1*Δ double mutant HU sensitivity (Figure 6.2). Double mutant *rnh1*Δ *rnh201*Δ sensitivity was diminished in the positive control, *rnh1*Δ *rnh201*Δ (pREP3X*::rnh1*), validating the use of pREP3X as an inducible system of plasmid expression.

A

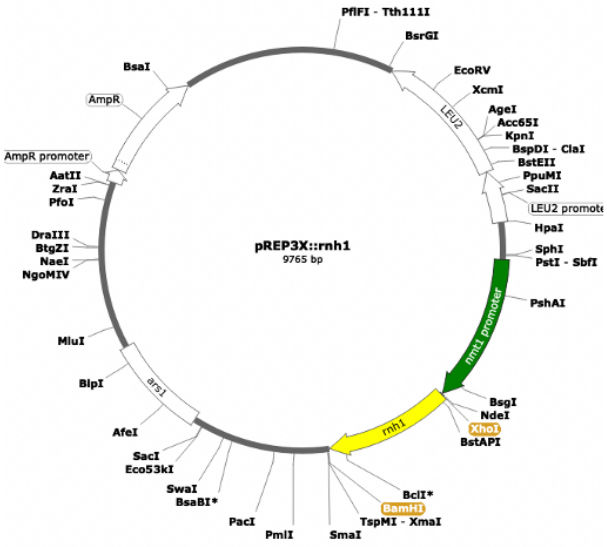


B

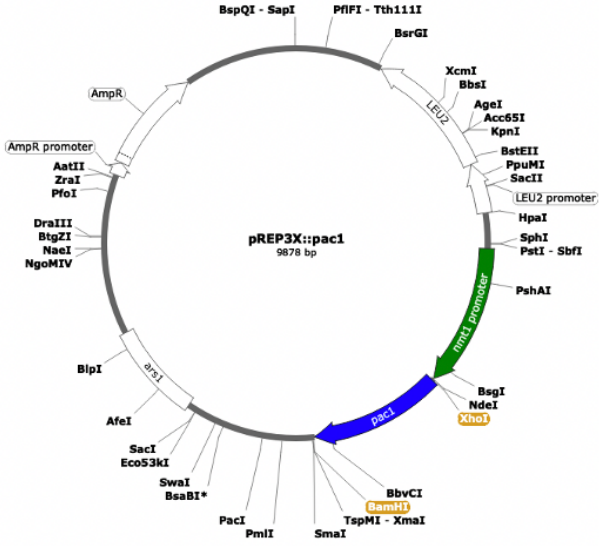


**Figure 6.1. Maps of fission yeast expression vector pREP3X with cloned *rnh1* and *pac1*.**

The pREP3X vector is an inducible expression plasmid system and it is derived from original pREP3 series by addition of a *Xho*I linker between *Bal*I and *Sal*I. This deletes the ATG within the polylinker, destroying a *Bal*I site and recreating a *Sal*I site. Note that we have supplied an ATG within the clone. This vector is composed of the *nmt* promoter, multiple cloning site (MCS), yeast selectable marker *LEU2* and an *E. coli* ampicillin resistance gene. The restriction enzymes *Xho*I and *Bam*HI were used in this study. A. is a map of the pREP3X*::rnh1*with size around 9765 bp while B. is a map of the pREP3X*::pac1*with size around 9878 bp.

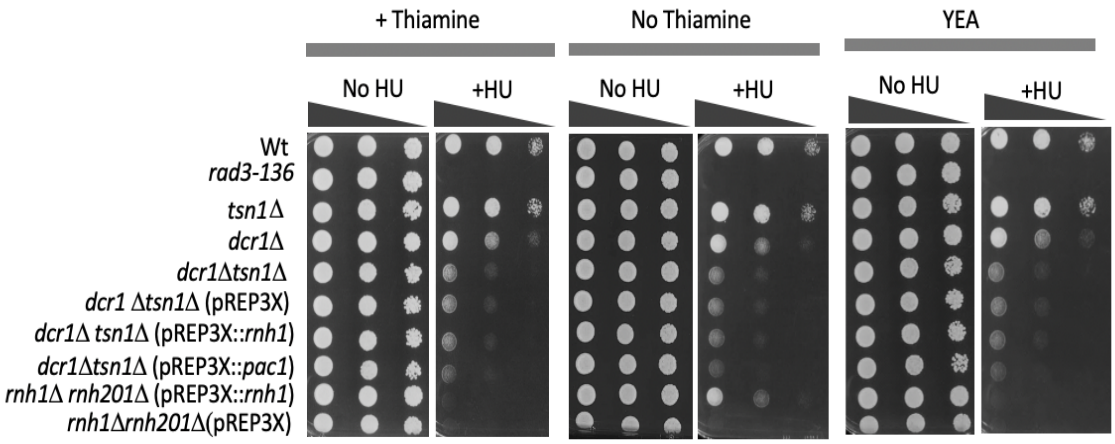


**Figure 6.2. Overexpression of *rnh1* and *pac1* fails to rescue *dcr1*Δ *tsn1*Δ double mutant replicative stress (HU sensitivity) phenotype.**

*S. pombe* cultures were serially diluted (x10 increments) then spotted onto 3 different types of media, EMMG with and without thiamine and YEA. Cells were spotted onto 10 mM HU and then incubated at 30°C for 3 days. *rad3-136* was used as a positive control. No HU sensitivity suppression was noted in *dcr1*Δ *tsn1*Δ (pREP3X::*rnh1*) or *dcr1*Δ *tsn1*Δ (pREP3X::*pac1*). *rnh1*Δ *rnh201*Δ(pREP3X) was used as negative control whereas *rnh1*Δ *rnh201*Δ (pREP3X*::rnh1*) was used as positive control; over expression of *rnh1* suppresses the *rnh1*Δ *rnh201*Δ HU sensitivity back to levels seen in the *rnh201*Δ single mutant, which indicates the over expression is working and the *rnh1* gene is functional.

### 6.2.2. Overexpression of *pac1* fails to suppress the *dcr1*Δ *tsn1*Δ replicative stress phenotype.

The *S. pombe* Pac1 ribonuclease belongs to the RNAse III class of double-strand-specific ribonucleases that destroy double stranded RNA (dsRNA) (Iino et al., 1991). Both Translin and Dicer have RNase activity and Dicer is classified as an RNase III enzyme. Therefore, to assess whether the *dcr1*Δ *tsn1*Δ replicative stress phenotype is caused by a failure to mediate an RNase III-like activity on dsRNA substrates the *pac1* gene was cloned into pREP3X (Figure 6.1B) to determine whether overexpression could suppress the need for either Dcr1 or Tsn1. The clone and the empty vector control were transformed into the *dcr1*Δ *tsn1*Δ double mutant strain. Subsequently, a spot test on media with/without thiamine was conducted to appraise the effect of the overexpression of *pac1* (Figure 6.2). The results demonstrated that in the thiamine lacking EMMG media, overexpression of *pac1* failed to suppress the *dcr1*Δ *tsn1*Δ double mutant HU sensitivity phenotype. The HU sensitivity phenotype of the *rnh1*Δ *rnh201*Δ strain was diminished using the pREP3X::*rnh1* the positive control, validating the use of pREP3X as an inducible system of plasmid expression.

### 6.2.3. Analysis of the overexpression of *rnh1* in the *rnh201*Δ *tsn1*Δ double mutant.

In view of the lack of suppression noted in *dcr1*Δ *tsn1*Δ (pREF3X*::rnh1*), the *rnh201*Δ *tsn1*Δ double mutant was also examined as it demonstrates a high sensitivity to DNA-damaging agents, such as HU. The aim was to further test the hypothesis that Tsn1 contributes to replicative stress sensitivity due to a failure to act on R-loops by overexpressing *rnh1* in this background. pREP3X*::rnh1* was transformed into the *rnh201*Δ *tsn1*Δ double mutant strain. The *rnh1*Δ *rnh201*Δ (pREP3X) and the *rnh1*Δ *rnh201*Δ (pREP3X:*:rnh1*) strains were used as negative and positive controls, respectively. The *rnh201*Δ *tsn1*Δ HU sensitivity phenotype was not suppressed by *rnh1* overexpression in EMMG media in the absence of thiamine (Figure 6.3). This observation is interesting as it indicates that the loss of Rnh201 cannot be suppressed by *rnh1* overexpression, suggesting the Rnh201 activity in question is not related to RNA:DNA hybrid removal activity.

### 6.2.4. Analysis of the overexpression of *pac1* in *rnh201*Δ *tsn1*Δ double mutant.

To assess whether HU sensitivity of the *rnh201*Δ *tsn1*Δ double mutant is related to dsRNA activity the pREP3X*::pac1* plasmid was transformed into the *rnh201*Δ *tsn1*Δ double mutant. The *rnh1*Δ *rnh201*Δ (pREP3X) and the *rnh1*Δ *rnh201*Δ (pREP3X:*:rnh1*) strains were used as negative and positive controls, respectively. The *rnh201*Δ *tsn1*Δ HU sensitivity phenotype was not suppressed following *pac1* overexpression in EMMG media in the absence of thiamine (Figure 6.3). This indicates that the replicative stress phenotype is unlikely to be related to a dsRNase activity.

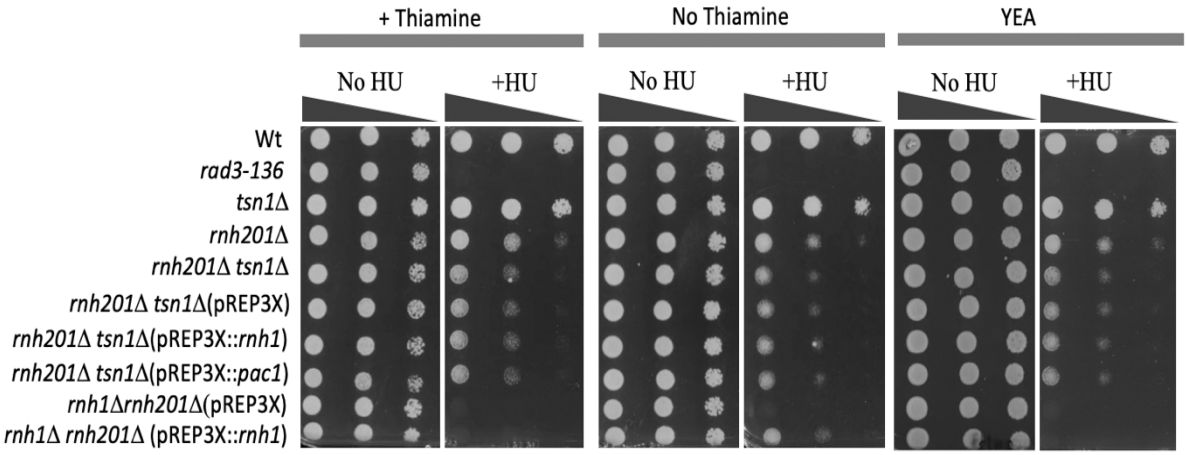


**Figure 6.3. Overexpression of *rnh1* and *pac1* does not rescue *rnh201*Δ *tsn1*Δ double mutant replicative stress (HU sensitivity) phenotype.**

*S. pombe* cultures were serially diluted (x10 increments) then spotted onto 3 different types of media, EMMG with and without thiamine and YEA. Cells were spotted onto 10 mM HU and then incubated at 30°C for 3 days. *rad3-136* was used as a positive control. No HU sensitivity suppression was notes in *rnh201*Δ *tsn1*Δ (*pREP3X::rnh1*) and *rnh201*Δ *tsn1*Δ (pREP3X*::pac1*). *rnh1*Δ *rnh201*Δ (pREP3X) was used as negative control and *rnh1*Δ *rnh201*Δ (pREP3X*::rnh1*) was used as positive control; over expression of *rnh1* suppresses the *rnh1*Δ *rnh201*Δ HU sensitivity back to levels seen in the *rnh201*Δ single mutant, which indicates the over expression is working and the *rnh1* gene is functional.

### 6.2.5. Analysis of the overexpression of *rnh1* in *dcr1*Δ single mutant

Since no suppression was seen in either *dcr1*Δ *tsn1*Δ (pREP3X::*rnh1*) or *rnh201*Δ*tsn1*Δ (pREP3X*::rnh1*), it was decided to investigate the single mutant, *dcr1*Δ. Castel et al. (2016) demonstrated that in the absence of Dcr1, RNA:DNA hybrid levels became elevated, and this was related to DNA replication difficulties, although they did show that this was independent of the Dcr1 ribonuclease catalytic activity. Whilst Castel et al. (2016) postulated the replicative stress was caused by increase RNA Pol II occupancy they did not overexpress *rnh1* to demonstrate whether the replicative issues were related to RNA:DNA hybrids per se. Despite the fact the double mutant data indicates there is no link to R-loops (above), in order to formally dismiss a role for increased R-loops driving the replicative stress phenotype of Dcr1 deficient cells the pREP3X*::rnh1* plasmid were transformed into the *dcr1*Δ strain. Negative and positive controls were formed by the *rnh1*Δ *rnh201*Δ (pREP3X) and *rnh1*Δ *rnh201*Δ (pREP3X::*rnh1*) strains, respectively. The results, shown in Figure 6.4 demonstrate a lack of suppression of the single mutant phenotype, supporting a model in which increased R-loops per se do not present a challenge to genome stability in Dcr1 deficiency.

### 6.2.6. Analysis the overexpression of *pac1* in *dcr1*Δ single mutant

Extending the above, to confirm that Dcr1 deficiency related genome instability was not related to dsRNase activity, it was decided to transform pREF3X*::pac1* plasmid into the *dcr1*Δ single mutant. Negative and positive controls were formed by the *rnh1*Δ *rnh201*Δ (pREP3X) and *rnh1*Δ *rnh201*Δ (pREP3X::*rnh1*) strains, respectively. The results, shown in Figure 6.4 demonstrate a lack of suppression of the single mutant phenotype, this further supports the postulate that replicative stress sensitivity observed in Dcr1 deficiency is not caused by loss of dsRNase activity.

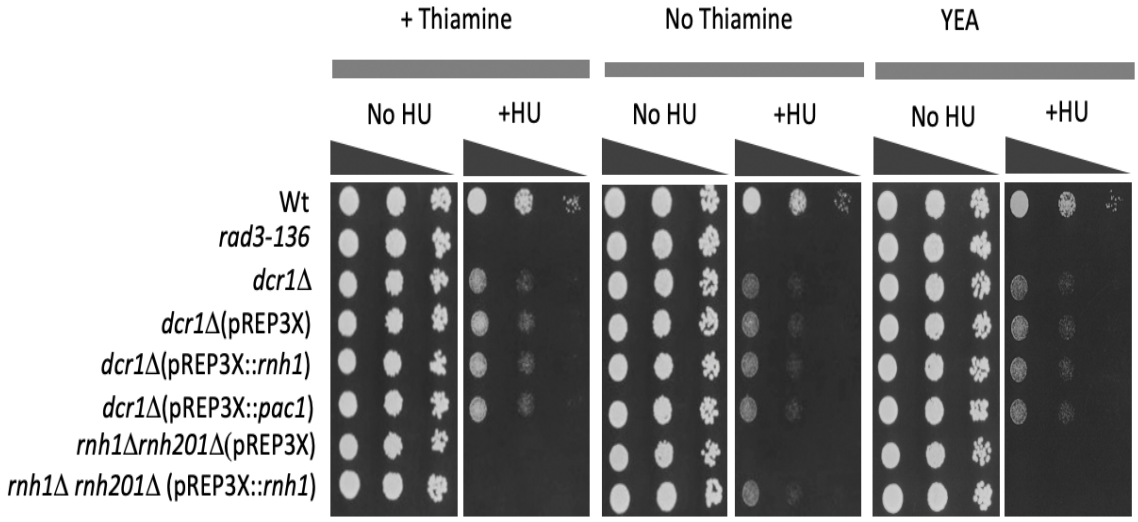


**Figure 6.4. Overexpression of *rnh1* and *pac1* does not rescue *dcr1*Δ single mutant replicative stress (HU sensitivity) phenotype.**

*S. pombe* cultures were serially diluted (x10 increments) then spotted onto 3 different types of media, EMMG with and without thiamine and YEA. Cells were spotted onto 10 mM HU and then incubated at 30°C for 3 days. *rad3-136* was used as a positive control. No HU sensitivity suppression was noted in *dcr1*Δ (pREP3X*::rnh1*) or *dcr1*Δ (pREP3X*::pac1*). *rnh1*Δ *rnh201*Δ (pREP3X) was used as negative control whereas *rnh1*Δ *rnh201*Δ (pREP3X*::rnh1*) was used as positive control; overexpression of *rnh1* suppresses the *rnh1*Δ *rnh201*Δ HU sensitivity back to levels seen in the *rnh201*Δ single mutant, which indicates the over expression is working and the *rnh1* gene is functional.

### 6.2.7. Verification of the overexpression of *rnh1*

Given that there was no evidence that overexpression of *rnh1* suppresses replicative stress phenotypes of the various strains (above), RT-PCR and qRT-PCR were performed in the cells with induced and non-induced *rnh1* expression to verify the gene was overexpressed in these cells.

RT-PCR was utilised to assess *rnh1* induction in the absence of thiamine. For a negative control strains transformed with the vector pREP3X only was employed (Figure 6.5A). EMMG liquid media without leucine (for plasmid maintenance) was used for incubation. Following cell harvesting and isolation of the total RNA, cDNA was made in order to appraise the expression of *rnh1* (see Sections 2.14.1 and 2.14.2.). The quality of the cDNA produced was assessed utilising expression of *act1* (Figure 6.5B). Sharp bands representing induced *rnh1* cDNA were seen in comparison to those from non-induced cells and the *act1* control, thus suggesting that *rnh1* overexpression was satisfactory (Figure 6.5C).

qRT-PCR studies were additionally performed in order to quantify the *rnh1* overexpression. cDNA was qPCR-amplified utilising the QuantiTect SYBR Green PCR Kit and CFX96 real-time system (Bio-Rad). The oligonucleotide sequences employed are described in Table 2.6. qRT-PCR data of the reference gene *act1* were used as controls for the *rnh1* data. The qRT-PCR correlated with the traditional RT-PCR results and demonstrated notable *rnh1* induction (Figure 6.5D).

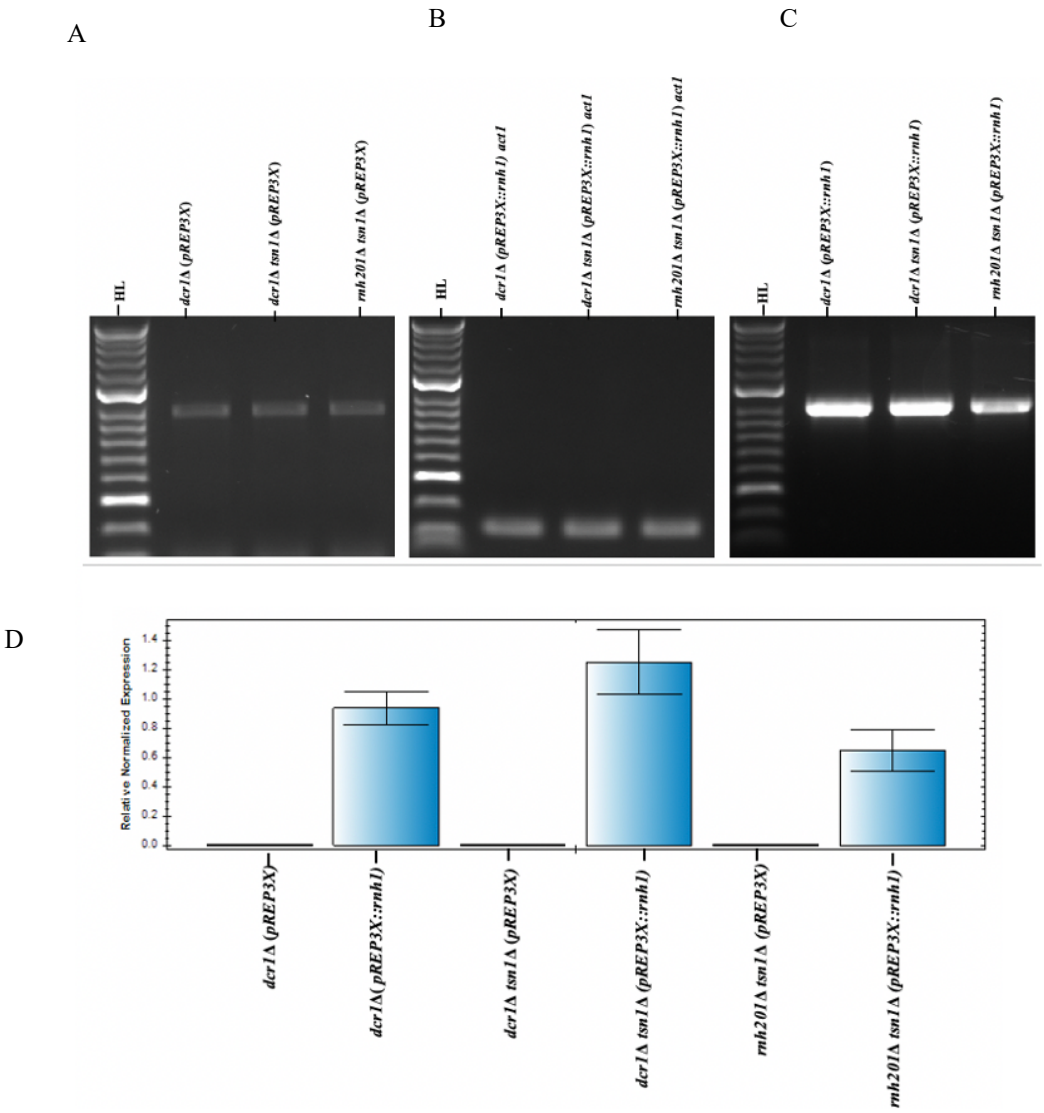


**Figure 6.5. Analysis of *rnh1* overexpression by RT-PCR and qRT-PCR.**

I) RT-PCR data depicting *rnh1*and *act1* expression in three mutant strains: *dcr1*Δ, *dcr1*Δ *tsn1*Δ and *rnh201* Δ*tsn1*Δ. The agarose gel images show: A) negative control, i.e., a strain vector (pREP3X)-transformed only; B) positive control, i.e., *act1* expression for cDNA quality appraisal; and C) a pREP3X::*rnh1* transformed strain to assess *rnh1* overexpression.

II) qRT-PCR analysis illustrating *rnh1* mRNA levels for the individual transformed strains; data for *rnh1* are presented relative to the qRT-PCR data for the *act1* reference gene.

### 6.2.8. Verification of the overexpression of *pac1*

Given that there was no evidence that overexpression of *pac1* suppresses replicative stress phenotypes of the various trains (above), RT-PCR and qRT-PCR were performed in the cells with induced and non-induced *pac1* expression to verify the gene was overexpressed in these cells.

The RT- PCR methods were utilised to assess *pac1* induction in the absence of thiamine. For a negative control strains transformed with the vector pREP3X only was employed (Figure 6.6A). EMMG liquid media without leucine (for plasmid maintenance) was used for incubation. Following cell harvesting and isolation of the total RNA, cDNA was made in order to appraise the expression of *pac1* (see Sections 2.14.1 and 2.14.2.). The quality of the cDNA produced was assessed utilising expression of *act1* (Figure 6.6B). Sharp bands representing induced *pac1* cDNA were seen in comparison to those from non-induced cells and the *act1* control, thus suggesting that *pac1* overexpression was satisfactory (Figure 6.6C).

qRT-PCR studies were additionally performed in order to quantify the *pac1* overexpression. cDNA was qPCR-amplified utilising the QuantiTect SYBR Green PCR Kit and CFX96 real-time system (Bio-Rad). The oligonucleotide sequences employed are described in Table 2.6. qRT-PCR data of the reference gene *act1* were used as controls for the *pac1* data. The qRT-PCR correlated with the traditional RT-PCR results and demonstrated notable *pac1* induction (Figure 6.6D).

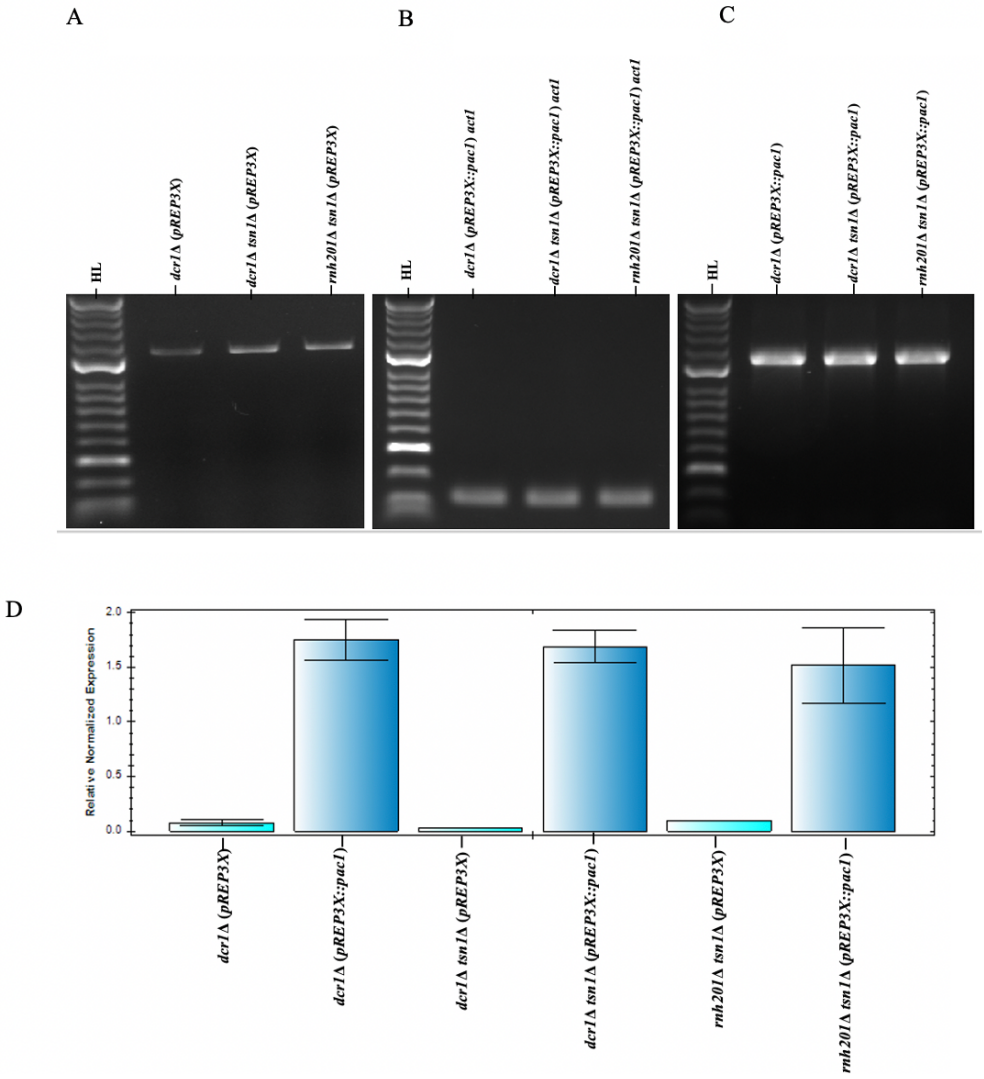


**Figure 6.6. Analysis of *pac1* overexpression by RT-PCR and qRT-PCR.**

I) RT-PCR data depicting *pac1* and *act1* expression in three mutant strains: *dcr1*Δ, *dcr1*Δ *tsn1*Δ and *rnh201*Δ *tsn1*Δ. The agarose gel images show: A) negative control, i.e., a strain vector (pREP3X)-transformed only; B) positive control, i.e., *act1* expression for cDNA quality appraisal; and C) a pREP3X*::pac1* transformed strain to assess *pac1* overexpression.

II) qRT-PCR analysis illustrating *pac1* mRNA levels for the individual transformed strains; data for *pac1* are presented relative to the qRT-PCR data for the *act1* reference gene.

### 6.2.9. Analysis of the overexpression of *rnh201* in the *dcr1*Δ *tsn1*Δ double mutant

Resolution of RNA:DNA hybrids can be accomplished by overexpression of RNase H family proteins, which eliminate the RNA strands of RNA:DNA hybrids (Gaillard et al. 2013; Lockhart et al. 2019). Deletion of the RNase H2, but not RNase H1, gene enhanced sensitivity to hydroxyurea (HU). This is explained by the fact that HU caused enhanced accumulation of rNTPs in genomic DNA, resulting in increased number of DSB (Kojima et al. 2019) .This evidence implies that RNase H2 decreases the existence of DSB.

Overexpression of *RNH201* alone in *S. cerevisiae* can suppress defects caused by the loss of a 5' to 3' RNA exonuclease, Rat1, implying Rnh201 can suppress other RNA processing activities (Luke et al., 2008). To discern if Tsn1 functions redundantly for processing another unidentified Rnh201 substrate, we overexpressed *rnh201* in the *dcr1*Δ *tsn1* Δmutant to assess whether *rnh201* overexpression could suppress HU sensitivity. The *rnh201* gene was cloned into pREP3X to determine whether overexpression could suppress the need for Tsn1. The clone and the empty vector control were transformed into the *dcr1*Δ *tsn1*Δ double mutant strain. Subsequently, a spot test on media with/without thiamine was conducted to appraise the effect of the overexpression of *rnh201* (Figure 6.7). The results demonstrated that in the thiamine lacking EMMG media, overexpression of *rnh201* failed to inhibit the *dcr1*Δ *tsn1*Δ double mutant HU sensitivity phenotype. The HU sensitivity phenotype of the *rnh1*Δ *rnh201*Δ strain was diminished using the pREP3X::*rnh201* the positive control, validating the use of pREP3X as an inducible system of plasmid expression.

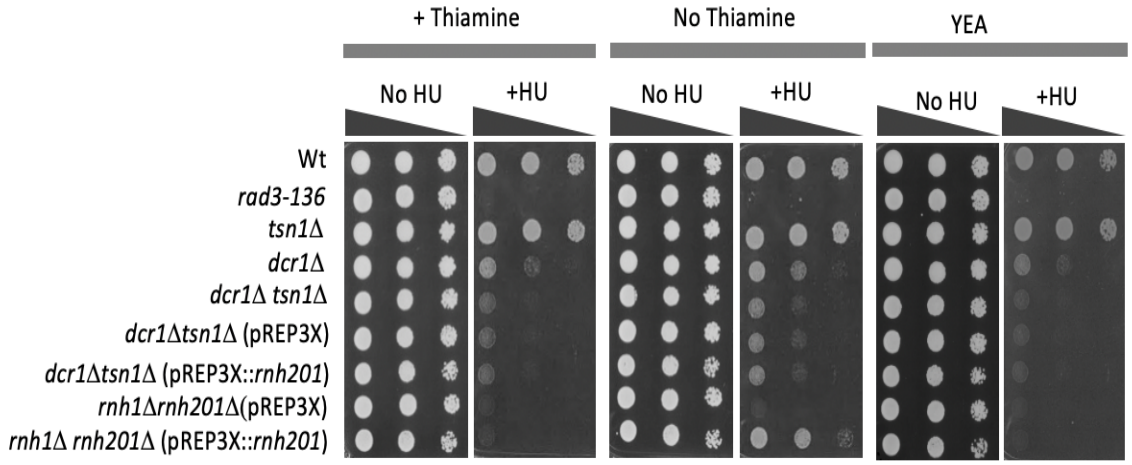


**Figure 6.7. Overexpression of *rnh201* does not rescue *dcr1*Δ *tsn1*Δ double mutant replicative stress (HU sensitivity) phenotype.**

*S. pombe* cultures were serially diluted (x10 increments) then spotted onto 3 different types of media, EMMG with and without thiamine and YEA. Cells were spotted onto 10 mM HU and then incubated at 30°C for 3 days. *rad3-136* was used as a positive control. No HU sensitivity suppression was noted in *dcr1*Δ *tsn1*Δ (pREP3X::*rnh201). rnh1*Δ *rnh201*Δ (pREP3X) was used as negative control whereas *rnh1*Δ *rnh201*Δ (pREP3X*::rnh201*) was used as positive control; overexpression of *rnh201* suppresses the *rnh1*Δ *rnh201*Δ HU sensitivity back to levels seen in the *rnh1*Δ single mutant, which indicates the over expression is working and the *rnh201* gene is functional.

### 6.2.10. Overexpression of *S. pombe tsn1* and Human *TSN* suppress replicative stress intolerance of the *dcr1*Δ *tsn1*Δ mutant

An essential question is whether within *S. pombe* the actions of Tsn1 bear any relation to the activity of human TSN. One method to investigate this is to construct a mutant of *S. pombe tsn1* and then to establish if human *TSN* has the capacity to suppress the mutant phenotype. If the latter occurs, the human gene synthesises a protein that is functional within *S. pombe* cells. Thus, *S. pombe tsn1* and human *TSN* genes were over expressed in the *dcr1*Δ *tsn1*Δ mutant to assess whether the HU sensitivity phenotype could be suppressed. Amino acid sequence alignment of the human and the *S.pombe* Translins showing in Figure 6.8

The McFarlane group cloned both *S. pombe tsn1* and human *TSN* into pREP3X, putting the genes under the control of the regulatable promoter *nmt*. The clones were transformed into the *dcr1*Δ *tsn1*Δ double mutant. Furthermore, *dcr1* was also cloned into pREP3X and transformed to the identical strain. An appraisal of excess *S. pombe tsn1, dcr1* and human *TSN* gene expression within the double mutant strain was performed (Figure 6.9). The data reveal that the *dcr1*Δ *tsn1*Δ HU sensitivity phenotype is supressed to some extent by over expression of both *tsn1* and *TSN*. There was complete suppression of the HU sensitivity from over expression of *dcr1,* as expected.

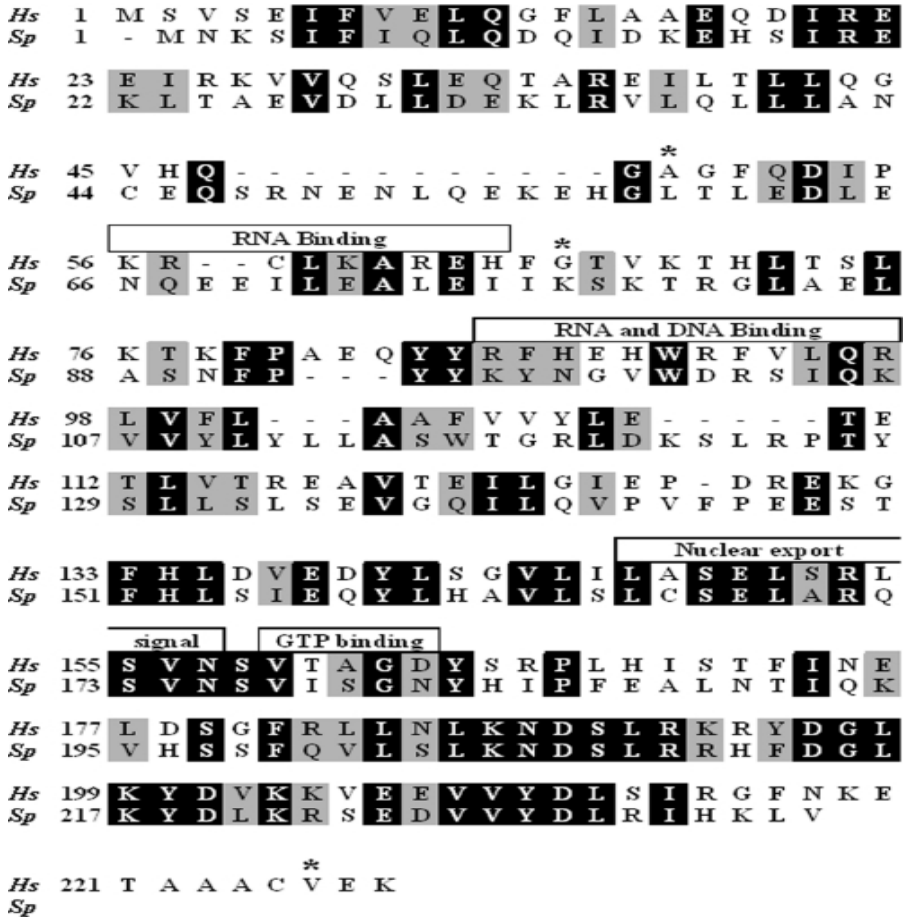


**Figure 6.8. Amino acid sequence alignment of the human and the *S.pombe* Translins.**

BLAST was used to align the sequences of the human Translin (*Hs*, *Homo sapiens*, GenBank™ gi: 12803111) and its *S.pombe* orthologue (*Sp*, *S.pombe*, GenBank™ gi: 19115469). The black highlight denotes perfectly conserved residues, whilst the grey highlight indicates residues that are similar. Boxes indicate those motifs that have been identified previously and are shared with mouse Translin; these are described in the Results section. Asterisks indicate amino acids in the human orthologue that are substituted with other amino acids in the mouse version (Gupta, G.D. and Kumar, V. 2018).

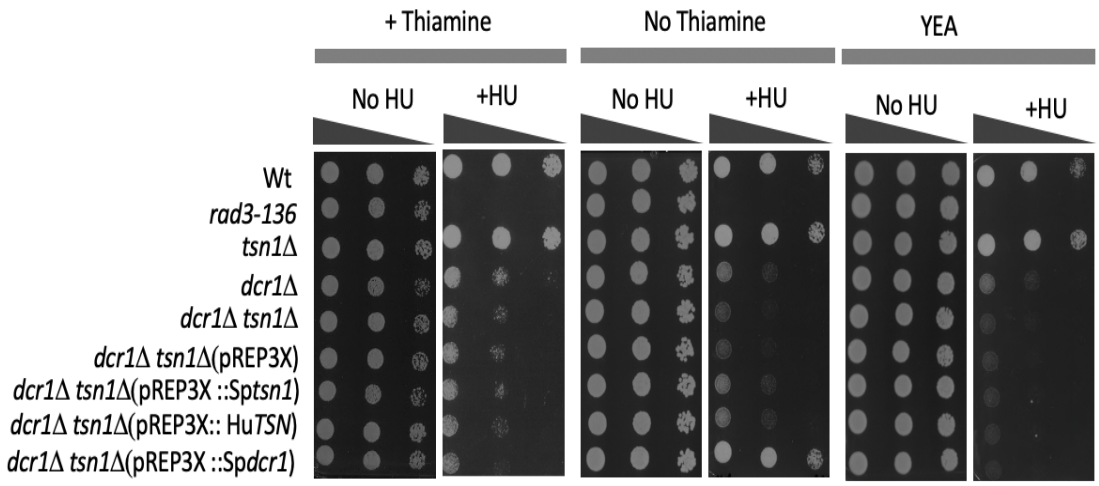


**Figure 6.9. Suppression of the *dcr1*Δ *tsn1*Δ double mutant replicative stress (HU sensitivity) phenotype.**

*S. pombe* cultures were serially diluted (x10 increments) then spotted onto 3 different types of media, EMMG with and without thiamine and YEA. Cells were spotted onto 10 mM HU and then incubated at 30°C for 3 days. *rad3-136* was used as a positive control. Moderate HU sensitivity suppression was noted in *dcr1*Δ *tsn1*Δ (pREP3X*::*Sp*tsn1*) and *dcr1*Δ *tsn1*Δ (pREP3X*::*Hu*TSN*), both back to *dcr1*Δ single mutant levels. *dcr1*Δ *tsn1*Δ (pREP3X*::*Sp*dcr1*) was used as positive control; over expression of *dcr1* suppresses the *dcr1*Δ *tsn1*Δ HU sensitivity back to levels seen in the *tsn1*Δ single mutant, which indicates the over expression is working.

### 6.2.10. Analysis of the overexpression of *S. pombe tsn1* and human *TSN* in the *rnh201*Δ *tsn1*Δ double mutant

As demonstrated in Figure 6.8, the *dcr1*Δ *tsn1*Δ HU sensitivity phenotype suppressed to *dcr1*D levels following *S. pombe tsn1* and human *TSN* overexpression, and completely, following *dcr1* overexpression. It was therefore decided to evaluate their overexpression in the *rnh201*Δ *tsn1*Δ double mutant strain to determine whether a similar suppression phenotype was apparent to assess whether this Tsn1 function could be equally met by human TSN.

pREP3X*::*Sp*tsn1*, pREP3X*::*Hu*TSN1* and pREP3X*::dcr1* (and vector control) were transformed into the *rnh201*Δ *tsn1*Δ double mutant. Again, overexpression of *S. pombe tsn1*, *dcr1* and human *TSN* genes was performed (Figure 6.10). Overexpression of *tsn1* and *TSN* suppressed the *rnh201*Δ *tsn1*Δ phenotype to an identical extent. This is in keeping with the data from the above experiment. Interestingly, over expression of *dcr1* did not suppress the HU sensitivity of the *rnh201*Δ *tsn1*Δ double mutant, indicating that Dcr1 function is not interchangeable with Rnh201 or Tsn1.

### 6.2.11. Analysis of the overexpression of *S. pombe* and human *TSN* in *dcr1*Δ single mutant

Figures 6.8 and 6.9 indicated that there was mild suppression of both *dcr1*Δ *tsn1*Δ and *rnh201*Δ *tsn1*Δ HU sensitivity phenotypes following the overexpression of either *S. pombe* or human *TSN*. However, *dcr1* overexpression did not suppress the *rnh201*Δ *tsn1*Δ double mutant. To explore the relationship between Tsn1 and Dcr1 further, *tsn1* and *TSN* were both overexpressed in the *dcr1*Δ mutant to determine whether the HU sensitivity could be suppressed. pREP3X*::*Sp*tsn1* and pREP3X*::*Hu*TSN* were transformed into the *dcr1*Δ single mutant and the two Translin genes were overexpressed (Figure 6.11). There was no evidence of HU sensitivity suppression.

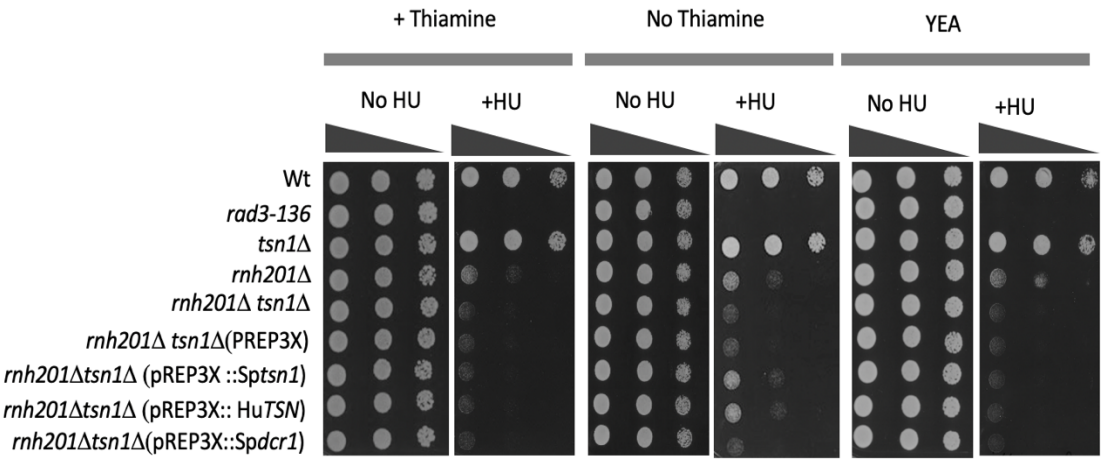


**Figure 6.10. Suppression of *rnh201*Δ *tsn1*Δ double mutant replicative stress (HU sensitivity) phenotype.**

*S. pombe* cultures were serially diluted (x10 increments) then spotted onto 3 different types of media, EMMG with and without thiamine and YEA. Cells were spotted onto 10 mM HU and then incubated at 30°C for 3 days. *rad3-136* was used as a positive control for the original strains. Mild HU sensitivity suppression was noted in *rnh201*Δ *tsn1*Δ (pREP3X*::*Sp*tsn1*) and *rnh201*Δ *tsn1*Δ (pREP3X*::*Hu*TSN*). No suppression of *rnh201*Δ *tsn1*Δ (pREP3X::Sp*dcr1*) was apparent.

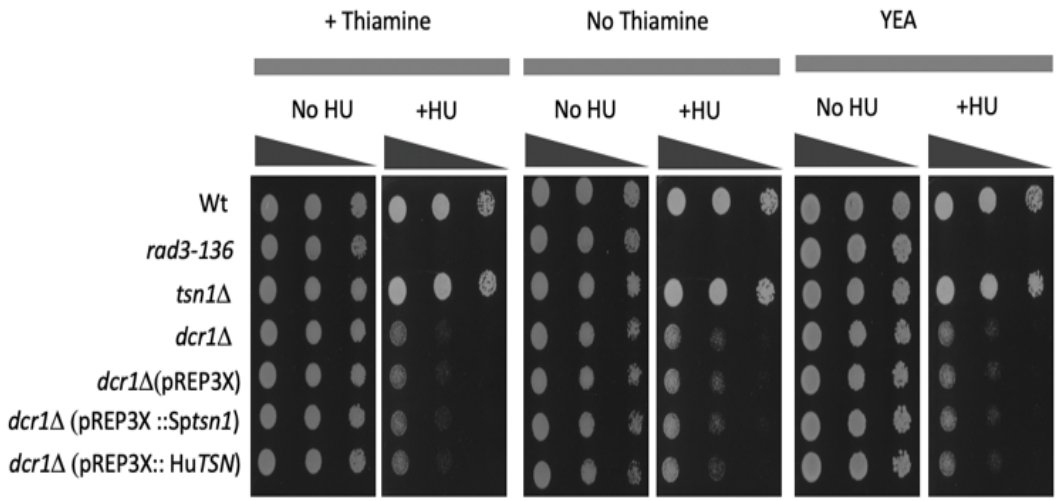


**Figure 6.11. Overexpression of human or *S. pombe* Translin genes does not suppress the *dcr1*Δ single mutant phenotype replicative stress (HU sensitivity) phenotype.**

*S. pombe* cultures were serially diluted (x10 increments) then spotted onto 3 different types of media, EMMG with and without thiamine and YEA. Cells were spotted onto 10 mM HU and then incubated at 30°C for 3 days. *rad3-136* was used as a positive control. No HU sensitivity suppression was noted for *dcr1*Δ (pREP3X*::*Sp*tsn1*) and *dcr1*Δ (pREP3X*::*Hu*TSN*) strains.

### 6.2.13. Analysis of the overexpression of *S. pombe tfx1* and human *TSNAX* in *dcr1*Δ *tsn1*Δ mutant

Much of the research published to date, which has evaluated the biological functions of Translin and Trax, has indicated an intimate functional relationship between these two proteins, even when there is little or no evidence of a C3PO-like complex (for example, see Gomez-Escobar et al., 2016). It has been shown here that Translin from humans and *S. pombe* exhibits suppression of the *dcr1*Δ *tsn1*Δ HU sensitivity phenotype (Figure 6.9). Thus, an appraisal of *S. pombe tfx1* and human *TSNAX* overexpression was undertaken in the *dcr1*Δ *tsn1*Δ strain.

The McFarlane group cloned *S. pombe tfx1* and human *TSNAX* into pREP3X. The clones were transformed into the *dcr1*Δ *tsn1*Δ double mutant. Overexpression of human *TSNAX* and *S. pombe tfx1* were then evaluated (Figure 6.12). The *dcr1*Δ *tsn1*Δ HU sensitivity phenotype was not suppressed by overexpression of either gene. The *rnh1*Δ *rnh201*Δ (pREP3X) strain was utilised as a negative control; the *rnh1*Δ *rnh201*Δ (pREP3X*::rnh201*) strain was a positive control for the overexpression media.

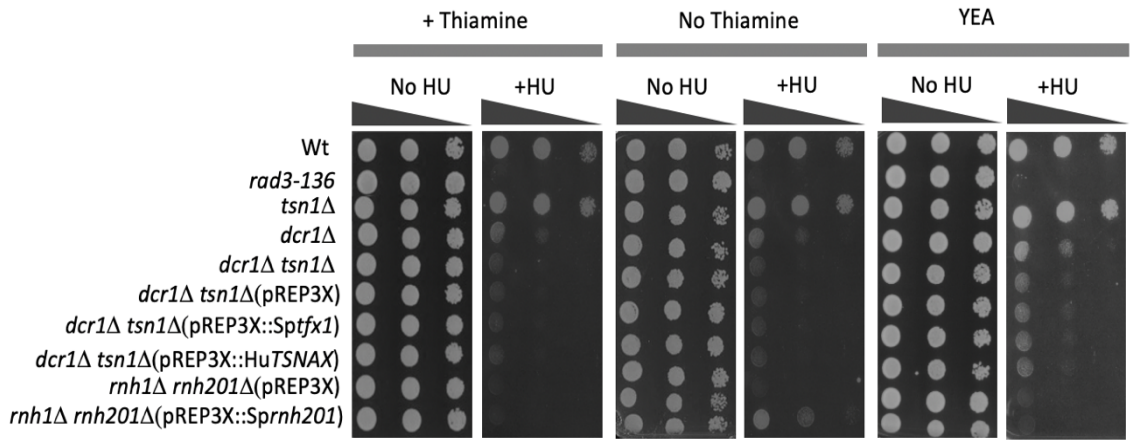


**Figure 6.12. Overexpression of S *pombe tfx1* and Human *TSNAX* fails to rescue *dcr1*Δ *tsn1*Δ double mutant replicative stress (HU sensitivity) phenotype.**

Appropriate *S. pombe* cultures were serially diluted (x10 increments) then spotted onto 3 different types of media, EMMG with and without thiamine and YEA. Cells were spotted onto 10 mM HU and then incubated at 30°C for 3 days. *rad3-136* was used as a positive control for the original strains. No HU sensitivity suppression was noted in *dcr1*Δ *tsn1*Δ (*pREP3X::*Sp*tfx1*) and *dcr1*Δ *tsn1*Δ (pREP3X-Hu*TSNAX*). *rnh1*Δ *rnh201*Δ (pREP3X) was used as negative control whereas *rnh1*Δ *rnh201*Δ (pREP3X*::rnh201*) was used as positive control ; over expression of *rnh201* suppresses the *rnh1*Δ *rnh201*Δ HU sensitivity back to levels seen in the *rnh201*Δ single mutant, which indicates the over expression system is working.

### 6.2.14. Analysis of point mutations of the RNase and RNA-binding domains of *S. pombe* Tsn1

It has been proposed that Trax exhibits RNase activity (Tian et al. 2011). Mammalian Translin also has RNase activity (Wang et al., 2004). The original three catalytic residue noted in human TNSAX were Glu126, Glu129 and Asp193, a fourth catalytic residue in human TSNAX, is maintained in Translin (including *S. pombe* Tsn1) and can be located within the 220 amino acid sequence by aligning amino acid sequences from both human and yeast (Ye et al. 2011). In Trax this moiety was mutated by Ye et al. (2011) with an E197A mutant to obtain a similar phenotype to the previous research, i.e., RNase dead, but with capacity for binding to RNA, thus reinforcing the concept that this residue was responsible for the RNase catalytic activity. So far, this residue has not undergone mutation in Translin from humans or any other species. Members of the McFarlane group mutated the *S. pombe* Tsn1 glutamic acid to alanine utilising site-directed mutagenesis. The plasmid containing this mutant allele was transformed into the double mutant strains, *dcr1*Δ *tsn1*Δ and *rnh201*Δ *tsn1*Δ, in order to generate the following strains: *dcr1*Δ *tsn1*Δ (pREP3X*::*Sp*tsn1::E152A*) and *rnh201*Δ *tsn1*Δ (pREP3X::Sp*tsn1::E152A*). The overexpression of this allele resulted in a level of suppressive activity similar to the unmutated wild- type in both strains **(**Figure 6.13 and 6.14). This suggests that the RNase domain is not required for Tsn1 function.

It has additionally been noted that in *S. pombe* arginine 86 is required for the majority (but not all) of the RNA binding function (Gupta et al., 2019). To assess whether loss of this RNA binding capacity interfered with Tsn1 function this residue was mutated (R86G) in the *tsn1* overexpression plasmid. Overexpression of *tsn1::R86G* resulted in full suppression of both double mutants suggestive that loss of some RNA binding capacity does not impair the Tsn1 function (Figure 6.13 and 6.14).

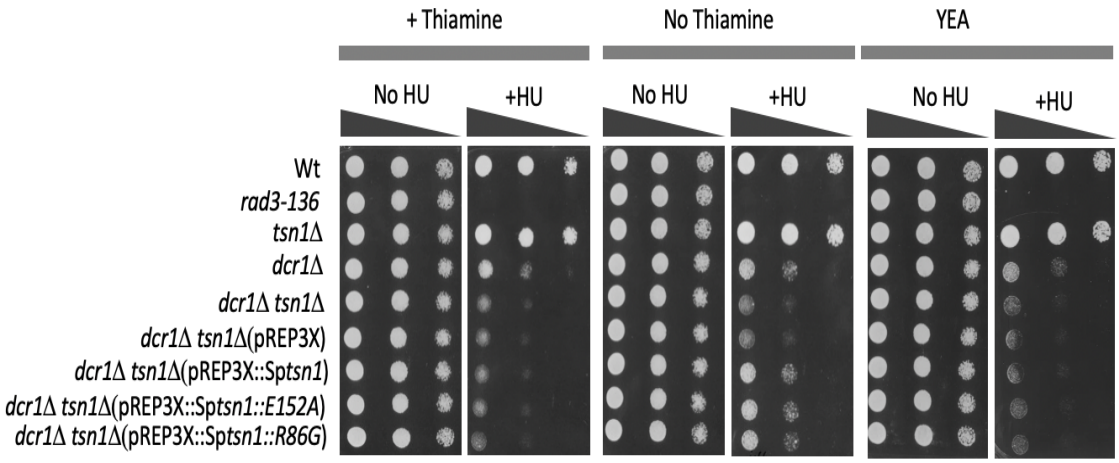


**Figure 6.13. Point mutation of RNase and RNA-binding domains of *S. pombe* Tsn1 supressed the *dcr1*Δ *tsn1*Δ double mutant replicative stress (HU sensitivity) phenotype.**

*S. pombe* cultures were serially diluted (x10 increments) then spotted onto 3 different types of media, EMMG with and without thiamine and YEA. Cells were spotted onto 10 mM HU and then incubated at 30°C for 3 days. *rad3-136* was used as a positive control. Full HU sensitivity suppression to *dcr1*Δ levels was noted in *dcr1*Δ *tsn1*Δ after mutating the RNase activity domain [*dcr1*Δ *tsn1*Δ (pREP3X*::*Sp*tsn1::E152A*) and RNA binding domain (*dcr1*Δ *tsn1*Δ pREP3X*::*Sp*tsn1::R86G*)].

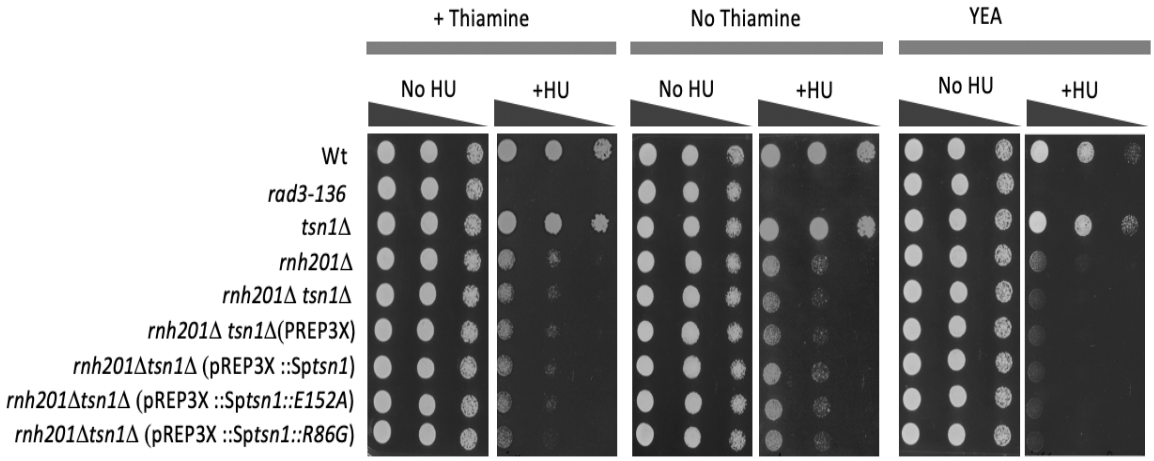


**Figure 6.14. Point mutation of RNase and RNA-binding domains of the *S. pombe* Tsn1 supressed *rnh201*Δ *tsn1*Δ double mutant replicative stress (HU sensitivity) phenotype.**

*S. pombe* cultures were serially diluted (x10 increments) then spotted onto 3 different types of media, EMMG with and without thiamine and YEA. Cells were spotted onto 10 mM HU and then incubated at 30°C for 3 days. *rad3-136* was used as a positive control. Full HU sensitivity suppression to *rnh201*Δ levels was noted after mutating RNase activity domain [*rnh201*Δ *tsn1*Δ (pREP3X::Sp*tsn1::E152A*) and RNA binding domain (*rnh201*Δ *tsn1*Δ pREP3X*::*Sp*tsn1::R86G*)].

### 6.2.15. RNase and RNA-binding domains of human Translin are not required for genome stability maintenance activity

Given that mutation of the *S. pombe* Tsn1 RNase and RNA-binding domains did not alter its ability to function in the replicative stress response, we set out to assess whether the human TSN behaved in the same RNase- and RNA-binding-independent fashion. Single base-pair substitutions in these domains were made in human *TSN*. In order to appraise RNase activity, the conserved glutamic acid residue at position 150 in the RNase domain was substituted with alanine in the pREP3X*::*Hu*TSN* plasmid to generate pREP3X*::*Hu*TSN::E150A*. Independently, the arginine residue at position 92 within the RNA binding domain was substituted for glycine within the pREP3X*::*Hu*TSN* plasmid to generate pREP3X-Hu*TSN::R92G.* The resulting plasmids were transformed into the double mutants *dcr1*Δ *tsn1*Δ and *rnh201*Δ *tsn1*Δ in order to assess their ability to suppress the loss of *S. pombe tsn1*$^{+}$ function. The overexpression of both alleles (*TSN::E150A* and *TSN::R92G)* resulted in a level of suppressive activity similar to the unmutated wild-type gene in both strains **(**Figures 6.15 and 6.16). This suggests that the RNase and RNA binding domains of human TSN are not required for TSN function to respond to replicative stress.

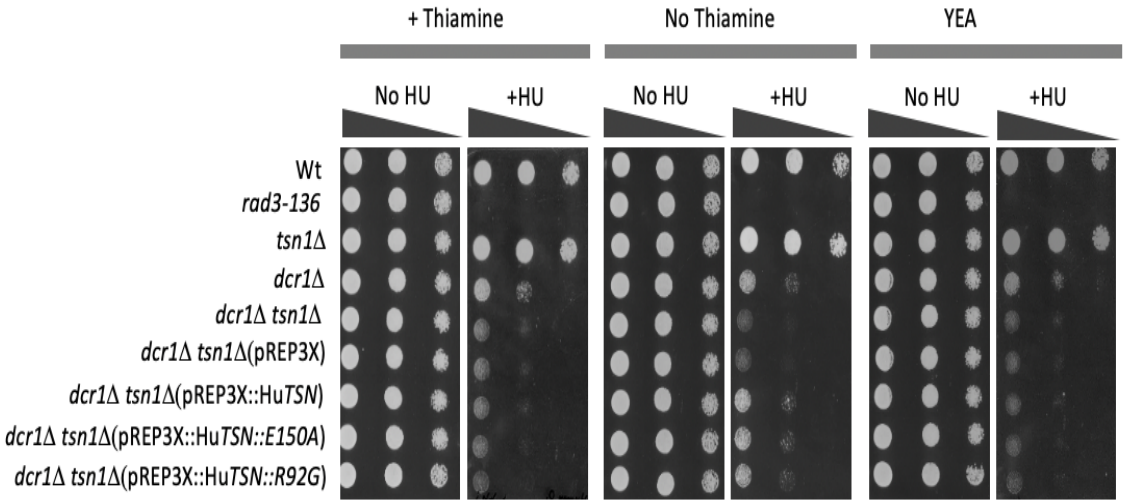


**Figure 6.15. Point mutation of RNase and RNA-binding domains of Human Translin supressed *dcr1*Δ *tsn1*Δ double mutant replicative stress (HU sensitivity) phenotype**

*S. pombe* cultures were serially diluted (x10 increments) then spotted onto 3 different types of media, EMMG with and without thiamine and YEA. Cells were spotted onto YEA containing 10 mM HU and then incubated at 30°C for 3 days. *rad3-136* was used as a positive control. Full HU sensitivity suppression to *dcr1*Δ levels was noted in *dcr1*Δ *tsn1*Δ after mutating the RNase activity domain [*dcr1*Δ *tsn1*Δ (pREP3X*::*Hu*TSN::E150A*)and RNA binding domain (*dcr1*Δ *tsn1*Δ pREP3X*::*Hu*TSN::R92G*)].

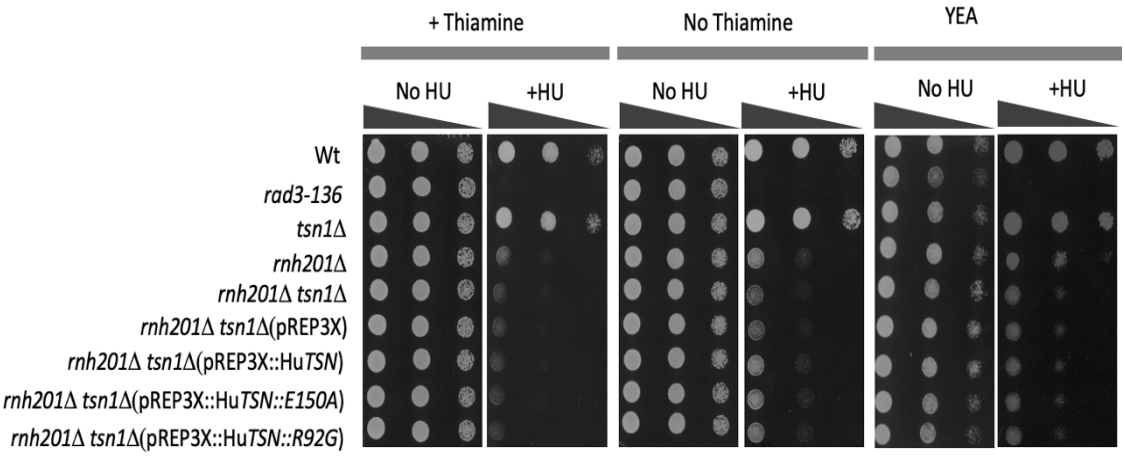


**Figure 6.16. Point mutation of RNase and RNA-binding domains of Human Translin supressed *rnh201*Δ *tsn1*Δ double mutant replicative stress (HU sensitivity) phenotype**

*S. pombe* cultures were serially diluted (x10 increments) then spotted onto 3 different types of media, EMMG with and without thiamine and YEA. Cells were spotted onto YEA containing 10 mM HU and then incubated at 30°C for 3 days. *rad3-136* was used as a positive control. Full HU sensitivity suppression to *rnh201*Δ levels was noted in *rnh201*Δ *tsn1*Δ after mutating RNase activity domain [(*rnh201*Δ *tsn1*Δ (pREP3X*::*Hu*TSN::E150A*) and RNA binding domain (*rnh201*Δ *tsn1*Δ pREP3X*::*Hu*TSN::R92G*) ].

# 6.3. Discussion

Translin and Trax, are associated with varying biological activities that appear to be related to RNA regulation rather than DNA. When Dcr1 is lacking it is clear from the data presented in this thesis that Tsn1 is required to maintain genome stability in response to some types of replicative stress. However, Tfx1 does not seem to be required. This observation is in keeping with the ability of Tsn1 to bind to nucleic acid and its RNAse function (Jaendling and McFarlane, 2010). It could also offer some insight into why Translin binds to chromosomal translocation break point junctions (to be discussed more in the final chapter). It is known that in the absence of Dcr1, RNA pol II accumulates on the genome, also increasing the associated RNA:DNA hybrids (Castel et al., 2014). These structures can threaten chromosomal integrity and predispose to pathologies such as malignancies (Zimmer et al., 2016).

In order to discourage the creation of structurally enduring RNA:DNA hybrids, two principal suppressor RNase H activities exist, RNase H1 and RNase H2. These enzymes are well-conserved ribonucleases, which have the capacity to eliminate RNA:DNA hybrids by catalysing the breakdown of the RNA residue (García-Muse and Aguilera, 2019). Furthermore, RNase H1 and RNase H2 are essential for the preservation of genomic integrity and the avoidance of replication conflicts (Cerritelli et al., 2009; Amon et al., 2016; Lockhart et al., 2019). Their activity also makes an important contribution to DSB reparation. If the genes that code for both RNase Hs are deleted, deficits in repair of DNA damage are observed and HR-governed DSB reparation is inhibited as a consequence. This therefore implies that the RNAse H pathways have a degree of redundancy in repair of the DSB (Ohle et al., 2016). The requirement for RNase H activity indicates that in DSB repair RNA:DNA hybrids play a positive function, and it has been proposed that RNA pol II and RNA pol III synthesises DSB response-specific RNAs at break sites to serve as a platform for the appropriately ordered recruitment of DSB repair factors (Michelini et al., 2017; Lui et al., 2021). Interestingly, this has recently been postulated to be related to a phase separation mechanism in which repair occurs in a phase separated from the aqueous phase (Pessina et al., 2021).

Here we have shown that Tsn1 may have a role that is redundant with an RNase H pathway (the Rnh201 pathway), but Tfx1 does not appear to be involved, again showing a separation of function for the *S. pombe* Translin family paralogues, as previously recorded for telomere transcript control (Gomez-Escobar et al., 2016). The absence of RNAse H2 (Rnh201) and Tsn1

gives rise to a more potent phenotype with respect to genomic instability. At the onset of the work, it was originally hypothesised that the HU sensitivity seen in the double mutants, *dcr1*Δ *tsn1*Δ and *rnh201*Δ *tsn1*Δ, and the single mutant, *dcr1*Δ*,* is connected to the integrity/levels of RNA:DNA hybrids, suggesting Tsn1 might have a role in suppressing RNA:DNA hybrids (i.e. possibly have an RNase H activity or an RNA:DNA hybrid helicase activity). If correct, the expression of an RNase H protein should eliminate the RNA:DNA hybrids and suppress the phenotypes observed (Drolet et al., 1995; Gaillard et al., 2013; Lockhart et al., 2019). This was not the case for any of the mutants, including the *dcr1*Δ single mutant, indicating that it is not elevated RNA:DNA hybrids *per se* that are causing the replicative stress phenotype in any of these mutants.

It is also worth noting that a colleague in the group has now demonstrated that in the *tsn1*Δ single mutant there are elevated levels of RNA:DNA hybrids. However, the single mutant exhibits no sensitivity to HU. Whilst these new data demonstrate a role for Tsn1 in RNA:DNA hybrid suppression, they support the view that these hybrids are not genotoxic under HU-induced replicative stress as no increase HU sensitivity is observed.

This view also supports the proposal of Castel et al. (2014) who suggested that the replicative stress in a *dcr1*Δ mutant is caused by the fact that loss of Dcr1 causes more RNA pol II to be retained on the genomic template, likely causing an intrinsic replicative stress, which is exacerbated by external stress from HU exposure. This indicates that the mechanism underlying the sensitivity is not connected to the RNA:DNA hybrids *per se* but to RNA Pol II retention. Despite overexpression of *rnh1,* RNA Pol II activity and association with the genome cannot be eliminated. The fact that Dcr1 is needed for RNA pol II template displacement suggests that Tsn1 might also function in this way; this possibility will be explored further in the final chapter.

In this chapter we also explored the possibility that Tsn1 has other activity that overlap with RNase III (dsRNA RNase activity) or unknown Rnh201 activities. To address both of these possibilities we overproduced the RNase III Pac1 and Rnh201 in various Tsn1-deficient cells. Neither suppressed the need for Dcr1 or Tsn1, strongly suggesting that the function of Tsn1 does not overlap with either of these functions.

The structure of Translin has been well-maintained during the development of eukaryotic organisms. In murine Translin (also known as TB-RBP), 225 of the 228 amino acids are similar

to the equivalent amino acids in human Translin. Analogous Translin proteins are found in many eukaryotes including chicken, *Xenopus*, *Drosophila* and *S. pombe*, which have 86%, 81%, 53% and 37.9% identity, respectively, with the human protein. It is noteworthy that whilst Archaea have only one Translin family paralogue, the eukaryotic budding yeast, *S. cerevisiae*, has none. *S. cerevisiae* does not have complex heterochromatin associated centromeres, like the fission yeast, but *S. pombe* Tsn1 and Tfx1 function are not related to siRNA regulated centromeric function as mutants are not defective in heterochromatic silencing (Gomez-Escobar et al., 2016). Thus, it remains unclear why *S. cerevisiae* does not have Translin orthologues, but *S. pombe* does.

In the current research, Translin genes from both *S. pombe* and human have been overexpressed in order to determine whether the activity of Tsn1 in *S. pombe* bears any relation to its function within human cells. Our data show that *S. pombe* Tsn1 defects in replicative stress response in the absence of Dcr1 can be suppressed by expression of human *TSN*. Importantly, this can be mediated in the absence of human *TSNAX* (Trax), suggesting that human TSN, like *S. pombe* Tsn1, can function in genome stability maintenance in response to replicative stress without interaction with its paralogous counterpart. The fission yeast can therefore be utilised to study the characteristics of the human Translin gene and protein. This obviates the necessity to employ human malignant cells to understand this newly revealed function, which is important as such cells do not represent the normal human state.

As Archaea only have on Translin family paralogue, which has been proposed to be more closely aligned to Trax than Translin (Parizotto et al., 2013), we assessed whether *S. pombe* Tfx1 or human TSNAX overproduction could substitute for the loss of Tsn1 in *S. pombe*. They could not. This further indicates that there is a clear functional separation between Translin and Trax for genome stability maintenance. This suggests that both paralogues have distinct and independent role in genome stability, as TSN can operate in DNA replication stress recovery (this thesis) and TSNAX function to mediate an appropriate DSB response by assisting ATM (Wang et al., 2016).

The initial work confirmed that C3PO had RNase activity was conducted in *Drosophila* (Liu et al., 2009). Multiple sequence alignments revealed three amino acids that are conserved in all the Trax proteins of higher eukaryotes, although these were less well conserved in *S. pombe.* Structural analysis revealed these groups were located within the magnesium binding area, which was postulated to be the RNase the catalytic site, despite not matching previously

defined RNase domains. These three residues were then mutated, and these proteins were found to be RNase defective. Ye et al. (2011) identified a fourth catalytic residue within human Trax, Glu197. The initial three residues in humans are Glu126, Glu129 and Asp193. Their exact locations, however, were dissimilar in the fly. The fourth residue associated with catalysis is conserved in Translin, including *S. pombe* Tsn1. This residue was mutated in Trax (Ye et al., 2011) (E197A) and was found to result in an RNase dead mutant that retained RNA binding activity. Thus, this residue is required for RNase catalysis. Here we mutated this residue in human and *S. pombe* Translin orthologues and find that these mutants retain function. This suggests that the activity is independent of RNase activity, which support the previous findings in which overexpression of RNase genes does not suppress the phenotype. It has bene proposed that human Trax has non-catalytic scaffold function in assisting ATM in responding to DSBs (Wang et al., 2016). The data presented here could indicate the activity of Translin in responding to replicative stress is also a scaffold-like function. This will be discussed further in the final Discussion chapter (Chapter 7).

We also mutated one of the codons for residues that are responsible for efficient nucleic acid binding. Both *S. pombe* and human versions could fully suppress the loss of Translin function. This is suggestive that RNA binding is not required. However, caution must be applied to this particular interpretation, as the *in vitro* analysis of the *S. pombe* mutant did not show full loss of nucleic acid binding capacity (Eliahoo et al., 2010; Gupta and Kumar., 2012). Indeed, it might be the case that sufficient RNA binding capacity is retained, particularly *in vivo*, and so whilst it might imply RNA binding is not important, this is not a robust conclusion from these data. This will be further discussed in the final chapter (Chapter 7).

There is one outstanding issue raised in this chapter that needs to be addressed. Even by using RT-PCR and Q-PCR, it is not possible to verify the overexpression of all genes mentioned previous (i.e. *rnh1*, *rnh201*, *pac1*, human TSNAX and *TSN,* and *S. pombe tsn1 and tfx1*,). Furthermore, the protein needs to be extracted and assess its level of expression is appropriate. This is achieved using the western blot technique, which is commonly in molecular biology and immunogenetics (Yang et al.,2012).

In summary, the data shown here indicate there is no phenotypic suppression of the double mutant strains, *dcr1*Δ *tsn1* and *rnh201* Δ *tsn1*Δ, and the single *dcr1*Δ mutant when *rnh1, pac1, rnh201 or tfx1* are overexpressed. The replicative stress sensitivity of these strains does not therefore appear to be associated with key ribonuclease activity of Translin. This is consistent with the findings from Castel et al. (2014) who demonstrated that the role of Dcr1 in maintaining genome stability is independent of its RNase capabilities. They extended this to demonstrate that Dcr1 functions in this RNase-independent fashion to remove RNA pol II from the genomic template to prevent increase replicative stress. The evidence we present here support a model in which Translin also functions in a nuclease-independent fashion in the absence of Dcr1 and the possibility that this might be associated with RNA pol II template dissociation is discussed in the following chapter.

# Chapter 7: Final Discussion

# 7. Final Discussion

## 7.1. Introduction

When human Translin was original identified as a protein that bound to the chromosomal breakpoint junctions of human malignancies it was inferred that it must play a role in the formation of these complex genetic rearrangement (Aoki et al., 1995). Indeed, soon after its identification Translin was referred to as a 'recombinase' (Kasai et al. 1997). Despite this, the direct evidence indicating that Translin functions in a homologous recombination mechanism has been exceptionally limited. Indeed, the co-discovery in mice of the TB-RBP (murine Translin) as an RNA binding protein indicated that even if Translin did function in recombination, the picture was not straightforward. Further complexity was added when work using *Drosophila* identified Translin, and its binding partner Trax, as the constituent part of the C3PO complex required to contribute to passenger strand remove in the RNAi pathway (Ye et al. 2011). Since these seminal discoveries, Transin and Trax have been implicated in a wide range of biological functions, including neuronal regulation through to oncogenic activity (Wang et al., 2004; Laufman et al., 2005; Gomez-Escobar et al., 2016). Additionally, evidence is emerging to indicate that Translin and Trax can function without the need to form the C3PO complex, with independent functions reported for both proteins, including telomeric transcript level regulation by Translin and an auxiliary role for Trax in ATM mediated response to DNA damage (Wang et al., 2016). These, and other features point to a complex, multifunctional role for both Translin and Trax.

The finding that Translin and Trax also function together as an oncogenic heterocomplex RNase in DICER-deficient tumours has also resulted in the development of small molecule inhibitors with an aim of developing anti-cancer therapeutic agents. This development makes it more pressing that the full functional role(s) of Translin and Trax are known to ensure that appropriate functions are targeted during therapeutic development.

At the onset of this study, co-workers within the McFarlane group had reveal that *S. pombe* Tsn1 was required to maintain genome stability in the absence of Dcr1. This function appeared to be totally independent of Tfx1. This seminal finding is one of the first direct and conclusive pieces of evidence for a role for Translin in genome stability maintenance (Gomez-Escobar et

al., 2021, in preparation; Appendix 5). Here, the findings from this thesis will be amalgamate with the findings of co-workers to offer a model for the mechanism of action of Translin in maintaining genome stability.

## 7.2. Addressing the RNase hypothesis

The discovery that the *tsn1* Δ *dcr1*Δ double mutant is hypersensitive to some DNA damaging agents, particularly those inducing certain types of DNA replication stress, suggests that Tsn1 plays an auxiliary or secondary role to Dcr1 (keep in mind *tsn1*Δ single mutants exhibit no DNA damage intolerance phenotype, suggesting that when cells are Dcr1 competent, there is no need for Tsn1). Importantly, it has previously been demonstrated that loss of Dcr1 function in fission yeast does render cells defective in DNA damage recovery and it does so in an RNAi-independent fashion (Roche et al. 2016). Castel and co-workers (2016) demonstrated that Dcr1 was required for the displacement of RNA pol II from template DNA. The model they proposed being that the retention of RNA pol II on the DNA template will form a 'roadblock' to the progression of the DNA replication machinery, which will ultimately result in replication fork collapse and the formation of recombination intermediates. Work from colleagues in the McFarlane group goes some way to support the proposal that Tsn1 functions in an auxiliary mechanism for RNA pol II displacement (see below; Gomez-Escobar et al., 2021, in preparation; Appendix 5). Castel and co-workers (2016) also fund that levels of RNA:DNA hybrids are also elevated in *dcr1*Δ cells. At the onset of this work, we speculated that further failure to process these hybrids might cause the added sensitivity of the *tsn1* Δ *dcr1* Δ to replication inhibitors. It is known that mutating both RNA:DNA hybrid processing RNase H pathways results in severe impediment to DNA repair and so we postulated that potentially Dcr1 functioned in one RNase H pathway and Tsn1 functioned in another RNase H pathway, thus, mutation of both *tsn1* and *dcr1* would offer repair defects similar to those seen in cells mutated for both RNase H encoding genes.

However, the data we have obtained here appears to dismiss this original hypothesis. Firstly, the demonstrable over expression of the gene for the primary RNase H, *rnh1*, to assess whether a phenotype can be suppressed is a good measure of whether that phenotype is caused by RNA:DNA hybrids. Interestingly, Castel and co-workers (2016) did not report over expressed

*rnh1* to determine whether they could suppress the defects they observed in the *dcr1*Δ mutant. Our data were unexpected; whilst we could show the over expressed *rnh1* was functional (it supported the HU sensitivity of the *rnh1*Δ*rnh201*Δ*)* it did not suppress the HU sensitivity of either the *dcr1* Δ single mutant or the enhanced HU sensitivity observed in the *tsn1* Δ *dcr1* Δ mutant. This suggests that neither Dcr1 nor Tsn1 are involved in removing RNA:DNA to maintain genome stability. Interestingly, a colleague (N. Gomez-Escobar) has demonstrated that both *tsn1*Δ mutants and *tfx1*Δ mutants do have elevated RNA:DNA hybrids at certain genomic loci. The consequences of this do not appear to manifest in genome instability phenotypes, as both single mutants exhibit no defect in genome stability. Moreover, the levels of RNA:DNA hybrids are not further increased in the *tsn1*Δ *dcr1*Δ double mutant, so there is no correlation between hybrid levels and measurable genome instability.

Secondly, our two RNase H pathway hypothesis was not supported when we explored mutational pairings. If Dcr1 and Tsn1 were contributing to distinct RNase H pathways, then this can be tested by constricting the appropriate double mutants of *dcr1*Δ and *tsn1*Δ with mutant in the two RNase H encoding genes (*rnh1* and *rnh201*). If the hypothesis is correct, then reciprocal pairings should have enhanced sensitivity to HU. Originally, in this work we noted that the *tsn1* Δ *rnh201* Δ double mutant was hypersensitive to HU (see table 6.1). For the hypothesis to be correct, this should mean that the *dcr1* Δ *rnh1* Δ was also hypersensitive. However, this was not the case and both *dcr1* Δ and *tsn1* Δ single mutations increased the HU sensitivity of the *rnh201* Δ mutant, but not the *rnh1* Δ mutant.

Together these findings indicate that the function of Tsn1 in maintaining genome stability does not appear to directly relate to RNA:DNA hybrid regulation/removal.

These genetic data point to a distinct explanation. They suggest that both Dcr1 and Tsn1 function in distinct pathways that when either is defective in the absence of Rnh201 this causes loss of replicative stress tolerance. RNase H2 (Rnh201) is known to be involved in an additional cellular function, the removal of mis-incorporated ribonucleotides. However, a co-worker in the group (N. Gomez-Escobar) also conducted alkali gel analysis to assess levels of alkali-sensitive genomic ribonucleotides and found no increase following mutation of either *dcr1* or *tsn1* in any background, suggesting that they are not functioning in auxiliary ribonucleotide removal pathways (Gomez- Escobar et al., in preparation; Appendix 5). This is

further confirmed by the fact that overexpression of *rnh201* in the *tsn1* Δ *dcr1* Δ double mutant does not suppress the HU sensitivity of these cells.

In fact, together, our findings might actually indicate that there is an additional, as yet unidentified role for RNase H2 (Rnh201). Indeed, the further observation that the *tsn1* Δ *rnh201* Δ double mutant exhibits enhanced HU sensitivity that cannot be suppressed by over expression of the RNase H gene, *rnh1*, suggest that Rnh201 is not functioning as an RNase H in this role. One possibility is that when Rnh201 is absent more ribonucleotides accumulate in the genome; this in turn puts added stress on replicative progression and now Tsn1 is required for RNA pol II removal (see below), despite Dcr1 proficiency in this mutant – i.e. the Tsn1-mediated auxiliary pathway is required under distinct conditions (e.g., Dcr1-deficiency and/or added ribonucleotide mis-incorporation).

Another explanation could be that Rnh201 has an as yet unidentified function that does not relate to removal of either RNA:DNA hybrids or mis-incorporated ribonucleotides. Some evidence to support this comes from the fact that mutations in human RNase H2 genes that do not cause loss of catalytic activity are linked to Aicardi-Goutieres syndrome (Feng & Cao, 2016). So, the data acquired in this thesis might be pointing to a new function for RNase H2.

Having speculated at the onset of this work that the added sensitivity to HU caused by mutating *tsn1* in the *dcr1* Δ background could be due to a failure to process RNA:DNA hybrids, we also set out to explore whether the RNA:DNA hybrid helicase Sen1 could be a factor. We found little evidence to support such a role and this further supported the conclusion that RNA:DNA hybrids *per se* are not an important molecular factor in the function of Tsn1 to maintain genome stability.

It is known that both DICER and Translin have RNase activity on double-stranded (ds) RNA (Wang et al. 2004). We also speculated that the functional role being played by either or both could be due to their dsRNse activity. Castel and co-workers (2016) had already demonstrated that the role of Dcr1 in removing RNA pol II was not dependent on the RNase catalytic activity of Dcr1. Given this, we suspected that Tsn1 RNase is also not required. However, we formally tested this in two ways. Firstly, we over expressing *pac1*, which encodes a primary dsRNase in *S. pombe*, in the *tsn1*Δ *dcr1*Δ and *tsn1* Δ *rnh201* Δ double mutants and no suppression was observed. Given that it remains possible that Pac1 might not favour the same dsRNA substrates.

Secondly, we also mutated the conserved RNAse residue in *S. pombe* Tsn1 and over expression of this mutant gene resulted in suppression of the phenotype caused by the loss of Tsn1. Together, these findings make it very unlikely that Tsn1 is functioning via an RNase mechanism to maintain genome stability.

**6.1. a table showing sensitivity profiles for each deletion mutant for each relevant drug.**

| **Drug type** | **Sensitive strains** | **Non sensitive strain** |
|---|---|---|
| Hydroxyurea (HU) | *rnh201*Δ<br>*rnh1*Δ *rnh201*Δ<br>*tsn1*Δ *rnh201*Δ<br>*sen1*Δ<br>*sen1*Δ *tfx1*Δ<br>*dcr1*Δ<br>*dcr1*Δ *rnh201*Δ | *tsn1*Δ<br>*rnh1*Δ<br>*tsn1*Δ *rnh1*Δ<br>*tfx1*Δ<br>*tfx1*Δ *rnh1*Δ<br>*tfx1*Δ *rnh201*Δ<br>*sen1*Δ *tsn1* Δ<br>*dcr1*Δ *rnh1*Δ |
| Phleomycin | *rnh1*Δ *rnh201*Δ<br>*tsn1*Δ *rnh201*Δ | *tsn1*Δ<br>*rnh1*Δ<br>*tsn1*Δ *rnh1*Δ<br>*tfx1*Δ<br>*tfx1*Δ *rnh1*Δ<br>*tfx1*Δ *rnh201*Δ |
| Camptothecin (CPT) | *rnh1*Δ *rnh201*Δ<br>*dcr1*Δ<br>*dcr1*Δ *rnh1*Δ | *tsn1*Δ<br>*rnh1*Δ<br>*tsn1*Δ *rnh1*Δ<br>*tsn1*Δ *rnh201*Δ<br>*tfx1*Δ<br>*tfx1*Δ *rnh1*Δ<br>*tfx1*Δ *rnh201*Δ<br>*sen1*Δ<br>*sen1*Δ *tfx1*Δ<br>*sen1*Δ *tsn1* Δ<br>*dcr1*Δ *rnh201*Δ |

| | | |
|---|---|---|
| Methyl Methanesulfonate (MMS) | *rnh1*Δ *rnh201*Δ | *tsn1*Δ<br>*rnh1*Δ<br>*tsn1*Δ *rnh1*Δ<br>*tsn1*Δ *rnh201*Δ<br>*tfx1*Δ<br>*tfx1*Δ *rnh1*Δ<br>*tfx1*Δ *rnh201*Δ<br>*sen1*Δ<br>*sen1*Δ *tfx1*Δ<br>*sen1*Δ *tsn1* Δ<br>*dcr1*Δ<br>*dcr1*Δ *rnh1*Δ<br>*dcr1*Δ *rnh201*Δ |
| Mitomycin C | *rnh1*Δ *rnh201*Δ | *tsn1*Δ<br>*rnh1*Δ<br>*tsn1*Δ *rnh1*Δ<br>*tsn1*Δ *rnh201*Δ<br>*tfx1*Δ<br>*tfx1*Δ *rnh1*Δ<br>*tfx1*Δ *rnh201*Δ<br>*sen1*Δ<br>*sen1*Δ *tfx1*Δ<br>*sen1*Δ *tsn1* Δ |

## 7.3. A model for Tsn1 function in genome stability control

The data within this thesis have revealed a more complex picture. An important feature to consider is the fact that Castel and co-workers (2016) found that Dcr1 was required to remove RNA pol II from the genomic template and that this was independent of Dcr1 RNase activity. The work here led us to speculate that Tsn1 too might have a role in removing RNA pol II from the template, similar to Dcr1, and that this was an auxiliary activity to that of Dcr1. A colleague in the lab (N. Gomez-Escobar) formally tested this after the completion of the laboratory work described within this thesis. She conducted chromatin immunoprecipitation of RNA pol II at genomic loci that are dependent upon Dcr1 for full RNA pol II displacement [tDNAs and the rDNA locus; important note: Castel et al. (2016) demonstrated that both RNA pol II and RNA pol III transcribe at tDNAs, in opposite orientations]. She found that in the presence of Dcr1, there is no increase in RNA pol II occupancy at these loci when *tsn1* is mutated (or *tfx1*) (Figure 5C, Gomez-Escobar et al., 2016; Appendix 5). However, when *dcr1* is mutated, an additional

mutation of *tsn1* significantly increases the RNA pol II retention at these loci, indicating that Tsn1 is required for full RNA pol II displacement when Dcr1 function is lost. The same increase in RNA pol II retention is not observed when *tfx1* is Mutated in the *dcr1*Δ background. These findings correlate well with the HU sensitivity patterns, so we can now present a postulate for a function for Tsn1 in suppression of genome stability in response to DNA replication stress. The model proposes that, under non-stress conditions that Dcr1 functions to offer sufficient RNA pol II displacement to avoid major impediment to the progression of the replisome. However, under replicative stress (e.g., HU), then loss of Dcr1 function causes genome instability due to retention of RNA pol II on the template, which causes barriers to replicative progression and is further exacerbated by loss of auxiliary RNA pol II displacement mechanism mediated by Tsn1.

Loss of Rnh201 function also puts an additional stress in the system via an unknown mechanism, which we postulate also required the maximal removal of RNA pol II from the genome, although this requires further experimental examination. Moreover, the extent to which Tsn1 is required for RNA pol II displacement through the genome at other loci remains undetermined. It could be that it only functions at these loci, which are known to cause replicative barriers. Indeed, tDNAs are frequently associated with genomic fragile sites and genomic rearrangement sites, which fits with a model linking the need for Tsn1 for RNA pol II displacement with the association of Translin with genomic rearrangement sites in human malignancies (Pryce et al. 2009). Such a model is further supported by the fact that other colleagues in the group demonstrate an increase in the recombinogenic nature of a specific test tDNA associated with an RNA pol II-replisome head-to-head collision in when both Dcr1 and Tsn1 functions are lost (Gomez-Escobar et al., in preparation; Appendix 5). Additionally, this increase in recombination is not observed for RNA pol III-replisome collisions, suggesting that the Tsn1 and Dcr1 functions are specific to RNA pol II.

## 7.4. So, how might Tsn1 (and Dcr1) function to displace RNA pol II?

Having established that Tsn1 functions to displace RNA pol II when Dcr1 is defective, the question remains as to how it might do this? Our data seem to indicate it is not via an RNase mechanism, but Tsn1 has the ability to bind to RNA, DNA and other proteins. Given this, a number of possibilities emerge (Figure 7.1). Firstly, both Dcr1 and Tsn1 might directly bind to RNA pol II to regulate its genome template association (Figure 7.1A&B). Secondly, Tsn1 might bind to ssRNA or dsRNA (generated by intra-molecular base pairing in the nascent transcript, or inter-molecular base paring between nascent transcripts produced from opposite strands); such binding might then mediate the displacement of the RNA pol II from the template DNA (Figure 7.1C-E). Alternatively, although Tsn1 is thought to have a preference for RNA, it can bind to DNA. It could mediate the removal of RNA pol II by binding to ssDNA caused by the transcription bubble and/or extensive RNA:DNA hybrid formation (although the latter is not fully supported by our RNase H over expression analysis) (Figure 7.1F).

There remains a further, intriguing possibility. *S. pombe* Tsn1 can bind to other proteins (Eliahoo et al., 2014), one of which is Srp1, a pre-mRNA splicing factor. It could be possible that the spliceosome proteins could be associated with RNA pol II removal (possibly via Dcr1 and or Tsn1). It is known that efficient splicing of pre-mRNAs is needed to suppress genome instability in response to replicative stress (Teloni et al., 2019) and that introns are protective from replicative stress (Bonnet et al., 2017), both facts that point to a model in which Tsn1 directly links to the spliceosome via a Tsn1-Srp1 interaction for the displacement of RNA pol II to prevent it becoming a recombinogenic replicative barrier (Figure 7.1G).

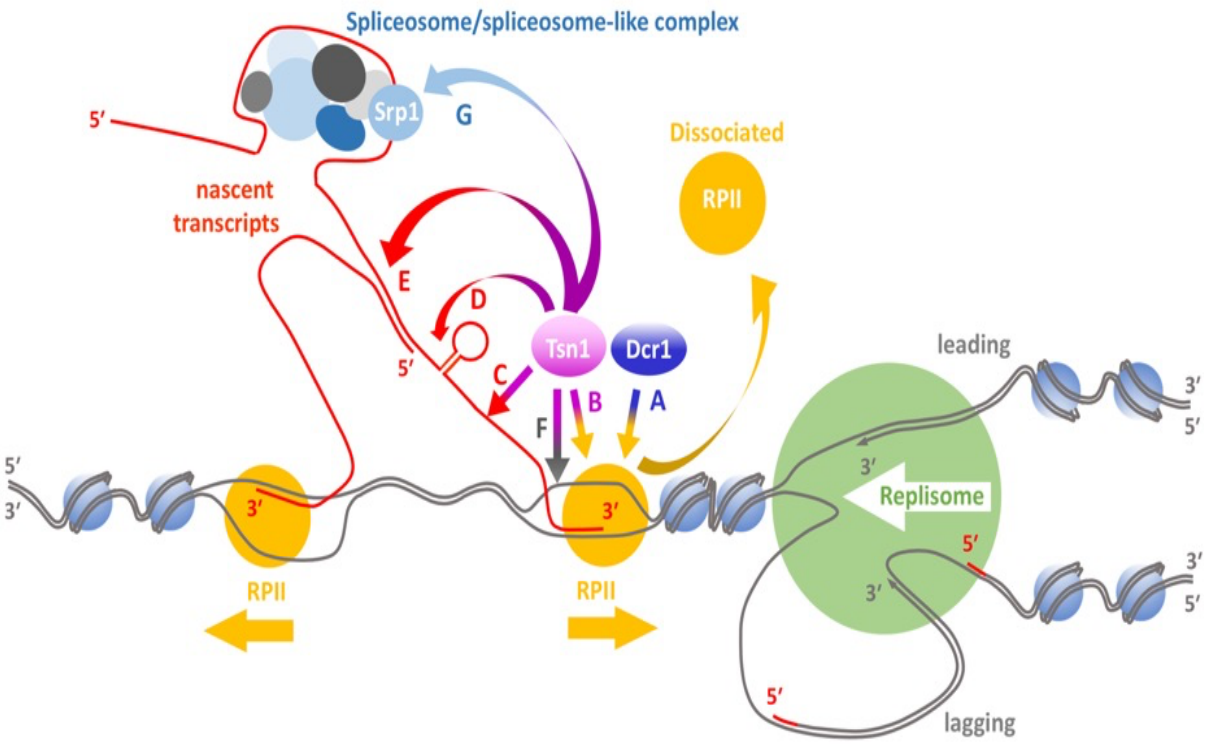


**Figure 7.1. Potential ways in which Tsn1 is involved in RNA pol II template displacement**

Refer to the text for overview.

## 7.5. Human Translin function in *S. pombe*

An important finding from this study is the demonstration that human TSN can function to suppress the loss of *S. pombe* Tsn1 and does so in the absence of co-expression of human TSNAX. This demonstrates that this genome stability regulation function of Translin is highly conserved and is independent of Trax. In humans Trax (TSNAX) has been shown to have a Translin-independent function in DNA damage response by providing a scaffold for ATM (Wang et al., 2016). Together, these findings show that both Translin and Trax have evolved distinct functions to maintain genome instability.

This becomes of considerable importance when considering these factors as drug targets for the treatment of cancer. Currently, it has been proposed that the human Translin-Trax complex RNase activity is an excellent target for anti-cancer agents in cancers that are DICER deficient (McFarlane and Wakeman 2020). In this case, it is proposed that inhibiting the Translin-Trax complex will prevent the aberrant destruction of tumour suppressing pre-miRNAs (Asada et al., 2016). However, it is known that targeting specific DNA repair pathways in cancers known to be defective on other redundant pathways can result in a synthetic lethality and greater sensitivity to genotoxic chemotherapeutic agents. It could be argued that by revealing a role for TSN in replication stress suppressing when cells are Dicer-defective, we have revealed a novel synthetic lethality that might provide a new avenue for therapeutic intervention.

## 7.6. Future experiment

As stated earlier, *sen1*Δ *tfx1*Δ double mutant is highly vulnerable to the HU, which may indicate that Sen1 has a role in regulating sub-telomeric ARRET. If a correlation between the HU sensitivity of the *sen1*Δ *tfx1*Δ double mutant and telomeric transcripts can be established, there might be some merit in undertaking research into this phenotype as it appears in the HAATI strain, which is telomere deficient.

Furthermore, through unknown mechanisms, the system experiences additional stress by the loss of functional Rnh201. We hypothesise that the mechanism requires maximal removal of RNA pol II from the genome. It might be possible to use chromatin immunoprecipitation to evaluate the function of rnh201 and its relationship to RNA polI. If the retention of RNA polI is elevated in rnh201 mutant background, the supposition is that rnh201 may have a secondary function of removing RNA polI.

Furthermore, the extent of Tsn1's involvement in displacing RNA pol II through the genome at other loci has yet to be determined. Potentially, Tsn1 only operates at these sites, giving rise to replicative barriers. Consequently, further research into this is warranted.

## 7.7. Closing remarks

For many years, since its first discovery, the binding of Translin to chromosomal break point junctions in human malignancies and other genetic diseases has resulted in an enigma. Despite some, albeit limited evidence coming forward linking Translin to genome instability, only Trax has previously been conclusively implicated in the DNA damage response. Work from this thesis, in combination with work from colleagues in the group, has resulted in plausible link between the need for Translin to remove RNA pol II and the formation of chromosomal translocation, so we believe that we have now offered sufficient insight into the long-standing question of why Translin associates with break point junctions to enable a more finely resolved answer to emerge in the future.

Importantly, we have also shown that the function of Translin in maintaining genome stability is Trax-independent and is highly conserved through evolution enabling us to point to a new therapeutic vulnerability in key cancers.

# References


Abeysinghe, S.S., Chuzhanova, N., Krawczak, M., Ball, E.V. & Cooper, D.N. 2003. Translocation and gross deletion breakpoints in human inherited disease and cancer I: Nucleotide composition and recombination-associated motifs. *Human mutation.* 22 (3). pp. 229-244.

Agrawal, N. et al. 2003. RNA Interference: Biology, Mechanism, and Applications. *Microbiology and Molecular Biology Reviews*,67(4). pp. 657–685.

Aguilera, A. and García-Muse, T. 2013. Causes of genome instability. *Annual Review of Genetics 47*, pp.1-32.

Ait Saada, A., Lambert, S.A.E. & Carr, A.M. 2018. Preserving replication fork integrity and competence via the homologous recombination pathway. *DNA Repair,* 71 pp. 135-147.

Ali Syeda, Z., Langden, S.S.S., Munkhzul, C., Lee, M. & Song, S.J. 2020. Regulatory Mechanism of MicroRNA Expression in Cancer. *International journal of molecular sciences,* 21 (5), pp. 1723.

Allison, D.F. and Wang, G.G. 2019. R-loops: Formation, function, and relevance to cell stress. *Cell Stress* 3(2), pp.28-47.

Almeida, M.V. et al. 2019. Function and evolution of nematode RNAi pathways. *Non-coding RNA*,155(1). pp.8.

Alper, B.J., Lowe, B.R. & Partridge, J.F. 2012. Centromeric heterochromatin assembly in fission yeast balancing transcription, RNA interference and chromatin modification. *Chromosome Research.* 20 (5). pp. 521-534.

Alzu A, Bermejo R, Begnis M, Lucca C, Piccini D, Carotenuto W, Saponaro M, Brambati A, Cocito A, Foiani M *et al* (2012) Senataxin associates with replication forks to protect fork integrity across RNA-polymerase-II-transcribed genes. Cell 151. pp. 835–846.

Amon JD, Koshland D. RNase H enables efficient repair of R-loop induced DNA damage. *Elife.* 2016;5:e20533.

Andrews AM, McCartney HJ, Errington TM, D'Andrea AD, Macara IG (2018) A senataxin-associated exonuclease SAN1 is required for resistance to DNA interstrand cross-links. *Nat Commun* 9, pp.2592.

Aoki, K., Ishida, R. & Kasai, M. 1997. Isolation and characterization of a cDNA encoding a Translin-like protein, TRAX. *FEBS Letters.* 401 (2-3). pp. 109-112.

Aoki, K., Suzuki, K., Ishida, R., Kasai, M., 1999. The DNA binding activity of Translin is mediated by a basic region in the ring-shaped structure conserved in evolution. FEBS Lett. 443, pp.363–366.

Aoki, K., Suzuki, K., Sugano, T., Tasaka, T., Nakahara, K., Kuge, O., Omori, A. & Kasai, M. 1995. A novel gene, Translin, encodes a recombination hotspot binding protein associated with chromosomal translocations. *Nature genetics.* 10 (2). pp. 167-174.

Arimbasseri AG, Rijal K, Maraia RJ (2013) Transcription termination by the eukaryotic RNA polymerase III. *Biochim Biophys Acta* 1829, pp 318–330.

Asada, K., Canestrari, E. & Paroo, Z. 2016. A druggable target for rescuing microRNA defects. *Bioorganic &Medicinal Chemistry Letters.* 26 (20). pp. 4942-4946.

Asada, K., Canestrari, E., Fu, X., Li, Z., Makowski, E., Wu, Y.C., Mito, J.K., Kirsch, D.G., Baraban, J. & Paroo, Z. 2014. Rescuing dicer defects via inhibition of an anti-dicing nuclease. *Cell reports.* 9 (4). pp. 1471-1481.

Atlas, M., Head, D., Behm, F., Schmidt, E., Zeleznik-Le, N., Roe, B., Burian, D., and Domer, P. 1998. Cloning and sequence analysis of four t (9; 11) therapy-related leukemia breakpoints. Leukemia 12, pp.1895-1902.

Au, C.H., Ho, D.N., Ip, B.B.K., Wan, T.S.K., Ng, M.H.L., Chiu, E.K.W., Chan, T.L. & Ma, E.S.K. 2019. Rapid detection of chromosomal translocation and precise breakpoint characterization in acute myeloid leukemia by nanopore long-read sequencing. *Cancer genetics.* 239 pp. 22-25.

Azzalin, C.M. & Lingner, J. 2015. Telomere functions grounding on TERRA firma. *Trends in Cell biology.* 25 (1). pp. 29-36.

Azzalin, C.M., Reichenbach, P., Khoriauli, L., Giulotto, E. & Lingner, J. 2007. Telomeric repeat containing RNA and RNA surveillance factors at mammalian chromosome ends. *Science.* 318 (5851). pp. 798-801.

Bach, D.H. et al. 2019. Chromosomal instability in tumor initiation and development. *Cancer Research*. pp.18-3235.

Bader, A.S., Hawley, B.R., Wilczynska, A. & Bushell, M. 2020. The roles of RNA in DNA double-strand break repair. *British Journal of Cancer,* 122 (5), pp. 613-623.

Badge, R.M., Yardley, J., Jeffreys, A.J. & Armour, J.A.L. 2000. Crossover breakpoint mapping identifies a subtelomeric hotspot for male meiotic recombination. *Human molecular genetics.* 9 (8). pp. 1239-1244.

Bah, A. et al. 2012. The telomeric transcriptome of Schizosaccharomyces pombe. *Nucleic Acids Research* 40 (7), pp.2995-3005.

Bähler, J., Wu, J.-Q., Longtine, M.S., Shah, N.G., Mckenzie III, A., Steever, A.B., Wach, A., Philippsen, P. and Pringle, J.R. 1998. Heterologous modules for efficient and versatile PCR-based gene targeting in *Schizosaccharomyces pombe*. Yeast, (14). pp.943-951.

Barroso, S. et al. 2019. The DNA damage response acts as a safeguard against harmful DNA–RNA hybrids of different origins. *EMBO report s20*. e47250.

Belotserkovskii, B.P., Tornaletti, S., D'Souza, A.D. & Hanawalt, P.C. 2018. R-loop generation during transcription: Formation, processing and cellular outcomes. *DNA repair.* 71 pp. 69-81.

Bennett, C.L. and La Spada, A.R. 2018. Senataxin, a novel helicase at the interface of RNA transcriptome regulation and neurobiology: From normal function to pathological roles in motor neuron disease and cerebellar degeneration. In: *Advances in Neurobiology* 20, pp.265-281.

Berti, M. & Vindigni, A. 2016. Replication stress: getting back on track. *Nature structural & Molecular Biology.* 23 (2). pp. 103-109.

Betermier, M., Borde, V. & de Villartay, J.P. 2020. Coupling DNA Damage and Repair: An Essential Safeguard during Programmed DNA Double-Strand Breaks? *Trends in cell biology.* 30 (2). pp. 87-96.

Bettin, N. et al. 2019. The Emerging Roles of TERRA in Telomere Maintenance and Genome Stability. *Cells 8*(3), pp.246.

Bhalla, P. et al. 2019. Yeast PAF1 complex counters the pol III accumulation and replication stress on the tRNA genes. *Scientific Reports* 9, pp.12892.

Bhargava, R., Onyango, D.O. & Stark, J.M. 2016. Regulation of Single-Strand Annealing and its Role in Genome Maintenance. *Trends in genetics: TIG,* 32 (9), pp. 566-575.

Bizard, A.H. & Hickson, I.D. 2014. The dissolution of double Holliday junctions. *Cold Spring Harbor perspectives in biology,* 6 (7), pp. a016477-a016477.

Blin M, Le Tallec B, Nähse V, Schmidt M, Brossas C, Millot GA, Prioleau MN, Debatisse M. 2019. Transcription-dependent regulation of replication dynamics modulates genome stability. *Nat Struct Mol Biol* 26, pp.58–66.

Boboila, C., Alt, F.W. & Schwer, B. 2012. 1 Classical and alternative end-joining pathways for repair of lymphocyte-specific and general DNA double-strand breaks. *Advances in Immunology.* 116 pp. 1.

Bonnet, A., Grosso, A.R., Elkaoutari, A., Coleno, E., Presle, A., Sridhara, S.C., Janbon, G., Géli, V., de Almeida, S.F., and Palancade, B. (2017) Introns protect eukaryotic genomes from transcription-associated genetic instability. Mol. Cell *67*, pp. 608-621.

Brambati, A., Colosio, A., Zardoni, L., Galanti, L. & Liberi, G. 2015. Replication and transcription on a collision course: eukaryotic regulation mechanisms and implications for DNA stability. *Frontiers in Genetics.* 6 pp. 166.

Brambati, A., Zardoni, L., Nardini, E., Pellicioli, A., and Liberi, G. (2020) The dark side of RNA:DNA hybrids. Mutate. pp.*784*.

Brieno-Enriquez, M.A., Moak, S.L., Abud-Flores, A. & Cohen, P.E. 2019. Characterization of telomeric repeat-containing RNA (TERRA) localization and protein interactions in primordial germ cells of the mousedagger. *Biology of reproduction.* 100 (4). pp. 950-962.

Buhler, M. & Gasser, S.M. 2009. Silent chromatin at the middle and ends lessons from yeasts. *EMBO Journal.* 28 (15). pp. 2149-2161.

Burgers, P.M.J. & Kunkel, T.A. 2017. Eukaryotic DNA Replication Fork. *Annual Review of Biochemistry,* 86 (1), pp. 417-438.

Burslem, G.M., Schultz, A.R., Bondeson, D.P., Eide, C.A., Savage Stevens, S.L., Druker, B.J. & Crews, C.M. 2019. Targeting BCR-ABL1 in Chronic Myeloid Leukemia by PROTAC-Mediated Targeted Protein Degradation. *Cancer research.* 79 (18). pp. 4744-4753.

Campbell, P.J., Getz, G., Korbel, J.O., Stuart, J.M., Jennings, J.L., Stein, L.D., Perry, M.D., et al. 2020. Pan-cancer analysis of whole genomes. *Nature*. 578(7793). pp.82-93.

Castel, S.E. & Martienssen, R.A. 2013. RNA interference in the nucleus: roles for small RNAs in transcription, epigenetics and beyond. *Nature Reviews Genetics.* 14 (2). pp. 100-112.

Castel, S.E., Ren, J., Bhattacharjee, S., Chang, A.Y., Sanchez, M., Valbuena, A., Antequera, F. & Martienssen, R.A. 2014. Dicer promotes transcription termination at sites of replication stress to maintain genome stability. *Cell.* 159 (3). pp. 572-583.

Ceccaldi, R., Rondinelli, B. & D'Andrea, A.D. 2016. Repair Pathway Choices and Consequences at the Double-Strand Break. *Trends in cell biology.* 26 (1). pp. 52-64.

Cerritelli, S.M. and Crouch, R.J. 2009. Ribonuclease H: The enzymes in eukaryotes. *FEBS Journal* ,276(6), pp.149401505.

Chang, H.H.Y., Pannunzio, N.R., Adachi, N. & Lieber, M.R. 2017. Non-homologous DNA end joining and alternative pathways to double-strand break repair. *Nature reviews. Molecular Cell Biology,* 18(8), p.495.

Chaplin, A.K. & Blundell, T.L. 2020. Structural biology of multicomponent assemblies in DNA double-strand-break repair through non-homologous end joining. *Current opinion in structural biology.* 61 pp. 9-16.

Chatterjee, S. 2017. Telomeres in health and disease. *Journal of Oral and Maxillofacial Pathology:* (1). pp. 87-91.

Chen, L., Chen, J.Y., Zhang, X., Gu, Y., Xiao, R., Shao, C., Tang, P., Qian, H., Luo, D., Li, H., Zhou, Y., Zhang, D.E. & Fu, X.D. 2017. R-ChIP Using Inactive RNase H Reveals Dynamic Coupling of R-loops with Transcriptional Pausing at Gene Promoters. *Molecular cell.* 68 (4). pp. 745-757.e5.

Chen, L., Ge, B., Casale, F.P., Vasquez, L., Kwan, T., Garrido-Martín, D., Watt, S., et al. 2016. Genetic Drivers of Epigenetic and Transcriptional Variation in Human Immune Cells. *Cell.* 167 (5). pp.1398-1414.e24.

Chen, X. et al. 2014. Saccharomyces cerevisiae Sen1 as a model for the study of mutations in human Senataxin that elicit cerebellar ataxia. *Genetics* 216(4).

Chennathukuzhi, V., Stein, J.M., Abel, T., Donlon, S., Yang, S., Miller, J.P., Allman, D.M., Simmons, R.A. & Hecht, N.B. 2003. Mice deficient for testis-brain RNA-binding protein exhibit a coordinate loss of TRAX, reduced fertility, altered gene expression in the brain, and behavioral changes. *Molecular and Cellular Biology.* 23 (18). pp. 6419-6434.

Chern, Y., Chien, T., Fu, X., Shah, A.P., Abel, T. & Baraban, J.M. 2019. Trax: A versatile signaling protein plays key roles in synaptic plasticity and DNA repair. *Neurobiology of learning and memory.* 159 pp. 46-51.

Chiaruttini, C., Vicario, A., Li, Z., Baj, G., Braiuca, P., Wu, Y., Lee, F.S., Gardossi, L., Baraban, J.M. & Tongiorgi, E. 2009. Dendritic trafficking of BDNF mRNA is mediated by translin and blocked by the G196A (Val66Met) mutation. *Proceedings of the National Academy of Sciences of the United States of America.* 106 (38). pp. 16481-16486.

Chien, T., Weng, Y.T., Chang, S.Y., Lai, H.L., Chiu, F.L., Kuo, H.C., Chuang, D.M., et al. 2018. GSK3β negatively regulates TRAX, a scaffold protein implicated in mental disorders, for NHEJ-mediated DNA repair in neurons. *Molecular Psychiatry*. 23. pp.2375–2390.

Chikashige, Y., Yamane, M., Okamasa, K., Tsutsumi, C., Kojidani, T., Sato, M., Haraguchi, T. & Hiraoka, Y. 2009. Membrane proteins Bqt3 and -4 anchor telomeres to the nuclear envelope to ensure chromosomal bouquet formation. *Journal of Cell Biology.* 187 (3). pp. 413-427.

Cho, Y.S., Chennathukuzhi, V.M., Handel, M.A., Eppig, J. & Hecht, N.B. 2004. The relative levels of translin-associated factor X (TRAX) and testis brain RNA-binding protein determine their nucleocytoplasmic distribution in male germ cells. *The Journal of biological chemistry.* 279 (30). pp. 31514-31523.

Chow, J.F.C., Cheng, H.H.Y., Lau, E.Y.L., Yeung, W.S.B. & Ng, E.H.Y. 2020. Distinguishing between carrier and noncarrier embryos with the use of long-read sequencing in preimplantation genetic testing for reciprocal translocations. *Genomics.* 112 (1). pp. 494-500.

Claussen, M., Koch, R., Jin, Z.Y. & Suter, B. 2006. Functional characterization of *Drosophila* Translin and Trax. *Genetics.* 174 (3). pp. 1337-1347.

Clouaire, T., Rocher, V., Lashgari, A., Arnould, C., Aguirrebengoa, M., Biernacka, A., Skrzypczak, M., Aymard, F., Fongang, B., Dojer, N., Iacovoni, J.S., Rowicka, M., Ginalski, K., Cote, J. & Legube, G. 2018. Comprehensive Mapping of Histone Modifications at DNA Double-Strand Breaks Deciphers Repair Pathway Chromatin Signatures. *Molecular cell.* 72 (2). pp. 250-262.e6.

Cohen, S., Puget, N., Lin, Y.L., Clouaire, T., Aguirrebengoa, M., Rocher, V., Pasero, P., Canitrot, Y. & Legube, G. 2018. Senataxin resolves RNA:DNA hybrids forming at DNA double-strand breaks to prevent translocations. *Nature communications.* 9 (1). pp. 533-018-02894-w.

Costantino, L. and Koshland, D. 2015. The Yin and Yang of R-loop biology. *Current Opinion in Cell Biology*. (2015) 34, pp.39-45.

Creamer, K.M. & Partridge, J.F. 2011. RITS-connecting transcription, RNA interference, and heterochromatin assembly in fission yeast. *RNA.* 2 (5). pp. 632-646.

Crickard, J.B., Moevus, C.J., Kwon, Y., Sung, P. & Greene, E.C. 2020. Rad54 Drives ATP Hydrolysis-Dependent DNA Sequence Alignment during Homologous Recombination *Cell.* 181 (6). pp. 1380-1394.e18.

Cristini, A., Gromak, N. & Sordet, O. 2020. Transcription-dependent DNA double-strand breaks and human disease. *Molecular & Cellular Oncology,* 7 (2), pp. 1691905.

Crossley, M.P. et al. 2019. R-Loops as Cellular Regulators and Genomic Threats. *Molecular Cell*. 73(3) pp.398-411.

Crossley, M.P., Bocek, M. & Cimprich, K.A. 2019. Review R-Loops as Cellular Regulators and Genomic Threats. *Molecular Cell,* 73 (3), pp. 398-411.

Cusanelli, E. & Chartrand, P. 2015. Telomeric repeat-containing RNA TERRA: a noncoding RNA connecting telomere biology to genome integrity. *Frontiers in genetics.* 6 pp. 143.

D'Alessandro, G., Whelan, D.R., Howard, S.M., Vitelli, V., Renaudin, X., Adamowicz, M., Iannelli, F., Jones-Weinert, C.W., Lee, M., Matti, V., Lee, W.T.C., Morten, M.J., Venkitaraman, A.R., Cejka, P., Rothenberg, E. & d'Adda di Fagagna, F. 2018. BRCA2 controls DNA:RNA hybrid level at DSBs by mediating RNase H2 recruitment. *Nature communications.* 9 (1). pp. 5376-018-07799-2.

Davis, A.J. & Chen, D.J. 2013. DNA double strand break repair via non-homologous end-joining. *Translational Cancer Research.* 2 (3). pp. 130-143.

Dewhurst, S.M. 2020. Chromothripsis and telomere crisis: engines of genome instability. *Current opinion in genetics & development.* 60 pp. 41-47.

Djupedal I, Ekwall K. Epigenetics: heterochromatin meets RNAi. Cell Res,19(3). pp.282-95.
Domingo-Prim, J. et al. 2020. RNA at DNA Double-Strand Breaks: The Challenge of Dealing with DNA:RNA Hybrids. *BioEssays* 42(5), pp.1900225.

Domingo-Prim, J., Endara-Coll, M., Bonath, F., Jimeno, S., Prados-Carvajal, R., Friedlander, M.R., Huertas, P. & Visa, N. 2019. EXOSC10 is required for RPA assembly and controlled DNA end resection at DNA double-strand breaks. *Nature communications.* 10 (1). pp. 2135-019-10153-9.

Domingo-Prim, J., Bonath, F. & Visa, N. 2020. RNA at DNA Double-Strand Breaks: The Challenge of Dealing with DNA: RNA Hybrids. *BioEssays,* 42 (5), pp. 1900225.

Donnianni, R.A., Zhou, Z., Lujan, S.A., Al-Zain, A., Garcia, V., Glancy, E., Burkholder, A.B., Kunkel, T.A. & Symington, L.S. 2019. DNA Polymerase Delta Synthesizes Both Strands during Break-Induced Replication. *Molecular Cell,* 76 (3), pp. 371-381.e4.

Drolet M, Phoenix P, Menzel R, Massé E, Liu LF, Crouch RJ. Overexpression of RNase H partially complements the growth defect of an Escherichia coli delta topA mutant: R-loop formation is a major problem in the absence of DNA topoisomerase I. Proc Natl Acad Sci U S A. 1995,11;92(8), pp.3526-30.

Duijf, P.H. & Benezra, R. 2013. The cancer biology of whole-chromosome instability. *Oncogene.* 32 (40). pp. 4727-4736.

Dumelie, J.G. & Jaffrey, S.R. 2017. Defining the location of promoter-associated R-loops at near-nucleotide resolution using bisDRIP-seq. *eLife.* 6 pp. 10.7554/eLife.28306.

Ďúranová, H. 2019. FISSION YEAST SCHIZOSACCHAROMYCES POMBE AS A MODEL SYSTEM FOR ULTRASTRUCTURAL INVESTIGATIONS USING TRANSMISSION ELECTRON MICROSCOPY, *Journal of Microbiology, Biotechnology and Food Sciences*, pp.160-165.

Dutertre, M., Lambert, S., Carreira, A., Amor-Guéret, M. & Vagner, S. 2014. DNA damage: RNA-binding proteins protect from near and far. *Trends in Biochemical Sciences,* 39 (3), pp. 141-149.

Dutta, A. et al. 2020. Senataxin: A Putative RNA: DNA Helicase Mutated in ALS4-Emerging Mechanisms of Genome Stability in Motor Neurons. In: *Amyotrophic Lateral Sclerosis - Recent Advances and Therapeutic Challenges* 6.

El Hage, A., French, S.L., Beyer, A.L. & Tollervey, D. 2010. Loss of Topoisomerase I lead to R-loop-mediated transcriptional blocks during ribosomal RNA synthesis. *Genes & development.* 24 (14). pp. 1546-1558.

Elango, R. *et al.* 2017. Break-induced replication promotes formation of lethal joint molecules dissolved by Srs2. *Nature Communications*, 8(1), pp. 1790.

Eliahoo, E., Litovco, P., Ben Yosef, R., Bendalak, K., Ziv, T. & Manor, H. 2014. Identification of proteins that form specific complexes with the highly conserved protein Translin in< i> Schizosaccharomyces pombe. *Biochimica et Biophysica Acta (BBA)-Proteins and Proteomics.* 1844 (4). pp. 767-777.

Emden, T.S., Forn, M., Forné, I., Sarkadi, Z., Capella, M., Martín Caballero, L., Fischer-Burkart, S., et al. 2019. Shelterin and subtelomeric DNA sequences control nucleosome maintenance and genome stability. *EMBO Reports*. pp.201847181.

Ensminger, M. & Löbrich, M. 2020. One end to rule them all: Non-homologous end-joining and homologous recombination at DNA double-strand breaks. *The British Journal of Radiology,* pp. 20191054.

Escorcia W, Forsburg SL. Tetrad Dissection in Fission Yeast. Methods Mol Biol 1721, pp.179-18.

Falquet, B. & Rass, U. 2019. Structure-Specific Endonucleases and the Resolution of Chromosome Underreplication. *Genes.* 10 (3). pp. 10.3390/genes10030232.

Fasching, C., Cejka, P., Kowalczykowski, S. & Heyer, W. 2015. Top3-Rmi1 Dissolve Rad51-Mediated D Loops by a Topoisomerase-Based Mechanism. *Molecular Cell,* 57 (4), pp. 595-606.

Felipe-Abrio, I., Lafuente-Barquero, J., Garcia-Rubio, M.L. & Aguilera, A. 2015. RNA polymerase II contributes to preventing transcription-mediated replication fork stalls. *The EMBO Journal.* 34 (2). pp. 236-250.

Feng, S., and Cao, Z. (2016) Is the role of human RNase H2 restricted to its enzyme activity? Prog. Biophys. Mol. Biol. *121*,pp. 66-73.

Feretzaki, M. & Lingner, J. 2017. A practical qPCR approach to detect TERRA, the elusive telomeric repeat-containing RNA. *Methods.* 114 pp. 39-45.

Feretzaki, M., Nunes, P.R. and Lingner, J. 2019. Expression and differential regulation of human TERRA at several chromosome ends. *RNA*,26 (10), pp.1470-1480.

Finkel, J.S. et al. 2010. Sen1p performs two genetically separable functions in transcription and processing of U5 small nuclear RNA in Saccharomyces cerevisiae. *Genetics* 148(1), pp.109-204.

Fischer, S.E.J. 2010. Small RNA-mediated gene silencing pathways in C. elegans. *International Journal of Biochemistry and Cell Biology*, 42(8). pp.1306-15.

Foulkes, W.D., Priest, J.R. & Duchaine, T.F. 2014. DICER1: mutations, microRNAs and mechanisms. *Nature Reviews Cancer,* 14 (10), pp. 662-672.

Fragkos, M. & Naim, V. 2017. Rescue from replication stress during mitosis. *Cell cycle (Georgetown, Tex.).* 16 (7). pp. 613-633.

Francia, S., Cabrini, M., Matti, V., Oldani, A. & Adda di Fagagna, F. 2016. DICER, DROSHA and DNA damage response RNAs are necessary for the secondary recruitment of DNA damage response factors. *Journal of Cell Science,* 129 (7), pp. 1468 LP - 1476.

Fu, X., Shah, A. & Baraban, J.M. 2016. Rapid reversal of translational silencing: Emerging role of microRNA degradation pathways in neuronal plasticity. *Neurobiology of learning and memory.* 133 pp. 225-232.

Gadaleta, M.C. & Noguchi, E. 2017. Regulation of DNA replication through natural impediments in the eukaryotic genome. *Genes.* 8 (3). pp. 10.3390/genes8030098.

Gaillard H, Herrera-Moyano E, Aguilera A. 2013. Transcription-associated genome instability. *Chem Rev* 113, pp.8638–8661.

Gajecka, M., Pavlicek, A., Glotzbach, C.D., Ballif, B.C., Jarmuz, M., Jurka, J. & Shaffer, L.G. 2006b. Identification of sequence motifs at the breakpoint junctions in three t (1; 9) (p36. 3; q34) and delineation of mechanisms involved in generating balanced translocations. *Human Genetics.* 120 (4). pp. 519-526.

Garcia-Muse, T. & Aguilera, A. 2016. Transcription-replication conflicts: how they occur and how they are resolved. *Nature Reviews. Molecular Cell Biology.* 17 (9). pp. 553-563.

García-Muse, T. and Aguilera, A. 2019. R Loops: From Physiological to Pathological Roles. *Cell* 179 (3), pp.604-618.

García-Rubio, M., Aguilera, P., Lafuente-Barquero, J., Ruiz, J.F., Simon, M.N., Geli, V., Rondón, A.G. & Aguilera, A. 2018b. Yra1-bound RNA–DNA hybrids cause orientation-independent transcription– replication collisions and telomere instability. *Genes and Development,* 32 (13-14), pp. 965-977.

Gerlitz, G. 2020. The Emerging Roles of Heterochromatin in Cell Migration. *Frontiers in Cell and Developmental Biology,* 8 pp. 394.

Ginno, P.A., Lott, P.L., Christensen, H.C., Korf, I. & Chedin, F. 2012. R-loop formation is a distinctive characteristic of unmethylated human CpG island promoters. *Molecular cell.* 45 (6). pp. 814-825.

Godin, S.K., Sullivan, M.R. & Bernstein, K.A. 2016. Novel insights into RAD51 activity and regulation during homologous recombination and DNA replication. *Biochemistry and Cell Biology,* 94 (5), pp. 407-418.

Gomez-Escobar, N. et al. 2016. Translin and Trax differentially regulate telomere-associated transcript homeostasis. *Oncotarget*, 7, pp.33809-33820.

Gómez-González, B. and Aguilera, A. 2019. Transcription-mediated replication hindrance: A major driver of genome instability. *Genes and Development*, 35, pp.5-6.

Gómez-González, B. et al. 2020. Spontaneous DNA-RNA hybrids: differential impacts throughout the cell cycle. *Cell Cycle* 19 (5).

Gomez-Herreros, F. 2019. DNA Double Strand Breaks and Chromosomal Translocations Induced by DNA Topoisomerase II. *Frontiers in molecular biosciences.* 6 pp. 141.

Grabarz, A., Barascu, A., Guirouilh-Barbat, J. & Lopez, B.S. 2012. Initiation of DNA double strand break repair: signaling and single-stranded resection dictate the choice between homologous recombination, non-homologous end-joining and alternative end-joining. *American Journal of Cancer Research.* 2 (3). pp. 249-268.

Greenstein, R.A., Ng, H., Barrales, R.R., Tan, C., Braun, S. & Al-Sady, B. 2020b. Local chromatin context dictates the genetic determinants of the heterochromatin spreading reaction. *bioRxiv,* pp. 2020.05.26.117143.

Greenwood, J. & Cooper, J.P. 2012a. Non-coding telomeric and subtelomeric transcripts are differentially regulated by telomeric and heterochromatin assembly factors in fission yeast. *Nucleic Acids Research.* 40 (7). pp. 2956-2963.

Groh M, Albulescu LO, Cristini A, Gromak N (2017) Senataxin: genome guardian at the interface of transcription and neurodegeneration. J Mol Bio 429, pp 3181–3195.

Gupta, A., Pillai, V.S. & Chittela, R.K. 2019. Role of amino acid residues important for nucleic acid binding in human Translin. *The international journal of biochemistry & cell biology.* 115 pp. 105593.

Gupta, A., Pillai, V.S. and Chittela, R.K. 2019a.Translin: A multifunctional protein involved in nucleic acid metabolism. *Journal of Biosciences*.44, pp.139.

Gupta, G.D., Kale, A., Kumar, V., 2012. Molecular evolution of Translin superfamily proteins within the genomes of eubacteria, archaea and eukaryotes. J. Mol. Evol. 75, pp.155–167.

Gurtner, A., Falcone, E., Garibaldi, F. & Piaggio, G. 2016. Dysregulation of microRNA biogenesis in cancer: the impact of mutant p53 on Drosha complex activity. *Journal of Experimental & Clinical Cancer Research.* 35 (1). pp. 45.

Gutbrod, M.J. & Martienssen, R.A. 2020. Conserved chromosomal functions of RNA interference. *Nature reviews.Genetics.* 21 (5). pp. 311-331.

Hamada M, Huang Y, Lowe TM, Maraia RJ (2001) Widespread use of TATA elements in the core promoters for RNA polymerases III, II, and I in fission yeast. *Mol Cell Biol* 21**,** pp 6870–6881.

Hamperl, S. et al. 2017. Transcription-Replication Conflict Orientation Modulates R-Loop Levels and Activates Distinct DNA Damage Responses. *Cell* 170(4), pp.774-786.

Han, J., Gu, W. & Hecht, N.B. 1995. Testis-brain RNA-binding protein, a testicular translational regulatory RNA-binding protein, is present in the brain and binds to the 3'untranslated regions of transported brain mRNAs. *Biology of Reproduction.* 53 (3). pp. 707-717.

Han, Z. et al. 2017. Biochemical characterization of the helicase Sen1 provides new insights into the mechanisms of non-coding transcription termination. *Nucleic Acids Research 45(3)*, pp. 1355–1370.

Han, Z. et al. 2020. Termination of non-coding transcription in yeast relies on both an RNA Pol II CTD interaction domain and a CTD-mimicking region in Sen1. *The EMBO Journal* 39 (7), pp. e101548.

Hanahan, D. & Weinberg, R.A. 2000. The hallmarks of cancer. *Cell,* 100 (1), pp. 57- 70.

Hanahan, D. & Weinberg, R.A. 2011. Hallmarks of cancer: the next generation. *Cell,* 144 (5), pp. 646-674.

Hansen, K.R., Ibarra, P.T. & Thon, G. 2006. Evolutionary-conserved telomere-linked helicase genes of fission yeast are repressed by silencing factors, RNAi components and the telomere-binding protein Taz1. *Nucleic Acids Research.* 34 (1). pp. 78-88.

Harewood, L. & Fraser, P. 2014. The impact of chromosomal rearrangements on regulation of gene expression. *Human Molecular Genetics.* 23 (R1). pp. R76-82.

Harland, J.L., Chang, Y.T., Moser, B.A. & Nakamura, T.M. 2014. Tpz1-Ccq1 and Tpz1-Poz1 interactions within fission yeast shelterin modulate Ccq1 Thr93 phosphorylation and telomerase recruitment. *PLoS Genetics.* 10 (10). pp. e1004708.

Hasegawa, T. & Isobe, K. 1999. Evidence for the interaction between Translin and GADD34 in mammalian cells. *Biochimica et Biophysica Acta (BBA)-General Subjects.* 1428 (2). pp. 161-168.

Hasegawa, T., Xiao, H., Hamajima, F. & Isobe, K. 2000. Interaction between DNA-damage protein GADD34 and a new member of the Hsp40 family of heat shock proteins that is induced by a DNA-damaging reagent. *Biochemical Journal.* 352 Pt 3 pp. 795-800.

Hata, A. & Kashima, R. 2016. Dysregulation of microRNA biogenesis machinery in cancer. *Critical Reviews in Biochemistry and Molecular Biology.* 51 (3). pp. 121-134.

Hawley, B.R., Lu, W.T., Wilczynska, A. and Bushell, M. 2017.The emerging role of RNAs in DNA damage repair, *Cell Death and Differentiation*, 24, pp.580–587.

Hayles, J. and Nurse, P. 2018.Introduction to fission yeast as a model system. *Cold Spring Harbor Protocols*, (10), pp. 1101.

Hegazy, Y.A., Fernando, C.M. and and Elizabeth, J.T. 2020. The balancing act of R-loop biology: The good, the bad, and', Vol. 295, pp. 905–913.

Hegazy, Y.A., Fernando, C.M., and Tran, E.J. (2020) The balancing act of R-loop biology: the good, the bad, and the ugly. J. Biol. Chem. *295*, pp. 905-913.

Helmrich, A. et al. 2013. Transcription-replication encounters, consequences and genomic instability. *Nature Structural and Molecular Biology* 20, pp.412–418.

Hizume, K. and Araki, H. 2019. Replication fork pausing at protein barriers on chromosomes. *FEBS Letters*, 593(13) pp.1449.1458.

Hoffman, C.S., Wood, V. & Fantes, P.A. 2015. An Ancient Yeast for Young Geneticists: A Primer on the Schizosaccharomyces pombe Model System. *Genetics.* 201 (2). pp. 403-423.

Holic, R., Pokorna, L. & Griac, P. 2020. Metabolism of phospholipids in the yeast Schizosaccharomyces pombe. *Yeast (Chichester, England).* 37 (1). pp. 73-92.

Holla, S., Dhakshnamoorthy, J., Folco, H.D., Balachandran, V., Xiao, H., Sun, L., Wheeler, D., Zofall, M. & Grewal, S.I.S. 2020a. Positioning Heterochromatin at the Nuclear Periphery Suppresses Histone Turnover to Promote Epigenetic Inheritance. *Cell,* 180 (1), pp. 150-164.e15.

Holoch, D. & Moazed, D. 2015. RNA-mediated epigenetic regulation of gene expression. *Nature Reviews Genetics.* 16 (2). pp. 71-84.

Hosaka, T., Kanoe, H., Nakayama, T., Murakami, H., Yamamoto, H., Nakamata, T., Tsuboyama, T., Oka, M., Kasai, M., and Sasaki, M. S. 2000. Translin binds to the sequences adjacent to the breakpoints of the TLS and CHOP genes in liposarcomas with translocation t (12; 6). Oncogene. pp.19, 5821.

HSU, M. and LUE, N.F., 2017. Analysis of Yeast Telomerase by Primer Extension Assays. *Telomeres and Telomerase.* Springer, pp. 83-93.

Hu, Y., Bennett, H.W., Liu, N., Moravec, M., Williams, J.F., Azzalin, C.M. & King, M.C. 2019b. RNA-DNA hybrids support recombination-based telomere maintenance in fission yeast. *bioRxiv,* pp. 458968.

Hustedt, N., Saito, Y., Zimmermann, M., Alvarez-Quilon, A., Setiaputra, D., Adam, S., McEwan, A., Yuan, J.Y., Olivieri, M., Zhao, Y., Kanemaki, M.T., Jurisicova, A. & Durocher, D. 2019. Control of homologous recombination by the HROB-MCM8-MCM9 pathway. *Genes & development.* 33 (19-20). pp. 1397-1415.

Hylton, H.M., Lucas, B.E. & Petreaca, R.C. 2020. Schizosaccharomyces pombe Assays to Study Mitotic Recombination Outcomes. *Genes.* 11 (1). pp. 10.3390/genes11010079.

Iino, Y. et al. 1991. S. pombe pac1+, whose overexpression imhibits sexual development, encodes a ribonuclease III-like RNase. *EMBO Journal*, 10(1), pp.221-6.

Iliakis, G., Murmann, T. & Soni, A. 2015. Alternative end-joining repair pathways are the ultimate backup for abrogated classical non-homologous end-joining and homologous recombination repair: Implications for the formation of chromosome translocations. *Mutation research.Genetic toxicology and environmental mutagenesis.* 793 pp. 166-175.

Ishida, R. et al. 2002. A role for the octameric ring protein, Translin, in mitotic cell division. *FEBS Letters* 525(1-3), pp.105-110.

Jackson, R.A., Wu, J.S. & Chen, E.S. 2016. C1D family proteins in coordinating RNA processing, chromosome condensation and DNA damage response. *Cell division.* 11 pp. 2-016-0014-5. eCollection 2016.

Jaendling, A. & Mcfarlane, R. 2010. Biological roles of translin and translin-associated factor-X: RNA metabolism comes to the fore. *Biochem.J.* 429 pp. 225-234.

Jaendling, A., Ramayah, S., Pryce, D.W. & McFarlane, R.J. 2008. Functional characterisation of the Schizosaccharomyces pombe homologue of the leukaemia-associated translocation breakpoint binding protein translin and its binding partner, TRAX. *Biochimica et biophysica acta.* 1783 (2). pp. 203-213.

Jain et al. (2010) HAATI survivors replace canonical telomeres with blocks of generic heterochromatin. Nature 467:223-227.

Jain, R., Aggarwal, A.K. & Rechkoblit, O. 2018. Eukaryotic DNA polymerases. *Current opinion in structural biology.* 53 pp. 77-87.

Jia, S., Noma, K. and Grewal, S.I.S. 2004. RNAi-independent heterochromatin nucleation by the stress-activated ATF/CREB family proteins.", *Science (New York, N.Y.)*, United States, Vol. 304 No. 5679, pp. 1971–1976.

Jimeno, S., Prados-Carvajal, R. & Huertas, P. 2019. The role of RNA and RNA-related proteins in the regulation of DNA double strand break repair pathway choice. *DNA repair,* 81 pp. 102662.

Johanson, T.M., Lew, A.M. & Chong, M.M. 2013. MicroRNA-independent roles of the RNase III enzymes Drosha and Dicer. *Open biology.* 3 (10). pp. 130144.

Kalantari, R., Chiang, C.M. & Corey, D.R. 2016. Regulation of mammalian transcription and splicing by Nuclear RNAi. *Nucleic acids research.* 44 (2). pp. 524-537.

Kanoe, H., Nakayama, T., Hosaka, T., Murakami, H., Yamamoto, H., Nakashima, Y., Tsuboyama, T., Nakamura, T., Ron, D., Sasaki, M.S. & Toguchida, J. 1999. Characteristics of genomic breakpoints in TLS-CHOP translocations in liposarcomas suggest the involvement of Translin and topoisomerase II in the process of translocation. *Oncogene.* 18 (3). pp. 721-729.

Kasai, M., Ishida, R., Nakahara, K., Okumura, K. and Aoki, K. 2018, Mesenchymal cell differentiation and diseases: involvement of translin/TRAX complexes and associated proteins. *Annals of the New York Academy of Sciences*, John Wiley & Sons, Ltd, Vol. 1421 No. 1, pp. 37–45.

Kasai, M., Matsuzaki, T., Katayanagi, K., Omori, A., Maziarz, R.T., Strominger, J.L., Aoki, K. & Suzuki, K. 1997. The translin ring specifically recognizes DNA ends at recombination hot spots in the human genome. *Journal of BiologicalChemistry.* 272 (17). pp. 11402-11407.

Kasparek, T.R. & Humphrey, T.C. 2011. DNA double-strand break repair pathways, chromosomal rearrangements and cancer. *Seminars in Cell & Developmental Biology.* 22 (8). pp. 886-897.

Kawakami, M., Liu, X. & Dmitrovsky, E. 2019. New Cell Cycle Inhibitors Target Aneuploidy in Cancer Therapy. *Annual Review of Pharmacology and Toxicology,* 59 (1), pp. 361-377.

Khan, F.A. & Ali, S.O. 2017. Physiological Roles of DNA Double-Strand Breaks. *Journal of Nucleic Acids,* 2017 pp. 6439169.

Kim HD, Choe J, Seo YS (1999) The sen1(+) gene of Schizosaccharomyces pombe, a homologue of budding yeast SEN1, encodes an RNA and DNA helicase. *Biochemistry* 38, pp14697–14710.

Klar, A.J. 2007. Lessons learned from studies of fission yeast mating-type switching and silencing. *Annual Review of Genetics.* 41 pp. 213-236.

Kojima, K., Baba, M., Tsukiashi, M., Nishimura, T. and Yasukawa, K. 2018. RNA/DNA structures recognized by RNase H2', *Briefings in Functional Genomics*, Vol. 18 No. 3, pp. 169–173.

Koyama, M., Nagakura, W., Tanaka, H., Kujirai, T., Chikashige, Y., Haraguchi, T., Hiraoka, Y. & Kurumizaka, H. 2017. In vitro reconstitution and biochemical analyses of the

*Schizosaccharomyces pombe* nucleosome. *Biochemical and Biophysical Research communications.* 482 (4). pp. 896-901.

Kramara, J., Osia, B. & Malkova, A. 2018. Break-induced replication: the where, the why, and the how. *Trends in Genetics,* 34 (7), pp. 518-531.

Kumar, V. and Gupta, G.D. 2012. Low-resolution structure of Drosophila translin. *FEBS Open Bio*,15;2. pp.37-46.

Kupfer, G.M., Wiese, C., Greene, E.C. & Sung, P. 2017. BRCA1-BARD1 promotes RAD51-mediated homologous DNA pairing. *Nature.* 550 (7676). pp. 360-365.

Kupiec, M. 2014. Biology of telomeres: lessons from budding yeast. *FEMS Microbiology Reviews.* 38 (2). pp. 144-171.

Kuznetsov, V.A. et al. 2018. Toward predictive R-loop computational biology: Genome-scale prediction of R-loops reveals their association with complex promoter structures, G-quadruplexes and transcriptionally active enhancers. *Nucleic Acids Research* 46 (15), pp 7566–7585.

Kwapisz, M. and Morillon, A. 2020. Subtelomeric Transcription and its Regulation. *Journal of Molecular Biology* 432 (15). 4199-4219.

Lalonde, M. and Chartrand, P. 2020. TERRA, a Multifaceted Regulator of Telomerase Activity at Telomeres. *Journal of Molecular Biology* 432(15), pp.4232-4243.

Lang, K.S. et al. 2017. Replication-Transcription Conflicts Generate R-Loops that Orchestrate Bacterial Stress Survival and Pathogenesis. *Cell 170 (4)*, pp. 787-799.

Larochelle M, Robert M-A, Hébert J-N, Liu X, Matteau D, Rodrigue S, Tian B, Jacques P-É, Bachand F (2018) Common mechanism of transcription termination at coding and noncoding RNA genes in fission yeast. *Nat Commun* 9, pp4364.

Laufman, O., Yosef, R.B., Adir, N. & Manor, H. 2005. Cloning and characterization of the Schizosaccharomyces pombe homologs of the human protein Translin and the Translin-associated protein TRAX. *Nucleic acids research,* 33 (13), pp. 4128-4139.

Lee, S.Y., Rozenzhak, S. & Russell, P. 2013. gammaH2A-binding protein Brc1 affects centromere function in fission yeast. *Molecular and Cellular Biology.* 33 (7). pp. 1410-1416.

Legros P, Malapert A, Niinuma S, Bernard P, Vanoosthuyse V (2014) RNA processing factors Swd2.2 and Sen1 antagonize RNA Pol III-dependent transcription and the localization of condensin at Pol III genes. *PLoS Genet* 10, pp e1004794.

Leman, A.R. & Noguchi, E. 2013. The replication fork: understanding the eukaryotic replication machinery and the challenges to genome duplication. *Genes.* 4 (1). pp. 1-32.

Lemay J-F, Marguerat S, Larochelle M, Liu X, van Nues R, Hunyadkürti J, Hoque M, Tian B, Granneman S, Bähler J *et al* (2016) The Nrd1-like protein Seb1 coordinates

cotranscriptional 3′ end processing and polyadenylation site selection. *Genes Dev* 30, pp1558–1572.

Lewis, J.S., Spenkelink, L.M., Schauer, G.D., Yurieva, O., Mueller, S.H., Natarajan, V., Kaur, G., Maher, C., Kay, C., O'Donnell, M.E. & van Oijen, A.M. 2020. Tunability of DNA Polymerase Stability during Eukaryotic DNA Replication. *Molecular cell.* 77 (1). pp. 17-25.e5.

Li, J. & Xu, X. 2016. DNA double-strand break repair: a tale of pathway choices. *Acta Biochimica Et Biophysica Sinica.* 48 (7). pp. 641-646.

Li, J.S., Miralles Fuste, J., Simavorian, T., Bartocci, C., Tsai, J., Karlseder, J. & Lazzerini Denchi, E. 2017. TZAP: A telomere-associated protein involved in telomere length control. *Science (New York, N.Y.).* 355 (6325). pp. 638-641.

Li, L., Gu, W., Liang, C., Liu, Q., Mello, C.C. & Liu, Y. 2012. The translin-TRAX complex (C3PO) is a ribonuclease in tRNA processing. *Nature Structural & Molecular Biology.* 19 (8). pp. 824-830.

Li, Y., Roberts, N.D., Wala, J.A., Shapira, O., Schumacher, S.E., Kumar, K., Khurana, E., Waszak, S., Korbel, J.O., Haber, J.E., Imielinski, M., PCAWG Structural Variation Working Group, Weischenfeldt, J., Beroukhim, R., Campbell, P.J. & PCAWG Consortium 2020. Patterns of somatic structural variation in human cancer genomes. *Nature.* 578 (7793). pp. 112-121.

Li, Z., Wu, Y. & Baraban, J.M. 2008. The Translin/Trax RNA binding complex: clues to function in the nervous system. *Biochimica Et Biophysica Acta.* 1779 (8). pp. 479-485.

Liao, H., Ji, F., Helleday, T. & Ying, S. 2018. Mechanisms for stalled replication fork stabilization: new targets for synthetic lethality strategies in cancer treatments. *EMBO reports.* 19 (9). pp. 10.15252/embr.201846263. Epub 2018 Aug 13.

Lin, Y.L. & Pasero, P. 2012. Interference between DNA replication and transcription as a cause of genomic instability. *Current Genomics.* 13 (1). pp. 65-73.

Liu, J., Ali, M. & Zhou, Q. 2020. Establishment and evolution of heterochromatin. *Annals of the New York Academy of Sciences.*

Liu, S., Hua, Y., Wang, J., Li, L., Yuan, J., Zhang, B., Wang, Z., Ji, J., and Kong, D. (2021) RNA polymerase III is required for the repair of DNA double-strand breaks by homologous recombination. Cell *184*, pp. 1314-1329.

Liu, Y., Fang, Y., Liu, Y., Wang, Z., Lyu, B., Hu, Y. & Zhou, X. 2019. Opposite effects of Drosophila C3PO on gene silencing mediated by esi-2.1 and miRNA-bantam. *Acta biochimica et biophysica Sinica.* 51 (2). pp. 131-138.

Liu, Y., Ye, X., Jiang, F., Liang, C., Chen, D., Peng, J., Kinch, L.N., Grishin, N.V. & Liu, Q. 2009. C3PO, an endoribonuclease that promotes RNAi by facilitating RISC activation. *Science.* 325 (5941). pp. 750-753.

Lluis, M., Hoe, W., Schleit, J., and Robertus, J. 2010. Analysis of nucleic acid binding by a recombinant translin–trax complex. Biochemical and biophysical research communications 396. PP.709-713.

Lockhart, A., Pires, V.B., Bento, F., Kellner, V., Luke-Glaser, S., Yakoub, G., Ulrich, H.D. & Luke, B. 2019. RNase H1 and H2 Are Differentially Regulated to Process RNA-DNA Hybrids. *Cell reports.* 29 (9). pp. 2890-2900.e5.

Lorenzi, L.E., Bah, A., Wischnewski, H., Shchepachev, V., Soneson, C., Santagostino, M. & Azzalin, C.M. 2015. Fission yeast Cactin restricts telomere transcription and elongation by controlling Rap1 levels. *EMBO Journal.* 34 (1). pp. 115-129.

Lu, W.-T., Hawley, B.R., Skalka, G.L., Baldock, R.A., Smith, E.M., Bader, A.S., Malewicz, M., et al. (2018), 'Drosha drives the formation of DNA:RNA hybrids around DNA break sites to facilitate DNA repair', *Nature Communications*, Vol. 9 No. 1, p. 532.

Lujan, S.A., Williams, J.S. & Kunkel, T.A. 2016. DNA Polymerases Divide the Labor of Genome Replication. *Trends in Cell Biology.* 26 (9). pp. 640-654.

Lyn Chan, F. and Wong, L.H. 2012.Transcription in the maintenance of centromere chromatin identity. *Nucleic Acids Research*, 40 (22). pp.11178-11188.

Maeshima, K., Imai, R., Tamura, S. & Nozaki, T. 2014. Chromatin as dynamic 10-nm fibers. *Chromosoma.* 123 (3). pp. 225-237.

Maicher, A., Lockhart, A. & Luke, B. 2014. Breaking new ground: digging into TERRA function. *Biochimica Et Biophysica Acta.* 1839 (5). pp. 387-394.

Mandell, J.G., Goodrich, K.J., Bahler, J. & Cech, T.R. 2005. Expression of a RecQ helicase homolog affects progression through crisis in fission yeast lacking telomerase. *Journal of Biological Chemistry.* 280 (7). pp. 5249-5257.

Marini, F., Rawal, C.C., Liberi, G. and Pellicioli, A. 2019.Regulation of DNA Double Strand Breaks Processing: Focus on Barriers.*Frontiers in Molecular Biosciences*.6. pp. 55.

Marsano, R.M., Giordano, E., Messina, G. & Dimitri, P. 2019. A New Portrait of Constitutive Heterochromatin: Lessons from Drosophila melanogaster. *Trends in genetics : TIG.* 35 (9). pp. 615-631.

Martin-Tumasz, S. and Brow, D.A. 2015. Saccharomyces cerevisiae sen1 helicase domain exhibits 5′- to 3′-helicase activity with a preference for translocation on DNA rather than RNA. *Journal of Biological Chemistry 290*, pp. 22880-22889.

Martinelli, G., Terragna, C., Amabile, M., Montefusco, V., Testoni, N., Ottaviani, E., De Vivo, A., Mianulli, A., Saglio, G. & Tura, S. 2000. Alu and translisin recognition site sequences flanking translocation sites in a novel type of chimeric bcr-abl transcript suggest a possible general mechanism for bcr-abl breakpoints. *Haematologica,* 85 (1), pp. 40-46.

Massirer, K.B. and Pasquinelli, A.E. 2013. MicroRNAs that interfere with RNAi. *Worm*, 2(1). pp. e21835.

Mawer, J. S. P. and Leach, D. R. F. 2014.Branch Migration Prevents DNA Loss during Double-Strand Break Repair.*PLOS Genetics*. Public Library of Science.10(8).pp. e1004485.

McFarlane, R.J. and Wakeman, J.A. 2020. Translin-Trax: Considerations for Oncological Therapeutic Targeting", *Trends in Cancer*, Vol. 6 No. 6, pp. 450–453.

McGinty, R.K. and Tan, S. (2015), "Nucleosome structure and function", *Chemical Reviews*, 115(6). pp.2255-2273.

Mei, F., Kehui, X. & Wenming, X. 2016. Research advances of Dicer in regulating reproductive function. *Yi chuan = Hereditas.* 38 (7). pp. 612-622.

Meiyanto, E. & Larasati, Y.A. 2019. The Chemopreventive Activity of Indonesia Medicinal Plants Targeting on Hallmarks of Cancer. *Advanced pharmaceutical bulletin.* 9 (2). pp. 219-230.

Meng, X., Yang, S. & Camp, V.J.A. 2020. The Interplay Between the DNA Damage Response, RNA Processing and Extracellular Vesicles. *Frontiers in Oncology,* 9 pp. 1538.

Meng, Z. & Lu, M. 2017. RNA interference-induced innate immunity, Off-Target effect, or immune Adjuvant? *Frontiers in Immunology.* 8, p.331.

Michelini, F., Pitchiaya, S., Vitelli, V., Sharma, S., Gioia, U., Pessina, F., Cabrini, M., Wang, Y., Capozzo, I., Iannelli, F., et al. (2017) Damage-induced lncRNAs control the DNA damage response through interaction with DDRNAs at individual double-strand breaks. Nat. Cell Biol. *19*, pp.1400-1411.

Mischo HE, Gómez-González B, Grzechnik P, Rondón AG, Wei W, Steinmetz L, Aguilera A, Proudfoot NJ (2011) Yeast Sen1 helicase protects the genome from transcription-associated instability. *Mol Cell* 41, pp 21–32.

Mishra S, Maraia RJ (2019) RNA polymerase III subunits C37/53 modulate rU:dA hybrid 3′ end dynamics during transcription termination. *Nucleic Acids Res* 47, pp 310–327.

Mizukoshi, E. & Kaneko, S. 2019.Telomerase-Targeted Cancer Immunotherapy. *International journal of molecular sciences.* 20 (8).

Mo, X., Yang, X. & Yuan, Y.A. 2018. Structural insights into Drosophila-C3PO complex assembly and 'Dynamic Side Port' model in substrate entry and release. *Nucleic acids research.* 46 (16). pp. 8590-8604.

Moazed, D. 2009. Small RNAs in transcriptional gene silencing and genome defence. *Nature* 457**,** pp.413–420.

Morati, F., Zagelbaum, J.A., Taylor, B., Desclos, E.C.B., Wang, R., Sullivan, M.R., Rein, H.L., et al.2020.Distinct pathways of homologous recombination controlled by the SWS1-SWSAP1-SPIDR complex. *BioRxiv*,05(15), pp.098848.

Moravec, M., Wischnewski, H., Bah, A., Hu, Y., Liu, N., Lafranchi, L., King, M.C. and Azzalin, C.M., 2016. TERRA promotes telomerase-mediated telomere elongation in *Schizosaccharomyces pombe*. *EMBO Reports*, *17*(7), pp.999-1012.

Moreno, S.P. and Gambus, A. 2020.Mechanisms of eukaryotic replisome disassembly. *Biochemical Society Transactions*, Vol. 48 No. 3, pp. 823–836.

Nadel, J. et al. 2015. RNA: DNA hybrids in the human genome have distinctive nucleotide characteristics, chromatin composition, and transcriptional relationships. *Epigenetics and Chromatin*. 8(46). pp.0040.

Nakano, K. and Takahashi, S. 2018.Translocation-related sarcomas.*International Journal of Molecular Sciences*.*19*(12). pp. 3784.

Nava, G.M. et al. 2020. One, no one, and one hundred thousand: The many forms of ribonucleotides in DNA. *International Journal of Molecular Sciences*.21(5), pp.1706.

Navarro, A.P. and Cheeseman, I.M. 2020.Chromosome Segregation: Evolving a Plastic Chromosome–Microtubule Interface, *Current Biology*,30 (4). pp. 561-572.e10.

Nenclares, P. and Harrington, K.J. 2020.The biology of cancer. *Medicine (United Kingdom)*.48(2). pp. 67-72.

Nierhs, C., and Luke, B. (2020) Regulatory R-loops as facilitators of gene expression and genome stability. Nat. Rev. Mol. Cell Biol. *21*, pp. 167-178.

Novo, C.L. Londoño-Vallejo, J.A. 2013. Telomeres and the nucleus. *Seminars in Cancer Biology.* Elsevier: pp. 116.

Nowell, P.C. and Hungerford, D.A. 1960.Chromosome studies on normal and leukemic human leukocytes. *Journal of the National Cancer Institute*. 25 (1). pp. 85-109.

Nussenzweig, A. and Nussenzweig, M.C. 2010.Origin of Chromosomal Translocations in Lymphoid Cancer. *Cell*.141(1). pp.27-38.

O'Brien, J., Hayder, H., Zayed, Y. & Peng, C. 2018. Overview of MicroRNA Biogenesis, Mechanisms of Actions, and Circulation. *Frontiers in endocrinology.* 9 pp. 402.

Ochi, T., Blackford, A.N., Coates, J., Jhujh, S., Mehmood, S., Tamura, N., Travers, J., Wu, Q., Draviam, V.M., Robinson, C.V., Blundell, T.L. & Jackson, S.P. 2015. DNA repair. PAXX, a paralog of XRCC4 and XLF, interacts with Ku to promote DNA double-strand break repair. *Science (New York, N.Y.).* 347 (6218). pp. 185-188.

Ohle, C., Tesorero, R., Schermann, G., Dobrev, N., Sinning, I. & Fischer, T. 2016. Transient RNA- DNA hybrids are required for efficient double-strand break repair. *Cell,* 167 (4), pp. 1001- 1013. e7.

Onaka, A.T., Su, J., Katahira, Y., Tang, C., Zafar, F., Aoki, K., Kagawa, W., Niki, H., Iwasaki, H. & Nakagawa, T. 2020. DNA replication machinery prevents Rad52-dependent single-strand annealing that leads to gross chromosomal rearrangements at centromeres. *Communications Biology,* 3 (1), pp. 202.

Paliwal, S., Kanagaraj, R., Sturzenegger, A., Burdova, K. & Janscak, P. 2013. Human RECQ5 helicase promotes repair of DNA double-strand breaks by synthesis-dependent strand annealing. *Nucleic Acids Research,* 42 (4), pp. 2380-2390.

Pan, L., Hildebrand, K., Stutz, C., Thoma, N. & Baumann, P. 2015. Minishelterins separate telomere length regulation and end protection in fission yeast. *Genes & Development.* 29 (11). pp. 1164-1174.

Parizotto, E.A., Lowe, E.D. & Parker, J.S. 2013. Structural basis for duplex RNA recognition and cleavage by Archaeoglobus fulgidus C3PO. *Nature Structural & Molecular Biology.* 20 (3). pp. 380-386.

Parizotto, E.A., Lowe, E.D., and Parker, J.S. (2013) Structural basis for duplex RNA recognition and cleavage by *Archaeoglobus fulgidus* C3PO. Nat. Struct. Mol. Biol. *20*, pp.380-386.

Park, A.J., Havekes, R., Fu, X., Hansen, R., Tudor, J.C., Peixoto, L., Li, Z., Wu, Y., Poplawski, S.G. & Baraban, J.M. 2017. Learning induces the translin/trax RNase complex to express activin receptors for persistent memory. *Elife,* 6 pp. e27872.

Park, A.J., Shetty, M.S., Baraban, J.M. & Abel, T. 2020. Selective role of the translin/trax RNase complex in hippocampal synaptic plasticity. *bioRxiv,* pp. 2020.05.19.105189.

Patterson, A.D., Hollander, M.C., Miller, G.F. & Fornace, A.J.,Jr 2006. Gadd34 requirement for normal hemoglobin synthesis. *Molecular and cellular biology.* 26 (5). pp. 1644-1653.

Pessina, F., Gioia, U., Brandi, O., Farina, S., Ceccon, M., Francia, S., and d'Adda di Fagagna, F. (2021) NA damage triggers a new phase in neurodegeneration. Trends Genet. *37*, pp.337-354.

Petermann, E., Orta, M.L., Issaeva, N., Schultz, N. & Helleday, T. 2010. Hydroxyurea-stalled replication forks become progressively inactivated and require two different RAD51-mediated pathways for restart and repair. *Molecular Cell.* 37 (4). pp. 492-502.

Petersen, J. & Russell, P. 2016. Growth and the Environment of Schizosaccharomyces pombe. *Cold Spring Harbor Protocols.* 2016 (3). pp. pdb.top079764.

Petrova, B., Dehler, S., Kruitwagen, T., Heriche, J.K., Miura, K. & Haering, C.H. 2013. Quantitative analysis of chromosome condensation in fission yeast. *Molecular and cellular biology.* 33 (5). pp. 984-998.

Porrua, O. and Libri, D. 2013. A bacterial-like mechanism for transcription termination by the Sen1p helicase in budding yeast. *Nature Structural and Molecular Biology* 20, pp.884-891.

Prado, F. 2018.Homologous recombination: To fork and beyond. *Genes*. 9(12).pp.603.

Pryce, D.W. et al. 2009. Recombination at DNA replication fork barriers is not universal and is differentially regulated by Swi 1. *Proceedings of the National Academy of Sciences of the United States of America* 9.

Pushpavalli, S.N., Bag, I., Pal-Bhadra, M. & Bhadra, U. 2012. Drosophila Argonaute-1 is critical for transcriptional cosuppression and heterochromatin formation. *Chromosome Research.* 20 (3). pp. 333-351.

Ramakrishnan, S., Kockler, Z., Evans, R., Downing, B.D. & Malkova, A. 2018. Single-strand annealing between inverted DNA repeats: Pathway choice, participating proteins, and genome destabilizing consequences. *PLOS Genetics,* 14 (8), pp. e1007543.

Rawal, C.C. et al. 2020. Senataxin Ortholog Sen1 Limits DNA: RNA Hybrid Accumulation at DNA Double-Strand Breaks to Control End Resection and Repair Fidelity. *Cell Reports* 31(5), pp.107603.

Remo, A., Li, X., Schiebel, E. and Pancione, M. 2020.The Centrosome Linker and Its Role in Cancer and Genetic Disorders, *Trends in Molecular Medicine*.26(4). pp.380-393.

Ren, J., Castel, S.E. & Martienssen, R.A. 2015. Dicer in action at replication-transcription collisions. *Molecular & Cellular Oncology.* 2 (3). pp. e991224.

Richard, P. et al. 2020. SETX (senataxin), the helicase mutated in AOA2 and ALS4, functions in autophagy regulation. *Autophagy* 20.

Rinaldi, C., Pizzul, P., Longhese, M.P., and Bonetti, D. (2021) Sensing R-loop-associated DNA damage to safeguard genome stability. Front. Cell Dev. Biol. *8*, pp. 618157.

Rippe, K. & Luke, B. 2015. TERRA and the state of the telomere. *Nature Structural & Molecular Biology.* 22 (11). pp. 853-858.

Rivosecchi, J. et al. 2019. Sen1 is required for RNA Polymerase III transcription termination in an R-loop independent manner. *bioRxiv* 11.

Rondón, A.G. and Aguilera, A. 2019. What causes an RNA-DNA hybrid to compromise genome integrity? *DNA Repair* 81, pp.102660.

Sabatinos, S.A. and Forsburg, S.L. 2010. Molecular genetics of schizosaccharomyces pombe", *Methods in Enzymology*. Elsevier, pp. 759-795.

Sadeghi, L., Prasad, P., Ekwall, K., Cohen, A. & Svensson, J.P. 2015. The Paf1 complex factors Leo1 and Paf1 promote local histone turnover to modulate chromatin states in fission yeast. *EMBO Reports.* 16 (12). pp. 1673-1687.

Sahu, S., Philip, F. & Scarlata, S. 2014. Hydrolysis rates of different small interfering RNAs (siRNAs) by the RNA silencing promoter complex, C3PO, determines their regulation by phospholipase Cbeta. *The Journal of Biological Chemistry.* 289 (8). pp. 5134-5144.

Sakofsky, C.J. & Malkova, A. 2017. Break induced replication in eukaryotes: mechanisms, functions, and consequences. *Critical Reviews in Biochemistry and Molecular biology.* 52 (4). pp. 395-413.

San Filippo, J., Sung, P. & Klein, H. 2008. Mechanism of Eukaryotic Homologous Recombination. *Annual Review of Biochemistry.* 77 (1). pp. 229-257.

Santos-Pereira, J.M. & Aguilera, A. 2015a. R loops: new modulators of genome dynamics and function. *Nature Reviews Genetics,* 16 (10), pp. 583.

Sanz, L.A., Hartono, S.R., Lim, Y.W., Steyaert, S., Rajpurkar, A., Ginno, P.A., Xu, X. & Chedin, F. 2016. Prevalent, Dynamic, and Conserved R-Loop Structures Associate with Specific Epigenomic Signatures in Mammals. *Molecular cell.* 63 (1). pp. 167-178.

Sarbajna, S. & West, S.C. 2014. Holliday junction processing enzymes as guardians of genome stability. *Trends in biochemical sciences.* 39 (9). pp. 409-419.

Sarek, G., Marzec, P., Margalef, P. & Boulton, S.J. 2015. Molecular basis of telomere dysfunction in human genetic diseases. *Nature Structural & Molecular Biology.* 22 (11). pp. 867-874.

Schoeftner, S. & Blasco, M.A. 2008. Developmentally regulated transcription of mammalian telomeres by DNA-dependent RNA polymerase II. *Nature Cell Biology.* 10 (2). pp. 228-236.

Schuster, S., Miesen, P. & van Rij, R.P. 2019. Antiviral RNAi in Insects and Mammals: Parallels and Differences. *Viruses.* 11 (5). pp. 10.3390/v11050448.

Schutte, J., Reusch, J., Khandanpour, C. & Eisfeld, C. 2019. Structural Variants as a Basis for Targeted Therapies in Hematological Malignancies. *Frontiers in oncology.* 9 pp. 839.

Scully, R., Panday, A., Elango, R. & Willis, N.A. 2019. DNA double-strand break repair-pathway choice in somatic mammalian cells. *Nature reviews.Molecular cell biology.* 20 (11). pp. 698-714.

Seike, T., Shimoda, C. & Niki, H. 2019. Asymmetric diversification of mating pheromones in fission yeast. *PLoS biology.* 17 (1). pp. e3000101.

Sengupta, K., Kamdar, R.P., D'souza, J.S., Mustafi, S.M., Rao, B.J., 2006. GTP-induced conformational changes in Translin: a comparison between human and Drosophila proteins. Biochemistry 45, pp.861–870.

Shah, R. *et al.* .2017. Resolution of single and double Holliday junction recombination intermediates by GEN1. 114(3), pp. 443–450.

Shibata, A. 2017.Regulation of repair pathway choice at two-ended DNA double-strand breaks. *Mutation Research/Fundamental and Molecular Mechanisms of Mutagenesis*, 803–805, pp. 51–55.

Shipkovenska, G., Durango, A., Kalocsay, M., Gygi, S.P. & Moazed, D. 2020. A conserved RNA degradation complex required for spreading and epigenetic inheritance of heterochromatin. *eLife.* 9 pp. 10.7554/eLife.54341.

Shukla, A. and Bhargava, P. 2018. Regulation of tRNA gene transcription by the chromatin structure and nucleosome dynamics. *Biochimica et Biophysica Acta (BBA) - Gene Regulatory Mechanisms* 1861(4), pp. 295–309.

Skourti-Stathaki K, Kamieniarz-Gdula K, Proudfoot NJ. 2014. R-loops induce repressive chromatin marks over mammalian gene terminators. *Nature* 516: pp. 436–439.

Skourti-Stathaki K, Proudfoot NJ, Gromak N (2011) Human senataxin resolves RNA/DNA hybrids formed at transcriptional pause sites to promote Xrn2-dependent termination. *Mol Cell* 42, pp794–805.

Smurova, K. and De Wulf, P. 2018.Centromere and Pericentromere Transcription: Roles and Regulation in Sickness and in Health. *Frontiers in Genetics*.9. pp.674.

Soniat, M.M., Myler, L.R., Kuo, H.C., Paull, T.T. & Finkelstein, I.J. 2019. RPA Phosphorylation Inhibits DNA Resection. *Molecular cell.* 75 (1). pp. 145-153.e5.

Stein, J.M., Bergman, W., Fang, Y., Davison, L., Brensinger, C., Robinson, M.B., Hecht, N.B. & Abel, T. 2006. Behavioral and neurochemical alterations in mice lacking the RNA-binding protein translin. *The Journal of neuroscience: the official Journal of the Society for Neuroscience.* 26 (8). pp. 2184-2196.

Steiner, F.A. & Henikoff, S. 2015. Diversity in the organization of centromeric chromatin. *Current Opinion in Genetics & Development.* 31 pp. 28-35.

Steinmetz, E.J. et al. 2006. Genome-Wide Distribution of Yeast RNA Polymerase II and Its Control by Sen1 Helicase. *Molecular Cell* 24(5), pp.735-746.

Stinson, B., Moreno, A., Walter, J. and Loparo, J. 2019. Non-homologous end joining minimizes errors by coordinating DNA processing with ligation. *Molecular Cell*.

Stinson, B.M., Moreno, A.T., Walter, J.C. & Loparo, J.J. 2020. A Mechanism to Minimize Errors during Non-homologous End Joining. *Molecular cell.* 77 (5). pp. 1080-1091.e8.

Stolz, R., Sulthana, S., Hartono, S.R., Malig, M., Benham, C.J. & Chedin, F. 2019. Interplay between DNA sequence and negative superhelicity drives R-loop structures. *Proceedings of the National Academy of Sciences of the United States of America.* 116 (13). pp. 6260-6269.

Storici, F. & Tichon, A.E. 2017. RNA takes over control of DNA break repair. *Nature cell biology.* 19 (12). pp. 1382-1384.

Sullivan, B.A. 2020. De Novo Centromere Formation: One's Company, Two's a Crowd. *Developmental cell.* 52 (3). pp. 257-258.

Suseendranathan, K., Sengupta, K., Rikhy, R., D'Souzaa, J.S., Kokkanti, M., Kolkarni, M.G., Kamdar, R., Changede, R., Sinha, R. & Subramanian, L. 2007. Expression pattern of Drosophila translin and behavioral analyses of the mutant. *European Journal of Cell Biology.* 86 (3). pp. 173-186.

Suwaki, N., Klare, K. & Tarsounas, M. 2011. RAD51 paralogs: roles in DNA damage signalling, recombinational repair and tumorigenesis. *Seminars in Cell & Developmental Biology.* 22 (8). pp. 898-905.

Symington, L.S. & Gautier, J. 2011. Double-strand break end resection and repair pathway choice. *Annual Review of Genetics.* 45 pp. 247-271

Szankasi, P. and Smith, G.R. 1995.A role for exonuclease I from S. pombe in mutation avoidance and mismatch correction. *Science*. 267{5201), pp.1166-1169.

Tadeo, X., Wang, J., Kallgren, S.P., Liu, J., Reddy, B.D., Qiao, F. & Jia, S. 2013. Elimination of shelterin components bypasses RNAi for pericentric heterochromatin assembly. *Genes & Development.* 27 (22). pp. 2489-2499.

Tadi, S.K., Tellier-Lebegue, C., Nemoz, C., Drevet, P., Audebert, S., Roy, S., Meek, K., Charbonnier, J.B. & Modesti, M. 2016. PAXX Is an Accessory c-NHEJ Factor that Associates with Ku70 and Has Overlapping Functions with XLF. *Cell reports.* 17 (2). pp. 541-555.

Takagi, M. 2017a. DNA damage response and hematological malignancy. *International journal of hematology,* 106 (3), pp. 345-356.

Talbert, P.B. and Henikoff, S. 2020.What makes a centromere? *Experimental Cell Research*.389(2). pp.111895.

Teloni, F., Michellena, J., Lezaja, A., Kilic, S., Ambrosi, C., Menon, S., Dobrovolna, J., Imhof, R., Janscak, P., Baubec, T., and Altmeyer, M. (2019) Efficient pre-mRNA cleavage prevents replication-stress-associated genome instability. Mol. Cell *73*, pp. 670-683.

Thakur, J. and Henikoff, S. 2016.CENPT bridges adjacent CENPA nucleosomes on young human α-satellite dimmers. *Genome Research*. 26.pp. 1178-1187.

Thon, G., Maki, T., Haber, J.E. & Iwasaki, H. 2019. Mating-type switching by homology-directed recombinational repair: a matter of choice. *Current genetics.* 65 (2). pp. 351-362.

Tian, H., Gao, Z., Li, H., Zhang, B., Wang, G., Zhang, Q., Pei, D. & Zheng, J. 2015. DNA damage response--a double-edged sword in cancer prevention and cancer therapy. *Cancer Letters.* 358 (1). pp. 8-

Timsina, R. and Qiu, X. 2019.Histone Tail-DNA Interactions: Charge Regulation and Sequence Specificity. *Biophysical Journal*, Vol. 116, pp. 73a.

Tirado, O.M. 2019.Targeting fusion proteins: a double edge sword?. *Expert Opinion on Therapeutic Targets*.23(8).pp.651-654.

Tolsma, T.O. and Hansen, J.C. 2019.Post-translational modifications and chromatin dynamics. *Essays in Biochemistry*, Vol. 63 No. 1, pp. 89–96.

Toomey, E.C., Schiffman, J.D. and Lessnick, S.L. 2010.Recent advances in the molecular pathogenesis of Ewing's sarcoma. *Oncogene*. (29). pp.4504–4516.

Toubiana, S. and Selig, S. 2018. DNA: RNA hybrids at telomeres – when it is better to be out of the (R) loop. *FEBS Journal* 285(14), pp.2552-2566.

Tran, P.L.T., Pohl, T.J., Chen, C.F., Chan, A., Pott, S. and Zakian, V.A. 2017.PIF1 family DNA helicases suppress R-loop mediated genome instability at tRNA genes. *Nature Communications*. (8). pp. 15025.

Tsukiashi, M., Baba, M., Kojima, K., Himeda, K., Takita, T. and Yasukawa, K. 2019. Construction and characterization of ribonuclease H2 knockout NIH3T3 cells. *The Journal of Biochemistry*, Oxford University Press, Vol. 165 No. 3, pp. 249–256.

Uckelmann, M. and Sixma, T.K., 2017. Histone ubiquitination in the DNA damageresponse. *DNA repair*, *56*, pp.92-101.

Udroiu, I. & Sgura, A. 2019. Alternative Lengthening of Telomeres and Chromatin Status. *Genes.* 11 (1). pp. 10.3390/genes11010045.

Ursic D, Chinchilla K, Finkel JS, Culbertson MR. Multiple protein/protein and protein/RNA interactions suggest roles for yeast DNA/RNA helicase Sen1p in transcription, transcription-coupled DNA repair and RNA processing. Nucleic Acids Res 32(8), pp.2441-52.

Ursic D, Himmel KL, Gurley KA, Webb F, Culbertson MR (1997) The yeast SEN1 gene is required for the processing of diverse RNA classes. *Nucleic Acids Res* 25, pp 4778–4785.

Vancevska, A., Douglass, K.M., Pfeiffer, V., Manley, S. and Lingner, J. 2017.The telomeric DNA damage response occurs in the absence of chromatin decompaction.*Genes & development, 31*(6), pp. 567-577.

Vanoosthuyse, V. 2018. Strengths and weaknesses of the current strategies to map and characterize R-loops. *Non-coding RNA* 4(2), *pp.9.*

Vargas-Rondon, N., Villegas, V.E. & Rondon-Lagos, M. 2017. The Role of Chromosomal Instability in Cancer and Therapeutic Responses. *Cancers.* 10 (1). pp. 10.3390/cancers10010004.

Verdel, A. & Moazed, D. 2005. RNAi-directed assembly of heterochromatin in fission yeast. *FEBS letters.* 579 (26). pp. 5872-5878.

Wahba, L., Gore, S.K. & Koshland, D. 2013. The homologous recombination machinery modulates the formation of RNA-DNA hybrids and associated chromosome instability. *eLife.* 2 pp. e00505.

Wang, C. et al. 2015. Role of TERRA in the regulation of telomere length. *International Journal of Biological Sciences* 11(3), pp.316-323.

Wang, J., Cohen, A.L., Letian, A., Tadeo, X., Moresco, J.J., Liu, J., Yates, J.R.,3rd, Qiao, F. & Jia, S. 2016a. The proper connection between shelterin components is required for telomeric heterochromatin assembly. *Genes & Development.* 30 (7). pp. 827-839.

Wang, J.Y., Chen, S.Y., Sun, C.N., Chien, T. & Chern, Y. 2016a. A central role of TRAX in the ATM-mediated DNA repair. *Oncogene,* 35 (13), pp. 1657.

Wang, Y. and Chen, Z. 2020.Mutation detection and molecular targeted tumor therapies. *STEMedicine*, Vol. 1 No. 1, pp. e11.

Waterman, D.P., Haber, J.E. & Smolka, M.B. 2020. Checkpoint Responses to DNA Double-Strand Breaks. *Annual Review of Biochemistry.* 89 pp. 103-133.

Wells, J.P., White, J., and Stirling, P.C. (2019) R loops and their composite cancer connections.

Trends Cancer *5*, pp.619-631.

Westhorpe, F.G. & Straight, A.F. 2014. The centromere: epigenetic control of chromosome segregation during mitosis. *Cold Spring Harbor Perspectives in Biology.* 7 (1). pp. a015818.

Wild, P., Susperregui, A., Piazza, I., Dorig, C., Oke, A., Arter, M., Yamaguchi, M., Hilditch, A.T., Vuina, K., Chan, K.C., Gromova, T., Haber, J.E., Fung, J.C., Picotti, P. & Matos, J. 2019. Network Rewiring of Homologous Recombination Enzymes during Mitotic Proliferation and Meiosis. *Molecular cell.* 75 (4). pp. 859-874.e4.

Williams, J.S. et al. 2016. Processing ribonucleotides incorporated during eukaryotic DNA replication. *Nature Reviews Molecular Cell Biology*. 17, pp.350–363.

Wong, R.P., Garcia-Rodriguez, N., Zilio, N., Hanulova, M. & Ulrich, H.D. 2020. Processing of DNA Polymerase-Blocking Lesions during Genome Replication Is Spatially and Temporally Segregated from Replication Forks. *Molecular cell.* 77 (1). pp. 3-16.e4.

Wood, V., Gwilliam, R., Rajandream, M., Lyne, M., Lyne, R., Stewart, A., Sgouros, J., Peat, N., Hayles, J. & Baker, S. 2002. The genome sequence of *Schizosaccharomyces pombe*. *Nature.* 415 (6874). pp. 871-880.

Wu, W. et al. 2020. The prevention and resolution of DNA replication–transcription conflicts in eukaryotic cells. *Genome Instability & Disease* 1, pp.114-128.

Wu, X., Gu, W., Meng, X. & Hecht, N.B. 1997. The RNA-binding protein, TB-RBP, is the mouse homologue of translin, a recombination protein associated with chromosomal translocations. *Proceedings of the National Academy of Sciences,* 94 (11), pp. 5640-5645.

Wyatt, H.D.M. and West, S.C. 2014.Holliday junction resolvases. *Cold Spring Harbor Perspectives in Biology*.12(10).

Yamada-Inagawa, T., Klar, A.J. & Dalgaard, J.Z. 2007. Schizosaccharomyces pombe switches mating type by the synthesis-dependent strand-annealing mechanism. *Genetics.* 177 (1). pp. 255-265.

Yang S, Cho YS, Chennathukuzhi VM, Underkoffler LA, Loomes K, Hecht NB. Translin-associated factor X is post-transcriptionally regulated by its partner protein TB-RBP, and both are essential for normal cell proliferation. J Biol Chem 26;279(13), pp.12605-14.

Yang, J. et al. 2018. Heterochromatin and RNAi regulate centromeres by protecting CENP-A from ubiquitin-mediated degradation. *PLoS Genetics*.

Yang, S. and Hecht, N.B. 2004. Translin associated protein X is essential for cellular proliferation. *FEBS Letters* 576(2), pp.221-225.

Yasuhara, T., Kato, R., Hagiwara, Y., Shiotani, B., Yamauchi, M., Nakada, S., Shibata, A. & Miyagawa, K. 2018. Human Rad52 Promotes XPG-Mediated R-loop Processing to Initiate Transcription-Associated Homologous Recombination Repair. *Cell.* 175 (2). pp. 558-570.e11.

Yavuzer, U., Smith, G.C., Bliss, T., Werner, D. & Jackson, S.P. 1998. DNA end-independent activation of DNA-PK mediated via association with the DNA-binding protein C1D. *Genes & development.* 12 (14). pp. 2188-2199.

Ye, X., Huang, N., Liu, Y., Paroo, Z., Huerta, C., Li, P., Chen, S., Liu, Q. & Zhang, H. 2011. Structure of C3PO and mechanism of human RISC activation. *Nature Structural & Molecular Biology.* 18 (6). pp. 650-657.

Yi, K. & Ju, Y.S. 2018. Patterns and mechanisms of structural variations in human cancer. *Experimental & molecular medicine.* 50 (8). pp. 98-018-0112-3.

Yu Y, Ren J-Y, Zhang J-M, Suo F, Fang X-F, Wu F, Du L-L (2013) A proteome-wide visual screen identifies fission yeast proteins localizing to DNA double-strand breaks. *DNA Repair* 12, pp 433–443.

Yüce-Petronczki, O. and West, S.C. 2013. Senataxin, defective in the neurogenerative disorder AOA-2, lies at the interface of transcription and the DNA damage response. *Molecular and cellular biology 33(2), pp.406*- 17.

Zaboikin, M., Zaboikina, T., Freter, C. & Srinivasakumar, N. 2017. Non-Homologous End Joining and Homology Directed DNA Repair Frequency of Double-Stranded Breaks Introduced by Genome Editing Reagents. *PloS One.* 12 (1). pp. e0169931.

Zhang, J., Liu, H., Yao, Q., Yu, X., Chen, Y., Cui, R., Wu, B., Zheng, L., Zuo, J. & Huang, Z. 2016. Structural basis for single-stranded RNA recognition and cleavage by C3PO. *Nucleic acids research,* 44 (19), pp. 9494-9504.

Zhang, Y., Gostissa, M., Hildebrand, D.G., Becker, M.S., Boboila, C., Chiarle, R., Lewis, S. & Alt, F.W. 2010. The role of mechanistic factors in promoting chromosomal translocations found in lymphoid and other cancers. In: Anon*Advances in immunology.* Elsevier. pp. 93-133.

Zhao, H. et al. 2018. RNase H eliminates R-loops that disrupt DNA replication but is nonessential for efficient DSB repair. *EMBO reports* 19(5), pp. e45335.

Zhao, W., Wiese, C., Kwon, Y., Hromas, R. & Sung, P. 2019. The BRCA Tumor Suppressor Network in Chromosome Damage Repair by Homologous Recombination. *Annual Review of Biochemistry.* 88 pp. 221-245.

Zhou, R., Yang, O., Declais, A.C., Jin, H., Gwon, G.H., Freeman, A.D.J., Cho, Y., Lilley, D.M.J. & Ha, T. 2019. Junction resolving enzymes use multivalency to keep the Holliday junction dynamic. *Nature chemical biology.* 15 (3). pp. 269-275.

Zimmer, A.D. and Koshland, D. 2016. Differential roles of the RNases H in preventing chromosome instability. *Proceedings of the National Academy of Sciences of the United States of America* 113(43), pp.12220-12225.

Zocco, M., Marasovic, M., Pisacane, P., Bilokapic, S. & Halic, M. 2016. The Chp1 chromodomain binds the H3K9me tail and the nucleosome core to assemble heterochromatin. *Cell discovery,* 2 pp. 16004.

# 9. Appendices

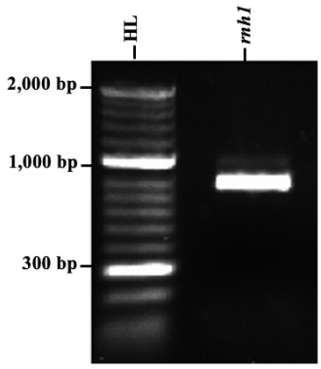


**Appendices 1: PCR amplification of *rnh1*.**

The entire length of the *rnh1* gene's open reading frame was amplified utilising RT-PCR. This was then imaged with peqGREEN DNA dye on a 1.0% agarose gel base. The band displays the anticipated estimated size of the *rnh1* open reading frame at 980 bp. HL includes 5 µl of Hyper Ladder 50 Kb**.**

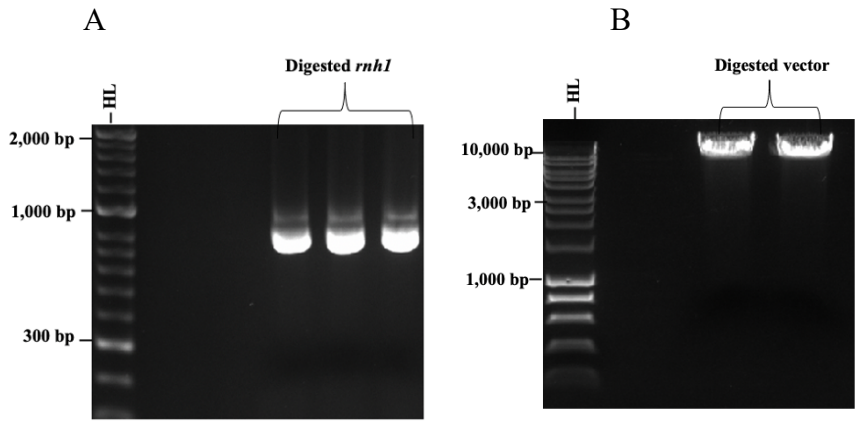


**Appendices 2: The Digestion and purification of *rnh1* and *pREP3X* plasmid.**

**A**. The dissected *rnh1 gene,* following digestion with the restriction enzymes, *Xhol and Bam*HI, was imaged on 1% agarose gel, and subsequently purified. Equivalent quantities of digested *rnh1* were split into 3 lanes. **B.** Following *Xhol and Bam*HI digestion, the linearised plasmid was imaged on 1% agarose gel, and subsequently purified. The HL lane included 5 µl of Hyper Ladder 50 and 1 Kb.

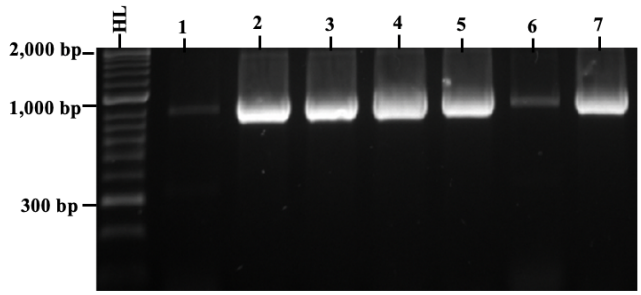


**Appendices 3: A PCR colony screen of the produced *E. coli* colony after the transformation process was completed.**

PCR screening data for transformed colonies of *E. Coli* depicted on agarose gel in order to identify recombinant plasmids using *rnh1* gene cloning primers. Numerous colonies, which had been transformed by the recombinant *pREP3X-rnh1* plasmid, demonstrated the insert. A single colony, i.e., colony number 2, was selected for further affirmation. The HL lane included 5 µl of Hyper Ladder 50 kb.

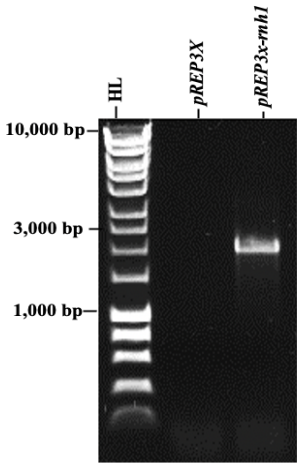


**Appendices 4: Confirmation of *rnh1* transformation into *pREP3X* by PCR screening**

The selected colony underwent RT-PCR, utilising the nmt Forward and the rnh1 cloning reverse primers, in order to check for the success of *rnh1* transformation into *pREP3X*. The first lane acted as a negative control which include the vector only; the second shows the anticipated size, 2043 bp, of the successful *rnh1* transformation. The HL lane includes 5 µl of Hyper Ladder 50 kb.

**Appendices 5: Draft manuscript**

**Translin prevents recombinogenic DNA replication-transcription conflicts during Dicer deficiency by limiting RNA polymerase II template association**

Natalia Gomez-Escobar[1], Ahad A.A. Alsaiari[1, †], Hanadi A.S. Alahamadi[1, †], Othman Alzahrani[1, †], Ellen Vernon[1], Hussam A.E. Althagafi[1,], Nasser S Almobadel[1], David W. Pryce[1], Jane A. Wakeman[1], Ramsay J. McFarlane[1,*]

1 – North West Cancer Research Institute, School of Medical Sciences, Bangor University, Brambell Building, Deiniol Road, Bangor, Gwynedd, LL57 2UW, United Kingdom.

* - Correspondence: r.macfarlane@bangor.ac.uk; Tel: +44 1248 382360; Fax: +44 1248 370731.

† -These authors contributed equally to this work.

**Summary**

The conserved nucleic acid binding protein Translin contributes to numerous facets of mammalian biology and genetic diseases and was first identified as a binder of cancer-associated chromosomal translocation breakpoint junctions. With a paralogous partner protein, Trax, Translin forms a hetero-octomeric RNase complex that drives some of its functions, including passenger strand removal in RNA interference (RNAi). The Translin-Trax complex also degrades the precursors to tumour suppressing microRNAs in cancers deficient for the RNase III Dicer. This oncogenic activity has resulted in the Translin-Trax complex being explored as a therapeutic target. Here we reveal a Trax- and RNAi-independent function for Translin in genome stability maintenance during Dicer-deficiency that serves to suppress DNA replication-associated recombination, a process mediated by dissociating RNA polymerase II from its genomic template. This addresses the longstanding question of how Translin influences chromosomal rearrangements in human genetic diseases and provides important functional understanding of an oncological therapeutic target.

Words: 150

## Introduction

DNA replicative stress arising from transcription-replication conflicts (TRCs) can result in genomic structural changes, including chromosomal translocations, drivers of evolution and genetic diseases (Achar and Foiani, 2017; Kotsantis et al., 2018; Gómez-González and Aguilera, 2019). Translin is a conserved nucleic acid binding protein first identified in humans by its binding to malignant disease associated chromosomal translocation breakpoint junctions (Aoki et al., 1995). Subsequently, it was found to form a hetero-octamer (also known as C3PO) with a paralogous protein, Translin-associated factor X (Trax) (Jaendling and McFarlane, 2010; Gupta et al., 2019). Translin and the Translin-Trax (Tn-Tx) complex can bind to both RNA and DNA, and the Tn-Tx complex possesses endoribonuclease activity, which facilitates passenger strand removal from small interfering RNAs during RNA interference (RNAi) in higher eukaryotes and can process other RNAs, including tRNA precursors (Liu et al., 2009; Ye et al., 2011; Tian et al., 2011; Li et al., 2012; Baraban et al., 2018). Translin and Trax (individually or in a Tn-Tx complex) are implicated in an array of biological processes, many of which influence human neurological function and disease, including cancer (Li et al., 2008; Jaendling and McFarlane, 2010; McFarlane and Wakeman, 2020).

Not all the functions of Translin and Trax require endoribonuclease activity; however, the RNase activity causes premature degradation of precursor-miRNAs (pre-miRNAs) of tumour suppressor miRNAs in cancers that have insufficiency in the RNase III Dicer, which, when at normal levels processes pre-miRNA to mature tumour suppressing miRNAs. Inhibition of Tn-Tx in Dicer-limited cancer cells permits the residual Dicer to re-establish appropriate maturation of pre-miRNAs (Asada et al., 2014). Indeed, small molecule inhibitors of Tn-Tx RNase activity have been developed that enable pre-miRNA maturation by Dicer, demonstrating the therapeutic potential of targeting Tn-Tx in Dicer-limited cancers (Asada et al., 2016).

The function of Translin in other processes also indicates that regulating its activity might be of clinical utility, for example, deletion of *Tsn* (Translin gene) in mice reduces hypertension-related vascular stiffening by maintaining levels of a regulatory miRNA (Tuday et al., 2019). Therapeutically targeting a specific function of a complex whose constituent parts, together or individually, act in a diverse range of processes requires an understanding of all functional roles to ensure disease-specific targeting. For example, murine Translin is also implicated in

survival of T cells required for immunological tumour suppression, so oncological therapeutic targeting needs to avoid such beneficial activities (Geiger et al., 2016).

The original finding that Translin can bind to chromosomal break point junctions in diseases resulted in the postulate that Translin functions in genetic recombination (Aoki et al., 1995; Kasai et al., 1997). To date, there is only limited evidence to support this. For example, Translin-deficient mice exhibit delayed proliferation in haemopoietic stem cells following ionizing irradiation (Fukuda et al., 2008), Translin migrates to the nucleus following DNA damage (Fukuda et al., 2008), Translin interacts with the DNA damage-inducible GADD34 (Hasegawa and Isobe, 1999) and recently Translin has been shown to specifically bind to short open reading frame-encoded peptides following UV irradiation (Koh et al., 2021). Trax, however, has a direct, Translin-independent mechanistic role as a scaffold protein in the DNA double-strand break (DSB) repair pathway by assisting the ATM kinase to establish an appropriate DNA damage response (Wang et al., 2016).

Here we use the RNAi-proficient model, *Schizosaccharomyces pombe*, to reveal a function for Translin (Tsn1) in maintaining genome stability and DNA replication stress tolerance in the absence of Dicer (Dcr1) and demonstrate it does so by recombination suppression mediated via a TRC avoidance mechanism. We show that this function is conserved in human Translin (TSN), revealing the first mechanistic link between Translin and disease-associated chromosomal recombination.

## Results

### *Tsn1 (Translin), but not Tfx1 (Trax), is required to maintain genome stability in Dcr1 deficiency*

Evidence for a direct role for Translin in genome stability maintenance is limited. *S. pombe* null mutants of either *tsn1*$^+$ or *tfx1*$^+$ exhibit no overt genome instability phenotype (Jaendling et al., 2008). The link between Tn-Tx (C3PO) and RNAi in higher eukaryotes led us to explore whether there is a functional relationship between Tsn1 and/or Tfx1 and RNAi components Dcr1 and Ago1 in *S. pombe*. We recently noted that the sensitivity of the RNAi defective *ago1*Δ mutant to the microtubule destabilizing drug TBZ could be partially suppressed by mutating *tfx1*$^+$, but not *tsn1*$^+$, which was attributed to loss of a telomere-associated function of Tfx1 (Gomez-Escobar et al., 2016). However, similar suppression is not observed for *ago1*Δ *tfx1*Δ double mutants exposed to the DNA replication inhibitor hydroxy urea (HU) (Figure 1A). Additionally, mutating *tsn1*$^+$ or *tfx1*$^+$ in the *ago1*Δ background does not increase HU sensitivity (Figure 1A), indicating there is no overt genetic interaction between *tsn1*$^+$ or *tfx1*$^+$ and the canonical RNAi pathway for replicative stress response.

Dcr1 has an RNAi-independent function in genome stability (Zaratiegui et al., 2011; Castel et al., 2014; Ren et al., 2015). Given this we tested *dcr1*Δ *tsn1*Δ and *dcr1*Δ *tfx1*Δ strains to assess potential genetic interaction between *dcr1*$^+$ and either *tsn1*$^+$ or *tfx1*$^+$ for replicative stress response. Exposure of the *dcr1*Δ *tsn1*Δ double mutant to HU revealed that loss of *tsn1*$^+$ in a *dcr1*Δ background increases sensitivity relative to the *dcr1*Δ mutant, indicative of a requirement for Tsn1 in Dcr1 deficiency (Figure 1B; increased sensitivity is suppressible by over expression of both *tsn1*$^+$ and *dcr1*$^+$, Figure S1A). There is no similar requirement for Tfx1 (Figure 1B), indicating this function of Tsn1 is not mediated by a Tn-Tx complex. We extended this by testing another DNA replication inhibitor, mitomycin C. No sensitivity was observed for any mutants (Figure 1B), indicating that Tsn1 and Dcr1 only regulate the response to specific replicative stresses.

To determine whether Tsn1 functions to maintain genome stability in the absence of externally induced replicative stress, we measured the instability of a mini, non-essential chromosome III derivative (Ch$^{16\text{-}23R}$; Niwa et al., 1986; 1989). *tsn1*Δ and *tfx1*Δ mutants both exhibit loss rates indistinguishable from the wild-type, but loss rates are elevated in the *dcr1*Δ mutant (Figure

1C). The *dcr1*Δ *tfx1*Δ strain loss rates are indistinguishable from the *dcr1*Δ mutant, whereas the *dcr1*Δ *tsn1*Δ double mutant exhibited a loss rate considerably higher than the *dcr1*Δ single mutant, indicating that without external insult Tsn1 is required to maintain genome stability in Dcr1 deficiency (Figure 1C).

***Tsn1 and Dcr1 are functionally redundant with RNase H2 (Rnh201)***

Dcr1 acts in an RNase-independent fashion to protect genome stability by removing RNA polymerase II (RPII) from the DNA template to avoid TRCs (Castel et al., 2014). In the absence of Dcr1 RPII retention is associated with elevated RNA:DNA hybrids (R-loops). Unprocessed R-loops can present a challenge to genome stability by perturbing replicative progression (Crossley et al., 2019; García-Muse and Aguilera, 2019; Wells et al., 2019; Brambati et al., 2020; Hegazy et al., 2020; Niehrs and Luke, 2020; Rinaldi et al., 2021). However, R-loops can also serve a positive function in DSB repair, during which RPII and/or RNA Polymerase III (RPIII) synthesize transcripts, including so called damage-induced long non-coding RNAs (dilncRNAs), at DSB sites to actively contribute to the hierarchical phase regulated repair structures (Michelini et al., 2017; Lui et al., 2021; Pessina et al., 2021). In all cases, R-loops must ultimately be removed to maintain genome integrity, and this is largely mediated by RNase H proteins (Hyjek et al., 2019). In most eukaryotes there are two conserved and redundant RNase H activities, RNase H1 (Rnh1 in *S. pombe*) and RNase H2 (a heterotrimeric complex containing Rnh201 in *S. pombe*). In humans both RNase H activities are essential, although H2 is thought to be the predominant activity (Feng and Cao, 2016). In *S. pombe* loss of both RNase H pathways results in loss of viability in response to replicative stress (Ohle et al., 2016; Zhao et al., 2018). Whilst the two RNase H activities are largely redundant, the *S. pombe rnh201*Δ single mutant exhibits sensitivity to HU, but only under logarithmic growth conditions (Zhao et al., 2018; Figure S2), possibly because Rnh201, but not Rnh1, is also required to remove mis-incorporated monoribonucleotides from DNA (Hyjek et al., 2019).

In higher eukaryotes the Tn-Tx complex (C3PO) has RNase activity, which is ascribed to Trax (Liu et al., 2009), although mammalian Translin also has RNase activity (Wang et al., 2004). This ribonuclease capability, in combination with the finding that Tsn1 is required for maintaining genome stability in the absence of Dcr1, loss of which results in R-loop accumulation, led us to explore the relationship between Tsn1, Tfx1 and Dcr1 and the two RNase H pathways. We firstly constructed double mutants of both *tsn1*$^{+}$ and *tfx1*$^{+}$ with null

mutants of both core RNase H (1 and 2) encoding genes, *rnh1*$^+$ and *rnh201*$^+$. The *rnh1*Δ *tfx1*Δ and *rnh201*Δ *tfx1*Δ double mutants exhibited no increased sensitivity to HU (Figure 2A). However, the *rnh201*Δ *tsn1*Δ double mutant, but not the *rnh1*Δ *tsn1*Δ double mutant, exhibited considerable HU sensitivity (Figure 2B), indicating that Tsn1 is functionally redundant with Rnh201.

RNase H2 can process R-loops and *Saccharomyces cerevisiae* RNase H1 and H2 appear to have distinct roles in R-loop processing (Zimmer and Koshland, 2016; Lockhart et al., 2019), whilst in humans RNase H2 provides the predominant activity (Feng and Cao, 2016). However, unlike RNase H1, RNase H2 has distinct, non-RNase H functions, such as the ability to remove mis-incorporated ribonucleotides (Hyjek et al., 2019). Based on our data (above) and the known roles for RNase H2, we hypothesized two possibilities for Tsn1. Firstly, it facilitates RNase H1-mediated R-loop removal. Secondly, it could function redundantly with Rnh201 in mis-incorporated ribonucleotide removal. To test the first possibility, we overexpressed the RNase H1 gene, *rnh1*$^+$, under a thiamine repressible promoter (*nmt*) plasmid in the *rnh201*Δ *tsn1*Δ double mutant, to assess whether the inability to cope with the replicative stress could be suppressed by elevated levels of R-loop processing RNase H activity. Over expression of *rnh1*$^+$ (no thiamine) did not alleviate the inability of the *rnh201*Δ *tsn1*Δ double mutant to tolerate HU, but did suppress the HU sensitivity of the *rnh1*Δ *rnh201*Δ double mutant back to *rnh201*Δ single mutant levels (Figure 2C). As mammalian Translin has RNase activity (the RNJase domain is conserved in *S. pombe*), and Tsn1 can bind to dsRNA (Wang et al., 2004; Liu et al., 2009; Eliahoo et al., 2010; Ye et al., 2011; Parizotto et al., 2013), we also over expressed the dsRNA-specific RNase encoding gene, *pac1*$^+$, but this also failed to suppress the HU sensitivity of the double mutant (Figure 2C). Together these data suggest that Tsn1 is not functioning via a dsRNase/RNase H activity.

To test the second possibility, that Tsn1 might function in a secondary pathway for mis-incorporated ribonucleotide removal, we assessed ribonucleotide levels in genomic DNA in distinct mutants using alkali gel electrophoresis; ribonucleotides in DNA are labile under alkali gel conditions, resulting in quantifiable loss of chromosomal DNA intensity on an alkali gel verses a neutral gel. Chromosomal DNA from null mutants of *rnh201*$^+$ exhibited elevated alkali-dependent degradation (Figure 2D). However, mutation of *tsn1*$^+$, alone or in a *rnh201*Δ

background, did not increase alkali-dependent sensitivity, indicating there is no discernable increase in chromosomal ribonucleotides in response to *tsn1*$^{+}$ loss (Figure 2D).

In *S. cerevisiae* over production of Rnh201 alone can suppress defects caused by the loss of Rat1, a 5' to 3' RNA exonuclease, indicting Rnh201 can suppress other RNA processing activities (Luke et al., 2008). To determine if Tsn1 functions redundantly for processing another undetermined Rnh201 substrate, we over expressed *rnh201*$^{+}$ in the *dcr1Δ tsn1Δ* mutant to assess whether Rnh201 over production could suppress HU sensitivity. This was not the case (Figure S1B), indicating that there is no biochemical mechanistic overlap between Rnh201 and Tsn1. Together, these findings indicate that Tsn1 does not function either as a ribonuclease (dsRNAs or RNase H), nor in the excision of mis-incorporated ribonucleotides.

That the *rnh201*Δ *tsn1*Δ strain HU sensitivity could not be suppressed by over production of RNase H1 indicates replicative stress intolerance due to loss of Tsn1 is not due to elevated R-loops that cannot be tolerated. However, *dcr1*Δ mutants do accumulate R-loops (Castel et al., 2014). To further explore the possibility that the role of Tsn1 in the *dcr1*Δ background could be to remove R-loops, we also over expressed *rnh1*$^{+}$ in the *dcr1*Δ *tsn1Δ* strain. This also failed to rescue the HU sensitivity (Figure 2E), indicating that unprocessed R-loops are not causing the replicative stress sensitivity. As Dcr1 has dsRNA specific RNase activity, we also over expressed the *pac1*$^{+}$ ribonuclease gene in the *dcr1*Δ *tsn1*Δ double mutant, but this too failed to suppress the HU sensitivity (Figure 2E). Interestingly, over expression of *rnh1*$^{+}$ (or *pac1*$^{+}$) also failed to rescue the HU sensitivity of the *dcr1*Δ single mutant in which R-loops accumulate (Figure S1C). Together these findings indicate replicative stress sensitivity is not caused by accumulation of R-loops or dsRNA, consistent with proposal that Dcr1 functions to maintain genome stability by an RNase-independent RPII template displacement mechanism (Castel et al., 2014).

Extending this, we used DNA:RNA-immunoprecipitation (DRIP) to directly measure R-loops at the rDNA locus and a tDNA gene, both of which accumulate R-loops in *dcr1*Δ cells (Castel et al., 2014). As expected, we observed increased R-loops at both loci in the *dcr1*Δ mutant (Figure 2F and Figure S3). However, surprisingly, R-loop levels were increased to the levels observed in the *dcr1*Δ mutant in both the *tsn1*Δ and *tfx1*Δ single mutants (Figure 2F and Figure S3), indicating both genes are required for suppressing R-loops, at least at these two loci. The

*dcr1*Δ *tsn1*Δ and *dcr1*Δ *tfx1*Δ double mutants did not show an increase in R-loops relative to the respective single mutants (Figure 2F and Figure S3). These data appear to demonstrate there is no correlation between R-loop levels and sensitivity to replicative stress, so R-loops alone are not sufficient to cause deleterious genome instability or a failure to cope with replicative stress in these mutants, supporting the data obtained from over expressing *rnh1*$^{+}$.

The genetic data suggest that *tsn1*$^{+}$ and *rnh201*$^{+}$ operate in redundant pathways. Moreover, *tsn1*$^{+}$ and *dcr1*$^{+}$ also contribute to distinct pathways. Together with the fact that Rnh1 and Rnh201 function in distinct pathways, one interpretation of our findings is that Tsn1 functions in a pathway with Rnh1 (although *rnh1*$^{+}$ overexpression does not support this being RNase H mediated), and so this led us to postulate that Dcr1 functions in a Rnh201-depedent pathway (i.e. Tsn1/Rnh1 function in one pathway and Dcr1/Rnh201 function in another, both pathways being redundant). This hypothesis predicts that the *dcr1*Δ *rnh1*Δ strain will be hypersensitive to HU and the *dcr1*Δ *rnh201*Δ strain will not be. We constructed the appropriate mutants and found that this hypothesis does not hold. Indeed, the *dcr1*Δ *rnh201*Δ double mutant was exquisitely sensitive to HU and the *dcr1*Δ *rnh1*Δ exhibited HU sensitivity similar to the *dcr1*Δ single mutant (Figure 2G). Together, these data indicate that Tsn1 and Dcr1 function redundantly with Rnh201 and with one another.

***Tsn1 functions to tolerate replicative stress independently of telomeres***

Loss of Tsn1 function results in elevated levels of telomeric transcripts termed TERRAs, which are associated with DNA damage tolerance (Gomez-Escobar et al., 2016). It is plausible that the requirement for Tsn1 in replicative stress tolerance is via TERRA regulation. To test this, we examined viable strains of *S. pombe* that lack telomeres, so called HAATI$^{STE}$ cells, that have linear telomere sequences replaced with stretches of subtelomeric elements (STEs; Figure 3A) (Jain et al., 2010). To check the need for Tsn1 in the telomere-free background we constructed *rnh1*Δ *tsn1*Δ and *rnh201*Δ *tsn1*Δ HAATI$^{STE}$ mutants (we did not use the *dcr1Δ* background as Dcr1 has a role in regulation of sub-telomeric regions). Similar to telomere-proficient cells, the HAATI$^{STE}$ *rnh201*Δ *tsn1*Δ double mutant exhibited considerable sensitivity to HU, comparable to the *rnh1*Δ *rnh201*Δ strain (Figure 3B). This demonstrates a requirement for Tsn1 in the absence of telomeres, indicating the function of Tsn1 is not associated with its

role in regulating TERRAs. As for the telomere proficient cells, HAATI$^{STE}$ strains exhibited no requirement for Tfx1 (Figure 3C).

Interestingly, the *rnh1*Δ *tsn1*Δ double mutant also exhibited a mild sensitivity to HU in this background, which is not observed in the telomere-proficient cells, but this was not as marked as the *rnh201*Δ *tsn1*Δ double mutant. Also, the *rnh201*Δ single mutant does not appear to exhibit the HU sensitivity observed in the telomere proficient strains. The meaning of these observations is currently unclear, but it suggests that without telomeres there are distinct requirements for the two RNase H pathways.

Further support for the role of Tsn1 in Dcr1 deficiency not being driven by elevated TERRAs comes from the unexpected finding that in telomere proficient cells mutation of *dcr1*$^{+}$ suppresses the elevated TERRA levels observed in the *tsn1*Δ mutant (Figure 3D). Whilst the biological relevance of this distinct Dcr1-Tsn1 relationship at telomeres remains unclear, it offers additional support to the idea that the role of Tsn1 in genome stability maintenance is independent of excessive TERRAs.

***Tsn1 is required to suppress TRC associated recombination***

The RNAi-independent function of Dcr1 mediates the removal of RPII from genomic regions, including tDNAs (Castel et al., 2014); the functional role of RPII at tDNAs is unknown, but R-loops, which could be generated by RPIII at tDNAs, serve as intrinsic RPII promoters (Tan-Wong et al., 2019). tDNAs can slow replicative progression and tDNA rich sites are overrepresented at sites of genomic rearrangements, including translocations (McFarlane and Whitehall, 2009; Guimarães et al., 2021). These factors led us to hypothesize that in the absence of Dcr1, Tsn1 is required to suppress recombination at loci which required Dcr1 to eject RPII, such as tDNAs.

To test this, we took advantage of the fact that tDNAs can be recombinogenic in *S. pombe* when recombination and replication systems are defective (Pryce et al., 2009; Steinacher et al., 2012; Jalan et al., 2019). We employed an established inter-molecular recombination assay, which involves a tDNA inserted into the genomic *ade6*$^{+}$ gene. In this case, *tRNA*$^{GLU}$ is inserted

into one of two orientations in distinct constructs (*tRNA$^{GLU}$* Ori1 and *tRNA$^{GLU}$* Ori2; Figure 4A). The *ade6$^{+}$* locus is predominantly replicated unidirectionally (Figure 4A) and the *ade6::tRNA$^{GLU}$* (Ori1 and Ori2) constructs serve as replicative pause sites, with neither orientation having greater pausing capacity than the other (Pryce et al., 2009). In the presence of an additional plasmid-borne mutant allele of *ade6$^{+}$*, *ade6-ΔG1483*, gene conversion via inter-molecular recombination can generate *ade6$^{+}$* cells, enabling recombination frequency to be measured via fluctuation analysis (*ade6$^{+}$* cells can be detected by plating cells on guanine containing media; Pryce et al., 2005) (Figure 4B).

For *tRNA$^{GLU}$* in the two orientations RPII and RPIII will transcribe in opposing orientations, presenting distinct head-to-head RNA polymerase challenges to the replisome. For Ori1, RPIII will be in a head-to-head configuration with the DNA replisome and in Ori 2 RPII will be in the head-to-head configuration (Figure 4A).

Mutants were constructed to assess inter-molecular recombination frequencies in the absence of *dcr1$^{+}$*, *tsn1$^{+}$* and *tfx1$^{+}$* for both orientations of *tRNA$^{GLU}$*. For Ori1 (RPIII in head-to-head conflict) none of the mutants exhibited difference in recombination frequency relative to the wild-type (Figure 4C). However, for Ori2 (RPII in head-to-head conflict) loss of *dcr1$^{+}$* results in a significant elevation in recombination frequency greater than 2-fold relative to the wild-type, consistent with the prediction that Dcr1 is required for RPII displacement to prevent TRCs (Figure 4D). The *tsn1*Δ and *tfx1*Δ single mutants exhibit no elevation relative to the wild-type (despite elevated R-loops). The *dcr1*Δ *tfx1*Δ double mutant exhibited levels similar to the *dcr1*Δ single mutant, but the *dcr1*Δ *tsn1*Δ double mutant exhibited a statistically significant elevation relative to the *dcr1*Δ single mutant (Figure 4D). These data are consistent with the HU sensitivity pattern and they demonstrate that loss of Tsn1 in Dcr1 deficiency elevates recombination associated with a head-to-head RPII TRC, but not a RPIII TRC. This indicates that, replicative pauses *per se* do not require Tsn1 and/or Dcr1 function to suppress recombination, but those associated with RPII head-to-head TRCs do.

***Tsn1 functions via an RNase-independent mechanism***

Dcr1 RNase activity is not required for its genome stability maintenance function (Castel et al., 2014). The RNase function of Tn-Tx in higher eukaryote RNAi passenger strand removal has been attributed to the Trax subunit, although mammalian Translin possesses ribonuclease

activity (Wang et al., 2004). However, over production of ribonucleases specific for R-loops (Rnh1) or RNA duplexes (Pac1) do not suppress the need for Tsn1 (above), suggesting the RNase activity of Tsn1 is not required (Figure 2C and 2E). Despite this, it remains a possibility that Tsn1 RNase activity is required and that the ribonucleases we have over produced (Rnh1/Pac1) do not target the same substrates, so cannot suppress the need for Tsn1. The Tsn1 RNase domain is within the 4$^{th}$ α helix, which is highly conserved within the Translin super family, including Trax orthologues (Figure S4) (Liu et al., 2009; Eliahoo et al., 2010; Ye et al., 2011; Parizotto et al., 2013). To explore whether Tsn1 function requires its RNase activity, we mutated the conserved glutamic acid within this domain (E152) to an alanine (E152A). Over expression of the wild-type *tsn1*$^{+}$ suppressed the loss of *tsn1*$^{+}$ (Figure 5A and 5B). Over expression of the *tsn1-E152A* catalytic mutant also fully reverted HU sensitivity to *dcr1*Δ levels, confirming that the Tsn1 function in genome stability maintenance, like that of Dcr1, does not appear to be mediated by its RNase activity (Figure 5A).

Our current and previous data demonstrate that *S. pombe* Tsn1 does not appear to function in a Tn-Tx-like complex, so we wanted to explore the functional overlap between the paralogous genes and so wild-type *tfx1*$^{+}$ was over expressed in the *dcr1*Δ *tsn1*Δ double mutant. It did not suppress the increased HU sensitivity caused by the loss of *tsn1*$^{+}$, confirming the functional independence of the paralogues (Figure S5).

***Tsn1 is required for RPII template displacement***

The loss of Tsn1 function elevates R-loops (above), but this does not appear to be directly linked to the cause of increased genome instability in the absences of Dcr1. Nor is the Tsn1 genome stability function dependent on RNase activity. The polar nature of recombination at a tDNA could suggest that Tsn1 functions in an auxiliary mechanism for template dissociation of RPII to prevent TRCs, the consequences which become exacerbated upon external replicative stress (e.g., HU). To test this, we assessed RPII occupancy using chromatin immunoprecipitation (ChIP) of RPII at loci previously demonstrated to require Dcr1 for RPII displacement, rDNA and tRNA loci (Castel et al., 2014). At both genomic elements, loss of *dcr1*$^{+}$ resulted in elevated RPII retention, consistent with the findings of Castel and co-workers (2014). Loss of *tsn1*$^{+}$ and *tfx1*$^{+}$ did not increase RPII occupancy (Figure 5C; Figure S6), despite loss of these two genes causing elevated R-loops (Figure 2F). However, when Tsn1 function is lost in the *dcr1*Δ background there is a significant rise in the levels of RPII retained on the

templated relative to the *dcr1*Δ mutant for both genomic regions (Figure 5C and Figure S6). This elevation is not observed when *tfx1*Δ is mutated in the *dcr1*Δ background (Figure 5C and Figure S6), indicating that Tsn1, but not Tfx1, functions to mediate an auxiliary RPII displacement mechanism in Dcr1 deficiency.

***Human TSN functions to mediate replicative stress tolerance***

Evolutionary conservation of Translin orthologue functions is evidenced by the fact that Tsn1 is required to maintain the stability of Tfx1 in *S. pombe* and mammals (Jaendling et al., 2008; Yang et al., 2004). However, there is no evidence for a Tn-Tx-like complex (C3PO) in *S. pombe* and Tsn1 and Tfx1 do not appear to be needed for centromeric heterochromatin formation, suggesting that they are not essential for canonical RNAi (Gomez-Escobar et al., 2016). This brings into question the relevance of this system for understanding human Translin (TSN) function. To directly address whether human TSN can function to maintain genome stability in response to replicative stress, we cloned the human *TSN* gene and over expressed it in the *dcr1*Δ *tsn1*Δ and *rnh201*Δ *tsn1*Δ double mutants. The expression of *TSN* suppressed the HU sensitivity of the double mutants to the same extent observed for *S. pombe tsn1*$^{+}$ (Figure 5B and 5D). Over expression of human *TSNAX* (Trax coding gene) did not suppress the HU sensitivity of the *dcr1*Δ *tsn1*Δ double mutant (Figure S7), so human TSN contributes to maintaining genome stability in a TSNAX-independent fashion, indicating functional independence of Translin for genome stability maintenance is apparent in humans. To confirm that this suppression was not due to the RNase activity of TSN (as is the case for *S. pombe* Tsn1), we mutated the conserved human TSN RNase catalytic residue to an alanine (E150A; Figure S4) and over expressed this allele (*TSN-E150A*) in the *dcr1*Δ *tsn1*Δ strain. This too could fully suppress the loss of *S. pombe tsn1*$^{+}$, indicating that the human TSN has a conserved TSNAX- and RNase-independent function in genome stability maintenance (Figure 5D).

**Discussion**

Since its discovery in humans as a chromosomal breakpoint junction binding protein (Aoki et al., 1995) and in mice as Testis-Brain RNA binding protein (Han et al., 1995; Wu et al., 1997), Translin has been implicated in a diverse range of fundamental biological processes, ranging from neurological regulation, including sleep and behavioural control (for example, see

Chiaruttini et al., 2009; Murakami et al., 2016; Park et al., 2017), through to oncogenic activity (Asada et al., 2014) and control of adiposity (Shah et al., 2020). In many cases, Translin operates in a heterocomplex with Trax, but independent functions are emerging. Moreover, Archaea only have one Translin/Trax paralogue, which is thought to be more similar to Trax, indicating the earliest function(s) to evolve were provided by one protein (Parizotto et al., 2013). The data presented here support previous findings that *S. pombe* Tsn1 and Tfx1 do not function together as a complex, despite a functional relationship in telomere transcript control (Gomez-Escobar et al., 2016), suggesting that C3PO-like activity has not evolved in lower eukaryotes, despite the Archaeal homocomplex having RNase activity. Here we demonstrate that a Trax-independent Translin function prevents genome instability in the absence of Dicer has been evolutionarily conserved from lower eukaryotes to humans.

Dicer deficiency is oncogenic in many cancers and is linked to poor prognosis (Kumar et al., 2009); moreover, a number of cancers carry mutations in *DICER1* (for example, see Vedanayagam et al., 2019). A primary tumour suppressing role of Dicer is to process miRNA precursors in the cytoplasm. However, evidence is emerging to indicate Dicer has nuclear function in response to DNA damage and replicative stress, which includes the processing of damage induced RNAs required for hierarchical DSB repair factor recruitment (Francia et al., 2012; Burger et al., 2017; Fragkos et al, 2019). These findings, added to the fact Dicer has RPII dissociation function, indicates the oncogenic nature of limited Dicer may extend beyond the loss of pre-miRNA maturation. Translin, in complex with Trax, shares pre-miRNA substrate capabilities with Dicer, but this is only oncogenic when Dicer is compromised (Asada et al., 2014). Here we now show that when Dicer is compromised, Translin, but not Trax, has additional functions, which could influence oncogenesis.

The mechanism by which Dcr1 removes RPII remains unclear, although it is independent of its RNase activity, which is also the case for Tsn1. Human Translin can compete for dilncRNAs with Dicer, but this function is likely to require the RNase activity (Michelini et al., 2017), so it is doubtful that this is directly linked to RPII displacement as this is RNase-independent. The function of Tsn1 is also unlikely to be indirect via regulation of other transcripts, as *tsn1*Δ mutants exhibit no transcript level changes relative to the wild-type, other than TERRAs (Gomez-Escobar et al., 2016), which we demonstrate are not essential for the replicative stress tolerance function of Tsn1.

It could be the case that the RPII displacement mechanism is mediated by a direct protein-protein association of either Dcr1 or Tsn1 with RPII (Figure 6A and 6B, respectively). In support of this, Trax does provide a nuclear scaffold role for ATM in the DNA damage response via direct interaction, and whilst this is Translin-independent it demonstrates the capacity for the Translin super family to directly interact with other non-paralogous proteins during the DNA damage response (Wang et al., 2016), something that has also been observed for Trax interaction with the NHEJ protein C1D (Erdemir et al., 2002). Additionally, Translin can interact with other proteins (see below), including the DNA repair factor GADD34 (Hasegawa and Isobe, 1999).

It is tempting to speculate that Translin, and Dicer, function to displace RPII via binding to one of the RNAs associated with RPII-TRC sites; this could be nascent single-stranded transcript (Figure 6C), double-stranded RNA structures generated by nascent transcript intra-molecular base pairing (Figure 6D) or by inter-molecular base pairing between nascent transcripts generated from opposing template DNA strands (Figure 6E). Whilst *S. pombe* Tsn1 appears to favour RNA binding, it does have DNA binding capability (Laufman et al., 2005) and single-stranded DNA generated at the transcriptional bubble or by the associated torsional stress could also be a substrate for Translin binding to target RPII displacement (Figure 6F). Notwithstanding this, it is not unreasonable to postulate that it is an RNA binding function of Translin that is require as this is consistent with its other known roles in RNA metabolism and mRNA binding, such as the direct binding to *BDNF* mRNA, where Translin binding defects can result in memory and psychiatric disorders (Chiaruttini et al. 2009).

Eliahoo and co-workers (2014) identified the *S. pombe* pre-mRNA splicing factor Srp1 as a putative Tsn1 binding partner. Efficient cleavage of pre-mRNAs is known to prevent genomic instability associated with DNA replication stress (Teloni et al., 2019) and introns protect genomes from replicative stress, indicating that some feature of spliceosome-associated processing is protective (Bonnet et al., 2017). However, we observed increased recombination associated with an RPII-TRCs that is associated with the production of a putative transcript that has no discernable intronic sequences (Figure 4A). It is known that some spliceosome components have non-canonical roles in genome stability maintenance (Tam and Stirling, 2019), so potentially Tsn1 functions in concert with the spliceosome-like Srp1 to act upon nascent transcripts in a splicing-independent fashion (Figure 6G). A role for

spliceosome/spliceosome-like function in *S. pombe* is further supported by the finding that the spliceosome-associated protein Nrl1 is involved in suppressing R-loop formation and homologous recombination (Aronica et al., 2015).

How might this connect Translin to chromosomal translocations? It has recently been demonstrated that cancer chromosomal translocations are linked to topoisomerase-mediated DSBs that are not associated with paused RPII *per se*, rather topoisomerase-induced DSBs are generated at sites from which paused RPII have been removed (Dellino et al., 2019). We propose a model in which Translin associates with pre-mRNA, possibly in conjunction with spliceosome factors, to assist the removal of paused RPII that triggers translocation-susceptible DSBs. This offers a plausible mechanism to address the longstanding question of why Translin associates with disease-linked translocation breakpoint junctions.

We have additionally revealed a functional redundancy between Rnh201 and Tsn1. RNase H activity is required for the removal of R-loops and the canonical view is that R-loops induce replicative stress and genome instability (Crossley et al., 2019; García-Muse and Aguilera, 2019; Wells et al., 2019; Brambati et al., 2020; Hegazy et al., 2020; Niehrs and Luke, 2020; Rinaldi et al., 2021). Originally, we had been working on the hypothesis that *S. pombe* Tsn1 might suppress R-loop levels and loss of Tsn1 function would further elevate potentially genotoxic levels of R-loops above the levels seen in following loss of Dcr1. However, this transpired not be the case. Surprisingly loss of both Tsn1 and Tfx1 elevate R-loops at tDNA and rDNA loci, to levels equal to those seen in the Dcr1-deficient cells. These levels of R-loops are not sufficient to increase genetic instability in replicative stress, indicating that R-loops *per se* are not problematic. Moreover, R-loop levels were not significantly increased in the *dcr1*Δ *tsn1*Δ double mutant relative to the *dcr1*Δ single mutant, despite there being an elevation in sensitivity to replicative stress and increased polar tDNA recombination. Whilst R-loops are elevated following loss of Tsn1 function in a Dcr1-proficient background, RPII is not retained at elevated levels indicting functional Dcr1 is sufficient for appropriate RPII displacement. This fits with the model describe above, in which Tsn1 functions to prevent further replicative stress by displacing RPII in Dcr1-deficiency.

This brings into question what causes enhanced replicative stress sensitivity in the *tsn1*Δ *rnh201*Δ background and suggests that this is not due to a failure to suppress R-loop levels,

which is supported by the failure to suppress this phenotype by overexpressing *rnh1*$^{+}$. We believe that these observations point to an additional, non-RNase H function for Rnh201. Mis-incorporated ribonucleotide can retard replication (Watt et al., 2011), so the need for RNase H2 for their removal could impair replicative progression in the *rnh201*Δ mutant. When this is combined with HU-induced stress Tsn1 becomes required for RPII template dissociation, despite Dcr1 proficiency; that is to say, under the elevated replicative stress caused by loss of Rnh201 the Tsn1-mediated auxiliary pathway for RPII template dissociation is required.

However, in humans RNase H2 has been proposed to also have non-enzymatic activities, this is partly based on the fact that mutations in the genes coding for the human RNASEH2B and RNASEH2C, which disrupt protein-protein interaction functions and not catalytic activity, are linked to Aicardi-Goutiéres syndrome (Feng & Cao, 2016). Given this, it is possible that Rnh201 provides another, as yet undetermined, non-enzymatic function to suppress susceptibility to replicative stress.

Previously, only relatively limited evidence linked Translin to the mechanisms of chromosomal translocation formation. Here we provide the first mechanistic insight into how Translin function might be linked to genomic changes such as translocations, drivers of evolution and disease. Importantly, given that Translin has been targeted as a potential therapeutic target in oncology and other disorders (Asada et al., 2014; 2016; Wakeman and McFarlane, 2020), these findings also provide insight to inform rational therapeutic design to ensure that only disease associated function(s) are targeted.

**References**


Achar, Y.J., and Foiani, M. (2017) Coordinating replication with transcription. Adv. Exp. Med. Biol. *1042*, 455-487. 10.1007/978-981-10-6955-0_20.

Aoki, K., Suzuki, K., Sugano, T., Tasaka, T., Nakahara, K., Kuge, O., Omori, A., and Kasai, M. (1995) a novel gene, Translin, encodes a recombination hotspot binding protein associated with chromosomal translocations. Nat. Genet. *10*, 167-174. 10.1038/ng0695-167.

Aronica, L., Kasparek, T., Ruchman, D., Marquez, Y., Cipak, L., Cipakova, I., Anrather, D., Mikolaskova, B., Radtke, M., Sarkar, S., et al. (2016) The spliceosome-associated protein Nrl1 suppresses homologous recombination-dependent R-loop formation in fission yeast. Nucleic Acids Res. *44*, 1703-1717. 10.1093/nar/gkv1473.

Asada, K., Canestrari, E., Fu, X., Li, Z., Makowski, E., Wu, Y.-C., Mito, J.K., Kirsch, D.G., Baraban, J., and Paroo, Z. (2014) Rescuing dicer defects via inhibition of an anti-dicing nuclease. Cell Rep. *9*, 1471-1481. 10.1016/j.celrep.2014.10.021.

Asada, K., Canestrari, E., and Paroo, Z. (2016) A druggable target for rescuing microRNA defects. Bioorg. Med. Chem. Lett. *26*, 4942-4946. 10.1016/j.bmcl.2016.09.019.

Bähler, J., Wu, J.Q., Longtine, M.S., Shah, N.G., McKenzie 3rd, A., Steever, A.B., Wach, A., Philippsen, P., and Pringle, J.R. (1998) Heterologous modules for efficient and versatile PCR-based gene targeting in *Schizosaccharomyces pombe*. Yeast *14*, 943-951.

Baraban, J.M., Shah, A., and Fu, X. (2018) Multiple pathways mediate microRNA degradation: focus on the Translin/Trax RNase complex. Adv. Pharmacol. *82*, 1-20. 10.1016/bs.apha.2017.08.003.

Bonnet, A., Grosso, A.R., Elkaoutari, A., Coleno, E., Presle, A., Sridhara, S.C., Janbon, G., Géli, V., de Almeida, S.F., and Palancade, B. (2017) Introns protect eukaryotic genomes from transcription-associated genetic instability. Mol. Cell *67*, 608-621. 10.1016/j.molcel.2017.07.002.

Brambati, A., Zardoni, L., Nardini, E., Pellicioli, A., and Liberi, G. (2020) The dark side of RNA:DNA hybrids. Mutat. Res. *784*, 108300. 10.1016/j.mrrev.2020.108300.

Burger, K., Schlackow, M., Potts, M., Hester, S., Mohammed, S., and Gullerova, M. (2017) Nuclear phosphorylated Diver processes double-stranded RNA in response to DNA damage. J. Cell Biol. *216*, 2373-2389. 10.1083/jcb.201612131.

Castel, S.E., Ren, J., Bhattacharjee, S., Chang, A.-Y., Sánchez, M., Valbuena, A., Antequera, F., and Martienssen, R.A. (2014) Dicer promotes transcription termination at sites of

replication stress to maintain genome stability. Cell *159*, 572-583. 10.1016/j.cell.2014.09.031.

Chiaruttini, C., Vicario, A., Li, Z., Baj, G., Braiuca, P., Wu, Y., Lee, F.S., Gardossi, L., Baraban, J.M., and Tongiori, E. (2009) Dendritic trafficking of BDNF mRNA is mediated by translin and blocked by the G196A (Val66Met) mutation. Proc. Natl. Acad. Sci. USA *106*, 16581-16486. 10.1073/pnas.0902833106.

Crossley, M.P., Bocek, M., and Cimprich, K.A. (2019) R-loops as cellular regulators and genomic threats. Mol. Cell *73*, 398-411. 10.1016/j.molcel.2019.01.024.

Dellino, G.I., Palluzzi, F., Chiariello, A.M., Piccioni, R., Bianco, S., Furia, L., De Conti, G., Bouwman, B.A.M., Melloni, G., Guido, D., et al. (2019) Release of paused RNA polymerase II at specific loci favors double-strand-break formation and promotes cancer translocations. Nat. Genet. *51*, 1011-1023. 10.1038/s41588-019-0421-z.

Eliahoo, E., Yosef, R.B., Pérez-Cano, L., Fernández-Recio, J., Glaser, F., and Manor, H. (2010) Mapping of interaction sites of the *Schizosaccharomyces pombe* protein Translin with nucleic acids and proteins: a combined molecular genetics and bioinformatics study. Nucleic Acids Res. *38*, 2975-2989. 10.1093/nar/gkp1230.

Eliahoo, E., Litovco, P., Yosef, R.B., Bendalak, K., Ziv, T., and Manor, H. (2014) Identification of proteins that form specific complexes with the highly conserved protein Translin in *Schizosaccharomyces pombe*. Biochim. Biophys. Acta. *1844*, 767-777. 10.1016/j.bbapap.2013.12.016.

Erdemir, T, Bilican, B., Oncel, D., Goding, C.R., and Yavuzer, U. (2002) DNA damage-dependent interaction of the nuclear matrix protein C1D with Translin-associated factor X (TRAX). J. Cell Sci. 115, 207-216.

Feng, S., and Cao, Z. (2016) Is the role of human RNase H2 restricted to its enzyme activity? Prog. Biophys. Mol. Biol. *121*, 66-73. 10.1016/j.pbiomolbio.2015.11.001.

Forsburg, S.L. (1993) Comparison of Schizosccharomyces pombe expression systems. Nucleic Acids Res. *21*, 2955-2956. 10.1093/nar/21.12.2955.

Forsburg, S.L., and Rhind, N. (2006) Basic methods for fission yeast. Yeast *23*, 173-183. 10.1002/yea.1347.

Fragkos, M., Barra, V., Egger, T., Bordignon, B., Lemacon, D., Naim, V., and Coquelle, A. (2019) Dicer prevents genome instability in response to replication stress. Oncotarget *10*, 4407-4423. 10.18632/oncotarget.27034.

Francia, S., Michelini, F., Saxena, A., Tang, D., de Hoon, M., Anelli, V., Mione, M., Carninci, P., and d'Adda di Fagagna, F. (2012) Site-specific DICER and DROSHA RNA

products control the DNA-damage response. Nature *488*, 231-235. 10.1038/nature11179.

Fukuda, K., Ishida, R., Aoki, K., Nakahara, K., Takashi, T., Mochida, K., Suzuki, O., Matsuda, J., and Kasai, M. (2008) Contribnution of Translin to hematopoitic regeneration after sublethal ionizing irradiation. Biol. Pharm. Bull. *31*, 207-211. 10.1248/bpb.31.207.

García-Muse, T., and Aguilera, A. (2019) R loops: from physiological to pathological roles. Cell *179*, 604-618. 10.1016/j.cell.2019.08.055.

Geiger, R., Rieckmann, J.C., Wolf, T., Basso, C., Feng, Y., Fuhrer, T., Kogadeeva, M., Picotti, P., Meissner, F., Mann, M., et al. (2016) L-Arginine modulates T cell metabolism and enhances survival and anti-tumor activity. Cell 167, 829-842. 10.1016/j.cell.2016.09.031.

Gomez-Escobar, N., Almobadel, N., Alzahrani, O., Feichtinger, J., Planells-Palop, V., Alshehri, Z., Thallinger, G.G., Wakeman, J.A., and McFarlane, R.J. (2016) Translin and Trax differentially regulate telomere-associated transcript homeostasis. Oncotarget *7*, 33809-33820. 10.18632/oncotarget.9278.

Gómez-González, B., and Aguilera, A. (2019) Transcription-mediated replication hinderance: a major driver of genomic instability. Genes Dev. *33*, 1008-1026. 10.1101/gad.324517.119.

Guimarães, A.R., Correia, I., Sousa, I., Oliveira, C., Moura, G., Bezerra, A.R., and Santos, M.A.S. (2012) tRNAs as a driving force of genome evolution in yeast. Front. Microbiol. 12, 634004. 10.3389/fmicb.2021.634004.

Gupta, A., Pillai, V.S., and Chittela, R.K. (2019) Translin: a multifunctional protein involved in nucleic acid metabolism. J. Biosci. *44*, 139. 10.1007/s12038-019-9947-6.

Han, J.R., Gu, W., and Hecht, N.B. (1995) Testis-brain RNA binding protein, a testicular translational regulatory RNA-binding protein, is present in the brain and binds to the 3' untranslated regions of transported brain mRNAs. Biol. Reprod. *53*, 707-717. 10.1095/biolreprod53.3.707.

Hasegawa, T., and Isobe, K. (1999) Evidence for the interaction between Translin and GADD34 in mammalian cells. Biochim. Biophys. Acta. *1428*, 161-168. 10.1016/s0304-4165(99)00060-4.

Hegazy, Y.A., Fernando, C.M., and Tran, E.J. (2020) The balancing act of R-loop biology: the good, the bad, and the ugly. J. Biol. Chem. *295*, 905-913. 10.1074/jbc.REV119.011353.

Hyjek, M., Figeil, M., and Nowotny, M. (2019) RNase H: structure and mechanism. DNA Repair *84*, 102672. 10.1016/j.dnarep.2019.102672.

Jaendling, a., Ramayah, S., Pryce, D.W., and McFarlane, R.J. (2008) Functional characterization of the *Schizosaccharomyces pombe* homologue of the leukaemia-associated translocation breakpoint junction binding protein translin and its binding partner, TRAX. Biochim. Biophys. Acta. *1783*, 203-213. 10.1016/j.bbamcr.2007.10.014.

Jaendling, A., and McFarlane, R.J. (2010) Biological roles of translin and trax-associated factor X: RNA metabolism comes to the fore. Biochem. J. *429*, 225-234. 10.1042/BJ20100273.

Jain, D., Hebden, A.K., Nakamura, T.M., Miller, K.M., and Cooper, J.P. (2010) HAATI survivors replace canonical telomeres with blocks of generic heterochromatin. Nature *467*, 223-227. 10.1038/nature09374.

Jalan, M., Oehler, J., Morrow, C.A., Osman, F., and Whitby, M.C. (2019) Factors affecting template switch recombination associated with restarted DNA replication. Elife *8*, e41697. 10.7554/eLife.41697.

Kasai, M., Matsuzaki, T., Katayanagi, K., Omori, A., Maziarz, R.T., Strominger, J.L., Aoki, K., and Suzuki, K. (1997) The translin ring specifically recognizes DNA ends at recombination hot spots in the human genome. J. Biol. Chem. *272*, 11402-11407. 10.1074/jbc.272.17.11402.

Koh, M., Ahmad, I., Ko, Y., Zhang, Y., Martinez, T.F., Diedrich, J.K., Chu, Q., Moresco, J.J., Erb, M.A., Saghatelian, A., et al. (2021) A short ORF-encoded transcriptional regulator. Proc. Natl. Acad. Sci. USA *118*, e2021943118. 10.1073/pnas.2021943118.

Kotsantis, P., Peterman, E., and Boulton, S.J. (2018) Mechanisms of oncogene-induced replication stress: jigsaw falling into place. Cancer Discov. *8*, 537-555. 10.1158/2159-8290.CD-17-1461.

Kumar, M.S., Pester, R.E., Chen, Y.C., Lane, K., Chin, C., Lu, J., Kirsch, D.G., Golub, T.R., and Jacks, T. (2009) Dicer1 functions as a haploinsufficient tumor suppressor. Genes Dev. *23*, 2700-2704. 10.1101/gad.1848209.

Laufman, O., Yosef, R.B., Adir, N., and Manor, H. (2005) Cloning and characterization of the *Schizosaccharomyces pombe* homologs of the human protein Translin and Translin-associated protein TRAX. Nucleic Acids Res. *33*, 4128-4139. 10.1093/nar/gki727.

Li, Z., Wu, Y., and Baraban, J.M. (2008) The Translin/Trax RNA binding complex: clues to fucntion in the nervous system. Biochim. Biophys. Acta. *1779*, 479-485. 10.1016/j.bbagrm.2008.03.008.

Li, L., Gu, W., Liang, C., Liu, Q., Mello, C.C., and Liu, Y. (2012) The translin-TRAX complex (C3PO) is a ribonuclease in tRNA processing. Nat. Struct. Mol. Biol. *19*, 824-830. 10.1038/nsmb.2337.

Liu, S., Hua, Y., Wang, J., Li, L., Yuan, J., Zhang, B., Wang, Z., Ji, J., and Kong, D. (2021) RNA polymerase III is required for the repair of DNA double-strand breaks by homologous recombination. Cell *184*, 1314-1329.

Liu, Y., Ye, X., Jiang, F., Liang, C., Chen, D., Peng, J., Kinch, L.N., Grishin, N.V., Liu, Q. (2009) C3PO, an endoribonuclease that promotes RNAi by facilitating RISC activation. Science *325*, 750-753. 10.1126/science.1176325.

Lockhart, A., Pires, V.B., Bento, F., Kellner, V., Luke-Glaser, S., Yakoub, G., Ulrich, H.D., and Luke, B. (2019) RNase H1 and H2 are differentially regulated to process RNA-DNA hybrids. Cell Rep. *29*, 2890-2900. 10.1016/j.celrep.2019.10.108.

Luke, B., Panza, A., Redon, S., Iglesias, N., Li, Z., and Lingner, J. (2008) The Rat1p 5' to 3' exonuclease degrades telomeric repeat-containing RNA and promotes telomere elongation in *Schaccharomyces cerevisiae*. Mol. Cell *32*, 465-477. 10.1016/j.molcel.2008.10.019.

Maundrell, K. (1993) Thiamine-repressible expression vectors pREP and pRIP for fission yeast. Gene *123*, 127-130. 10.1016/0378-1119(93)90551-d.

McFarlane, R.J., and Wakeman, J.A. (2020) Translin-Trax: considerations for oncological therapeutic targeting. Trends Cancer *6*, 450-453. 10.1016/j.trecan.2020.02.014.

McFarlane, R.J., and Whitehall, S.K. (2009) tRNA genes in eukaryotic genome organization and reorganization. Cell Cycle *8*, 3102-3106. 10.4161/cc.8.19.9625.

Michelini, F., Pitchiaya, S., Vitelli, V., Sharma, S., Gioia, U., Pessina, F., Cabrini, M., Wang, Y., Capozzo, I., Iannelli, F., et al. (2017) Damage-induced lncRNAs control the DNA damage response through interaction with DDRNAs at individual double-strand breaks. Nat. Cell Biol. *19*, 1400-1411. 10.1038/ncb3643.

Murakami, K., Yurgel, M.E., Stahl, B.A., Masek, P., Mehta, A., Heidker, R., Bollinger, W., Gingras, R.M., Kim, Y.-J., Ja, W.W. et al. (2016) Translin is required for metabolic regulation of sleep. Curr. Biol. *26*, 972-980. 10.1016/j.cub.2016.02.013.

Nierhs, C., and Luke, B. (2020) Regulatory R-loops as facilitators of gene expression and genome stability. Nat. Rev. Mol. Cell Biol. *21*, 167-178. 10.1038/s41580-019-0206-3.

Niwa, O. (2018) Determination of the frequency of minichromsome loss to assess chromosome stability in fission yeast. Cold Spring Harb. Protoc. 2018. 10.1101/pdb.prot091991.

Niwa, O., Matsumoto, T., and Yanagida, M. (1986) Construction of a mini-chromosome by deletion and its mitotic and meiotic behaviour in fission yeast. Mol. Gen. Genet. *203*, 397-405.

Niwa, O., Matsumoto, T., Chikashige, Y., and Yanagida, M. (1989) Characterization of Schizosaccharomyces pombe minichromosome deletion derivatives and a functional allocation of their centromere. EMBO J 8, 3045-3052. 10.1002/j.1460-2075.1989.tb08455.x

Ohle, C., Tesorero, R., Schermann, G., Dobrev, N., Sinning, I, and Fischer, T. (2016) Transient RNA-DNA hybrids are required for efficient double-strand break repair. Cell *167*, 1001-1013. 10.1016/j.cell.2016.10.001.

Parizotto, E.A., Lowe, E.D., and Parker, J.S. (2013) Structural basis for duplex RNA recognition and cleavage by *Archaeoglobus fulgidus* C3PO. Nat. Struct. Mol. Biol. *20*, 380-386. 10.1038/nsmb.2487.

Park, A.J., Shetty, M.S., Baraban, J.M., and Abel, T. (2020) Selective role of the translin/trax RNase complex in hippocampal synaptic plasticity. Mol. Brain *13*, 145. 10.1186/s13041-020-00691-5.

Pessina, F., Gioia, U., Brandi, O., Farina, S., Ceccon, M., Francia, S., and d'Adda di Fagagna, F. (2021) DNA damage triggers a new phase in neurodegeneration. Trends Genet. *37*, 337-354. 10.1016/j.tig.2020.09.006.

Pryce, D.W., Lorenz, A., Smirnova, J.B., Loidl, J., and McFarlane, R.J. (2005) Differential activation of M26-containing meiotic recombination hot spots in *Schizosaccharomyces pombe*. Genetics *170*, 95-106. 10.1534/genetics.104.036301.

Pryce, D.W., Ramayah, S., Jaendling, A., and McFarlane, R.J. (2009) Recombination at DNA replication fork barriers is not universal and is differentially regulated by Swi1. Proc. Natl. Acad. Sci. USA *106*, 4770-4775. 10.1073/pnas.0807739106.

Ren, J., Castel, S.E., and Martienssen, R.A. (2015) Dicer in action at replication-transcription collisions. Mol. Cell. Oncol. *2*, e991224. 10.4161/23723556.2014.991224.

Rinaldi, C., Pizzul, P., Longhese, M.P., and Bonetti, D. (2021) Sensing R-loop-associated DNA damage to safeguard genome stability. Front. Cell Dev. Biol. *8*, 618157. 10.3389/fcell.2020.618157.

Sabatinos, S.A., and Forsburg, S.L. (2010) Molecular genetics of *Schizosaccharomyces pombe*. Methods Enzymol. *470*, 759-795. 10.1016/S0076-6879(10)70032-X.

Shah, A.P., Johnson, M.D., Fu, X., Boersma, G.J., Shah, M., Wolfgang, M.J., Tamashiro, K.L., and Baraban, J.M. (2020) Deletion of translin (Tsn) induces robust adiposity and

hepatic steatosis without impairing glucose tolerance. Int. J. Obes (Lond). *44*, 254-266. 10.1038/s41366-018-0315-7.

Steinacher, R., Osman, F., Dalgaard, J.Z., Lorenz, A., and Whitby, M.C. (2012) The DNA helicase Pfh1 promotes fork merging at replication termination sites to ensure genome stability. Genes Dev. *26*, 594-602. 10.1101/gad.184663.111.

Tam, A.S., and Stirling, P.C. (2019) Splicing, genome stability and disease: splice like your genome depends on it! Curr. Genet. *65*, 905-912. 10.1007/s00294-019-00964-0.

Tan-Wong, S.M., Dhir, S., and Proudfoot, N.J. (2019) R-loops promote antisense transcription across the mammalian genome. Mol. Cell *76*, 600-616. 10.1016/j.molcel.2019.10.002.

Teloni, F., Michellena, J., Lezaja, A., Kilic, S., Ambrosi, C., Menon, S., Dobrovolna, J., Imhof, R., Janscak, P., Baubec, T., and Altmeyer, M. (2019) Efficient pre-mRNA cleavage prevents replication-stress-associated genome instability. Mol. Cell *73*, 670-683. 10.1016/j.molcel.2018.11.036.

Tian, Y., Shimanshu, D.K., Ascano, M., Diaz-Avalos, R., Park, A.Y., Juranek, S.A., Rice, W.J., Yin, Q., Robinson, C.V., Tuschl, T., and Patel, D.J. (2011) Multimeric assembly and biochemical characterization of the Trax-translin endonuclease complex. Nat. Struct. Mol. Biol. *18*, 658-664. 10.1038/nsmb.2069.

Tuday, E., Nomura, Y., Ruhela, D., Nakano, M., Fu, X., Shah, A., Roman, B., Yamaguchi, A., An, S.S., Steenbergen, C., et al. (2019) Deletion of the microRNA-degrading nuclease, translin-trax, prevents pathogenic vascular stiffness. Am. J. Physiol. Heart Circ. Physiol. *317*, H1116-H1124. 10.1152/ajpheart.00153.2019.

Vedanayagam, J., Chatila, W.K., Aksoy, B.A., Majumdar, S., Skanderup, A.J., Demir, E., Schultz, N., Sander, C., and Lai, E.C. (2019) Cancer-associated mutations in DICER1 RNase IIIa and IIIb domains exerts similar effects on miRNA biogenesis. Nat. Commun. *10*, 3682. 10.1038/s41467-019-11610-1.

Wakeman, J.A., and McFarlane, R.J. (2020) translin-Trax: considerations for oncological therapeutic targeting. Trends Cancer *6*, 450-453. 10.1016/j.trecan.2020.02.014.

Wang, J., Boja, E.S., Oubrahim, H., and Chock, P.B. (2004) Testis brain ribonucleic acid-binding protein/translin possesses both single-stranded and double-stranded ribonuclease activities. Biochemistry *43*, 13424-13431. 10.1021/bi048847l. 10.1021/bi048847l.

Wang, J.-Y., Chen, S.-Y., Sun, C.-N., Chien, T., and Chern, Y. (2016) A central role of TRAX in the ATM-mediated DNA repair. Oncogene *35*, 1657-1670. 10.1038/onc.2015.228.

Wells, J.P., White, J., and Stirling, P.C. (2019) R loops and their composite cancer connections. Trends Cancer *5*, 619-631.

Watt, D.L., Johansson, E., Burgers, P.M., and Kunkel, T.A. (2011) Replication of ribonucleotide-containing DNA templates by yeast replicative polymerases. DNA Repair *10*, 897-902. 10.1016/j.dnarep.2011.05.009.

Wu, X.Q., Gu,. W., Meng, X., and Hecht, N.B. (1997) The RNMA-binding protein, TB-RBP, is the mouse homologue of translin, a recombination protein associated with chromosomal translocations. Proc. Natl. Acad. Sci. USA *94*, 5640-5645. 10.1073/pnas.94.11.5640.

Yang, S., Cho, Y.S., Chennathukuzhi, V.M., Underkoffler, L.A., Loomes, K., and Hecht, N.B. (2004) Translin-associated factor X is post-transcriptionally regulated by its partner protein TB-RBP, and both are essential for normal cell proliferation. J. Biol. Chem. *279*, 12605-12614. 10.1074/jbc.M313133200.

Ye, X., Huang, N., Liu, Y., Paroo, Z., Huerta, C., Li, P., Chen, S., Liu, Q., and Zhang, H. (2011) Structure of C3PO and mechanism of human RISC activation. Nat. Struct. Mol. Biol. *18*, 650-657. 10.1038/nsmb.2032.

Zaratiegui, M., Castel, S.E., Irvine, D.V., Kloc, A., Ren, J., Li, F., de Castro, E., Marín, L., Chang, A.-Y., Goto, D., et al. (2011) RNAi promotes heterochromatic silencing through replication-coupled release of RNA Pol II. Nature *479*, 135-138. 10.1038/nature10501.

Zhao, H., Zhu, M., Limbo, O., and Russell, P. (2018) RNase H eliminates R-loops that disrupt DNA replication but is nonessential for efficient DSB repair. EMBO Rep. *19*, e45335. 10.15252/embr.201745335.

Zimmer, A.D., and Koshland, D. (2016) Differential roles of the RNases H in preventing chromosome instability. Proc. Natl. Acad. Sci. USA *113*, 12220-12225. 10.1073/pnas.1613448113.

## Figure Legends

**Figure 1. *tsn1*$^+$, but not *tfx1*$^+$, is require to maintain genome stability in Dcr1-deficiency, but not Ago1-deficiency**

(A) 10-fold serial dilutions of indicated strains were spotted onto YEA with or without HU (10 mM).

(B) 10-fold serial dilutions of indicated strains were spotted onto YEA with or without HU (10 mM) or mitomycin C (150 nM).

(C) Percentage of mini chromosome loss values are offered for the indicated strains.

**Figure 2. tsn1$^+$ and dcr1$^+$ are both functionally redundant with rnh201$^+$**

(A) 10-fold serial dilutions of indicated strains were spotted onto YEA with or without HU (10 mM).

(B) 10-fold serial dilutions of indicated strains were spotted onto YEA with or without HU (10 mM).

(C) 10-fold serial dilutions of indicated strains were spotted onto EMM with thiamine (with and without HU; 10 mM) or without thiamine (with or without HU;10 mM). OE-overexpression.

(D) Top: Alkali and native gels showing genomic DNA extracted from the indicated strains. Arrows indicate the undegraded genomic DNA and the single asterisk indicates the region of degraded genomic DNA. Bottom: Quantification of undegraded genomic DNA intensity from the alkali gel (values normalized against the intensity of the undegraded chromosomal DNA in the native gel). *P>0.05, **P>0.01, ***P>0.001 from *t*-test in pairwise comparisons relative to wild-type. Bars represent standard deviation.

(E) 10-fold serial dilutions of indicated strains were spotted onto EMM with thiamine (with and without HU; 10 mM) or without thiamine (with or without HU;10 mM). OE-overexpression.

(F) Quantification of DRIP for the rDNA (18S) locus for the indicated strains. *P>0.05, **P>0.01, ***P>0.001, ns – not significant, from *t*-test in pairwise comparisons relative to relative to wild-type (black) or to *dcr1Δ* (red). Bars represent standard deviation.

(G) 10-fold serial dilutions of indicated strains were spotted onto YEA with or without HU (10 mM).

**Figure 3. t*sn1*$^{+}$, but *not tfx1*$^{+}$, is require for replicative stress response in Dcr1-deficiency in the absence of telomeres**

(A) Schematic of the *S. pombe* chromosome structure for wild-type (Wt) and HAATI$^{STE}$ strain. The three Wt chromosomes are shown on the top (I, II and III represent the Wt chromosome designations); the three HAATI$^{STE}$ chromosomes are shown on the bottom. *cen* = centromere; STE = subtelomeric elements; TEL = telomere, template for TERRAs; rDNA= ribosomal DNA. Adapted from Begnis et al., 2018.

(B) 10-fold serial dilutions of indicated strains were spotted onto YEA with or without HU (10 mM).

(C) 10-fold serial dilutions of indicated strains were spotted onto YEA with or without HU (10 mM).

(D) Agarose gel images showing reverse transcriptase PCR products for RNA extracted from the indicated strains. Left hand set is as previously reported (Gomez-Escobar et al., 2016); right hand set from this study. *taz1*Δ – control for elevated TERRA; O*trt1*Δ – no telomere control. NP – No primer control. Primers to *act1*$^{+}$ used as cDNA positive control.

**Figure 4. *tsn1*$^{+}$ is required to suppress recombination in a polar fashion at a tDNA in Dcr1-deficiency**

(A) Schematic of the *ade6::tRNA$^{GLU}$* allele showing the approximate position of the tDNAs inserted into the *ade6*$^{+}$ gene in different configurations (Ori1 and Ori2). The orientation that gives an RPII head-to-head TRC is shown in red.

(B) Schematic of the intermolecular recombination assay.

(C) Quantification of recombination frequency for *tRNA$^{GLU}$* Ori1 for the indicated strains. Bars represent standard deviation.

(D) Quantification of recombination frequency for *tRNA$^{GLU}$* Ori2 for the indicated strains. *P>0.05, **P>0.01, ns – not significant from *t*-test in pairwise comparisons relative to relative to the wild-type (black) or to *dcr1*Δ (red). Bars represent standard deviation.

**Figure 5. Translin prevents replicative stress associated genome instability via an RNase-independent RPII displacement mechanism**

(A) 10-fold serial dilutions of indicated strains were spotted onto EMM with thiamine (with and without HU; 10 mM) or without thiamine (with or without HU;10 mM). OE-Sp*tsn+* - overexpressed *S. pombe tsn1*$^{+}$; OE-Sp*tsn1-E152A* – overexpression of *S. pombe tsn1*$^{+}$ RNase catalytic mutant.

(B) 10-fold serial dilutions of indicated strains were spotted onto EMM with thiamine (with and without HU; 10 mM) or without thiamine (with or without HU;10 mM). OE-Sp*tsn+* - overexpressed *S. pombe tsn1*$^{+}$; OE-Sp*tsn1-E152A* – overexpression of *S. pombe tsn1*$^{+}$ RNase catalytic mutant.

(C) Quantification of rDNA locus RPII ChIP for the indicated strains. **P>0.01, ***P>0.001, ns – not significant, relative to the wild-type (black) or to *dcr1* (red). Bars represent standard deviation.

(D) 10-fold serial dilutions of indicated strains were spotted onto EMM with thiamine (with and without HU; 10 mM) or without thiamine (with or without HU;10 mM). OE-Hu*TSN*$^{+}$ - overexpressed human *TSN*$^{+}$; OE-Hu*TSN-E150A* – overexpression of human *TSN*$^{+}$ RNase catalytic mutant.

**Figure 6. Possible mechanisms for the contribution of Tsn1 for RPII template displacement**

The schematic represents a replication fork with the replisome (green) encountering RPII in a head-to-head configuration. The letters and associated arrows indicate the possible pathways by which Drc1 and Tsn1 might interact with the macromolecules associated with RPII to mediate its dissociation with the DNA template. A – Direct Dcr1-RPII interaction; B – Direct Tsn1-RPII interaction; C – Tsn1 direct interaction with ssRNA of nascent transcript; D – Tsn1direct interaction with dsRNA formed by intramolecular pairing in the nascent transcript; E – Tsn1 direct association with dsRNA formed by intermolecular association of nascent transcripts produced from opposite strands; F- Tsn1 direct interaction with ssDNA associated with the transcription bubble; G – Tsn1 indirect interaction with nascent transcript via binding to spliceosome-like factor Srp1.

43,058

Figure 1

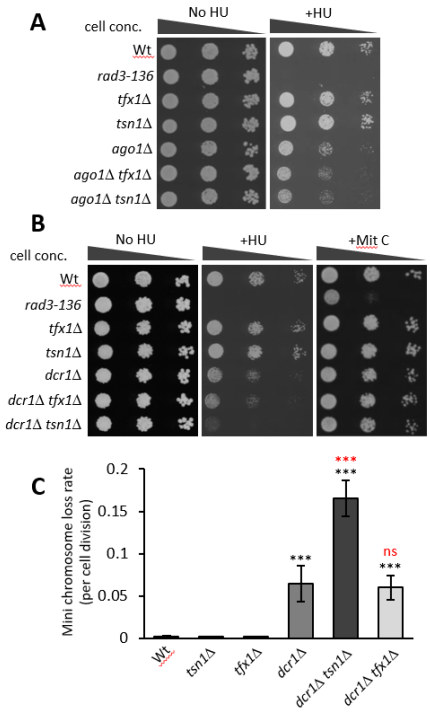
A
cell conc.
No HU
+HU
Wt
rad3-136
tfx1Δ
tsn1Δ
ago1Δ
ago1Δ tfx1Δ
ago1Δ tsn1Δ
B
cell conc.
No HU
+HU
+Mit C
Wt
rad3-136
tfx1Δ
tsn1Δ
dcr1Δ
dcr1Δ tfx1Δ
dcr1Δ tsn1Δ
C
Mini chromosome loss rate (per cell division)
0.2
0.15
0.1
0.05
0
***
***
***
***
ns
Wt
tsn1Δ
tfx1Δ
dcr1Δ
dcr1Δ tsn1Δ
dcr1Δ tfx1Δ

Figure 2

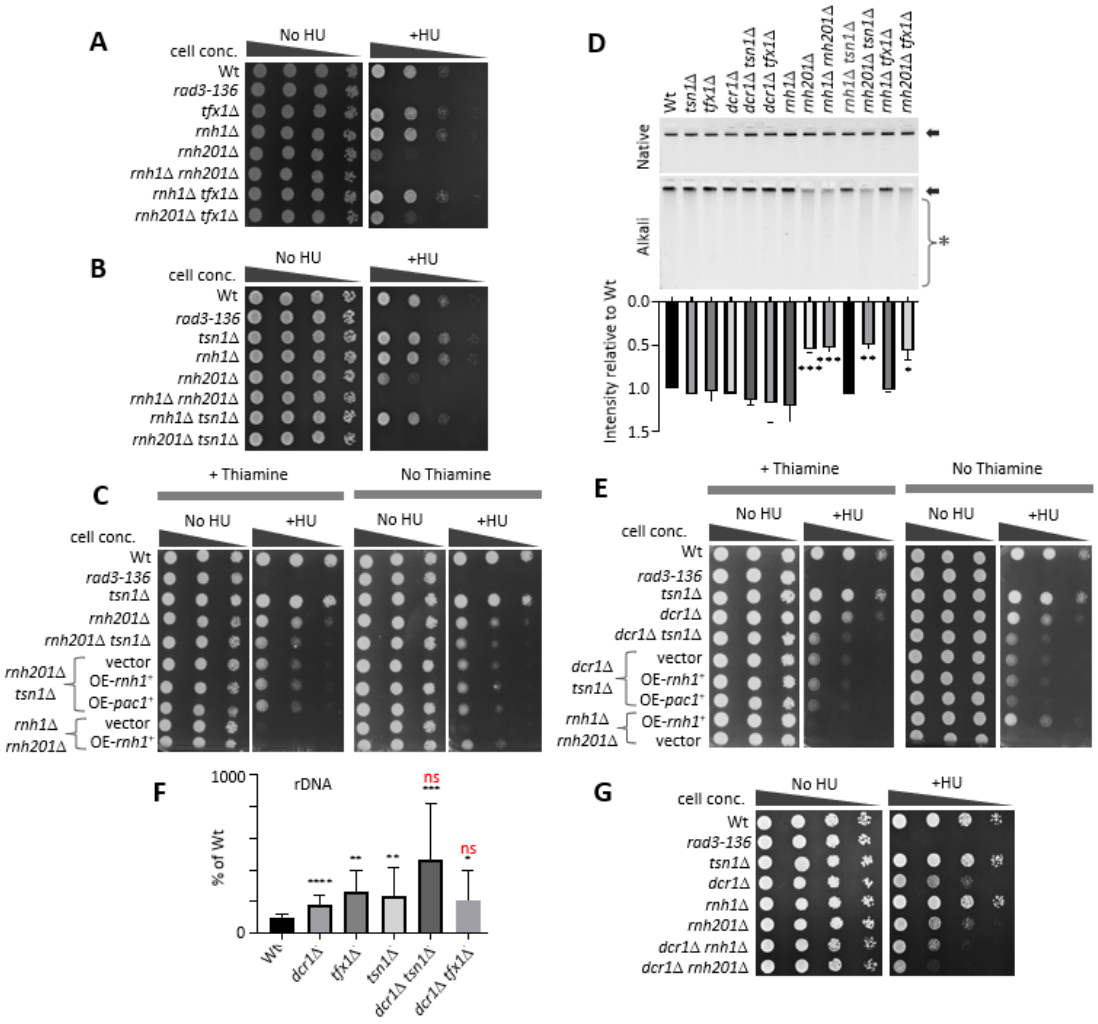
A
No HU
+HU
cell conc.
Wt
rad3-136
tfx1Δ
rnh1Δ
rnh201Δ
rnh1Δ rnh201Δ
rnh1Δ tfx1Δ
rnh201Δ tfx1Δ
B
No HU
+HU
cell conc.
Wt
rad3-136
tsn1Δ
rnh1Δ
rnh201Δ
rnh1Δ rnh201Δ
rnh1Δ tsn1Δ
rnh201Δ tsn1Δ
C
+ Thiamine
No Thiamine
No HU
+HU
No HU
+HU
cell conc.
Wt
rad3-136
tsn1Δ
rnh201Δ
rnh201Δ tsn1Δ
rnh201Δ tsn1Δ
vector
OE-rnh1+
OE-pac1+
rnh1Δ rnh201Δ
vector
OE-rnh1+
D
Wt
tsn1Δ
tfx1Δ
dcr1Δ
dcr1Δ tsn1Δ
dcr1Δ tfx1Δ
rnh1Δ
rnh201Δ
rnh1Δ rnh201Δ
rnh1Δ tsn1Δ
rnh201Δ tsn1Δ
rnh1Δ tfx1Δ
rnh201Δ tfx1Δ
Native
Alkali
*
Intensity relative to Wt
0.0
0.5
1.0
1.5
E
+ Thiamine
No Thiamine
No HU
+HU
No HU
+HU
cell conc.
Wt
rad3-136
tsn1Δ
dcr1Δ
dcr1Δ tsn1Δ
dcr1Δ tsn1Δ
vector
OE-rnh1+
OE-pac1+
rnh1Δ rnh201Δ
OE-rnh1+
vector
F
rDNA
1000
0
% of Wt
ns
ns
Wt
dcr1Δ
tfx1Δ
tsn1Δ
dcr1Δ tsn1Δ
dcr1Δ tfx1Δ
G
No HU
+HU
cell conc.
Wt
rad3-136
tsn1Δ
dcr1Δ
rnh1Δ
rnh201Δ
dcr1Δ rnh1Δ
dcr1Δ rnh201Δ

Figure 3

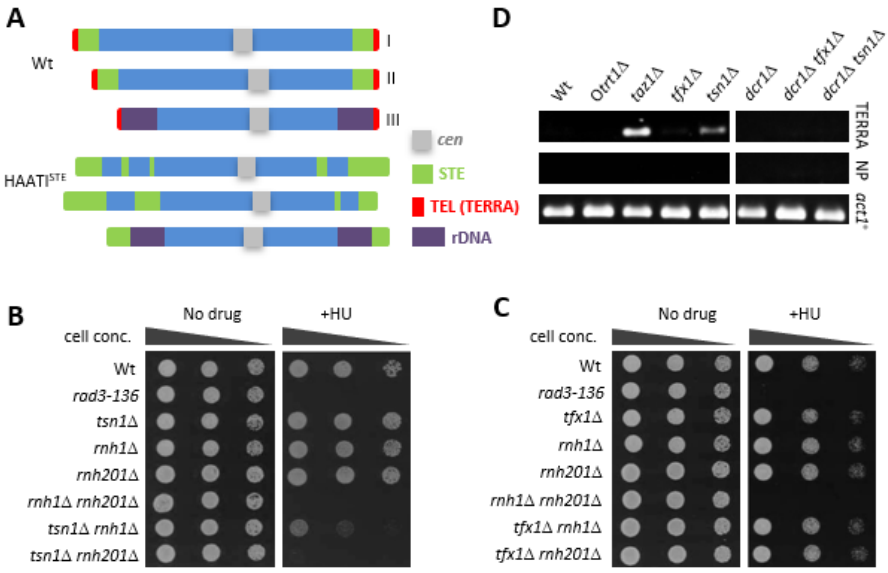
A
Wt
I
II
III
HAATI^STE
cen
STE
TEL (TERRA)
rDNA
D
Wt
Otr1Δ
taz1Δ
tfx1Δ
tsn1Δ
dcr1Δ
dcr1Δ tfx1Δ
dcr1Δ tsn1Δ
TERRA
NP
act1+
B
No drug
+HU
cell conc.
Wt
rad3-136
tsn1Δ
rnh1Δ
rnh201Δ
rnh1Δ rnh201Δ
tsn1Δ rnh1Δ
tsn1Δ rnh201Δ
C
No drug
+HU
cell conc.
Wt
rad3-136
tfx1Δ
rnh1Δ
rnh201Δ
rnh1Δ rnh201Δ
tfx1Δ rnh1Δ
tfx1Δ rnh201Δ

Figure 4

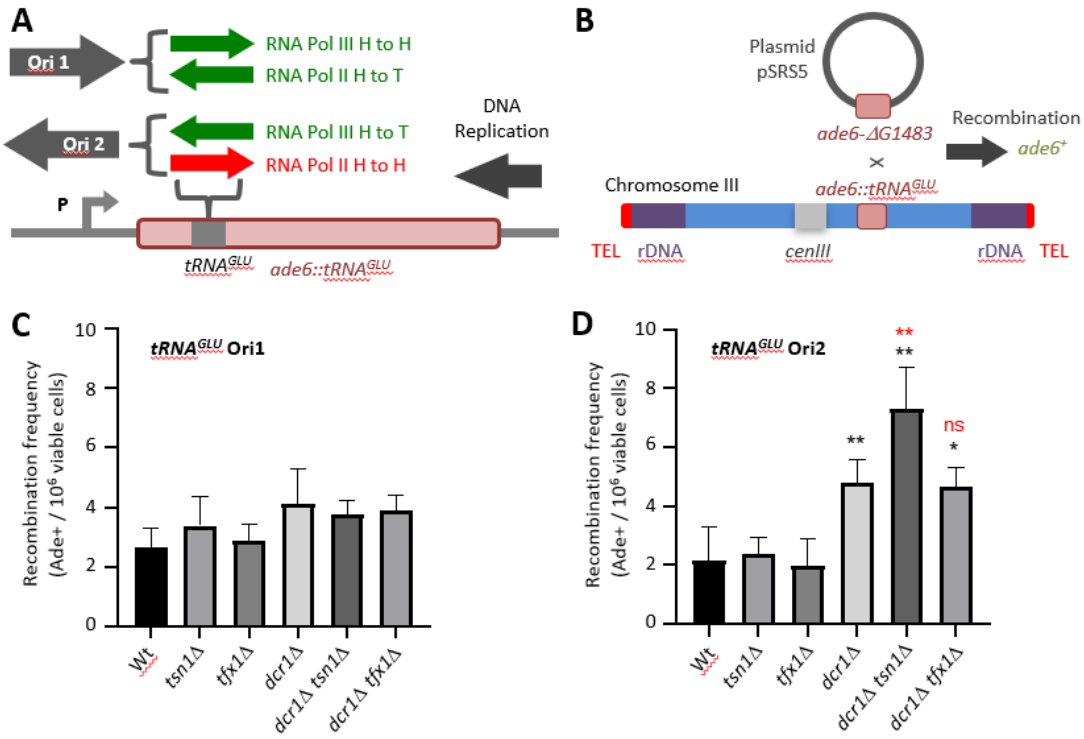
A
Ori 1
RNA Pol III H to H
RNA Pol II H to T
Ori 2
RNA Pol III H to T
RNA Pol II H to H
DNA Replication
P
tRNAGLU
ade6::tRNAGLU
B
Plasmid pSRS5
ade6-ΔG1483
Recombination
ade6+
Chromosome III
ade6::tRNAGLU
TEL
rDNA
cenIII
rDNA
TEL
C
tRNAGLU Ori1
Recombination frequency (Ade+ / 10⁶ viable cells)
Wt
tsn1Δ
tfx1Δ
dcr1Δ
dcr1Δ tsn1Δ
dcr1Δ tfx1Δ
D
tRNAGLU Ori2
ns

Figure 5

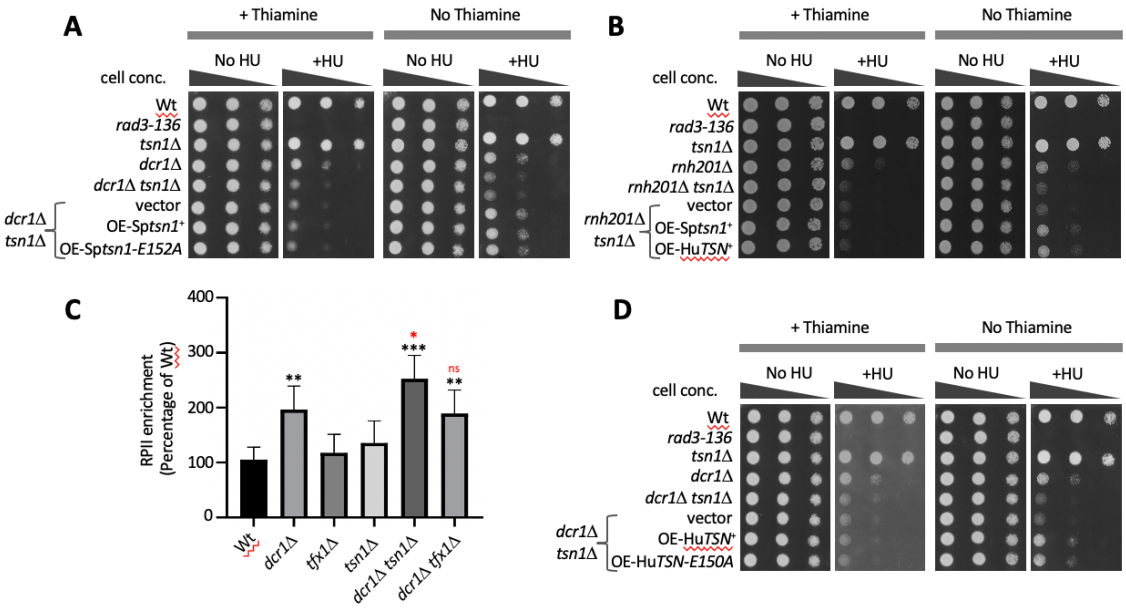
A
+ Thiamine
No Thiamine
No HU
+HU
cell conc.
Wt
rad3-136
tsn1Δ
dcr1Δ
dcr1Δ tsn1Δ
vector
OE-Sptsn1+
OE-Sptsn1-E152A
dcr1Δ
tsn1Δ
B
rnh201Δ
rnh201Δ tsn1Δ
OE-Hu TSN+
C
RPII enrichment (Percentage of Wt)
400
300
200
100
0
Wt
dcr1Δ
tfx1Δ
tsn1Δ
dcr1Δ tsn1Δ
dcr1Δ tfx1Δ
ns
D
OE-Hu TSN-E150A

Figure 6

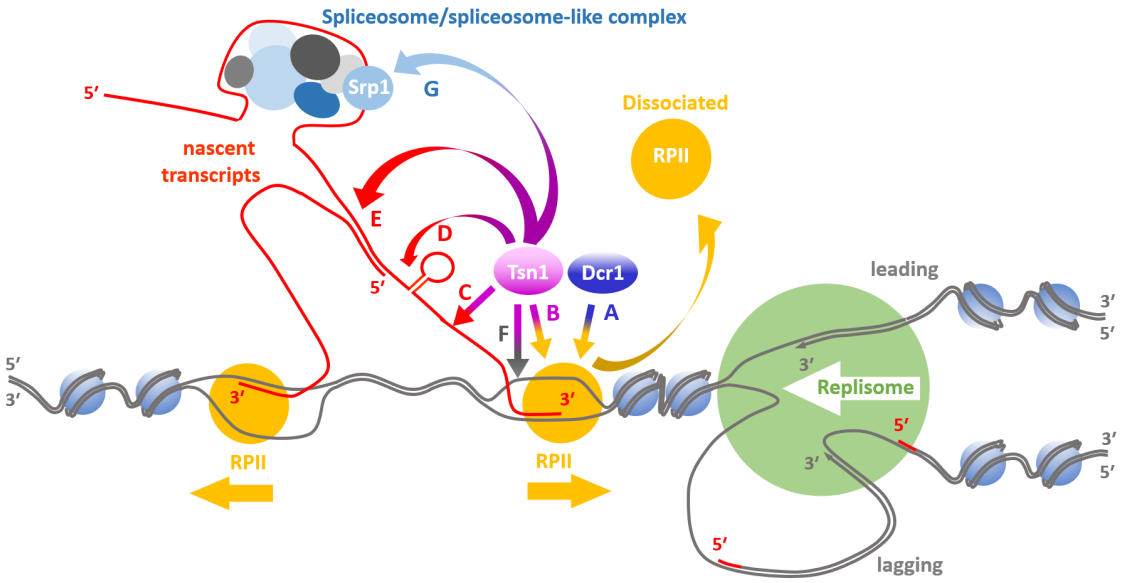
Spliceosome/spliceosome-like complex
Srp1
G
5′
nascent
transcripts
Dissociated
RPII
E
D
C
5′
Tsn1
Dcr1
F
B
A
leading
3′
5′
Replisome
3′
5′
3′
5′
3′
5′
3′
RPII
RPII
5′
lagging

Figure S1

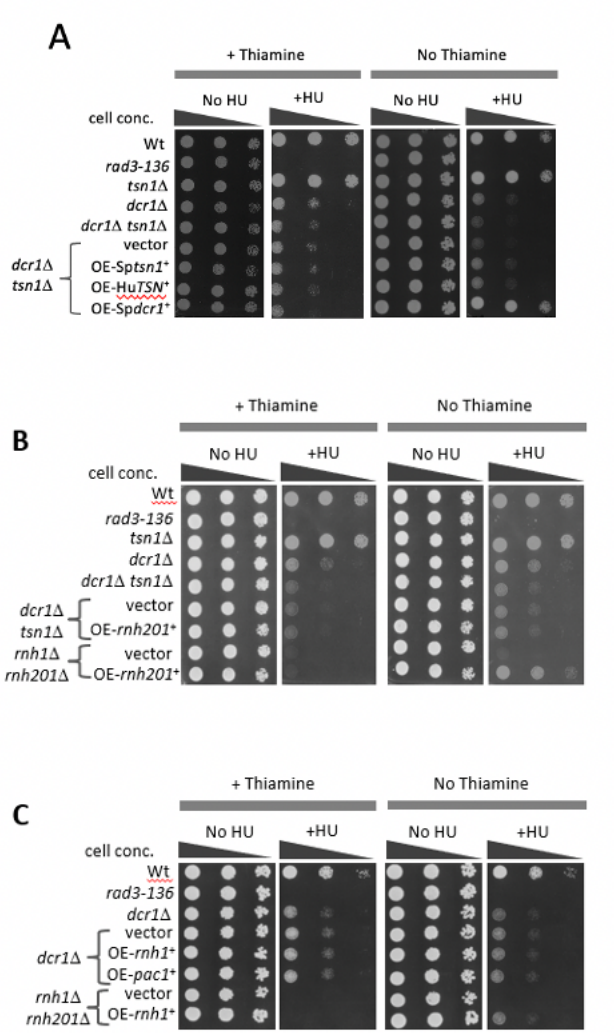
A
+ Thiamine
No Thiamine
No HU
+HU
No HU
+HU
cell conc.
Wt
rad3-136
tsn1Δ
dcr1Δ
dcr1Δ tsn1Δ
vector
OE-Sptsn1+
OE-HuTSN+
OE-Spdcr1+
dcr1Δ
tsn1Δ
B
+ Thiamine
No Thiamine
No HU
+HU
No HU
+HU
cell conc.
Wt
rad3-136
tsn1Δ
dcr1Δ
dcr1Δ tsn1Δ
vector
OE-rnh201+
dcr1Δ
tsn1Δ
vector
OE-rnh201+
rnh1Δ
rnh201Δ
C
+ Thiamine
No Thiamine
No HU
+HU
No HU
+HU
cell conc.
Wt
rad3-136
dcr1Δ
vector
OE-rnh1+
OE-pac1+
dcr1Δ
vector
OE-rnh1+
rnh1Δ
rnh201Δ

Figure S2

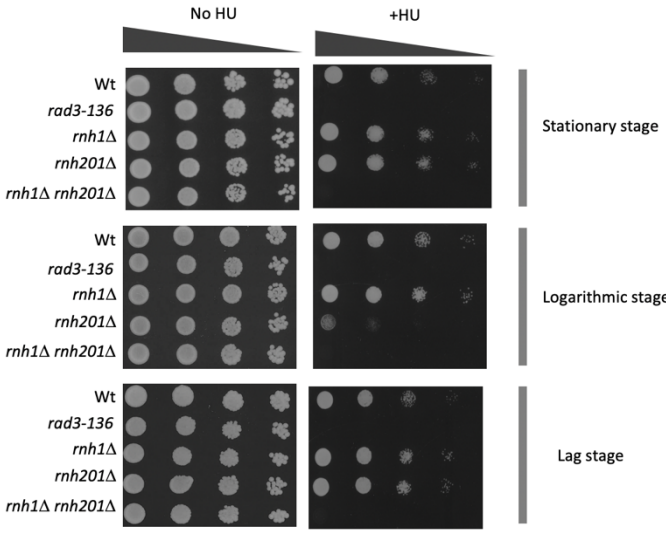
No HU
+HU
Wt
rad3-136
rnh1Δ
rnh201Δ
rnh1Δ rnh201Δ
Stationary stage
Wt
rad3-136
rnh1Δ
rnh201Δ
rnh1Δ rnh201Δ
Logarithmic stage
Wt
rad3-136
rnh1Δ
rnh201Δ
rnh1Δ rnh201Δ
Lag stage

Figure S3

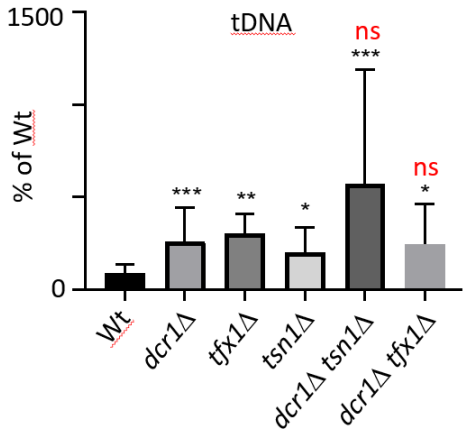
1500
0
% of Wt
tDNA
***
**
*
ns
***
ns
*
Wt
dcr1Δ
tfx1Δ
tsn1Δ
dcr1Δ tsn1Δ
dcr1Δ tfx1Δ

Figure S4

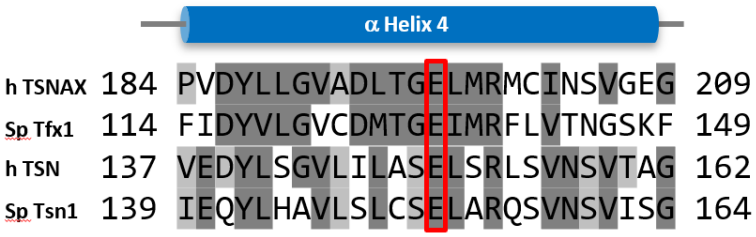
α Helix 4
h TSNAX 184 PVDYLLGVADLTGELMRMCINSVGEG 209
Sp Tfx1 114 FIDYVLGVCDMTGEIMRFLVTNGSKF 149
h TSN 137 VEDYLSGVLILASELSRLSVNSVTAG 162
Sp Tsn1 139 IEQYLHAVLSLCSELARQSVNSVISG 164

Figure S5

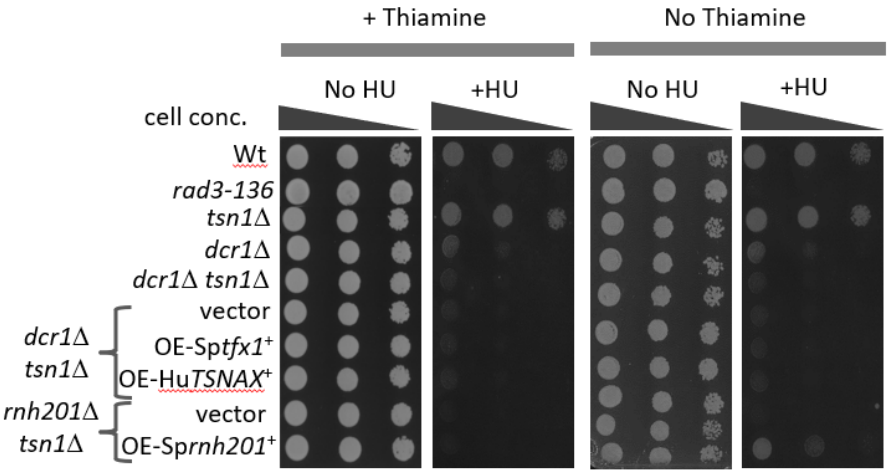
+ Thiamine
No Thiamine
No HU
+HU
No HU
+HU
cell conc.
Wt
rad3-136
tsn1Δ
dcr1Δ
dcr1Δ tsn1Δ
vector
dcr1Δ
tsn1Δ
OE-Sptfx1+
OE-HuTSNAX+
rnh201Δ
tsn1Δ
vector
OE-Sprnh201+

Figure S6

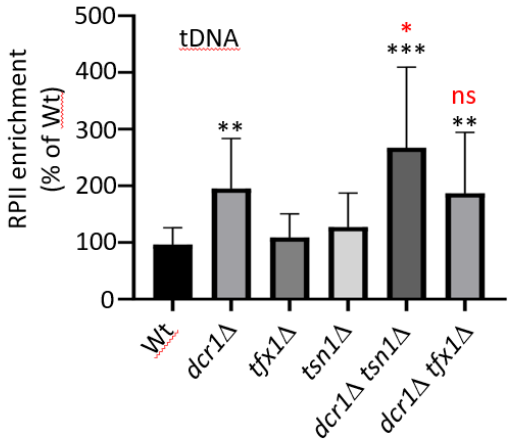
tDNA
RPII enrichment
(% of Wt)
500
400
300
200
100
0
**
*
***
ns
**
Wt
dcr1Δ
tfx1Δ
tsn1Δ
dcr1Δ tsn1Δ
dcr1Δ tfx1Δ

## STAR★METHODS

## KEY RESOURCE TABLE

| REAGENT OR RESOURCE | SOURCE | IDENTIFIER |
|---|---|---|
| **Antibodies** | | |
| S9.6 antibody | Kerafast | ENH001 |
| anti-RNA polymerase II antibody | Abcam | ab5408 |
| **Bacterial strains** | | |
| NEB® 10-beta competent E. coli (High Efficiency) | NEB | C3019H |
| **Chemicals** | | |
| Hydroxyurea | Sigma | H8627-5G |
| Mitomycin C | Sigma | M4287-2MG |
| Adenine | Sigma | A8626-100G |
| Guanine | Sigma | G11950-10G |
| Thiamine | Sigma | T4625-250G |
| **Reagents** | | |
| Human total RNA | Takara | 636533 |
| 6x loading buffer | AlfaAesar | J62157 |
| 6x loading dye | NEB | B7024s |
| BamHI | NEB | R3136S |
| DdeI | NEB | R0175s |
| SYBR Gold | ThermoFisher Scientific | S11494 |
| RNaseH | NEB | M0297s |
| Protein G-coupled Dynabeads | Life Technologies | 10003D |
| Chelex resin | BioRad | 1421253 |
| Paraformaldehyde | Electron Microscopy Sciences | 15714-5 |
| PMSF | Sigma | P7626-5G |
| Halt Protease Inhibitors | ThermoFisher Scientific | 78430 |
| Glass Beads | Sigma | G8772-500G |
| Dynabeads M-280 sheep anti-mouse IgG | ThermoFisher Scientific | 11201D |
| Proteinase K | Qiagen | 19131 |
| **Critical Commercial Assays** | | |
| MasterPure Yeast RNA Purification Kit | Cambio | MPY03100 |
| Epicenter MasterPure Yeast DNA Purification Kit | Cambio | MPY80200 |
| Superscript III First-Strand Synthesis System | ThermoFisher Scientific | 18080-051 |
| Phusion High-Fidelity DNA Polymerase | NEB | M0530s |
| QuickChangeLightning site-directed mutagenesis system | Agilent | 210515 |
| **Oligonucleotides** | | |
| Primes for DRIP-qPCR see Table S1 | this paper | N/A |
| Primers for ChIP-qPCR see Table S1 | this paper | N/A |

| Recombinant DNA | | |
|---|---|---|
| pREP3X | Forsburg, 1993 | N/A |
| pSRS5 | Pryce *et al*., 2009 | N/A |
| pREP3X::Sp*tsn1*$^{+}$ | this study | N/A |
| pREP3X::HuTSN$^{+}$ | this study | N/A |
| pREP3X::Sp*tsn1-E152A* | this study | N/A |
| pREP3X::Hu*TSN-E150A* | this study | N/A |

## RESOURCE AVAILABILITY

### Lead contact

Further information and requests for resources and reagents should be directed to and will be fulfilled by Ramsay McFarlane (r.macfarlane@bangor.ac.uk).

### Materials available

Plasmids and *Schizosaccharomyces pombe* strains generated during this study are available from the corresponding author upon request.

### Data code and availability

This study did not generate/analyze datasets/code.

## EXPERIMENTAL MODEL AND SUBJECT DETAILS

### *Schizosaccharomyces pombe*

This study was conducted using the model organism *Schizosaccharomyces pombe*. Extended information and genome resources for this model organism can be found at PomBase (RRID:SCR_006586; www.pombase.org/). A list of *S. pombe* strains used in this study can be found in Table S2. Lineage of strains can be obtained from the corresponding author upon request.

*S. pombe* cells were maintained and cultured in standard media [yeast extract liquid (YEL), yeast extract agar (YEA) or Edinburgh Minimal Medium + Glutamic Acid (20 mM) (EMMG)] as required with addition or omission of reagents as required/specified (Forsburg and Rhind, 2006; Sabatinos and Forsburg, 2010). Strain construction, storage, gene deletions and transformations used standard *S. pombe* protocols described by Bähler et al. (1998), Forsburg and Rhind (2006) and Sabatinos and Forsburg (2010).

## METHOD DETAILS

### Spot assays

Required strains were cultured in appropriate liquid media to mid log phase ($OD_{600}$ of ~0.5). Cells were subjected to a 10-fold serial dilution ($10^{-1}$-$10^{-5}$) and 10 µl of each dilution were spotted onto agar plates of appropriate media. Plates were incubated for 3 days at 30ºC unless otherwise stated.

### Estimation of mini chromosome instability

$Ch^{16\text{-}23R}$ is a derivative of *S. pombe* Chromosome III and it carries the *ade6-M216* allele, which interallelically complements an *ade6-M210* allele located on the full-length Chromosome III (Niwa et al., 1986; 1989). Strains containing a mini chromosome *ade6-M216* allele and a full-length chromosome *ade6-M210* allele will be Ade+ (these cells produce colonies that are white on YEA plates without supplemental adenine, whereas cells that have lost the minichromosome and only carry the *ade6-M210* allele are Ade- and grow as red colonies); loss of the mini chromosome will result in Ade-. To calculate the rate of minichromosome loss we employed the method of Niwa (2018). In brief, appropriate strains containing the minichromosome were cultured in liquid EMMG medium containing appropriate supplements, but no adenine (for minichromosome maintenance selection). Cultures were incubated until late log-phase, subjected to serial dilutions, and then plated out onto YEA without supplemental adenine to give plates with approximately 100-200 colonies per plate. Loss of the minichromosome prior to plating will result in colonies that are completely red. Cells that retain the minichromsome in both daughter cells after the first mitotic division post-plating (i.e. one cell to two cell stage) will either be all white or have red/white sectored colonies with the ratio of white being greater than red (the latter arising due to minichromosome loss after the first division). Half sectored colonies (50% white and 50% red) represent a minichromosome loss event in the first division of the single colony forming cell. Counting the half-sectored colonies as a fraction of the total number of cells gives a relatively accurate approximation of the minichromosome loss rate per cell division [see Niwa (2018) for further details and limitations]. Colony colours were counted to quantify cells that had retained the minichromsome at the first post-plating division (white or sectored with the majority white), cells that did not contain the minichromosome at plating

(totally red) and cells that had lost the minchromosome at the first division post-plating (half sectored 50:50 red:white).

### Determination of recombination frequency

Appropriate *S. pombe* strains containing the plasmid pSRS5 (Pryce et al., 2009) were cultured to mid-log phase in liquid EMMG medium containing appropriate supplements. Cells were subjected to serial dilution and plated out on EMMG agar containing appropriate supplements at a dilution that resulted in well-dispersed single colonies following incubation at 30ºC. Colonies were permitted to grow until visible, but not permitted to reach greater than 1 mm in diameter. At this point a minimum of 7 whole colonies were individually picked and inoculated into individual 5 ml volumes of sterile liquid EMMG containing appropriate supplements, ensuring all the cells from the colony were transferred to the liquid medium. Cultures were incubated at 30ºC with shaking until very early stationary phase. Serial dilutions were made for each culture and these were plated onto YEA (dilution range $10^{-4}$ to $10^{-6}$) and YEA containing 20 mg/ml guanine (pH 6.5) (dilution range neat – $10^{-2}$), which prevents the uptake of adenine because of purine antagonism (Pryce *et al*., 2005). Plates were incubated at 30ºC for 3 days.

### Gene overexpression

Genes were cloned into the *S. pombe* expression vector pREP3X (Forsburg, 1993) under the control of the regulatable *nmt* (no message in thiamine) promoter, which is repressed when cells are cultured in media containing thiamine (Maundrell, 1993). pREP3X contains a *LEU2*$^{+}$ marker gene for selection in *S. pombe* (Forsburg, 1993). Strains containing genes cloned into pREP3X were cultured in liquid EMMG with appropriate strain-specific supplements and 2% thiamine, but without leucine (for plasmid maintenance). Cells were cultured in a rotary incubator at 30ºC to mid log-phase ($OD_{600}$ of ~0.5). For gene expression during spot analysis strains were spotted onto EMMG agar without thiamine. EMMG agar plates containing thiamine (2%) and YEA were used as a ‘gene off’ controls.

### Cloning and site directed mutagenesis

RNA was extracted from *S. pombe* wild-type using the MasterPure™ Yeast RNA Purification Kit (Cambio; MPY03100). Human uterus RNA was obtained from Takara (Takara; 636551). cDNA was synthesized using the Superscript™ III First-Strand Synthesis System

(ThermoFisher Scientific; 18080-051). Genes of interest were amplified from cDNA using primers shown in Table S2. A *Bam*HI (New England Biolabs; R3136s) restriction site was added to each primer sequence for cloning into the pREP3X expression vector (Forsburg, 1993). Amplification from human and *S. pombe* cDNA was done using Phusion® High-Fidelity DNA polymerase (New England Biolabs; M0530S). DNA sequencing of both strands (performed by Eurofins Genomics) of the cloned genes of interest confirmed that no mutations were introduced during the PCR and cloning procedures. Point mutations in human *TSN* and *S. pombe tsn1*$^{+}$ were introduced using the QuickChange Lightning site-directed mutagenesis system (Agilent; 210515). Following the mutagenesis procedure all mutant genes were re-sequenced to ensure the correct mutations had been made and no additional mutations had been added.

### Genomic alkali lability assay

Appropriate *S. pombe* strains were cultured in YEL to mid log phase (~0.5 $OD_{600}$). DNA was extracted using the Epicentre MasterPure™ Yeast DNA Purification Kit (Cambio; MPY80200). Either KOH or KCl was added to 1 µg of genomic DNA to a final concentration of 0.2 M in 40 µl volumes and incubated at 55ºC for 2 hours. 6X loading buffer (alkaline; AlfaAesar; J62157) was added to the KOH-treated samples and 6X loading dye (non-alkaline; New England Biolabs; B7024s) was added to the KCl-treated samples. Alkali treated samples were loaded onto a 1%alkaline agarose gel (1% agarose, 1 mM EDTA, 50 mM NaOH) and run in alkaline electrophoresis buffer (1 mM EDTA, 50 mM NaOH). Electrophoresis of KCl treated samples was performed using a 1% agarose gel run in tris-borate-EDTA (TBE) buffer (130 mM tris [pH 7.6], 45 mM boric acid, 2.5 mM EDTA). Gels were run at 1 V/cm for 18 hours. Alkaline gels were neutralized by soaking in 1 M tris HCl (pH8.0) for 1 hour prior to staining with SYBR Gold (Thermo Fisher Scientific; S11494) and imaged on a UV transilluminator (BioRad; Molecular Imager Gel Doc XR System).

### DNA:RNA immunoprecipitation (DRIP)

DNA extraction was performed as described in Forsdurg and Rhind (2006). DNA was fragmented using *Dde*I (10U/µg of DNA) for 2 hours at 37ºC (New England Biolabs; R0175s). DNA samples were divided into two and one sample was treated with RNase H (New England Biolabs; M0297s) for 2 hours at 37ºC, the other sample was left untreated. For DRIP, DNA samples were then incubated overnight at 4ºC in immunoprecipitation (IP) buffer [100 mM

MES (pH 6.6), 500 mM NaCl, 0.05% Triton, 2 mg/ml BSA] in the presence of Protein G-coupled Dynabeads (Life Technologies; 10003D) previously incubated with S9.6 antibody (Kerafast; ENH001) according to the manufacturer's instructions. The beads were then washed three times in IP buffer. After two additional washes in Tris-EDTA (TE) buffer [10 mM tris-HCl (pH 8.0), 1 mM EDTA] the beads were resuspended in 10% Chelex resin (BioRad; 1421253) and incubated at 98ºC for 5 minutes. The mixture was then incubated with 20 µg of proteinase K (Qiagen; 19131) at 43ºC for 30 minutes and then at 98ºC for 5 minutes. After centrifugation for 5 minutes at 6000 r.p.m. in a benchtop microcentrifuge, DRIP-qPCR was performed using the supernatant.

## DRIP-qPCR

Real-time PCR was performed using 25 ng of input DNA and 1/20 of the input immunoprecipitated DNA (above) in the presence of GoTaq® Green Master Mix (Promega; A6002). Reactions were done in duplicate and standard curves were calculated on serial dilutions (100 ng – 0.1 ng) of input genomic DNA. IP enrichment was calculated relative to RNase H treated IP using the following formula: DRIP enrichment = {[IP amount (ng) (no RNase H) / input amount (ng) (no RNase H)] / [IP amount (ng) (+ RNase H) / input amount (ng) (+ RNase H)]}.The resulting values were then presented as a percentage of the wild-type value. Primer sequences are given in Table S2.

## Chromatin immunoprecipitation (ChIP)

Appropriate *S. pombe* strains were cultured in 50 ml of YEL to mid log-phase. Cells were crosslinked with 1% paraformaldehyde solution (Electron Microscopy Sciences; 15714-5) at room temperature for 15 minutes. Reactions were quenched by addition of 2 ml of 2.5 M glycine for 15 minutes at room temperature. Cells were harvested by centrifugation for 5 minutes at 1000g, washed twice with ice-cod phosphate-buffer saline (PBS) (137 mM NaCl, 2.7 mM KCl, 10 mM $Na_2HPO_4$, 1.8 mM $KH_2PO_4$) and resuspended in 400 µl of Buffer A [50 mM HEPES (pH 7.5), 140 mM NaCl, 1 mM EDTA, 1% Triton X-100, 0.1% sodium deoxycholate] supplemented with 1 mM PMSF (Sigma; P78830-1G) and 1 x Halt protease inhibitors (ThermoFisher Scientific; 78430). After an addition of an equal volume of acid washed glass beads (Sigma; G8772-500G), cells were vortexed for 60 minutes at 4ºC using a disruptor genie(Scientific Industries) with a Turbomix attachment. Lysates were recovered from the beads and sonicated using a bath Bioruptor Sonicator (Diagenode) at 30 seconds on

followed by 30 seconds off for 10 minutes to obtain chromatin fragments in the range of 200-800 base pairs. The total volume was increased to 1 ml by addition of Buffer A and the sonicate was centrifuged at 4ºC in a benchtop microfuge at 14,000 r.p.m. for 10 minutes. The soluble chromatin was retained.

20 µl of washed Dynabeads M-280 sheep anti-mouse IgG (Thermofisher Scientific; 11201D) were added to the chromatin sample and incubated for 2 hours at 4ºC. 20 µl of the pre-cleared sample was kept for the 'input' fraction and the rest was incubated overnight at 4ºC with 2 µg of anti-RNA polymerase II antibody (Abcam; ab5408) or in the absence of antibody. 20 µl of washed Dynabeads were added and after 2 hours at 4ºC they were washed sequentially three times with Buffer A, twice with Buffer A with 500 mM NaCl, twice with 250 mM LiCl, 1% NP-40, 1% sodium deoxycholate, 1 mM EDTA, 10 mM tris-HCl (pH8.0) and twice with 10 mM Tris-HCl (pH 8.0), 1 mM EDTA (pH 8.0). The beads and 'input' were resuspended in 100 µl of 10% Chelex (BioRad; 1421253) and incubated at 98ºC for 5 minutes. The mixture was then incubated with 20 µg of proteinase K (Qiagen; 19131) at 43ºC for one hour and then at 98ºC for 5 minutes. After centrifugation for 5 minutes at 6000 r.p.m. in a benchtop microcentrifuge, the supernatant was collected and analyzed by qPCR (below).

### ChIP-qPCR

qPCR was performed using the primers listed in Table S2. Average CT was calculated across technical triplicates for each sample. IP enrichment was calculated as percentage of input (whole cell extract) and presented relative to the wild-type value.

## QUANTIFICATION AND STATISTICAL ANALYSIS

### Mini Chromosome Loss

**Colony counts** were used to gain an approximate value for loss rate per cell division using the equation $N_{hs}/(N_{total}/N_r)$, where $N_{hs}$ = number of half-sectored, $N_{total}$ = total number of colonies, $N_r$ = total number of all red colonies (Niwa, 2018). *P* values were calculated using Student's t-test and error bars represent standard deviation.

### Recombination frequency

The numbers of colony forming units per ml of culture were counted to determine recombination frequencies (Ade+ cells / $10^6$ viable cells). The recombination frequency was determined for 7 independent cultures for each strain to be tested and the median value was used for the recombination frequency (to avoid 'jackpot' values). This was repeated a minimum of three times for each strain to obtain mean values of independent biological repeats. P values were calculated using Student's *t*-test and error bars represent standard deviation.

### Alkaline and native gels

Quantification of undegraded genomic DNA intensity from alkali and native gels was performed using ImageQuant software. Values from the intensity of undegraded genomic DNA from alkali gels were normalized against the values of the chromosomal DNA in the native gel. *P* values were calculated using one sample Student's *t*-test and error bars represent standard deviation.

### qPCR

Quantification for DRIP-qPCR was accomplished using Ct values and a standard curve of ten-fold dilutions of input genomic DNA from the wild-type strain. Experiments were performed in duplicates. Ct values for ChIP-qPCR were normalized using the Percent Input analysis method which represents the amount of DNA pulled down by using the antibody of interest in the ChIP reaction, relative to the amount of starting material ('input' fraction). Experiments were done in triplicate. *P* values were calculated using Student's unpaired *t*-test with Welch's correction, and error bars represent standard deviation.

**Table S1.** Primers used in this study.

| Primer designation | Primer sequence (5'-3') |
|---|---|
| rDNA qPCR F | TTTCTAGGACCGCCGTAATG |
| rDNA qPCR R | TGCTTTCGCAGTAGTTCGTC |
| HIS.02 qPCR F | CTGGTGTGGGCACTTACTAT |
| HIS.02 qPCR R | ATGGATCTATTTGGGATGC |
| MET.06 qPCR F | TCCTGGGACCTACGGGTTAT |
| MET.06 qPCR R | AACGGATATAGGTTCAT |
| ARG.09 qPCR F | GGTTAAGGCGCTTGACTACG |
| ARG.09 qPCR R | ACATCCTTTTTGCACTCGAA |
| PRO.01 qPCR F | CACAATATCAACTGAGGCTTCG |
| PRO.01 qPCR R | AAATTTAAAGGCTTTGGGCTTC |
| VAL.01 qPCR F | ACAACCAACAGTCCCGTGTT |
| VAL.01 qPCR R | TGGTTCAAGTTCGCTATTGTTG |
| ASN.03 qPCR F | AAGCAAGAAGGTCGGGTAG |
| ASN.03 qPCR R | TGTGCGTTTGTCTATCCTTTGT |
| TYR.01 qPCR F | AACTCCTGATGGTGTAGTTGGT |
| TYR.01 qPCR R | TTTACCAGGTGGAAGCA |
| pac-1 cloning F* | ccgctcgagATGGGACGGTTTAAGAGGCA |
| pac-1 cloning R* | cgcggatccTTAACGGGCAAACTTAGAGTAATC |
| rnh1 cloning F* | cgcggatccATGGGTGGAAATAAGCGTGC |
| rnh1 cloning R* | cgcggatccTTACTCAGAAGCTCCTCGCC |
| rnh201 cloning F* | cgcggatccATGAAAGATGATCACGATGC |
| rnh201 cloning R* | cgcggatccCTAAAAATAAAACTCTGATC |
| dcr1 cloning F* | cgcggatccATGGATATTTCAAGTTTTCTACTTC |
| dcr1 cloning R* | cgcggatccTCAAGTCAAACTTTTAACTTTTCC |
| Sp Tsn1 cloning F* | cgcggatccATGAATAAATCAATATTTATTCAGCTA |
| Sp Tsn1 cloning R* | cgcggatccTTAAACCAATTTATGTATCCGAAG |
| Hs TSN cloning F* | cgcggatccATGTCTGTGAGCGAGATCTTCG |
| Hs TSN cloning R* | cgcggatccCTATTTTTCAACACAAGCTGCTG |
| Sp Tfx1 cloning F* | cgcggatccATGGAAGAGGAATTCCTCTCA |
| Sp Tfx1 cloning F* | cgcggatccTTATGTGGACCGTAATCGTTTC |
| Hs TSNAX cloning F* | cgcggatccATGAGCAACAAAGAAGGATCAG |
| HS TSNAX cloning R* | cgcggatccCTAAGAAATGCCCTCTTCTTG |

*Lower case = restriction site

**Table S2.** Strains used in this study

| Strain | Genotype | Source |
|---|---|---|
| BP90 | *h⁻ ade6-M26 ura4-D18 leu1-32* | McFarlane Collection |
| BP118 | *h⁻ ade6-M216 ura4-D18 leu1-32 taz1::ura4⁺* | McFarlane Collection |
| BP743 | *h⁻ rad3-136* | McFarlane Collection |
| BP1080 | *h⁻ ade6-M26 ura4-D18 leu1-32 tsn1::kanMX6* | McFarlane Collection |
| BP1089 | *h⁻ ade6-M26 ura4-D18 leu1-32 tfx1::kanMX6* | McFarlane Collection |
| BP1534 | *h⁻ ura4-D18 leu1-32 his3-D1 ade6::tRNA$^{GLU}$ (1) lys1-37* (pSRS5) | McFarlane Collection |
| BP1535 | *h⁻ ura4-D18 leu1-32 his3-D1 ade6::tRNA$^{GLU}$ (2) lys1-37* (pSRS5) | McFarlane Collection |
| BP2294 | *h⁻ ade6-M210 ura4-D18 leu1-32* Ch$^{16\text{-}23R}$ | This study |
| BP2406 | *h⁻ ade6-M210 ura4-D18 leu1-32 tfx1::kanMX6* Ch$^{16\text{-}23R}$ | This study |
| BP2421 | *h⁻ ade6-M210 ura4-D18 leu1-32 tsn1::kanMX6* Ch$^{16\text{-}23R}$ | This study |
| BP2747 | *h⁻ ade6-M26 ura4-D18 leu1-32 dcr1::natMX6* | McFarlane Collection |
| BP2748 | *h⁻ ade6-M26 ura4-D18 leu1-32 dcr1::natMX6 tsn1::kanMX6* | McFarlane Collection |
| BP2750 | *h⁻ ade6-M26 ura4-D18 leu1-32 dcr1::natMX6 tfx1::kanMX6* | McFarlane Collection |
| BP2757 | *h⁻ ade6-M26 ura4-D18 leu1-32 ago1::ura4⁺* | McFarlane Collection |
| BP2759 | *h⁻ ade6-M26 ura4-D18 leu1-32 tsn1::kanMX6 ago1::ura4⁺* | McFarlane Collection |
| BP2761 | *h⁻ ade6-M26 ura4-D18 leu1-32 tfx1::kanMX6 ago1::ura4⁺* | McFarlane Collection |
| BP2894 | *h⁻ ade6-M210 ura4-D18 leu1-32 dcr1::ura4⁺* Ch$^{16\text{-}23R}$ | This study |
| BP2897 | *h⁻ ade6-M210 ura4-D18 leu1-32 tfx1::kanMX6 dcr1::ura4⁺* Ch$^{16\text{-}23R}$ | This study |
| BP2899 | *h⁻ ade6-M210 ura4-D18 leu1-32 tsn1::kanMX6 dcr1::ura4⁺* Ch$^{16\text{-}23R}$ | This study |
| BP3301 | *h⁻ ade6-M210 ura4-D18 leu1-32 his3-D1* O*trt1::his3⁺* | McFarlane Collection |
| BP3305 | *h+ ade6-M210 leu1-32 his3-D1 trt1::his3⁺* (HAATI$^{STE}$) | J. Cooper[1] |
| BP3322 | *h⁻ ura4-D18 leu1-32 his3-D1 ade6::tRNA$^{GLU}$ (1) lys1-37 tsn1::kanMX6* (pSRS5) | McFarlane Collection |
| BP3324 | *h⁻ ura4-D18 leu1-32 his3-D1 ade6::tRNA$^{GLU}$ (1) lys1-37 dcr1::natMX6* (pSRS5) | McFarlane Collection |
| BP3326 | *h⁻ ura4-D18 leu1-32 his3-D1 ade6::tRNA$^{GLU}$ (1) lys1-37 dcr1::natMX6 tsn1::kanMX6* (pSRS5) | McFarlane Collection |
| BP3344 | *h⁻ ura4-D18 leu1-32 his3-D1 ade6::tRNA$^{GLU}$(2) lys1-37 tsn1::kanMX6* (pSRS5) | McFarlane Collection |
| BP3348 | *h⁻ ura4-D18 leu1-32 his3-D1 ade6::tRNA$^{GLU}$(2) lys1-37 dcr1::kanMX6* (pSRS5) | McFarlane Collection |
| BP3364 | *h⁻ ura4-D18 leu1-32 his3-D1 ade6::tRNA$^{GLU}$(2) lys1-37 tsn1::kanMX6 dcr1::natMX6* (pSRS5) | McFarlane Collection |
| BP3382 | *h+ ade6-M210 leu1-32 his3-D1 trt1::his3⁺* (HAATI$^{STE}$) *tsn1::kanMX6* | This study |
| BP3384 | *h+ ade6-M210 leu1-32 his3-D1 trt1::his3⁺* (HAATI$^{STE}$) *tfx1::kanMX6* | This study |
| BP3401 | *h⁻ ade6-M26 ura4-D18 leu1-32 rnh1::kanMX6* | This study |
| BP3405 | *h⁻ ade6-M26 ura4-D18 leu1-32 rnh201::kanMX6* | This study |
| BP3410 | *h⁻ ade6-M26 ura4-D18 leu1-32 rnh1::kanMX6 rnh201::hphMX6* | This study |
| BP3412 | *h⁻ ade6-M26 ura4-D18 leu1-32 tfx1::natMX6 rnh1::kanMX6* | This study |
| BP3414 | *h⁻ ade6-M26 ura4-D18 leu1-32 tfx1::natMX6 rnh201::kanMX6* | This study |
| BP3417 | *h⁻ ade6-M26 ura4-D18 leu1-32 rnh201::kanMX6 tsn1::natMX6* | This study |
| BP3426 | *h⁻ ade6-M26 ura4-D18 leu1-32 tsn1::kanMX6 rnh1::natMX6* | This study |
| BP3428 | *h⁻ ura4-D18 leu1-32 his3 ade6::tRNA$^{GLU}$ (1) lys1-37 tfx1::kanMX6* (pSRS5) | McFarlane Collection |
| BP3431 | *h⁻ ura4-D18 leu1-32 his3 ade6::tRNA$^{GLU}$ (2) lys1-37 tfx1::kanMX6* (pSRS5) | McFarlane Collection |
| BP3433 | *h⁻ ura4-D18 leu1-32 his3-D1 ade6::tRNA$^{GLU}$ (1) lys1-37 dcr1::natMX6 tfx1::kanMX6* (pSRS5) | McFarlane Collection |
| BP3435 | *h⁻ ura4-D18 leu1-32 his3 ade6::tRNA$^{GLU}$(2) lys-37 dcr1::natMX6 tfx1::kanMX6* (pSRS5) | McFarlane Collection |
| BP3450 | *h+ ade6-M210 leu1-32 his3-D1 trt1::his3⁺* (HAATI$^{STE}$) *tsn1::kanMX6 rnh201::natMX6* | This study |
| BP3451 | *h+ ade6-M210 leu1-32 his3-D1 trt1::his3⁺* (HAATI$^{STE}$) *tsn1::kanMX6 rnh1::natMX6* | This study |
| BP3453 | *h+ ade6-M210 leu1-32 his3-D1 trt1::his3⁺* (HAATI$^{STE}$) *rnh201::natMX6* | This study |
| BP3454 | *h+ ade6-M210 leu1-32 his3-D1 trt1::his3⁺* (HAATI$^{STE}$) *rnh1::natMX6* | This study |
| BP3456 | *h+ ade6-M210 leu1-32 his3-D1 trt1::his3⁺* (HAATI$^{STE}$) *rnh201::natMX6 tfx1::kanMX6* | This study |
| BP3458 | *h+ ade6-M210 leu1-32 his3-D1 trt1::his3⁺* (HAATI$^{STE}$) *rnh1::natMX6 tfx1::kanMX6* | This study |
| BP3459 | *h+ ade6-M210 leu1-32 his3-D1 trt1::his3⁺* (HAATI$^{STE}$) *rnh201::natMX6 rnh1::kanMX6* | This study |
| BP3461 | *h⁻ ade6-M26 ura4-D18 leu1-32 rnh201::kanMX6 dcr1::natMX6* | This study |
| BP3472 | *h⁻ ade6-M26 ura4-D18 leu1-32 rnh1::kanMX6 rnh201::hphMX6* (pREP3X) | This study |
| BP3473 | *h⁻ ade6-M26 ura4-D18 leu1-32 rnh1::kanMX6 rnh201::hphMX6* (pREP3X-*rnh1⁺*) | This study |
| BP3474 | *h⁻ ade6-M26 ura4-D18 leu1-32 dcr1::natMX6 tsn1::kanMX6* (pREP3X) | This study |
| BP3475 | *h⁻ ade6-M26 ura4-D18 leu1-32 dcr1::natMX6 tsn1::kanMX6* (pREP3X-*rnh1⁺*) | This study |
| BP3476 | *h⁻ ade6-M216 ura4-D18 leu1-32 dcr1::natMX6* (pREP3X) | This study |
| BP3477 | *h⁻ ade6-M26 ura4-D18 leu1-32 dcr1::natMX6* (pREP3X-*rnh1⁺*) | This study |
| BP3478 | *h⁻ ade6-M26 ura4-D18 leu1-32 rnh201::hphMX6 tsn1::kanMX6* (pREP3X) | This study |
| BP3479 | *h⁻ ade6-M26 ura4-D18 leu1-32 rnh201::hphMX6 tsn1::kanMX6* (pREP3X-*rnh1⁺*) | This study |
| BP3482 | *h⁻ ade6-M26 ura4-D18 leu1-32 dcr1::natMX6* (pREP3X-*pac1⁺*) | This study |
| BP3483 | *h⁻ ade6-M26 ura4-D18 leu1-32 dcr1::natMX6 tsn1::kanmx6* (pREP3X-*pac1⁺*) | This study |
| BP3484 | *h⁻ ade6-M26 ura4-D18 leu1-32 rnh201::kanMX6 tsn1::natMX6* (pREP3X-*pac1⁺*) | This study |
| BP3488 | *h⁻ ade6-M26 ura4-D18 leu1-32 dcr1::natMX6 tsn1::kanMX6* (pREP3X-Sp*tsn1⁺*) | This study |
| BP3489 | *h⁻ ade6-M26 ura4-D18 leu1-32 dcr1::natMX6 tsn1::kanMX6* (pREP3X-Hs*TSN⁺*) | This study |
| BP3491 | *h- ade6-M26 leu1-32 ura4-D18 rnh201::kanMX6 tsn1::natMX6* (pREP3X-Sp*tsn1⁺*) | This study |
| BP3492 | *h- ade6-M26 leu1-32 ura4-D18 rnh201::kanMX6 tsn1::natMX6* (pREP3X-Hs*TSN⁺*) | This study |
| BP3493 | *h- ade6-M26 leu1-32 ura4-D18 nh201::kanMX6tsn1::natMX6* (pREP3X-*dcr1⁺*) | This study |
| BP3497 | *h⁻ ade6-M26 ura4-D18 leu1-32 dcr1::natMX6 tsn1::kanMX6* (pREP3X-Sp*tsn1-E152A*) | This study |
| BP3499 | *h⁻ ade6-M26 ura4-D18 leu1-32 dcr1::natMX6 tsn1::kanMX6* (pREP3X-Hs*TSN-E150A*) | This study |

| | | |
|---|---|---|
| BP3510 | *h⁻ ade6-M26 ura4-D18 leu1-32 dcr1::natMX6 tsn1::kanMX6* (pREP3X-*rnh201*⁺) | This study |
| BP3511 | *h⁻ ade6-M26 ura4-D18 leu1-32 rnh1::kanMX6 rnh201::hphMX6* (pREP3X-*rnh201*⁺) | This study |
| BP3512 | *h- ade6-M26 leu1-32 ura4-D18 tsn1::kanMX6 dcr1::natMX6* (pREP3X-Hu*TSNAX*⁺) | This study |
| BP3513 | *h- ade6-M26 leu1-32 ura4-D18 tsn1::kanMX6 dcr1::natMX6* (pREP3X-Sp*tfx1*⁺) | This study |
| BP3518 | *h⁻ ade6-M26 ura4-D18 leu1-32 dcr1::ura4⁺ rnh1::kanMX6* | This study |

[1]Jain *et al*. (2010) *Nature 467*, 223-227.